Deytec Technical Report No. 2009-01

Validation of the CFAST and FDS Fire Models with Full-Scale Nuclear Power Plant Compartment Fire Experiments

Deytec, Inc.

Nuclear Engineering Services

Validation of the CFAST and FDS Fire Models with Full-Scale Nuclear Power Plant Compartment Fire Experiments

March 2009

Prepared by
Dr. Monideep K. Dey,

HC-64, Box 100-27
Yellow Spring, WV 26865
USA

Deytec, Inc.
Nuclear Engineering Services

Abstract

A comprehensive series of full-scale fire experiments was designed to simulate single compartment fire scenarios in nuclear power plants. The main purpose of the test series was to provide data to validate fire models over a wide range of conditions. The fire size and location, type of fuel, natural and mechanical ventilation, and cable type and configuration were varied to provide a comprehensive data set for model validation. The CFAST (Consolidated Model for Fire Growth and Smoke Transport), a two-zone fire model and; FDS (Fire Dynamics Simulator), a computational fluid dynamics fire model, have been validated using the data from the these full-scale compartment fire experiments. Both CFAST and FDS demonstrated capabilities for modeling the phenomena in the transients investigated in this validation study. The prediction of open door tests is more simple and accurate. This is because the extinction models in CFAST and FDS employ simple algorithms for predicting fire extinction. Generally, the predictions of global parameters such as hot gas layer temperature and interface height, oxygen, carbon dioxide, carbon monoxide, and smoke concentrations, and door heat and mass flows are more accurate. Larger discrepancies in the predictions of heat fluxes and target responses by both codes were observed in this study. Improvements in the calculation of heat fluxes, coupling of the mechanical ventilation system to the fire compartment, near-field environment, and fire extinction will improve the predictive capabilities of both codes.

Table of Contents

List of Tables

List of Figures

Executive Summary

A comprehensive series of full-scale fire experiments was designed to simulate single compartment fire scenarios in nuclear power plants. The main purpose of the test series was to provide data to validate fire models over a wide range of conditions. The fire size and location, type of fuel, natural and mechanical ventilation, and cable type and configuration were varied to provide a comprehensive data set for model validation. Fifteen experiments were conducted in a large compartment (584 m3) constructed with marinite boards to provide about 300 channels of data. Overall, about 10 million discrete pieces of data were recorded. These tests were designed by the NRC staff and conducted in collaboration with the National Institute of Standards and Technology (NIST) at its Large Fire Facility in Gaithersburg, Maryland. This test series provided validation data for an international benchmark exercise in the International Collaborative Fire Model Project (ICFMP).

The CFAST (Consolidated Model for Fire Growth and Smoke Transport), a two-zone fire model and; FDS (Fire Dynamics Simulator), a computational fluid dynamics fire model, have been validated using the data from these full-scale compartment fire experiments. These codes were developed at NIST and exercised by NRC staff for the validation study reported herein. The code predictions for this validation study were made before the tests were conducted.

Both CFAST and FDS demonstrated capabilities for modeling the phenomena in the transients investigated in this validation study. Generally, the prediction of open door tests is more simple and accurate. This is because the extinction models in CFAST and FDS employ simple algorithms for predicting fire extinction. However, even with these simple models, the codes provided fairly accurate predictions of fire extinction for closed door scenarios without mechanical ventilation. This is in part due to the accurate prediction of oxygen concentrations in most cases. The predictions of global parameters such as hot gas layer temperature and interface height, oxygen, carbon dioxide, carbon monoxide, and smoke concentrations, and door heat and mass flows are more accurate than the prediction of heat fluxes and target responses. The sub-models in both codes for predicting global parameters are generally robust.

The limitations of CFAST and FDS determined from this validation study is discussed below. The limitations are discussed to provide information for improving the models.

Both codes employ simple algorithms for fire behavior in under ventilated conditions. Although the predictions of fire extinction were reasonably good for some scenarios, the codes have difficulty predicting the effects of mechanical ventilation on the mixing and concentration of oxygen in the compartment. The lack of ability to model the coupling of the compartment with the mechanical ventilation system results in errors in the predicted compartment pressure, ventilation flowrates, and oxygen concentration.

Large uncertainties are noted in the prediction of heat fluxes to targets and walls, and the thermal response of the targets. Results of this study shows that FDS consistently under predicts the convective and radiative heat fluxes to targets and walls. The CFAST predictions vary, and are sometimes much larger than measured values. The errors of the flux predictions by the codes are much larger than the expected uncertainty of the heat flux due to measurement uncertainties. Experimental observation indicates a larger convective heat flux (total heat flux - radiative heat flux) than predicted by both CFAST and FDS for all the experiments. The prediction of the spatial temperature distribution in vertical cable trays when fires sources are in its immediate vicinity was challenging, even for FDS. The prediction of heat fluxes in or near a fire plume is also difficult, even for CFD codes.

The prediction of carbon monoxide and smoke, products of incomplete combustion, posed a challenge for the closed door experiments in which the fire became under ventilated. Both, CFAST and FDS do not account for the effects of under ventilation on carbon monoxide or smoke production. A constant yield for the quantities is used by the codes through the transient, whereas in reality the production of these species changes with the availability of oxygen during the combustion process. The smoke yield used in the calculations may also be dependent on the size of the fire.

Certain increases and oscillations in the hot gas temperature or target temperature in localized areas were observed in the experiments. Some of these oscillations are due to the movement of the fire plume, particularly if the fire is under ventilated. Oscillations in the local oxygen concentration due to the incomplete mixing of gases in closed compartment experiments were also observed. Prediction of these localized phenomena is difficult, even with a CFD code like FDS. The evaluation of target response in or near the fire can be challenging due to plume tilting and behavior.

Although relatively good performance is noted above for most parameters, this study shows that the calculation of heat flux to targets and walls require improvement for both CFAST and FDS. It should be noted that this validation test series was designed for and contains extensive data that can be used to improve the models for calculating heat fluxes.

The prediction of the effects of under ventilation on a fire is complex. Research is ongoing to improve the understanding of the basic combustion processes to be able to develop more robust combustion models. Although the simple combustion models in CFAST and FDS performed well in most of the scenarios examined here, further examination and improvement of combustion sub-models to cover a wide range of conditions is needed.

Acknowledgments

This verification and validation (V&V) study for CFAST and FDS has been conducted by the U.S. Nuclear Regulatory Commission (NRC) in collaboration with the National Institute of Standards and Technology (NIST) Building and Fire Research Laboratory (BFRL) , U.S. Department of Commerce. Since the inception of this project in 1999, the NRC has collaborated with NIST through an inter-agency memorandum of understanding (MOU) and conducted research to provide the necessary technical data and tools to support the use of fire models in nuclear power plant fire hazard analysis (FHA). Specifically, the collaboration included the evaluation of the NIST fire models, CFAST and FDS, for use in NRC's regulatory framework. The full-scale nuclear power plant compartment fire experiments used in the validation study reported here were jointly sponsored by the NRC and NIST, and conducted jointly by NRC and NIST staff. NIST has reported on these experiments separately in NIST reports, and has utilized material prepared by NRC staff assigned to NIST for their reports. Likewise, this report contains limited material prepared by NIST staff and is acknowledged. This validation study for CFAST and FDS was part of an international benchmarking and validation study in which several organizations from various countries exercised zone, lumped-parameter, and computational fluid mechanics (CFD) models. The NRC appreciates the efforts of organizations participating in the International Collaborative Fire Model Project (ICFMP) for providing comments and input for the design of the experiments, interpretation of the experimental results, and sharing their results and insights gained from their respective analyses.

Acronyms and Initialisms

1 Introduction

1.1 Purpose of Document

Section 2.4.1.2 of NFPA 805 requires that only fire models acceptable to the NRC [(Authority Having Jurisdiction (AHJ)] shall be used in fire modeling calculations. Further, NFPA 805, Sections 2.4.1.2.2 and 2.4.1.2.3 state that the fire models shall only be applied within the limitations of that fire model, and shall be verified and validated. The NRC has proposed to endorse V&V documents for specific fire models that will be acceptable to the NRC if they are used within the ranges identified in the V&V documents. The specific fire models include the Consolidated Model of Fire Growth and Smoke Transport (CFAST), and the Fire Dynamics Simulator (FDS) developed by the National Institute of Standards and Technology (NIST) . Draft NUREG-1824, presented as a main report and six volumes, includes the V&V documents for these two models. The documentation follows the outline of ASTM E 1355-04, "Evaluating the Predictive Capability of Deterministic Fire Models," [ASTM, 2004]. This report is a technical supporting document for Draft NUREG-1824 and presents the validation study of CFAST and FDS with full-scale nuclear power plant fire experiments conducted by the NRC. The results of this validation study have been used toward formulating the verification and validation information presented in Draft NUREG-1824.

This validation study for CFAST and FDS was conducted as part of an international benchmarking and validation study in which several organizations from various countries exercised zone, lumped-parameter, and computational fluid mechanics (CFD). This report only presents the validation study for CFAST and FDS. The results of the international benchmarking and validation study, including validation of the other models exercised and collective insights on the validity of classes of models for these fire scenarios will be published in the near future.

1.2 Background

Activities conducted by the NRC office of Nuclear Regulatory Research (RES) to support development of the technical basis for fire model applications in nuclear power plants (NPPs) since 1999 include the establishment of an interagency agreement between the NRC and NIST Building and Fire Research Laboratory (BFRL) for the NRC to develop the capability to use the CFAST and FDS fire computer codes for NPP applications.

NRC has also co-organized an International Collaborative Fire Model Project (ICFMP) to evaluate fire models for NPP Applications. The collaborative project is divided into two phases. The objective of the first phase is to evaluate the capability and limitations of current state-of-the-art fire models for FHA in NPPs. The second phase of the project is aimed at improving fire modeling methods and tools in order to support their extended use for FHA for NPPs. Five benchmarking and validation exercises have been conducted in the ICFMP to evaluate the predictive capability and limitations of fire models (both zone and CFD) to simulate several NPP fire scenarios, and develop generic conclusions on the use of fire models in the NRC regulatory process.

A test program for fire model evaluation, validation, and improvement has been conducted as part of RES anticipatory research efforts in collaboration with NIST. Full-scale NPP compartment fire experiments with cable targets were conducted in 2003 for the specific purpose of verifying and validating fire models for NPP applications. This work was performed by NRC staff with support of NIST BFRL staff. Other international fire tests and validation exercises include those that examined fires in large halls such as a turbine building, large pool fires in compartments, cable tray fires, and flame spread. NRC staff exercised CFAST and FDS in the international benchmarking and validation exercises for CFAST and FDS. The titles of the five benchmarking and validation exercises are listed below:

1. Cable Tray Fires [NRC, 2002]
2. Pool Fires in Large Halls [NRC, 2004a]
3. Full-Scale Nuclear Power Plant Compartment Fire Experiments [This report]
4. Large Fires in Compartments [NRC, 2005b]
5. Cable Tray Flame Spread Experiments [NRC, 2005c]

Additionally, the NRC has initiated a 5-Year collaborative program with Institut de Radioprotection et de Surete Nucleaire (IRSN), France for validating CFAST and FDS for multi-compartment fire scenarios.

1.3 Format of Document

The document is formatted in seven chapters. Chapter 2 provides the specification of the international benchmarking and validation exercise, followed by Chapter 3 that presents the main experimental results. Chapter 4 provides a summary of the main issues that arose in the consideration of input parameters and assumptions for the scenarios in the exercise. Chapter 5 provides the main comparison of model predictions with experimental results, followed by the general conclusions and recommendations from the validation study in Chapter 6. Finally, Chapter 7 provides the references for the study.

2 Specification of Benchmark Exercise

2.1 Introduction

The results of Benchmark Exercise # 1 [NRC, 2002] provided a certain degree of confidence in the current fire models for single compartment fire analysis, however, benefits to extending the validation database were identified. The sub model for the target, and issues regarding the thermal environment of the target, was identified as sources of uncertainty for the types of scenarios analyzed. The target response is sensitive to the magnitude and duration of the heat flux incident on it. A target may be more sensitive to the duration of the exposure than the magnitude of the heat flux and intensity of the thermal environment if it has a high thermal inertia. It was concluded [NRC, 2002] that it would be useful to have international collaborative validation exercises in which the sensitivity of target response is explored and the predictive capability of target damage is the main focus of the program. Also, more refined measurements and data analyses will be useful to estimate the quantitative uncertainties of the parameters predicted in the analyses of these fire scenarios. The computer code results, with quantitative estimates of the uncertainties in the predicted parameters, will extend the confidence in the models for supporting engineering judgments in nuclear power plant fire safety analysis. The data from these tests can also be used for improving target models, and developing models for target heating in the ceiling jet and plume regions.

The following sections present the specification of ICFMP Benchmark Exercise # 3. In Section 2.2, previous related tests conducted by the NRC and IRSN (Institut de Radioprotection et de Sûreté Nucléaire), and the lessons learned from them, are summarized. This specification incorporates the lessons learned from previous studies, especially regarding the measurement uncertainties and challenges faced in previous tests. Previous tests sponsored by the NRC in the early 1980s have been used by various organizations to validate their respective fire models. The NRC sponsored the experiments for ICFMP Benchmark Exercise # 3 to conduct specified[1] simulations of test results to enhance the confidence in the use of the models in NRC's regulatory framework. The use of newer measurement and test methods will also provide up to date data for the validation exercises. Insights gained from the use of various models in the international validation exercises will add to the technical basis for their use in a regulatory framework. The determination of the uncertainties in model predictions is a key goal for this benchmark exercise. Therefore, the quantification of measurement uncertainties, especially for measurements that have been challenging in previous studies, are addressed in this exercise.

2.2 Review of Previous Related Work

In the past NRC has sponsored three large-scale fire test series. One of the objectives of the earlier work included using data from the large-scale experiments for fire model validation. Sandia National Laboratories (SNL) conducted an "Investigation of Twenty Foot Separation Distance as a Fire Protection Method as Specified in 10 CFR 50 Appendix R" [NRC, 1983]. SNL conducted two additional test series for the NRC; "Enclosure Environment Characterization Testing for the Base Line Validation of Computer Fire Simulation Codes" [NRC, 1987], and "An Experimental Investigation of Internally Ignited Fires in Nuclear Power Plant Control Cabinets"

[1] Per ASTM 1355-05 [ASTM, 2005].

[NRC, 1988]. The Laboratory on Research and Modeling of Fires, Institut de Radioprotection et de Sûreté Nucléaire, France, also conducted a single test. The test and results are described in "Probability Study on Fire Safety" [IRSN, 1997]. A brief description of each test series follows.

2.2.1 Investigation of Twenty-Foot Separation Distance

The tests were conducted at Underwriters Laboratories and the work reported in 1983. The primary purpose of these tests was to evaluate the effectiveness of the fire protection afforded by the separation of redundant safety related cables by a horizontal distance of twenty 6.1 m (20 feet) with no intervening combustibles or hazards. Four preliminary experiments were conducted and modeled using the Harvard Fire Code [Mitler, 1981]. The experiments and the model were used to design and execute the six full-scale tests. The full-scale test compartment was 7.6 m x 4.3 m x 3.0 m (25 x 14 x 10 ft). Construction was hollow core concrete blocks laid with mortar. The ceiling was of 12 mm inorganic board fastened to steel form and coated with cementious mixture (6mm - 19 mm). There was a 4 ft x 8 ft opening. The fire was a 1 ft x 5 ft steel pan filled with five gallons of heptane. The pan was placed against the wall. The compartment contained two vertical trays with 43 cables, corresponding to a 12.5% fill. The vertical trays were directly above the heptane pan. Two horizontal cable trays, also filled at 12.5% fill, were located 20 ft from the fire. The horizontal trays were energized. Ventilation was free convective movement through the compartment opening. Tests were run for 25 minutes.

2.2.2 Base Line Validation of Computer Fire Simulation Codes

Tests were conducted by SNL at Factory Mutual Research Center (FMRC) and reported March 1987. The primary purpose of these tests was to provide data against which to validate fire models. The test compartment was 18.3 m x 12.2 m x 6.1 m (60 x 40 x 20 ft). Interior ceiling and walls were lined with 2.5 cm thick Marinite I. The floor was concrete slab. Fuels used were gas burner, heptane pool, methanol pool, and solid polymethylmethacrylate (PMMA) with fires ranging from 500 kW to 2000 kW. All of the tests utilized forced ventilation. The series was divided into two parts. The first part is described here; the second part is the following test series description. During the first part of the series a total of 22 tests were conducted. The first 18 tests were conducted with nothing in the enclosure. The final four tests used 6 real electrical control cabinets and eight mock cabinets composed of Marinite I and metal framing. Forced ventilation was used during the tests ranging form one to ten room air changes per hour. Test variables were fire intensity, enclosure ventilation rate, and fire location.

2.2.3 Internally Ignited Fires in Nuclear Power Plant Control Cabinets

This work reported in October 1988, describes the second part of the two-part series of full-scale electrical cabinet fire tests described above. Both series utilized the same test compartment. The second series tests were designed to investigate the effects of fuel type, cabinet configuration and enclosure ventilation rate on the development of the enclosure environment. Forced ventilation was used ranging from one to eight room air changes per hour. Compartment contents were six electrical control cabinets containing cables to represent all cabinet fuels, eight cable bundles placed throughout the enclosure (exposed to room conditions) and eight mock cabinets of Marinite and metal framing. Five tests were conducted all involving a fire in a control cabinet.

2.2.4 Probability Study Program on Fire Safety

The single test was conducted at the Laboratory on Research and Modeling of Fires in the Pluton chamber at the Galaxie facility in IRSN, Cadarache, France. The objectives of this test were to provide quantitative information to safety analysts and contribute data to the qualification of the FLAMME_S fire model. The test was conducted on March 28, 1996 and reported in April 1997. The test was designed to simulate a cable room. Compartment construction was reinforced concrete with walls 0.25 m thick. Compartment dimensions were 9 m x 6 m x 7.5 m. Forced ventilation system consisted of a floor blower, and an extractor located high on the wall. The ventilation flow rate was set at five air changes per hour. The compartment contained five bundles of 20 cables mounted on a ladder-like support. Four were set horizontally with voltage supplied to them (two near the ceiling and two near the fire). One was vertical without any voltage applied to them. One electrical cabinet was also included (1 m x 0.3 m x 1.2 m) with metal plates inside to represent electrical equipment. One hundred liters of MOBIL DTE medium oil preheated to 250 ºC were used for the fire that yielded a peak heat release rate of 940 kW. Temperature measurements were made along each cable run on either side of the bundle using 2 mm diameter type K thermocouples.

2.3 Lessons Learned from Previous Tests

An analysis of the early NRC model validation fire testing (NUREG/CR-4681) has revealed the following information, limitations, and lessons learned:

! Data was recorded every five seconds, introducing a 5 second uncertainty in the measurements.

! The difference between nominal and actual ventilation rates appears to have been as high as 20%. The measured values should be used whenever possible in lieu of the nominal ventilation rates.

! During testing, significant air leakage was noted from the enclosure. It appears that typical outlet duct flow was only about 70-80% of the inlet flow implying significant leakage. If an estimate of the total outflow rate is needed, it is recommended that a full mass balance on the room be performed. The room "storage" term can be estimated using the measured internal room temperatures at various locations. At approximately 5 minutes into Test 3, one entire wall of the test enclosure shifted at the wall/floor interface.

! The enclosure exhaust gas represents only a very small fraction of the total flow through the fire products collector. The exhaust gas stream was diluted significantly by air drawn into the collector from the general enclosure. Hence the actual concentration values, smoke density, and temperature data all represent a mixture of ambient and enclosure gas streams.

! Due mostly to the very large volume of the test enclosure, there is a significant lag time between the fire behaviors within the room and sensing of the associated effects at the fire products collector.

! Not all the fire products from the test fires where actually collected, as there was significant leakage of air from the room.

! All the data from the surface heat flux probes as reported in the main data reports is in error. It appears that the problem occurred when the raw data was converted to engineering units.

! The density of Marinite board ranges from 700-1000 km/m3. The original assumed value of 737 kg/m3 was found to be just a nominal value reported in the literature. SNL chose to "experiment" with the assumed property values to obtain a better fit between the predictions and the data.

! Thermal conductivity varies with material density with the higher density material having higher thermal conductivity than the lower density version of the same material. To explore the impact of material properties, SNL assumed that the panels used in construction were at the upper end of the manufacturers density range. Hence a density of 1000 kg/m3 was assumed.

! In the transient thermal model the thermal parameter of interest is actually the thermal diffusivity. This parameter was adjusted to obtain the best possible fit between predictions and data for a number of locations in several tests. The best results were obtained assuming a thermal diffusivity of 2.0E-7m2/s, which given the materials specific heat and density values implies a thermal conductivity of 0.23W/m K.

! SNL had no specific information regarding the properties of the floor.

! Power/signal cables should not be run on the top of the test enclosure, when possible, to limit the potential of failures due to elevated temperatures.

An analysis of the Probability Study Program on Fire Safety report revealed the following information:

! K type thermocouples were glued even with the concrete

! No measurement was taken within the thickness of the wall

! The thermal loss through the walls was about 650 kW, which is 70% of the energy emitted by the initiating blaze (~940 kW). This percentage is in the same range as the earlier studies by the French Laboratory on Research and Modeling of Fires.

The above lessons learned were considered in the development of the test plan for the benchmark exercise and in analyzing the data.

2.4 Experiment Design Process for ICFMP Benchmark Exercise # 3

The experiments and draft specification of the ICFMP Benchmark Exercise # 3 was designed and developed by NRC staff and incorporated into an implementing test plan by NIST experimentalists. A draft specification of ICFMP Benchmark Exercise # 3 was issued to participants in the International Collaborative Fire Model Project (ICFMP) on September 6, 2002 to solicit comments, further ideas, and suggestions. Written comments on the draft specification were received from participants. The draft specification was also presented at the 6th ICFMP meeting at British Research Establishment (BRE), UK on October 10-11, 2002 when verbal comments from participants in the meeting were received and documented. Appendix A provides the written and verbal comments received on the draft specification of the ICFMP Benchmark Exercise # 3, including the resolution and disposition of the comments. The final specification used for ICFMP Benchmark Exercise # 3 and presented below includes the modifications resulting from the extensive comments received and presented in Appendix A.

2.5 Specification of Experiments

The following sections describe the facility, experiments, and instrumentation for ICFMP Benchmark Exercise # 3. A complete description of the instrumentation and procedures developed by NIST for the experiments designed by the NRC may be found in NIST, 2005.

2.5.1 Test Facility Description

As the US federal government's principal fire research laboratory, Building and Fire Research Laboratory (BFRL) at NIST maintains some of the country's best and most extensive fire testing facilities. More than 400 fire experiments are performed each year in the specially equipped, 27 m (90 ft) x 37 m (120 ft), Large Fire Laboratory. The facility has several instrumented hoods or calorimeters for measuring heat release rate. The smallest calorimeter has a capacity of 50 kW and a hood 1.2 m (4 ft) on each side. It is used for measuring the heat release rate of small objects or samples removed from larger objects. A medium sized calorimeter or furniture calorimeter, has a capacity of approximately 750 kW. This calorimeter is sized for burning individual pieces of furniture or other objects of similar size with a hood measuring 3 m (10 ft) on each side.

Two large hoods are available for burning multiple items at one time. One hood is approximately 6 m (20 ft) x 6 m (20 ft) and has a capacity of 3 MW (3,000 kW). The largest hood is approximately 9 m (30 ft) x 12 m (40 ft) and has a capacity of approximately 10 MW (10,000 kW). Burn rooms built to simulate portions of a building or a house can be installed adjacent to or under the large hoods. The smoke from the room fires flows into the large hood for measurement and exhaust from the building.

The Large Fire Research Facility has a variety of instrumentation for measuring temperature, mass, pressure, thermal radiation, real time gas concentrations for oxygen, carbon dioxide, carbon monoxide, nitrogen oxides and hydrocarbons, and smoke concentration. Several computerized data acquisition systems are available in the facility for recording the inputs from the instrumentation.

The facility has been used for measuring the heat release rate of a wide variety of items including crude oils, office and home furnishings, and transportation vehicle components. Data from many of the large fire experiments are used to develop or evaluate mathematical models and to study the fire performance of furnishings and interior finish materials. The open space in the facility has housed structures built to simulate living rooms, kitchens, offices, corridors, townhouses, buses, and portions of a train car. Measurements on fire suppression systems, such as sprinklers, water mist and gaseous agents have also been conducted in the Large Fire Research Facility. Figure 2.1 shows the compartment used for ICFMP Benchmark Exercise # 3 being built under the largest hood in the Large Fire Facility.

Figure 2.1 Test Compartment in Large Fire Facility

2.5.2 Test Compartment and Contents

Figure 2.2 is a photo of the compartment taken from the door in the west wall, looking east. The compartment was 7.04 m x 21.66 m x 3.82 m in dimension, designed to represent a realistic-scale cable room in a nuclear power plant. The total compartment volume was 582 m3. Looking in from the 2.0 m by 2.0 m double door, Fig. 2.2 shows the right (South), back (East), and left (North) walls. Walls and ceiling were covered with two layers of 25 mm marinite

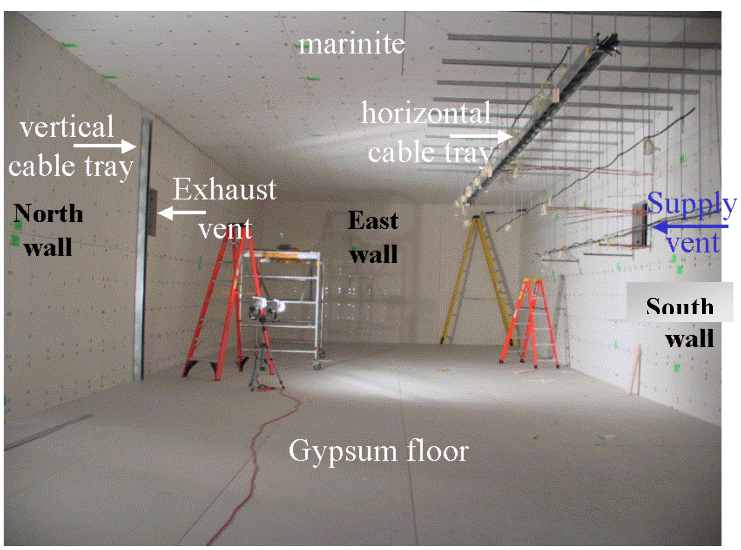

Figure 2.2 Main Features in Test Compartment

boards[2], while the floor was covered with two layers of 25 mm gypsum boards. The supply duct and horizontal cables are evident on the right of Fig. 2.2, while the vertical cable tray and exhaust duct are on the left. Figures 2.3-2.5 are schematic drawings of the compartment in which the location of some of the compartment features are shown including the Targets (A-F), ventilation ducts, thermocouple trees, junction box, fire pan, and door.

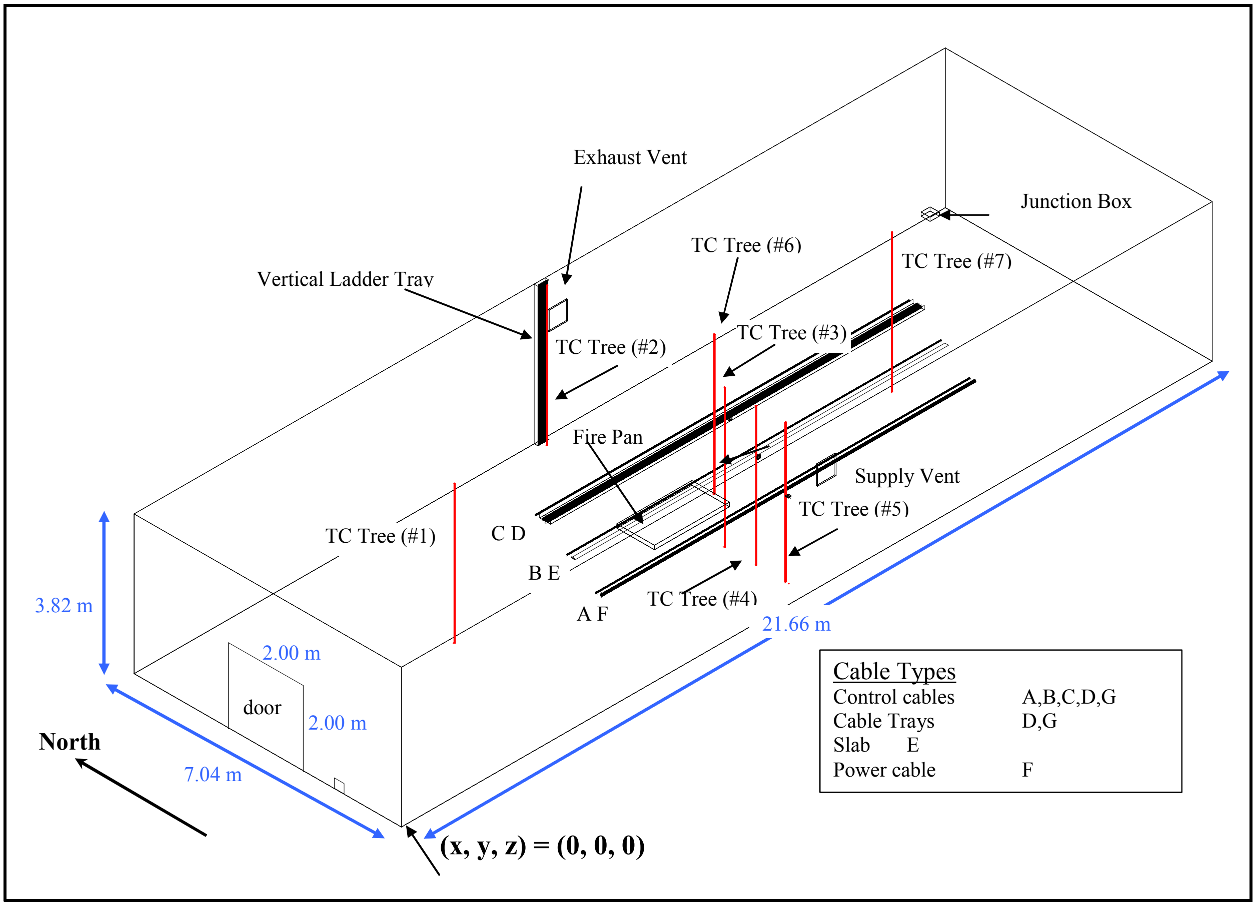

Figure 2.3 Compartment Isometric with Thermocouple Trees

The compartment contained three control cables (A, B, C), a horizontal (Target D) and a vertical cable tray (Target G) with control cables, a solid polyvinyl chloride (PVC) slab "target" (E), a single power cable (F), and a junction box. The targets were arranged to examine the following effects:

- Modeling one cable versus cables bundled in a cable tray
- Modeling a cable as composed of a slab with uniform material versus a real cable geometry and composition
- Heating characteristics of cables with a large diameter versus smaller cables
- Elevation of the target in the hot gas layer

---

[2]The thermal and optical properties of the marinite boards specifically used in the experiments were measured for this benchmark exercise and are listed in Appendix A of NIST, 2005.

- Vertical versus horizontal cable target
- Heating of a junction box on the ceiling

One goal of the target selections and locations was to develop data that could be used in establishing the degree of conservatism and margin in cable damage criteria that are currently used in the field.

The control cables had seven conductors (# 14 American Wire Gauge, AWG). The power cable had three conductors (# 6 AWG). For the primary tests in the series, all the cables were constructed of XPE (crosslinked polyethylene) insulation and Hypalon jacket materials. For the replicate tests, all the cables were based on PVC jacket and PVC/Nylon insulation materials. Further information on the thermal and optical properties, and morphology of the cables is given in NIST, 2005 (App. A). Significant resources and rigor were applied in the measuring the properties of the cables specifically used for this benchmark exercise.

In order to examine the effects on target heating listed above, the following targets were included in the experiments:

! A horizontal ladder type cable tray (Target D) was 0.3 m wide and 0.1 m deep. The tray contained two layers of control cables constructed of XPE insulation and Hypalon jacket materials in the primary tests, and three layers of control cables constructed of PVC jacket and PVC/Nylon insulation materials in the replicate tests. The center of the bottom of the tray was located 2.0 m meters from the right wall, 3.2 m above the floor. It was 10 m long, extending from 5.85 m from the front wall to 5.85 m from the back wall. Figure 2.6 shows the horizontal cable tray in the compartment at the top tier of the targets. Figure 2.7 shows the instrumented cable in the tray.

! The bottom of the center of a rectangular slab target (E) was located 1.25 meters from the right wall, 2.7 m above the floor and centrally located between the front and back walls. The slab was composed of PVC. The PVC slab was located in the middle tier of the targets.

! The bottom of the center of the power cable (F) was located 0.5 meters from the right wall, 2.2 m above the floor and extended 10 m from 5.85 m from the front wall to 5.85 m from the back wall. Figure 2.6 shows the power cable in the lower tier of the targets.

! The three control cables A, B and C were located at the same elevation and 0.1 m from the left edge of the power cable, slab target, and cable tray respectively to provide comparisons and information on target heating effects. They extended 10 m from 5.85 m from the front wall to 5.85 m from the back wall. Figure 2.6 shows the location of the control cables in the three tiers of the targets. Figure 2.7 shows the cable tray and the control cable C adjacent to each another at the same elevation in the compartment. Figure 2.8 shows the PVC slab and the adjacent control cable. Figure 2.9 shows the power cable adjacent to the control cable in the same lower tier of targets.

! The ladder type vertical cable tray (G) was 0.3 m wide and 0.1 m deep. The tray contained one layer of control cables constructed of XPE (polyethylene) insulation and Hypalon jacket materials in the primary tests, and PVC (polyvinyl chloride) jacket and PVC/Nylon insulation materials in the replicate tests. The tray was located on the surface at the center of the north wall, extending from the floor to the ceiling. Figure 2.10 shows the vertical cable tray with the cables instrumented with thermocouples adjacent to flux gauges.

! The junction box was a WCB Junction Box. It was heavy-duty, dust-tight, weatherproof, rain and watertight, with nominal inside dimensions, 30 cm length x 30 cm width x 10 cm depth. It had an approximate wall thickness of 0.7 cm. The junction box was mounted on the ceiling and located on the compartment centerline (see Figure 2.11), with its center 17.7 meters from the door. The box was made of Feraloy (see NIST, 2005; App. H for thermal properties).

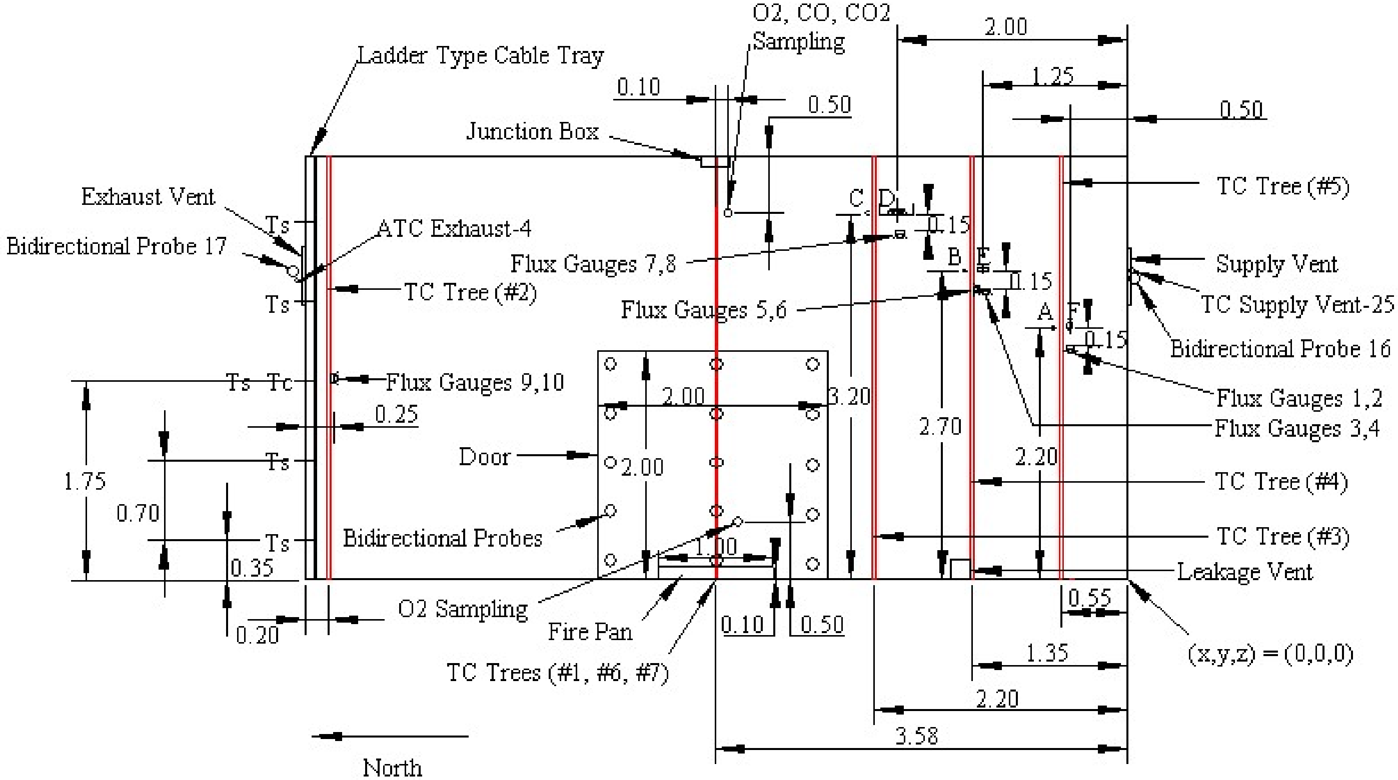

Figure 2.4 Compartment Contents and Selected Instrumentation (to scale)

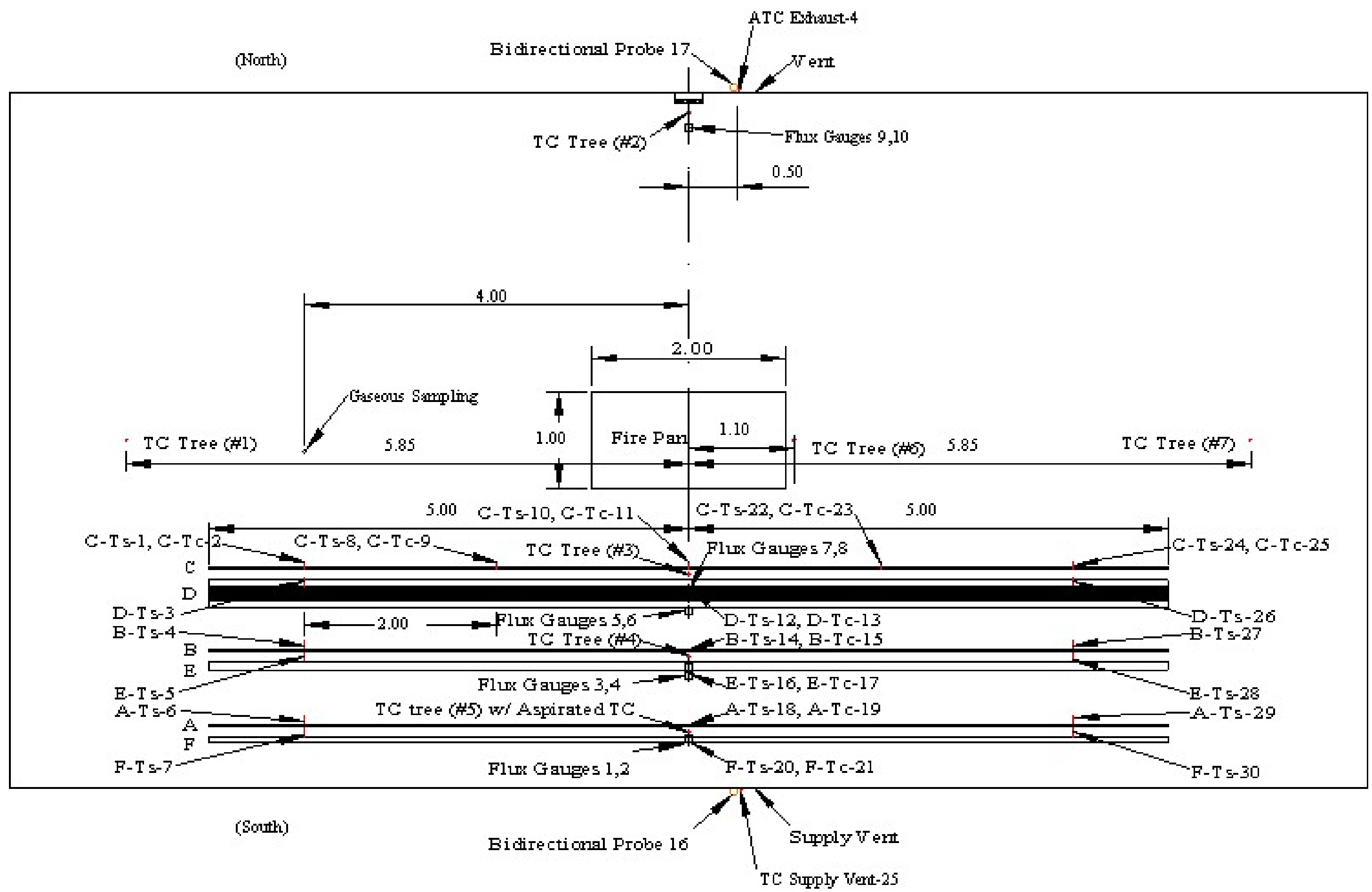

Figure 2.5 Plan View of Compartment Mid-Section (to scale)

Figure 2.6 Cable Targets in Compartment

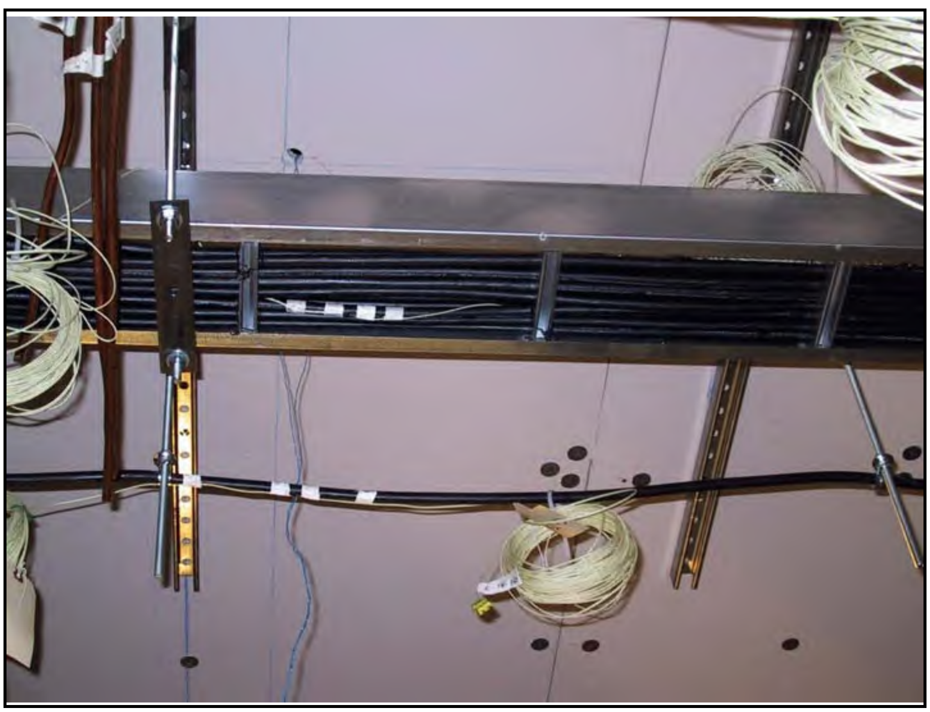

Figure 2.7 Instrumented Horizontal Cables

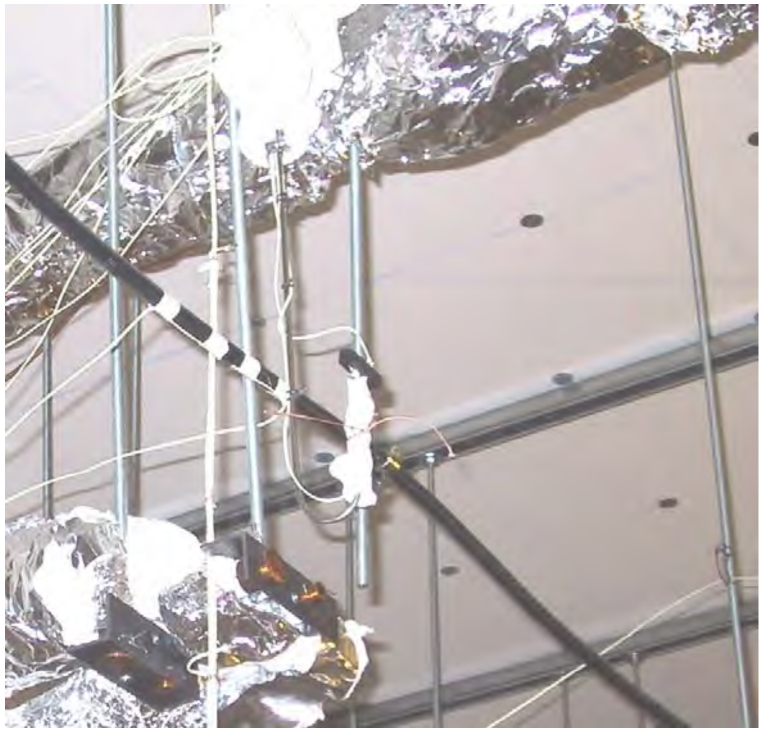

Figure 2.8 PVC Slab E with Adjacent Control Cable

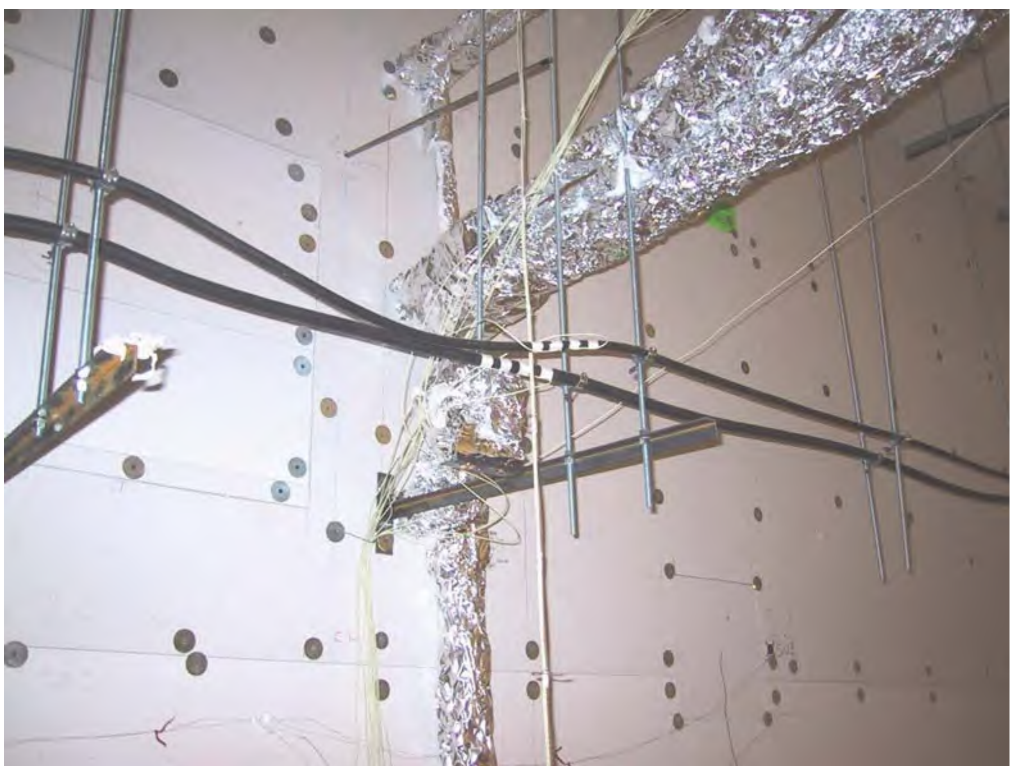

Figure 2.9 Power Cable with Adjacent Power Cable


Figure 2.10 Instrumented Vertical Cable with Flux Gauge

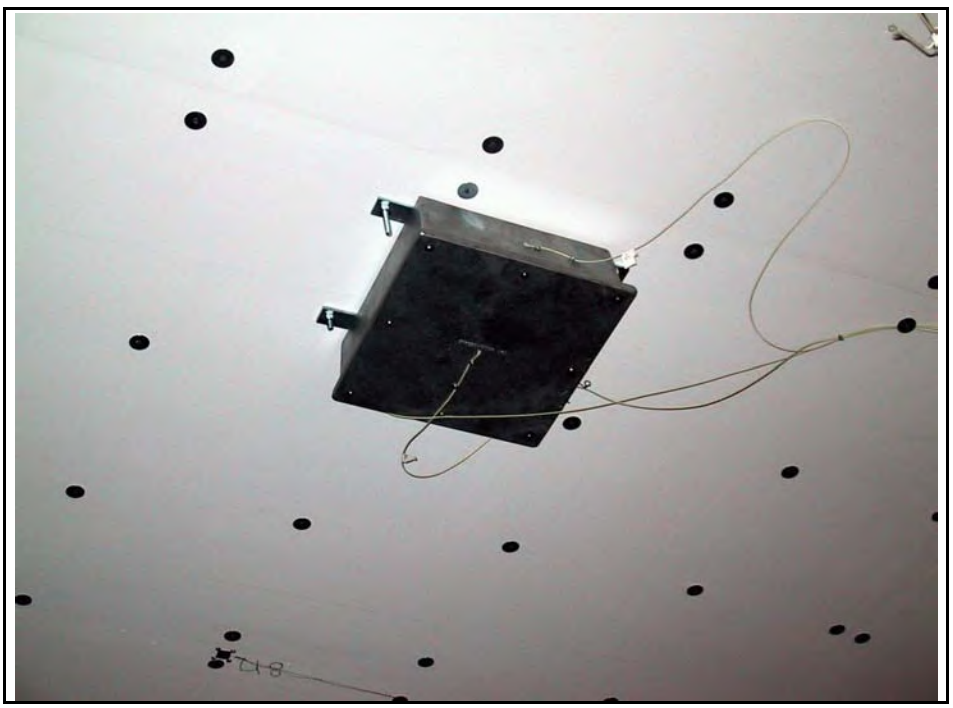
Figure 2.11 Instrumented Junction Box with Thermocouples

Several thermocouples were placed along the lengths of the cables in all the targets to examine the effect of elevation and distance from the fire on cable heating.

2.5.3 Fire Scenarios

The test configuration and fire scenarios have been selected to examine the following effects:

1. Heat release rate
2. Natural ventilation with open door
3. Mechanical ventilation system operation
4. Combination of mechanical and natural ventilation
5. Distance between fire and target
6. Target heating directly in the plume region

The fire will be located in the center of the compartment, at floor level for tests 1 through 13 (see Test Matrix in Table 2.1). Test 14 was conducted with the center of the fire at floor level and 1.8 m from the North wall at the east-west centerline. Test 15 was conducted with center of the fire at floor level and 1.25 m from the South wall at the east-west centerline. Test 18 was conducted with the center of the fire at the floor level, 1.55 m from the south wall and 1.5 m east of the east-west centerline. All tests were conducted with the fuel pan positioned with its length (2 m) parallel to the north and south walls, except for Test 18 in which the length of the pan was parallel to the east and west walls. The fuel used was heptane, except toluene was used for Test 17. To limit the potential of reflash, the fuel was secured and the test terminated when the lower level oxygen concentration dropped below ~ 15% by volume. The fuel was delivered through a positive displacement pump with a constant delivery pressure. The combustion properties of the fuel specifically used in the experiments were measured for this benchmark exercise and are listed in NIST, 2005 (Ch. 3).

The fire was located in the center of the compartment at floor level for most of the tests. For a number of tests the fire pan was moved away from the center of the compartment (see Table 2.1). Figure 2.12 shows the fuel pan used in the experiments. Although two spray nozzles are shown in Figure 2.12, one spray nozzle was found to provide optimal performance and was used in all the experiments.

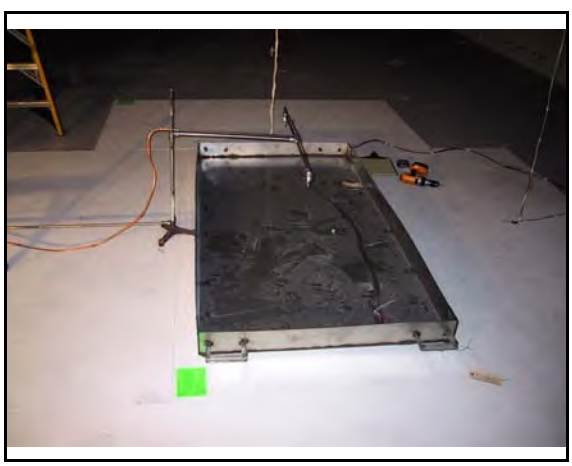

Figure 2.12 Fuel Pan with Spray Nozzle

Table 2.1 Test Matrix and Experimental Conditions.

Test	Peak HRR (kW)	Cable Type	Fuel: Burner Location	Door	Ventilation
1	410	XPE[3]	Heptanes[4]; Center	Closed	Off
2	1190	XPE	Heptanes; Center	Closed	Off
3	1190	XPE	Heptanes; Center	Open	Off
4	1190	XPE	Heptanes; Center	Closed	On
5	1190	XPE	Heptanes; Center	Open	On
6	Not conducted				
7	Replicate Test 1	PVC[5]	Heptanes; Center	Closed	Off
8	Replicate Test 2	XPE	Heptanes; Center	Closed	Off
9	Replicate Test 3	XPE	Heptanes; Center	Open	Off
10	Replicate Test 4	PVC	Heptanes; Center	Closed	On
11	Replicate Test 5	Not conducted			
12	Replicate Test 6	Not conducted			
13	2330	XPE	Heptanes; Center	Closed	Off
14	1180	XPE	Heptanes; 1.8 m from N wall	Open	Off
15	1180	PVC	Heptanes; 1.25 m from S wall	Open	Off
16	2300	PVC	Heptanes; Center	Closed	On
17	1160	XPE	Toluene; Center	Closed	Off
18	1180	XPE	Heptanes; 1.55 m from S wall & 1.50 m E of centerline	Open	Off

During the experiments, observations to determine if experimental conditions deviated from nominal conditions were made and listed in Table 2.2 below.

[3]XPE cable has crosslinked polyethylene insulation

[4]Heptanes is a commercial blend of heptane isomers

[5]PVC cable has a polyvinylchloride jacket

Table 2.2 Test Observations

Test Order	Test	Observations
1	1	No observations noted.
2	2	No observations noted.
3	5	N_2 purge flow for soot laser was low for first 5 min after ignition. Slab E appeared melted after test.
4	4	Slab E not present.
5	3	Slab E not present.
6	8	Slab E not present. Leakage around door during testing. Cable burned at Ts-10 and Tc-11 during test.
7	9	Slab E not present. Cable C charred after test.
8	13	Slab E not present.
9	14	Wall flux gauges not functioning. Slab E not present. Cables in vertical cable tray damaged during test.
10	18	Smoke coming out of south wall-ceiling joint 17 min after ignition. Doused with water at 18 min 30 s. Flux Gauge #8 not functioning before test start. Slab E not present.
11	7	New PVC cables and slab E installed before test. Biderectional Probes #13 & #14 not functioning properly before test start.
12	10	Wall flux gauges (N6, S6, C4, C5, C8) not functioning before test start. Slab E and cables partially melted during test.
13	16	Flux Gauge #8 not functioning before test start.
14	15	Flux Gauge #7 erratic behavior noticed at 730 s after ignition. Vertical tray melted above 2 m.
15	17	Fuel secured when loss of visibility completely obstructed the fire. Slab E not present. Flux Gauge #1 low water flow before test start. Flux Gauge #5 not working before test start.

2.5.4 Ventilation

A 2.00 m by 2.00 m door was present in the middle of the west wall (see Figs. 2.1 and 2.2).

The compartment was equipped with supply and exhaust forced ventilation. The midpoint of the supply and exhaust vents was located 11.22 m from the door and 2.40 m above the floor. The vents were square (0.70 m x 0.70 m) with an area of 0.5 m2 each. The supply vent is shown in Figure 2.1, and both vents are shown in Figure 2.3. The ventilation flow rate was approximately 5 volume air changes per hour. The exact values of the flows through the vents and the door were measured and are discussed in detail in NIST, 2005 (Ch. 7).

The intrinsic leakage associated with the compartment was measured before initiation of the first experiment and a number of times during the test series (see NIST 2005; App. C). An additional opening to simulate compartment leakage was not added to the compartment as originally planned because the "intrinsic" leakage of the compartment was larger than an equivalent leakage area of 0.17 m x 0.17 m which is typical of NPP compartments.

2.5.5 Measurements

Measurements were made of the following parameters:

- Heat release rate
- Upper layer temperature
- Lower layer temperature
- Depth of the hot gas layer
- Plume temperatures
- Pressure
- Oxygen content (upper and lower layer)
- CO, CO2 concentrations
- Flow rates through door and mechanical vents
- Heat flux on the cables (total + radiative)
- Cable surface and inside temperatures
- Total heat loss to boundaries
- Video and infrared recording
- Visibility

The above measurements were accomplished through the use of the following instrumentation:

- thermocouple trees with ten K-type thermocouples on each tree were used for measuring upper and lower layer temperatures as well as depth of hot layer.
- Calorimeters and radiometers were used to measure fluxes (total and radiative) on the cables. The measurement technique that utilizes different size thermocouples to estimate uncertainties in convective and radiative fluxes is not appropriate in a soot-filled environment where the effective size of a thermocouple changes as soot deposits occur. Instead, heat flux measurements were undertaken using a number of Schmidt-Bolter total heat flux gauges and ellipsoidal radiometers. The Schmidt Bolter gauges were cooled by an elevated temperature water flow to avoid condensation on the sensing element of the gauge. The radiometers are wide-angle, N2 purged devices. The comparison of the fluxes between the ellipsoidal and Schmidt-Bolter measurements allowed differentiation of radiative and convective heat flux. The convective heat flux is

expected to be small compared to the radiative heat flux. Additional instrumentation measured heat flux to the walls and ceiling.

- For open door tests oxygen concentration of the effluent from the compartment was also used to determine heat release rate.
- A compartment pressure transducer was used to measure compartment pressure.
- Paramagnetic analyzers were used for measuring upper and lower layer oxygen concentrations. Continuous sampling mitigated the need for grab sampling.
- Bi-directional probes were used for measuring air velocities.
- Thermocouples were used to measure surface and core cable temperatures.
- A laser extinction measurement was made in the upper layer near to determine the visibility.

The list of instrumentation, including locations, were designed and developed by NRC staff and implemented by NIST. A complete description of the measuring devices and systems may be found in NIST, 2005. A comprehensive list of instruments and their locations can be found in NIST 2005; App. D.

Other appendices in NIST, 2005 provide information on the ambient humidity and temperature during testing (Appendix B), the compartment leakage area determination (Appendix C), format of the electronic data (Appendix D), non-functioning instrument channels (Appendix E), and the pressure curves for the ventilation supply fan (Appendix G).

3 Experimental Results

The following sections provide data and results from the experiments for ICFMP Benchmark Exercise # 3. This comprehensive and extensive data set provides the analyst an opportunity for a complete analysis of the experiments, as well as comparison of model predictions with experimental data. Experimental uncertainties are also discussed here as their consideration was a major objective of the exercise. Sample experimental results and an expanded discussion of experimental uncertainties may also be found in NIST, 2005. The experimental results were presented and discussed at the 7th ICFMP Meeting at WPI. NIST, 2005 (Appendix F) documents responses to questions and comments on the experimental report from the participants of the 7th ICFMP Meeting.

3.1 Experimental Data and Recordings

The following provides the experimental electronic data and video recordings of the benchmark exercise.

3.1.1 Electronic Data

The CD included with this report, entitled, “Experimental Data for Full-Scale Nuclear Power Plant Compartment Fire Experiments,” contains the experimental data developed for and utilized in ICFMP Benchmark Exercise # 3. The CD also includes (1) digital pictures recording observations of the experiments, including cable damage; (2) a text file that describes the format of the electronic data; and (3) the NIST experimental report (NIST, 2005) that provides detailed descriptions and procedures of the instrumentation and measurement systems used for the test series. NIST, 2005 also provides sample results of the measurements made of the following:

- Fuel flow and heat release rate
- Heat flux to cables and walls
- Smoke concentration
- Target temperatures
- Vent and doorway flows
- Gaseous concentrations
- Gas temperatures
- Heat loss to boundaries
- Compartment pressure

3.1.2 Video Recordings

In order to allow for a complete observation and understanding of the fire phenomena, video and infrared recordings of the experiments were made. A video recording was made with cameras located in the south and west walls, and infrared recordings were made with a camera in the west wall. The recordings have been processed and compiled into the three DVDs included with this report, entitled, “Full-Scale Nuclear Power Plant Compartment Fire Experiments, Video DVDs 1, 2, and 3.” The DVDs contain several single views of the fires, as well as composites to allow simultaneous viewing of the fire from two angles, video and infrared recordings, replicate tests, fires of different sizes or affected by other conditions. The layout of the DVDs is shown in Table 3.1. The clock in the videos was set to start at the beginning of increased burning, i.e., the first video frame where the visible size of the fire increased from the pilot flame. In the case of composites where two or more views of the same test are shown on the video, the fires were synchronized by examining various distinctive points during burning such as the start of the fire and the separation of a flame mass from the main flame. The end of the test was defined as the time when the fire went out or the time the flames became invisible.

Table 3.1 DVD Layout

No.	DVD	Tests	Duration (min)
1	1	Test 1 West View	25
2	1	Test 1 South View	25
3	1	Test 2 West View	10 ½
4	1	Test 2 South View	10 ½
5	1	Test 3 West View	26
6	1	Test 3 South, West, & IR Views	26
7	2	Test 4 South & West Views	13 ½
8	2	Test 5 South, West, & IR Views	26
9	2	South Views of Test 1 Replicates [Test 1 & Test 7]	25
10	2	West Views of Test 2 Replicates [Test 2 & Test 8]	10 ½
11	2	West Views of Test 3 Replicates [Test 3 & Test 9]	26
12	2	South Views of Test 4 Replicates [Test 4 & Test 10]	13 ½
13	3	Test 13 West View	6
14	3	Test 13 South View	6
15	3	Test 13 South & West Views	6
16	3	South Views of Test 13 & Test 16	6
17	3	West Views of Test 13 & Test 2	10 ½
18	3	Test 14 South View	26
19	3	Test 15 South View	26
20	3	Test 16 South View	6 ½
21	3	Test 17 South View	4 ½
22	2	Test 18 IR View	26

3.2 Experimental Uncertainties

Determination of the experimental uncertainties in the measurements made was a major objective for this benchmark exercise. Significant resources and rigor were applied in the determination of the uncertainties of the measurements which is documented in NIST, 2005. Table 3.2 summarizes the findings.

As indicated earlier, the extent to which one is able to validate predictive models is dependent on the degree of accuracy of the experimental measurements. Table 3.2 shows that the main source of uncertainty and limitation in validating models is the measurement of the HRR, a key input parameter that affects the thermal environment of the compartment. The uncertainty of the HRR is estimated to be 15 - 20 % and thereby deviations of model predictions with experimental data that are within this range may be generally be considered to fall within experimental uncertainty.

Table 3.2 Measurement Uncertainties

Measurement	Uncertainty[6]	Notes
Heat Release Rate	± 15 %	Originally, a 20 % discrepancy was noted between the heat release rate measured for Test 3 using the fuel mass flow and calorimetry.
Heat Flux to Cables Total heat flux Radiative flux	 ± 3 %[7] ± 6 %	Total heat flux: Uncertainty quoted is due to calibration uncertainty; uncertainty due to soot deposition is difficult to quantify. There is no effect of soot on the radiometers.
Smoke Concentration	± 0.02 g/m3 (17%)	For Test 3 with peak smoke conc. = 0.116 g/m3
Target Temperatures	± 4 C	Effect of cable morphology and TC placement relative to cable structure on measurement was not quantified.
Vent and Doorway Flows Door Vent	 ± 0.6 kg/s ± 0.2 kg/s	 Peak net mass flow for Test 3 was 2.0 kg/s (uncertainty = 30 %) Peak supply vent flow for Test 3 was 1.3 kg/s (uncertainty=15 %)
Gaseous Concentrations O2 CO2 CO	 ± 0.01 vol. frac. ± 0.0025 vol. frac. ±	 Corresponds to 7 % for safety cut-off at 0.15 vol. frac. Corresponds to 6 % uncertainty for 0.04 peak value for Tests 1 CO measurements showed unexpected anomalies.
Gas Temperatures	± 10 C	Except for Tests 15 & 18 in which TCs were close to fire and exposed to higher radiative heat flux.
Heat Loss to Boundaries	± 11 %	Estimated for Test 3 only, measurement may be less robust for other tests. Uncertainty from use of FDS to design sensor layout is unknown.
Compartment Pressure	± 40 Pa	Corresponds to 14 % uncertainty for peak pressure of 293 Pa for Test 2.

A 20 % discrepancy was noted between the heat release rate measured for Test 3 using the fuel mass flow and calorimetry. The nominal HRRs for the tests shown in Table 2.1 were corrected in NIST, 2005 to account for variations in fuel flow caused by temperature increases during the experiments. The development of this correction factor was not robust due to lack of resources and limited to the simulation of the environment for one test in a different size compartment. As a result of the issues associated with this correction factor and uncertainty in the most probable values, the HRRs used as input for the models used in this benchmark exercise range from the nominal values to ± 20 % of nominal values. The experimental uncertainty is noted in the comparison of the different model predictions with experimental data.

3.3 Summary of Tests

[6]The uncertainties in Table 3.2 are expressed as the expanded relative uncertainty with an expansion factor equal to two (i.e., 2.F), which represents a 95 % confidence interval.

The following are objectives and observations of the experiments conducted for the international benchmark exercise.

Test 1

This test was designed to serve as a preliminary test to determine if the compartment features and instrumentation were functioning adequately, and also to include a test with a smaller fire. The nominal peak HRR was 350 kW with a heptane fire located in the center of the compartment. The door was closed during this test and the mechanical ventilation was turned off with the supply and exhaust vents sealed. XPE cable type was installed during this test.

This was the only test conducted with one spray nozzle. All other tests in the series were conducted with two nozzles since it was determined that the use of one nozzle caused oscillations in the burning of the fire between the nozzles. The fire diameter for this test was about 74 cm through observation of the fire pan after the test. The flame height was observed to be about 3/4 of the compartment height. Further observations of the flame height and smoke layer development may be made from the videos in the accompanying DVDs. The smoke layer became progressively more opaque through the transient, and the flame was observed to oscillate more during the end of the transient with the depletion of the oxygen in the compartment. The oxygen near the fire (sensor O2-2) reached 15 % by volume at the end of the transient. The test was run to the planned completion time of 25 min. The average HGL temperature and cable surface temperature (B-TS-14) reached 146 C and 130 C, respectively at the peak of the transient. There was no visible damage to the cables during this test.

Test 2

Test 2 was designed as the base test for providing data to determine the predictively capability of models for scenarios with under ventilated conditions. The nominal peak HRR was 1 MW with a heptane fire located in the center of the compartment. The door was closed during this test and the mechanical ventilation was turned off with the supply and exhaust vents sealed. XPE cable type was installed during this test

The fire diameter for this test was about 1 m through observation of the fire pan after the test. The flame was observed to reach the ceiling of the compartment. The oxygen near the fire (sensor O2-2) reached 14 % by volume at about 630 s when the test was terminated prior to the planned 26 min. run. The fire was observed to initially be engulfing and then becoming under ventilated through the transient becoming smaller and weaker toward the end of the transient. The visible color changed from yellow at the beginning of the transient to bluish-red toward the end possibly due to the under-ventilation of the fire and the flame temperature. Further observations of the effects of oxygen depletion on the fire may be made from the videos in the accompanying DVDs. The average HGL temperature and cable temperature (B-TS-14) reached 235 C and 200 C, respectively during the peak of the transient. There was no visible damage to the cables during this test.

Test 3

Test 3 was designed as the base test for providing data to determine the predictively capability of models for scenarios with well ventilated conditions. The nominal peak HRR was 1 MW with a heptane fire located in the center of the compartment. The door was open during this test and the mechanical ventilation was turned off with the supply and exhaust vents sealed. XPE cable type was installed during this test.

The fire diameter for this test was about 1 m through observation of the fire pan after the test (see Figure 3.1). The flame was observed to reach the ceiling of the compartment. The fire tilted toward the east wall away from the door due to the inflow of air (see Figure 3.2). The oxygen near the fire (sensor O2-2) was maintained at ambient conditions through the transient by the air flow into the compartment through the open door, and the test was run to the planned completion time of 26 min. The smoke layer in the compartment was steady with slight oscillations of wave like motion in the layer. Figures 3.3 shows the formation of the smoke layer, and the smoke exhausting through the door during the test. The steady state smoke layer height during this test can be approximated to be at 1.3 m above the compartment floor from Figure 3.1. Further observations of the smoke layer development and tilting of the fire may be made from the videos in the accompanying DVDs. The average HGL temperature and cable temperature (B-TS-14) reached 227 C and 255 C, respectively during the peak of the transient. There was no visible damage to the cables during this test, however, some discoloration (whitish) of the cables was observed.

Figure 3.1 Fuel Pan after Test 3

Figure 3.2 Fire Plume Tilt in Test 3

Figure 3.3 Hot Gas Layer in Test 3

Test 4

Test 4 was designed as a variation of Test 2 for providing data to determine the predictively capability of models for closed door scenarios with the mechanical ventilation system on. The nominal peak HRR was 1 MW with a heptane fire located in the center of the compartment. The door was closed during this test and the mechanical ventilation was turned on with the supply and exhaust vents open. XPE cable type was installed during this test

The fire diameter for this test was about 1 m through observation of the fire pan after the test. The flame was observed to reach the ceiling of the compartment. The oxygen near the fire (sensor O2-2) reached 14.8 % by volume at about 838 s when the test was terminated prior to the planned 26 min. run, extending the duration of the run and fire by only 200 s as compared to Test 2. The fire was observed to become under ventilated through the transient becoming smaller and weaker toward the end of the transient. Further observations of the effects of oxygen depletion on the fire may be made from the videos in the accompanying DVDs. The average HGL temperature and cable temperature (B-TS-14) reached 219 C and 174 C, respectively during the peak of the transient. There was no visible damage to the cables during this test.

Test 5

Test 5 was designed as a variation of Test 3 for providing data to determine the predictively capability of models for fires in well ventilated conditions with natural and mechanical ventilation. The nominal peak HRR was 1 MW with a heptane fire located in the center of the compartment. The door was open during this test and the mechanical ventilation was turned on with the supply and exhaust vents open. XPE cable type was installed during this test.

The fire diameter for this test was about 1 m through observation of the fire pan after the test. The fire tilted toward the east wall away from the door due to the inflow of air. The flame was observed to reach the ceiling of the compartment. The oxygen near the fire (sensor O2-2) was maintained at ambient conditions through the transient by the air flow into the compartment through the open door and by the mechanical ventilation system, and the test was run to the planned completion time of 26 min. The smoke layer in the compartment was steady with slight oscillations of wave like motion in the layer. The smoke layer development and height for this test were similar to that in Test 3. Further observations of the smoke layer development may be made from the videos in the accompanying DVDs. The average HGL temperature and cable temperature (B-TS-14) reached 200 C and 169 C, respectively during the peak of the transient. There was no visible damage to the cables during this test.

Tests 7 to 10

Tests 7 to 10 were replicate tests of Tests 1, 2, 3, and 4. A discussion of the replicate tests and comparison of the results with the base tests is presented in the next section. A description and pictures of cable damage during these tests is presented below.

Figures 3.4 an 3.5 show softening and damage to PVC cables after Test 7 (Replicate of Test 1) in a mild environment created by a 350 KW fire. Test 7 is the first test conducted in the series after PVC were installed in the compartment. Figures 3.6 and 3.7 show localized damage of XPE cables after Test 9 which was the 7th test conducted in the series with XPE cables. The XPE cables had a slight whitish discoloration after the first few tests, and were only damaged in local hot spots after repeated insults. Figure 3.8 shows the bending and damage to control cables in the vertical tray after Test 10.

Figure 3.4 Softening of PVC Cables in Vertical Tray after Test 7

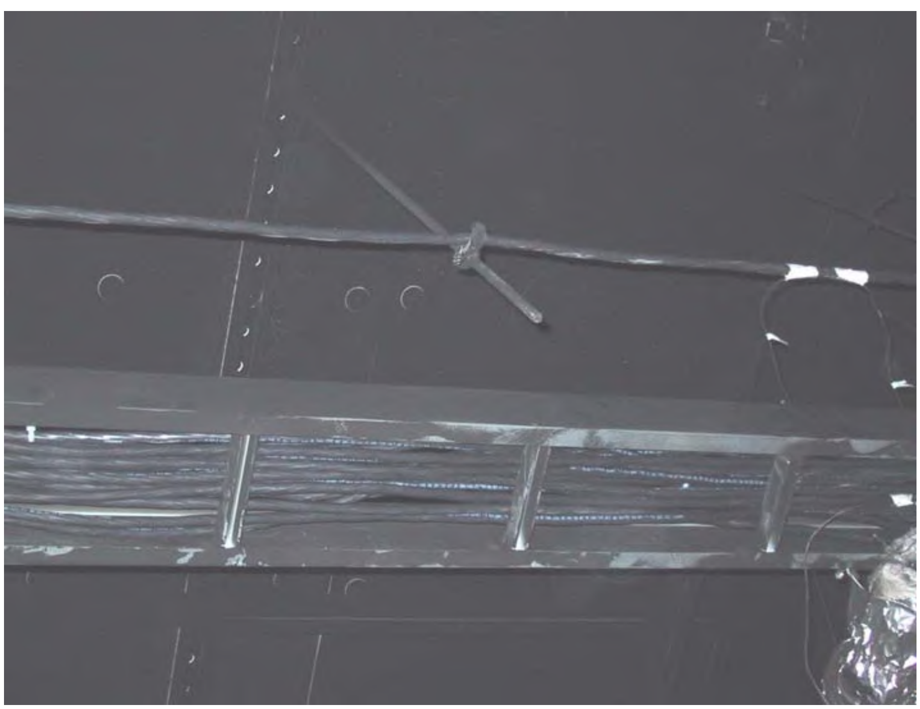

Figure 3.5 Softening of Cables in Horizontal Tray after Test 7

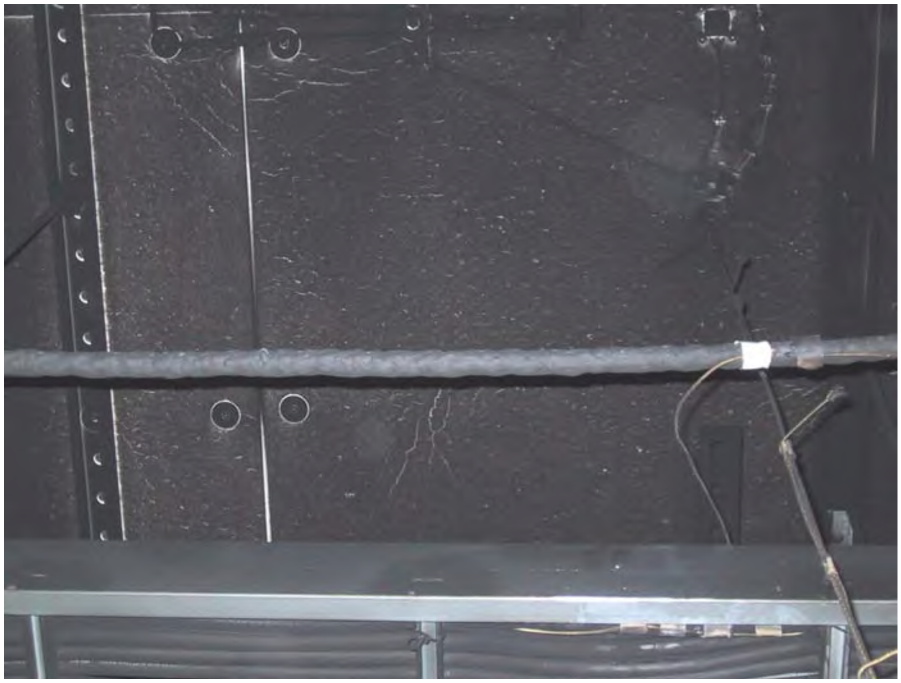

Figure 3.6 Localized Damage to XPE Control Cable after Test 9

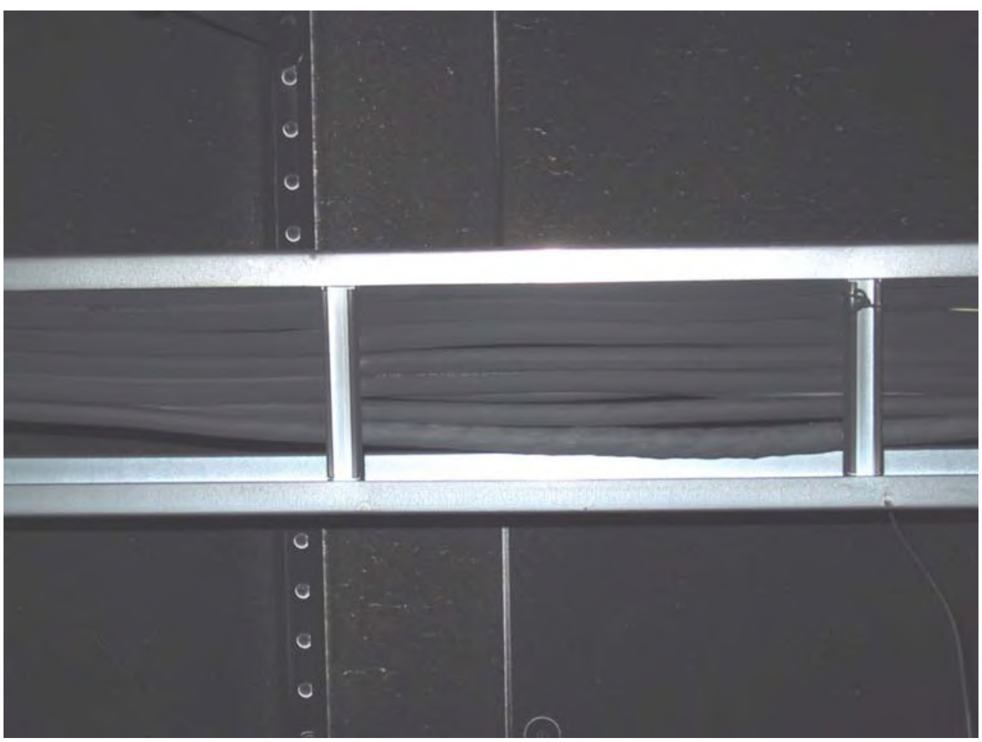

Figure 3.7 Localized Damage to XPE Control Cables in Horizontal Tray after Test 9

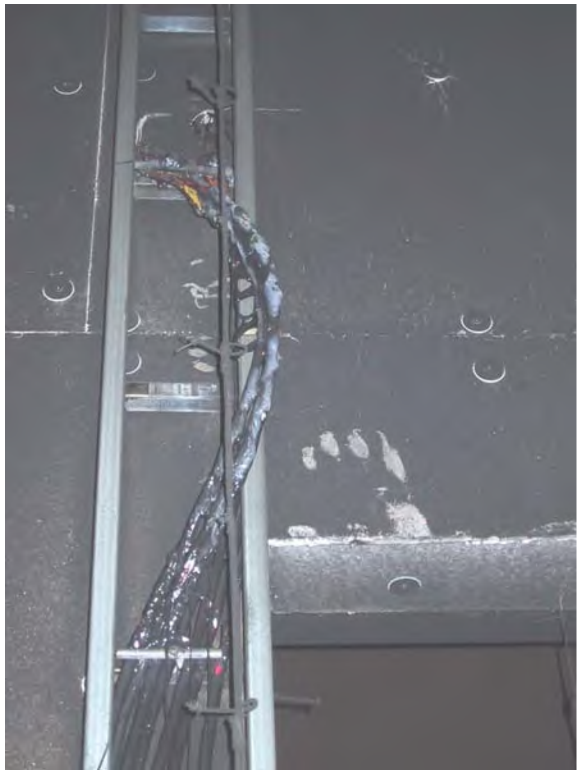

Figure 3.8 Bending and Damage to PVC Cables in Vertical Tray after Test 10

Test 13

Test 13 was designed as a variation of Test 2 to provide data to determine the predictively capability of models for large fires in under ventilated conditions. The nominal peak HRR was 2 MW with a heptane fire located in the center of the compartment. The door was closed during this test and the mechanical ventilation was turned off with the supply and exhaust vents sealed. XPE cable type was installed during this test

The fire diameter for this test was also about 1 m through observation of the fire pan after the test. The flame was observed to engulf the ceiling of the compartment over the fire. The oxygen near the fire (sensor O2-2) reached 13.8 % by volume at about 400 s when the test was terminated prior to the planned 26 min. run. The fire was observed to initially be large and engulfing and then becoming under ventilated through the transient becoming smaller and weaker toward the end of the transient. Figures 3.9 and 3.10 are pictures of the fire toward the end of the transient with the fire in a partial and severely under ventilated environment, respectively. The visible color changed from yellow at the beginning of the transient to bluish-red toward the end possibly due to the under-ventilation of the fire and the flame temperature. Further observations of the effects of oxygen depletion on the fire may be made from the videos in the accompanying DVDs. The average HGL temperature and cable temperature (B-TS-14) reached 295 C and 218 C, respectively during the peak of the transient. There was no visible damage to the cables during this test.

Figure 3.9 Partially Under Ventilated Fire in Test 13 (2 MW)

Figure 3.10 Severely Under Ventilated Fire in Test 13 (2 MW)

Test 14

Test 14 was designed as a variation of Test 3 to provide data to determine the predictively capability of models for scenarios involving cable damage in an extreme thermal environment in well ventilated conditions that would sustain the fire through the transient. The nominal peak HRR was 1 MW with a heptane fire located 1.8 m from the north wall near the vertical cable tray. The door was open during this test and the mechanical ventilation was turned off with the supply and exhaust vents sealed. XPE cable type was installed during this test.

The fire diameter for this test was about 1 m through observation of the fire pan after the test. The fire tilted toward the east wall away from the door due to the inflow of air. However, there was no visible tilt of the fire toward the north wall even though the fire was near the wall. The flame was observed to reach the ceiling of the compartment. Like Test 3, the oxygen near the fire (sensor O2-2) was maintained at ambient conditions through the transient by the air flow into the compartment through the open door, and the test was run to the planned completion time of 26 min. The smoke layer in the compartment was steady with slight oscillations of wave like motion in the layer. Figures 3.11 and 3.12 show the hot gas smoke layer and the fire near the vertical cable tray. Further observations of the smoke layer development and tilting of the fire may be made from the videos in the accompanying DVDs. The average HGL temperature and cable temperature (TC-VS-32) reached 230 C and 378 C, respectively during the peak of the transient. There was extensive damage to the cables in the vertical cable tray (see Figure 3.13). The bottom of the cables in the tray reached higher temperatures than the top, as in Test 3. The damage appeared to be extensive around the center of the vertical run of the cables. Off-gases were observed to be emitted from the cables during the transient. Even though the fire was near the wall, there was no visible tilt of the fire toward the wall.

Test 15

Test 15 was designed as a variation of Test 3 to provide data to determine the predictively capability of models for scenarios with well ventilated conditions would sustain a fire, with the fire directly under cable targets. The nominal peak HRR was 1 MW with a heptane fire located 1.25 m from the south wall directly under cable B. The door was open during this test and the mechanical ventilation was turned off with the supply and exhaust vents sealed. PVC cable type was installed during this test.

The fire diameter for this test was about 1 m through observation of the fire pan after the test. The flame was observed to reach the ceiling of the compartment. The fire tilted toward the east wall away from the door due to the inflow of air. The fire was also observed to be drawn toward the south wall. The oxygen near the fire (sensor O2-2) was maintained at ambient conditions through the transient by the air flow into the compartment through the open door, and the test was run to the planned completion time of 26 min. The smoke layer in the compartment was steady with slight oscillations of wave like motion in the layer. Further observations of the smoke layer development and tilting of the fire may be made from the videos in the accompanying DVDs. The average HGL temperature and cable temperature (B-TS-14) reached 227 C and 262 C, respectively during the peak of the transient. There was extensive damage to the cables, including combustion in localized areas (see Figures 3.15, 3.16, and 3.17). The heating and combustion of the cables may be observed through the infrared camera recordings in the accompanying DVDs.

Figure 3.11 Hot Gas Layer and Fire in Test 14

Figure 3.12 Fire Near Vertical Tray in Test 14

Figure 3.13 Damage to XPE Cables in Vertical Tray after Test 14

Figure 3.14 Fire in Test 15


Figure 3.15 Melted PVC Control and Power Cable after Test 15

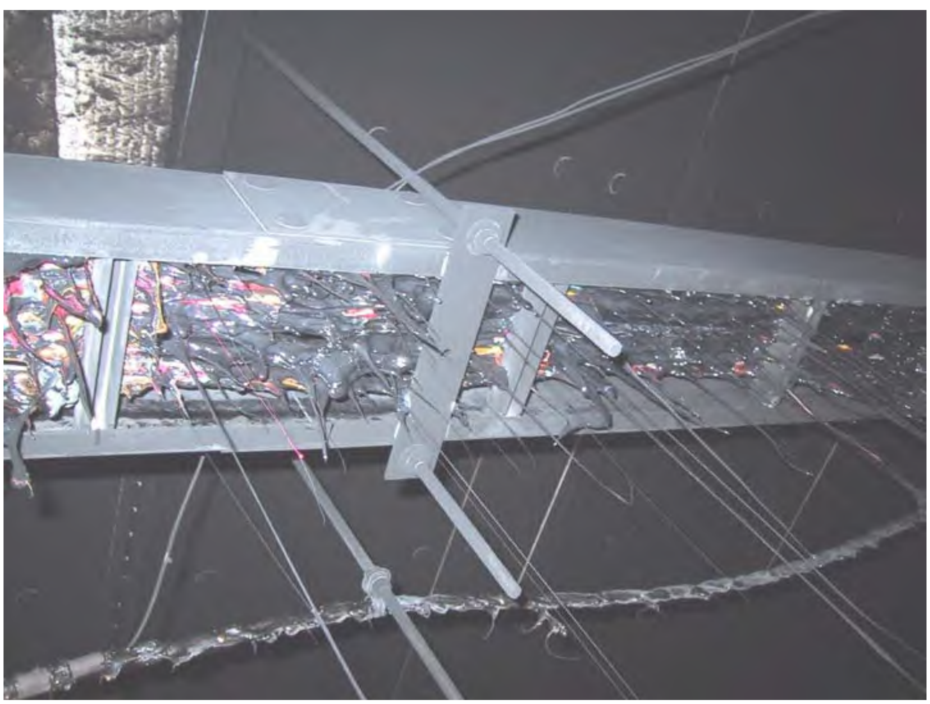
Figure 3.16 Melted PVC Cables In Horizontal Tray after Test 15

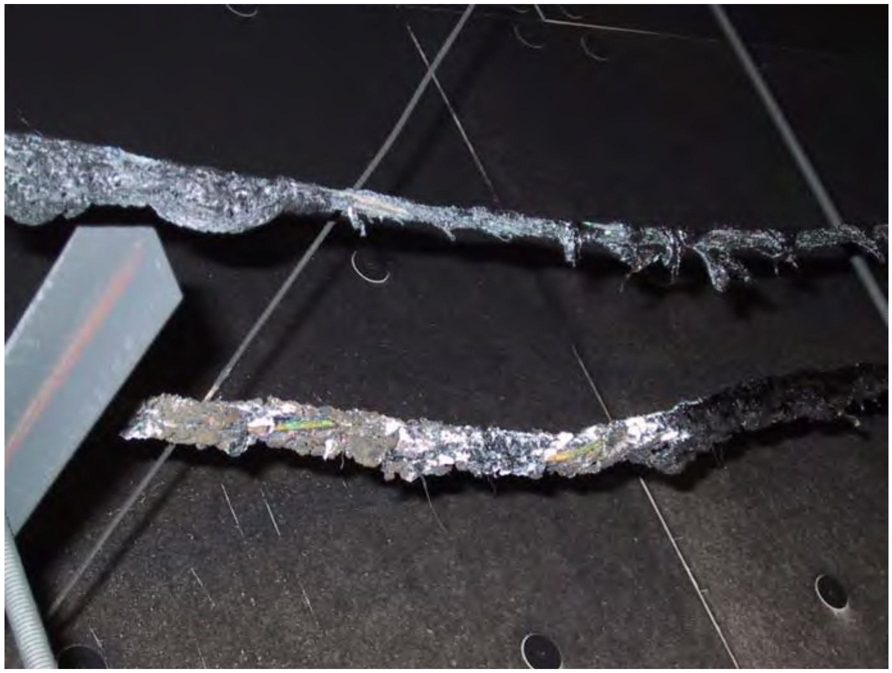
Figure 3.17 Localized Combustion of PVC Cables in Test 15

Test 16

Test 16 was designed as a variation of Test 13 to provide data to determine the predictively capability of models for large fires in under ventilated conditions with the mechanical ventilation system on. The nominal peak HRR was 2 MW with a heptane fire located in the center of the compartment. The door was closed during this test and the mechanical ventilation was turned on with the supply and exhaust vents open. PVC cable type was installed during this test

The fire diameter for this test was also about 1 m through observation of the fire pan after the test. The flame was observed to engulf the ceiling of the compartment over the fire. The oxygen near the fire (sensor O2-2) reached 14 % by volume at about 425 s when the test was terminated prior to the planned 26 min. run, extending the run and fire by only 25 s when compared to Test 13. The fire was observed to initially be large and engulfing at first and then becoming under ventilated through the transient, becoming smaller and weaker toward the end of the transient. The visible color changed from yellow at the beginning of the transient to bluish-red toward the end possibly due to the under-ventilation of the fire and the flame temperature. Further observations of the effects of oxygen depletion on the fire may be made from the videos in the accompanying DVDs. The average HGL temperature reached 263 C during the peak of the transient. There was melting of the PVC cables during this test.

Test 17

Test 17 was designed as a variation of Test 2 to provide data to determine the predictively capability of models for a different fuel, toluene, with under ventilated conditions. The nominal peak HRR was 1 MW with a toluene fire located in the center of the compartment. The door was closed during this test and the mechanical ventilation was turned off with the supply and exhaust vents sealed. PVC cable type was installed during this test

The fire diameter for this test was about 1 m through observation of the fire pan after the test. The flame was observed to reach the ceiling of the compartment. The smoke development for this transient was much faster and dense when compared to Test 2. The fire was completely obstructed by the smoke and not visible at 240 s into the transient. At this point, the fuel was turned off for safety. Further observations of the dense smoke development from the fire may be made from the video in the accompanying DVDs.

Test 18

Test 18 was designed as a variation of Test 15 to provide data to determine the predictively capability of models for scenarios with well ventilated conditions sustaining the fire, with the fire directly under cable targets. The nominal peak HRR was 1 MW with a heptane fire located 1.55 m from the south wall and 1.5 m east of the centerline directly under cable B. This test is similar to Test 15, except the fire was located east of the centerline compared to being located at the center between the east and west walls in Test 15. The door was open during this test and the mechanical ventilation was turned off with the supply and exhaust vents sealed. XPE cable type was installed during this test.

The fire diameter for this test was about 1 m through observation of the fire pan after the test. The flame was observed to reach the ceiling of the compartment. There was no visible tilt of the fire toward the wall even though the fire was near the south wall. The oxygen near the fire (sensor O2-2) was maintained at ambient conditions through the transient by the air flow into the compartment through the open door, and the test was run to the planned completion time of 26 min. The smoke layer in the compartment was steady with slight oscillations of wave like motion in the layer. Further observations of the smoke layer development may be made from the videos in the accompanying DVDs. The average HGL temperature reached 227 C during the peak of the transient. There was extensive damage to the cables, including combustion in localized areas with more damage to the control cables compared with the power cables (see Figures 3.18 and 3.19). The inside insulators of the power cables were intact at the end of the transient, whereas the copper wires were visible in the control cables. A thin whitish layer formed underneath the HGL possibly from off-gases from combustion of the cables, and char from combusted cables was observed to fall to the floor during the transient. The smoke exhausting through the door also appeared to be whitish. The heating and combustion of the cables may be observed through the infrared camera recordings in the accompanying DVDs. The videos did not appear to indicate any flame spread during the transient.


Figure 3.18 Localized Combustion of XPE Control Cable in Test 18


Figure 3.19 Localized Combustion of XPE Control Cable in Test 18

3.4 Reproducibility of Experiments

The reproducibility of experiments is an important consideration when drawing conclusions on the validation and performance of fire models by comparison of model prediction with experimental measurements. The extent to which an accuracy may be attributed to the model predictions is limited by (1) the uncertainty in the fire phenomenon and reproducibility of the fire environment; and (2) the uncertainty in the measurements of the parameters predicted by models. The 2nd issue was discussed and covered earlier. The uncertainty in the fire phenomenon and reproducibility of the fire environment is discussed below.

Figures 3.20 to 3.25 present measurements of main parameters of interest for Test 2 and its replicate test, Test 8. Replicate tests of Test 1, 3, and 4 were also conducted. The results of Test 2 and Test 8 for closed door and under ventilated conditions are presented since these tests would be the most difficult to reproduce and provide a bound on the uncertainty in reproducing the experiments in this test series. Figures 3.20 to 3.25 show that the variation in most of the measurements of the main parameters in the two tests was small, except for pressure. The pressure development during the transient is dependent on the compartment leakage. As noted in Table 2.2, leakage around the door was observed during Test 8, thereby leading to a smaller pressure increase in the compartment. Figure 3.24 shows some oscillations in the O2 concentration toward the end of the transient measured at O2-2 which is in the lower part of the compartment near the fire. These oscillations were observed in other experiments with under ventilated fires and may be caused by the oscillations in the flow and mixing in that region of the compartment. The mixing phenomenon appears to be stochastic and not reproducible since the magnitude and nature of the measured oscillations of O2-2 are not similar for the two tests. Table 3.2 lists the variation in the measurements for the main parameters in the two tests. Further observations of the replicate tests may made by viewing the accompanying DVDs which include composite views of the replicate tests (see Table 3.1).

Table 3.3 Variation in Measurements for Tests 2 and 8

Parameter	Variation
HGL Temperature	2.5 %
Interface Height	2.3 %
Temperatures in TC Tree 7	1.1 % (avg.)
Pressure	35 %
O2 concentration	4 %
CO2 concentration	3.5 %

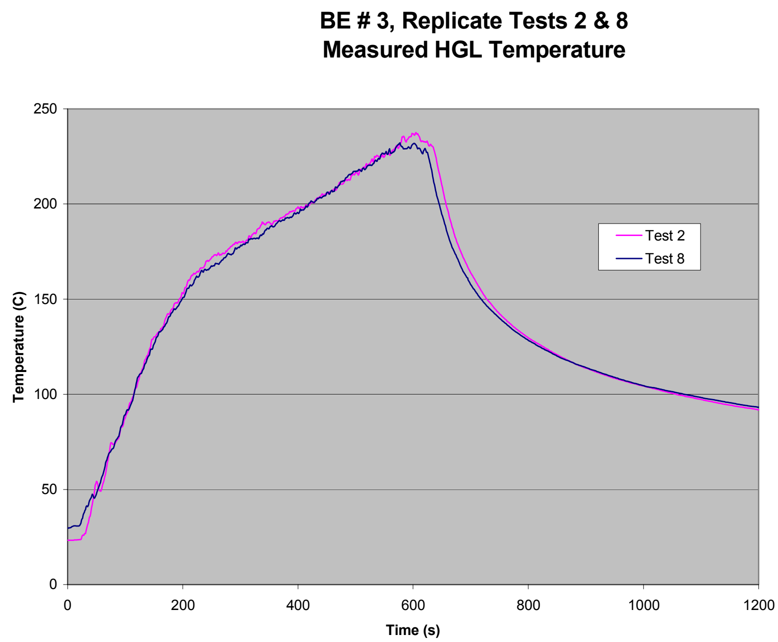

Figure 3.20 HGL Temperature in Replicate Tests 2 and 8

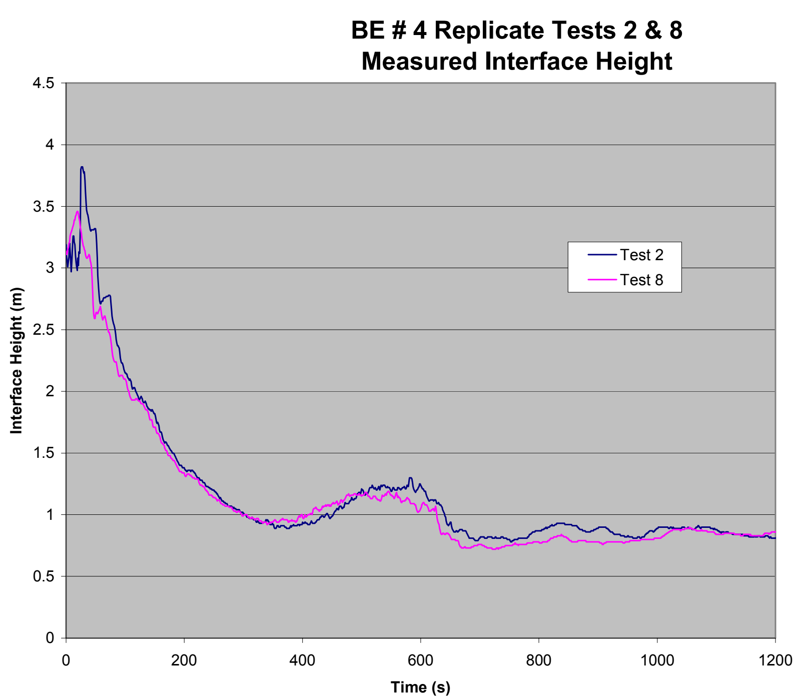

Figure 3.21 Interface Height in Replicate Tests 2 and 8

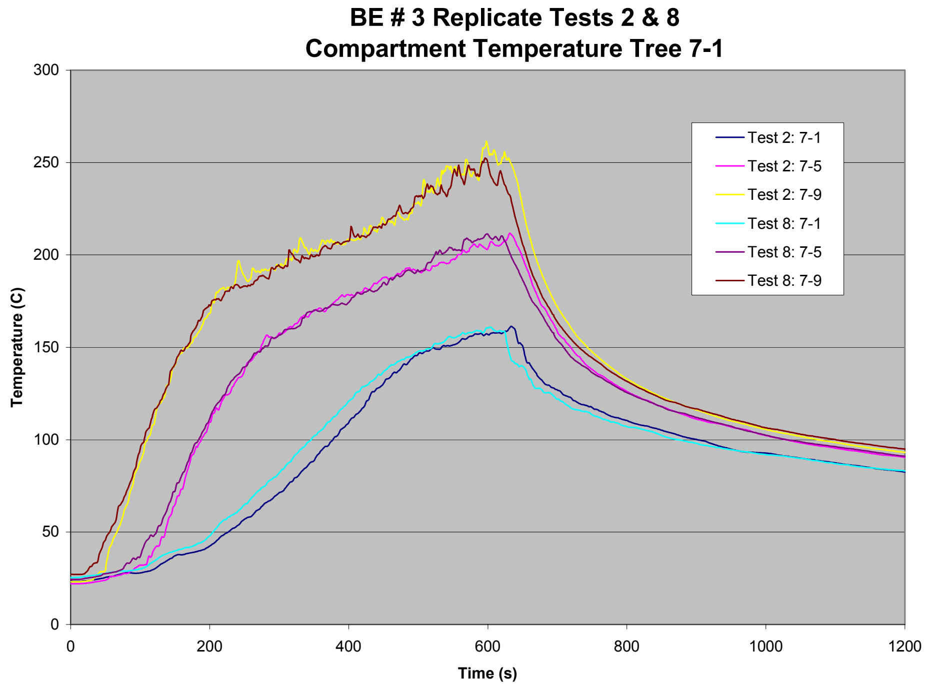

Figure 3.22 TC Tree 7 in Replicate Tests 2 and 8

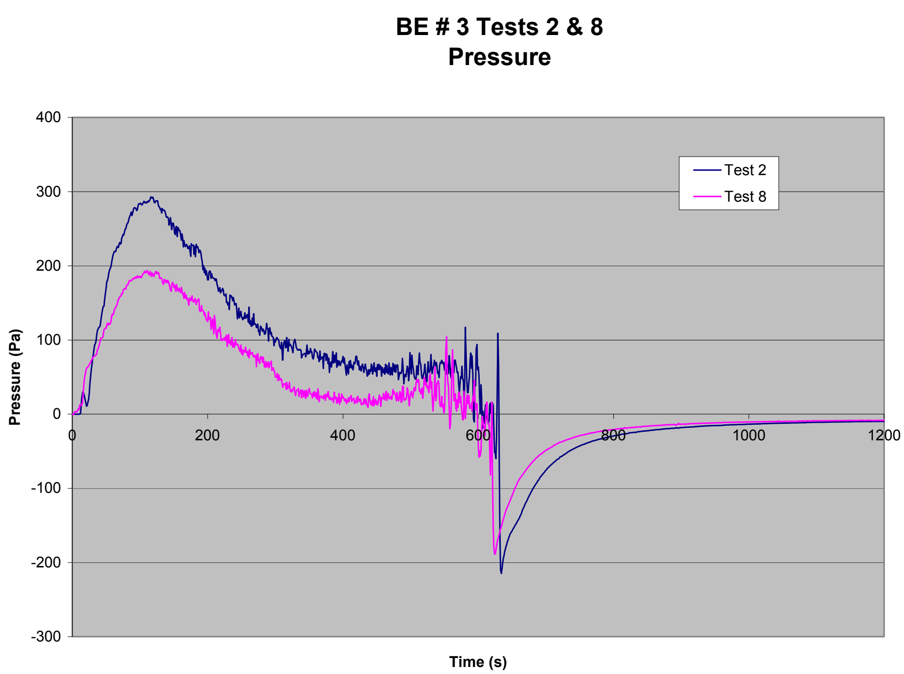

Figure 3.23 Pressure in Replicate Tests 2 and 8

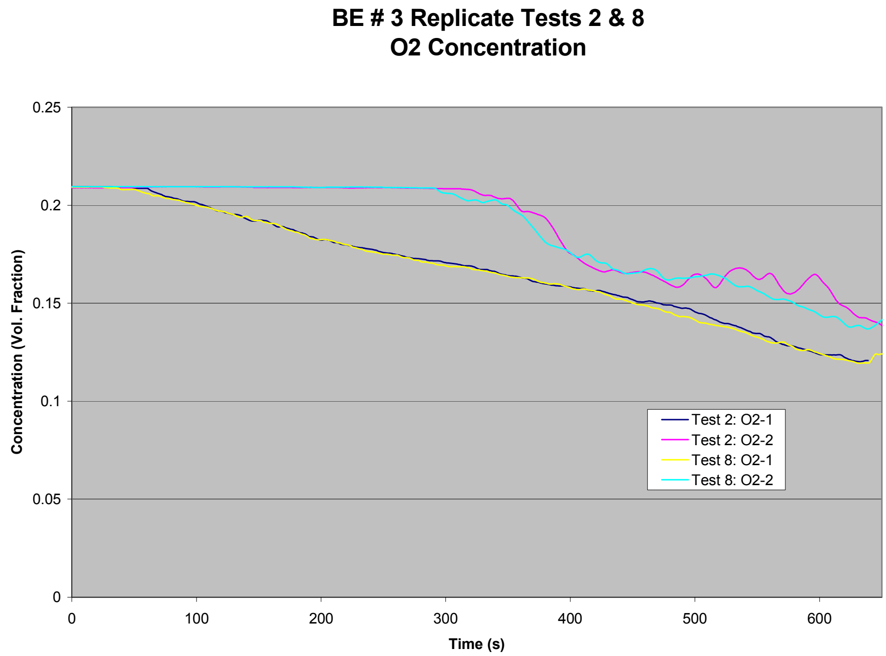

Figure 3.24 Oxygen in Replicate Tests 2 and 8

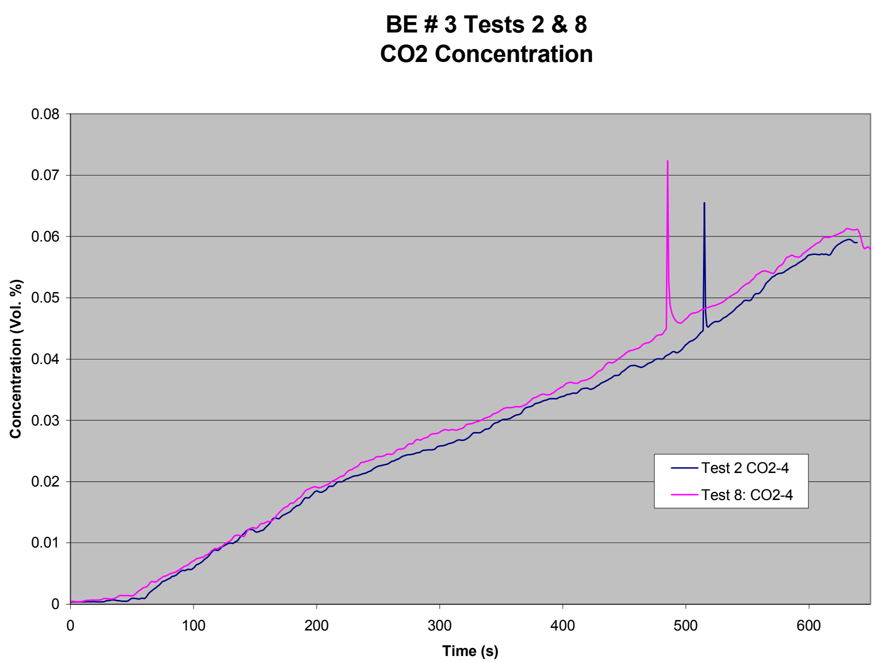

Figure 3.25 CO2 in replicate Tests 2 and 8

3.5 Parameter Uncertainty

Experimental uncertainties due to the imprecision of measurement devices were presented in Section 3.2. The parameter with the largest measurement uncertainty of ± 15 % is the heat release rate (see Table 3.2). It is acknowledged that the uncertainty in the heat release rate, a fundamental input parameter for the fire model simulations, will have an impact on the output parameters of interest such as gas temperature and the heat flux to targets. In order to determine the impact of the uncertainty of the HRR on the output parameters, a set of simulations were conducted with the HRR set at ~ 15 % below the measured HRR for all the tests. Table 3.4 shows the results of the model predictions for Test 3 for select parameters discussed later in Chapter 5. Results of model predictions are shown for the HRR set at the measured steady state HRR of 1190 kW and at 1000 kW (~ 15 % less than measured). The parameter uncertainties for CFAST and FDS for each selected parameter are shown on the two columns at the right side of the Table. The values in the Table show that the parameter uncertainty for the predictions of gas temperature and heat flux by the models is in the order of ~ 10 % and ~ 20 %, respectively. Therefore, it can approximately deduced that the total parameter uncertainty for the predictions of gas temperature and heat flux by the models is in the order of ~ ± 10 % and ~ ± 20 %, respectively. Although the results of all the tests are not reported, it is expected that the parameter uncertainties due to the uncertainty of the HRR measurement for the other tests will be of the same order as Test 3.

Table 3.4 Parameter Uncertainty[8]

Parameter	Sensor	Model prediction at peak (for HHR=1190 kW) CFAST	FDS	Model prediction at peak (for HHR=1000 kW) CFAST	FDS	Parameter Uncertainty CFAST	FDS
Global Parameters							
HGL Temp. (avg.)-C	Tree 7	283.0	247.0	256.0	227.0	-10%	-8%
HGL Interface Ht -	Fire videos	1.1	1.0	1.1	1.0	0.0	0.0
Smoke Conc. - mg/m3 - NA	Smoke Obs./Conc.	120.0	144.0	115.0	137.0	-4%	-5%
O2 Conc.[9] - Vol %	O2-1	10.1	11.4	11.4	12.9	13%	13%
CO2 Conc. - Vol %	CO2	2.6	2.6	2.3	2.5	-12%	-4%
CO Conc. - ppm	CO	NA					
Pressure[2] - Pa	Comp P	835.0	298.0	629.0	240.0	-25%	-19%
Flame Height - m	From fire videos	NA					
Local Gas Temperature							
Hot Gas Temp. (point values) - C	Tree 4.8		241.0		229.0		-5%
	Tree 2-1		91.0		87.0		-4%
	Tree 2-5		227.0		207.0		-9%

[8]Based on analysis of results for Test 3 for most parameters, unless noted otherwise.

[9]Based on results of Test 2

	Tree 2-7		246.0		226.0		-8%
	Tree 3-9		263.0		237.0		-10%
	Tree 5-6		229.0		209.0		-9%
	Tree 7-1		114.0		105.0		-8%
	Tree 7-5		231.0		210.0		-9%
Plume Temp.- C	NA						
Ceiling Jet Temp.-C	Tree 7-10		281.0		258.0		-8%
Heat Flux to Cables							
Radiative Heat Flux to Cables - kW/m2	Cable Rad Flux Gauge 1	5.1	3.4	4.1	2.6	-20%	-24%
	Cable Rad Flux Gauge 3	5.5	4.2	4.5	3.2	-18%	-24%
	Cable Rad Flux Gauge 5	5.6	4.8	4.6	3.7	-18%	-23%
	Cable Rad Flux Gauge 10	6.0	3.8	5.0	3.0	-17%	-21%
Total Heat Flux to Cables - kW/m2	Cable Total Flux Gauge 2	5.4	3.8	4.7	3.0	-13%	-21%
	Cable Total Flux Gauge 4	5.6	4.4	5.1	4.0	-9%	-9%
	Cable Total Flux Gauge 6	5.6	4.8	5.0	4.2	-11%	-12%
	Cable Total Flux Gauge 9	6.0	3.7	5.3	3.6	-12%	-3%

Cable Temperature							
Cable Surface Temp. - C	B-TS-14 (control cable)	257.0	201.0	224.0	174.0	-13%	-13%
	TS-33 (vertical cable)	254.0	153.0	225.0	136.0	-11%	-11%
	E-TS-16 (slab)	NA					
	D-TS-12 (cable in bundle/tray) -	230.0	188.0	230.0	188.0	0%	0%
	F-TS-20 (power cable)	215.0	164.0	188.0	141.0	-13%	-14%
Heat Flux to Walls							
Total Heat Flux to Walls - kW/m2	East U-4	5.4	1.3	4.4	1.2	-19%	-8%
	West U-4	5.4	1.3	4.4	1.2	-19%	-8%
	Ceiling C-5	5.5	3.2	4.5	2.5	-18%	-22%
	Floor U-8	4.1	1.0	3.3	0.9	-20%	-10%
Wall Temperature							
Wall Surface Temp. - C	TC East U-4-2	255.0	193.0	225.0	175.0	-12%	-9%
	TC West U-4-2	255.0	186.0	225.0	171.0	-12%	-8%
	TC Ceiling C-5-2	255.0	270.0	228.0	245.0	-11%	-9%
	TC Floor U-8-2	206.0	148.0	178.0	133.0	-14%	-10%

4 Input Parameters and Assumptions

A comprehensive specification of Benchmark Exercise # 3 was developed such that there would be a minimal amount of unspecified parameters and assumptions for the analysts conducting specified[10] predictions for the exercise. Specific efforts were also made to measure the properties of the materials used in the experiments, including for cables and walls. However, there were still some parameters for which values had to be assumed to conduct the specified calculations. These are listed and discussed below:

1. Compartment Leakage: It is not possible to specify the leakage in the compartment until the leakage tests are completed just before the experiments are conducted. Even then, some additional leakage area may be created during the tests. Therefore, precise specification of this parameter is difficult and results in uncertainty for the prediction of compartment over pressure.

2. Heat Release Rate (HRR): The nominal HRR of the tests were specified for the benchmark exercise. However, the heat release rates measured during the tests varied from the nominal values due to the lack of measurements of fuel flow during the experiments. A large uncertainty for this parameter was reported (see Table 3.2 in the main text). This parameter is likely to be the largest source of uncertainty in the predicted results.

3. Ventilation Flow Pattern: The mechanical ventilation rate for the compartment was specified. The flow from the vents into the compartment was assumed to be horizontal, i.e. parallel to the floor, for the FDS calculations. The actual flow from the vents in the experiments was determined to be upward toward the ceiling due to the design of the mechanical ventilation system. The flow pattern from mechanical ventilation systems will affect the temperatures in local areas predicted by CFD codes, and will be a source of uncertainty for such calculations.

4. Lower Oxygen Limit (LOL): The lower oxygen limit needs to be input for the CFAST code for the simplistic sub-model in it for predicting the extinction of the fire. There was no value for LOL included in the specifications, allowing judgment from users to define the most appropriate value for the experiments in this series. A value of 12 % was used in the CFAST calculations. The specification of this parameter has a large effect on the prediction of extinction and could be a large source of user effects. The FDS code uses a similar scheme to extinguish the fire when oxygen level and temperature decreases below a preset value, however, the user does not need to specify the value.

5. Target Specification: A detailed heat transfer model for a cable or cable tray will be fairly complex. Cable trays generally have a number of cables bundled together in layers, and most cables consist of several conductors. Cables configured in a single layer will get damaged and ignite at a lower flux than cables in a multilayer configuration because the flux to a single layer will not be shielded by cables above that layer. The damage or ignition temperature for cables in a multilayer configuration will depend on the volume-to-surface area ratio. The CFAST and FDS fire models are not capable of modeling such complex cable configurations. The target in these models is simply represented as rectangular slabs for use in a 1-D heat conduction calculation. The slabs were assumed to be of the same thickness as the cables.

---

[10]Per ASTM 1355-05 [ASTM, 2005].

6. <u>Grid Size</u>: A grid size of 15 cm was used for the FDS calculations. It is recognized that CFD calculations are generally sensitive to the grid used. A grid size of 15 cm may be optimal for the type of scenarios simulated, however, this was not confirmed through a grid sensitivity analysis.

7. <u>Multi-Layer Boundaries</u>: Walls and ceilings were covered with two layers of 25 mm marinite boards, while the floor was covered with two layers of 25 mm gypsum boards. The two layers of insulation covering the walls and floor were neglected in the CFAST and FDS calculations since the layers could not be directly modeled in CFAST or FDS. The two layers were combined to form one 50 mm board for the input to the model. This assumption may affect the insulating effects of the air gap in between the boards.

8. <u>Heat Flux Comparisons</u>: The comparison of heat flux prediction with measured data poses several challenges. It is important that equivalent measures of heat flux are used in the comparison. The total flux gauges in the experiments in Benchmark Exercise # 3 were cooled and maintained at a constant temperature (75 C). The CFAST and FDS codes normally output the net heat flux on targets based on the target temperature. It is important that these fluxes be modified to the incident radiative heat flux and the convective heat flux to a block at constant temperature for comparison with measured heat fluxes. Even with the modifications to account for the differences between measured and predicted values, an exact comparison is not possible due to the lack of ability to precisely measure the calculated values from models. Therefore, the comparison of heat fluxes will have some additional uncertainty due to this limitation.

5 Evaluation of Specified Model Predictions

The following provides a comparison of ***specified***[11] predictions by CFAST and FDS for the tests conducted for ICFMP Benchmark Exercise # 3. The results of CFAST, a zone model, and FDS, a CFD code, are presented together to allow a comparison and discussion of the capabilities and limitations of the two types of models. The predictions using CFAST and FDS were made before the experiments were conducted. The results of the calculations were sent to an impartial referee, Professor Jonathan Barnett, Worcester Polytechnic Institute, for the benchmark exercise who certified the authenticity of the specified calculations. Subsequently, the data files used for the specified predictions were used to recalculate the results utilizing heat release rates measured during the experiments. No other changes to the data files were made other than the revised HRRs input to the codes.

The following is a list of the major sub-models implemented in the two fire computer codes for modeling the physical phenomena in the scenarios:

combustion chemistry (tracking concentrations of oxygen and combustion products)
plume and ceiling jet flow
mass and energy balance
ventilation through doors and cracks
forced ventilation
heat transfer to boundaries
heat transfer to targets
thermal response of the target

The FDS code computes the flows from first principles based on mostly fundamental fluid dynamic equations, whereas CFAST utilizes correlations developed from experimental data. The performance of the above sub-models is discussed below based on comparison of predicted results with experimental measurements. The theoretical formulation of the two models may be found in Jones, 2004 for CFAST, and McGrattan, 2004 for FDS. The theoretical formulation of these codes are presented in these reports according to the format and content required by ASTM - 1355, “Evaluating the Predictive Capability of Deterministic Fire Models,” [ASTM, 2004]. These reports were sponsored by the U.S. Nuclear Regulatory Commission for referencing in its validation studies as that reported herein.

The following presents the comparison of predictions by the CFAST and FDS code with experimental data for tests in the series. The discussion is grouped in categories presented below to evaluate the predictive capability of the models according to the general features and sub-models of the codes:

- Global parameters
- Local gas temperature
- Heat flux to targets
- Target temperature
- Wall temperature

[11] Per ASTM 1355-05.

The figures show the comparison of the trends of the predictions of CFAST and FDS with experimental data, and the Tables shows the peak values predicted by the models and that measured, and the uncertainty of the predictions. The uncertainty value tabulated is:

(model prediction at peak- measured value at peak)/(measured value at peak - initial measured value)

A + sign in the uncertainty value means that the model prediction was greater than the measured value, and a - sign means that the model prediction was less than measured value.

The following analysis presents a significant number of comparisons of code predictions with experimental data. Figures are presented to show the trends of the predicted and measured parameters, and Tables are used to list peaks of the predicted and measured parameters, and the uncertainty in the predictions as discussed above. The reader should refer to the Tables consistently as they are not cited in the discussion presented in each section.

5.1 Test 1

This test was designed to include a test with a smaller fire. The peak HRR was 410 kW with a heptane fire located in the center of the compartment. The door was closed during this test and the mechanical ventilation was turned off with the supply and exhaust vents sealed. XPE cable type was installed during this test.

This was the only test conducted with one spray nozzle. All other tests in the series were conducted with two nozzles since it was determined that the use of one nozzle caused oscillations in the burning between the nozzles for 1-MW fires. The fire diameter for this test was about 74 cm through observation of the fire pan after the test. The flame height was observed to be about 3/4 of the compartment height. The smoke layer became progressively more opaque through the transient, and the flame was observed to oscillate more during the end of the transient with the depletion of oxygen in the compartment. The oxygen near the fire (sensor O2-2) reached 16 % by volume at the end of the transient. The test was run to the planned completion time of 25 min.

5.1.1 Global Compartment Parameters

Figure 5.1.1 shows the HRR input and used by the CFAST and FDS codes. The HRR was not measured through calorimetry in this test because the compartment was sealed and had no openings. The HRR input to the CFAST and FDS codes were set at the nominal peak value of 410 kW for 20 minutes after a 3-minute linear increase to the peak value. Although oxygen depletion was expected in this test, the internal algorithms in CFAST and FDS did not decrease the specified HRR. As indicated above, the oxygen near the fire (sensor O2-2) reached 16 % by volume at the end of the transient, and therefore the test was run to the planned completion time of 25 min.

Figure 5.1.2 compares the predicted hot gas layer development predicted by CFAST and FDS with that measured in the experiment. CFAST, a two zone model, calculates the interface height directly. However, the interface height is calculated from temperatures at a specific thermocouple tree for the experimental value and FDS calculation. CFAST predicts the interface height to reach the floor at ~ 500 s. FDS and experimental observation indicate that the interface layer height levels at 0.5 m and 1.2 m, respectively. The interface layer height is deduced through an algorithm using temperature data in thermocouple Tree 7. The algorithm used will result in erroneous predictions when a clear interface cannot be deduced from the temperature profile. Therefore, the measured (through Tree 7) and FDS prediction of interface height is erroneous. Video data indicates the HGL reaches the floor at 510 s. Based on this, the uncertainty on the CFAST prediction for the HGL to reach the floor is - 2 %.

Figure 5.1.3 shows the hot gas layer (HGL) temperature. The HGL temperature increases rapidly when the fire is increased and the heat lost to the boundaries is less rapid than the increase in the HRR of the fire. The measured HGL temperature starts to transition to a new rate of increase in temperature at ~ 180 s when the fire reaches a steady value of 410 kW. The measured HGL increases until ~ 1380 s when the fuel is ramped down. CFAST over predicts the peak HGL temperature by + 30 %, whereas FDS over predicts the temperature by + 12 %.

Figure 5.1.4 shows a comparison of the O2 concentration predicted by CFAST and FDS with experimental measurement. Comparisons for FDS are shown for locations at O2-1 and O2-2. The trend predicted by CFAST and FDS are similar to measurements at O2-1. Measurements at O2-2 show oscillations in the O2 concentration which is not predicted by FDS. These oscillations are possibly due to the lack of complete mixing of the hot gas that results in pockets of the gas containing higher levels of O2. The uncertainties of the CFAST and FDS predictions at O2-1 are - 55 % and - 55 %, respectively.

Figure 5.1.5 compares the concentration of CO2 predicted by CFAST and FDS in the HGL with experimental observation. CFAST and FDS predictions, and experimental observation show that the CO2 from the combustion process builds up in the compartment since there are no vents releasing gases. The uncertainties in the predictions of CFAST and FDS are + 23 % and +18 %, respectively.

Figure 5.1.6 compares the concentration of smoke predicted by CFAST and FDS in the HGL with experimental observation. A large discrepancy is noted between the predictions and experimental observations. This discrepancy may be due to a measurement error or that the smoke yield used for the code predictions are not applicable to small fires. The ratio of the soot concentrations predicted by the codes for this test and in Test 2 (discussed below), about 0.34, is the same as the ratio of the fire sizes (410 kW/1190 kW). However, the ratio of the measured soot concentrations is only about 0.14. The smoke yield factor used was determined from measurements for larger fires which may not be applicable to the small fire in this test.

Figure 5.1.7 compares the compartment pressure predicted by CFAST and FDS with experimental observation. The predicted and measured trends are similar. Both positive and negative peaks in the predictions and measurements are noted. The positive peak occurs at ~ 180 s when the fire reaches the peak HRR and the negative peak occurs at ~ 1500 s when the fire is terminated. The measured leakage in the compartment during the test was used in these computations as compared to the design leakage which was used in calculations conducted before the test. The uncertainties in the predictions of CFAST and FDS are + 92 % and - 29 %, respectively.

5.1.2 Local Gas Temperature

Figure 5.1.8 compares the gas temperatures in thermocouple Tree 2 predicted by FDS with measurement. The predicted and measured trends are similar. FDS predicts oscillations in the temperature, especially at 2-7 near the ceiling, possibly from the ceiling jet flow. The uncertainties of the predictions at 2-1, 2-5, and 2-7 are + 43 %, + 20 %, and + 15 %.

Figure 5.1.9 compares the gas temperatures in thermocouple Tree 4 predicted by FDS with measurement. The predicted and measured trends are similar. The uncertainty of the predictions at 4-8 is + 21 %.

Figure 5.1.10 compares the gas temperatures in thermocouple Tree 7 predicted by FDS with measurement. The predicted and measured trends are similar. The uncertainties of the predictions at 7-1, 7-5, and 7-10 are + 56 %, + 28 %, and + 1 %.

The temperature profiles of the hot gases at the above locations are similar to that of the average hot gas layer temperature discussed above. Note, the average HGL temperature is deduced from Tree 7.

5.1.3 Heat Flux to Cable Targets

The following figures show comparisons of the incident radiative flux and the total heat flux predicted by CFAST and FDS with experimental data. As indicated earlier, the total heat flux is measured by a gauge maintained at a constant temperature of ~ 75 C. The outputs from CFAST and FDS were modified to the extent possible to compare similar output quantities.

Figure 5.1.11 compares the radiative and total heat flux predicted by CFAST and FDS at Rad Gauge 1 and Total Gauge 2 with measurement. The trends of the predicted values are similar to experimental observation. The uncertainties in the predictions for CFAST at Rad Gauge 1 and Total Gauge 2 are + 133 % and + 50 %, respectively and; for FDS are + 22 % and - 6 %, respectively. Experimental observation indicates a larger convective heat flux (total heat flux - radiative heat flux) than predicted by both CFAST and FDS. The large discrepancy for CFAST prediction at Rad Gauge 1 is probably due to the use of the point source model in the code, and the height and orientation of the gauge.

Figure 5.1.12 compares the radiative and total heat flux predicted by CFAST and FDS at Rad Gauge 3 and Total Gauge 4 with measurement. The trends of the predicted values are similar to experimental observation. The uncertainties in the predictions for CFAST at Rad Gauge 3 and Total Gauge 4 are + 100 % and + 33 %, respectively and; for FDS are + 27 % and - 6 %, respectively. Experimental observation indicates a larger convective heat flux (total heat flux - radiative heat flux) than predicted by both CFAST and FDS. The large discrepancy for CFAST prediction at Rad Gauge 3 is probably due to the use of the point source model in the code, and the height and orientation of the gauge.

Figure 5.1.13 compares the radiative and total heat flux predicted by CFAST and FDS at Rad Gauge 5 and Total Gauge 6 with measurement. The trends of the predicted values are similar to experimental observation. The uncertainties in the predictions for CFAST at Rad Gauge 5 and Total Gauge 6 are + 5 % and - 14 %, respectively and; for FDS are - 23 % and - 32 %, respectively. Experimental observation indicates a larger convective heat flux (total heat flux - radiative heat flux) than predicted by both CFAST and FDS.

Figure 5.1.14 compares the radiative and total heat flux predicted by CFAST and FDS at Rad Gauge 10. The uncertainties in the predictions for CFAST and FDS at Rad Gauge 10 are + 53 % and - 7 %, respectively. The measured radiative flux reaches a steady level at ~ 700 s possible due to the shielding of the radiative heat flux from the fire to the gauge by the developing hot gas layer.

Interpretation of experimental results, and comparison of predictions with measurement, of radiative and total heat flux is complicated by the various components of radiative heat flux from the fire, hot gas, and hot wall surfaces. Generally, experimental observations indicate higher convective heat fluxes than predicted by the codes.

5.1.4 Cable Temperature

Figure 5.1.15 shows a comparison of the control cable surface temperature at B-TS-14 predicted by CFAST and FDS with measurement. The uncertainties in the peak temperatures for CFAST and FDS are + 11 % and - 25 %, respectively.

Figure 5.1.16 shows a comparison of the surface temperature of the power cable at F-TS-20 predicted by CFAST and FDS with measurement. The uncertainties in the peak temperatures for CFAST and FDS are + 11 % and - 24 %, respectively.

Figure 5.1.17 shows a comparison of the surface temperature of Slab E predicted by CFAST and FDS with measurement. The trends of the predictions are similar to experimental observation. The uncertainties in the peak temperatures for CFAST and FDS are + 4 % and - 30 %, respectively.

Figure 5.1.18 shows a comparison of the surface temperature of the vertical cable at TS-33 predicted by CFAST and FDS with measurement. The uncertainties in the peak temperatures for CFAST and FDS are + 72 % and 0 %, respectively.

5.1.5 Heat Flux to Walls

Figure 5.1.19 shows a comparison of the net heat flux to walls predicted by CFAST with experimental observations. The net heat fluxes to the east and west walls predicted by CFAST are identical and overlap. Although the trend of the net heat flux to the ceiling is similar to experimental observation, the trend of the heat flux to the east and west walls, and the floor following the peak is the reverse of experimental observation. The uncertainties in the heat flux predicted by CFAST for East U-4, West U-4, Ceiling C-5, and Floor U-8 are + 67 %,+ 67 %, + 50 %, and + 167 %, respectively.

Figure 5.1.20 shows a comparison of the net total heat flux to walls predicted by FDS with experimental observations. The net heat flux to the ceiling peaks at ~ 300 s after the fire peaks and then decreases due to the heat up of the ceiling and radiative heat flux emitted from it. The trend of the heat flux to the ceiling predicted by FDS is similar to experimental observation. The heat flux to the floor increases sharply initially due to the ramp up of the fire and then increases with a smaller slope through the transient. The increase is due to the increase of temperature of the hot gas above it through the transient. This trend is also predicted by FDS. The measured net heat flux to the east and west walls initially increases rapidly with the fire and then transitions to a rate with a smaller slope. This trend is also predicted by FDS, but with a smaller rate of increase. The uncertainties in the heat flux predicted by FDS for East U-4, West U-4, Ceiling C-5, and Floor U-8 are - 22 %, - 22 %, + 10 %, and - 0 %, respectively.

5.1.6 Wall Temperature

Figure 5.1.21 shows a comparison of the wall temperatures predicted by CFAST with experimental measurements. The predictions by CFAST are much higher than observed and almost overlap. These predictions are probably due to errors in code implementation as opposed to weaknesses in the sub-models that predict these parameters.

Figure 5.1.22 shows a comparison of the wall temperatures predicted by FDS with experimental measurements. The trends predicted by FDS are similar to experimental observation. The uncertainties of the predictions by FDS for TC East U-4-2, TC West U-4-2, TC Ceiling C-5-2, and TC Floor U-8-2 are + 47 %, + 56 %, - 19 % and + 107 %, respectively.

5.1.7 Conclusion

In this test, CFAST and FDS predictions were similar to experimental observations for most parameters. Global parameters such as the HGL temperature, interface height, and CO2 were within 30 % of experimental values for both CFAST and FDS. A large deviation was observed for O2 predictions by both codes, and the prediction of compartment pressure by CFAST. The local gas temperatures in the compartment predicted by FDS were within 28 % of experimental observations for most locations except at Tree 2-1 and Tree 7-1 where the deviations were as high as 56 %.

The heat flux to the cables predicted by CFAST and FDS deviated by as much as 133 % and 32 % from experimental observation, respectively. The large discrepancy for CFAST is probably due to the use of the point source model in the code. The corresponding cable surface temperatures predicted by CFAST and FDS deviated by as much as 72 % and 30 % from experimental observation, respectively. The heat flux to the walls predicted by CFAST and FDS deviated by 167 % and 22 % from experimental observation, respectively and; the corresponding wall surface temperatures predicted by CFAST and FDS deviated by as much as 290 % and 107 % from experimental observation, respectively.

The analysis shows that the CFAST predictions were generally more accurate for global parameters (except for O2) than for heat fluxes and target responses. The uncertainties in the FDS predictions were similar for global parameters, local gas temperatures, and target heat fluxes and temperatures.

5.2 Test 2

Test 2 was designed as the base test for providing data to determine the predictively capability of models for scenarios with under ventilated conditions. The peak HRR was 1190 kW with a heptane fire located in the center of the compartment. The door was closed during this test and the mechanical ventilation was turned off with the supply and exhaust vents sealed. XPE cable type was installed during this test

The fire diameter for this test was about 1 m through observation of the fire pan after the test. The flame was observed to reach the ceiling of the compartment. The oxygen near the fire (sensor O2-2) reached 14 % by volume at about 630 s when the test was terminated prior to the planned 26-minute transient. The fire was observed to initially be engulfing and then becoming under ventilated through the transient, becoming smaller and weaker, and leading to extinction toward the end of the transient. The visible color changed from yellow at the beginning of the transient to bluish-red toward the end possibly due to the under-ventilation of the fire and the decreased flame temperature. There was no visible damage to the cables during this test.

5.2.1 Global Compartment Parameters

Figure 5.2.1 shows the HRR input and calculated by the CFAST and FDS codes. The HRR was not measured through calorimetry in this test because the compartment was sealed and had no openings. The HRR input to the CFAST and FDS codes were set at 1190 kW for 20 minutes after a 3-minute increase to the peak value. The lower oxygen limit (LOL) needs to be input for the CFAST code for the simplistic sub-model in it for predicting the extinction of the fire. A value of 12 % was used in the CFAST calculations. The FDS code uses a similar scheme to extinguish the fire when oxygen level and temperature decreases below a preset value, however, the user does not need to specify the value. FDS and CFAST start to decrease the HRR at ~ 550 s to account for under-ventilated conditions. The oscillation in the CFAST trend is due to limitations of the algorithm used to decrease the HRR. The FDS computations of the HRR also results in oscillations in this parameter.

Figure 5.2.2 compares the compartment pressure predicted by CFAST and FDS with experimental observation. The CFAST and FDS calculations were conducted with the leakage measured just before the test. CFAST and FDS predict pressure peaks at ~ 180 s when the HRR reaches its peal value. The measured peak occurs earlier at ~ 115 s possibly due to the leakage area becoming larger as the pressure builds up in the compartment. A negative peak is predicted by both codes and measured at the end of the transient when the fuel is shut off. The uncertainties in the CFAST and FDS predictions are 190 % and + 3 %, respectively.

Figure 5.2.3 compares the predicted hot gas layer development predicted by CFAST and FDS with measurements in the experiment. CFAST, a two-zone model, calculates the interface height directly. However, the interface height is calculated from temperatures at a specific thermocouple tree for the experimental data and FDS calculation. CFAST predicts the interface height to reach the floor at ~ 230 s. FDS and experimental observation indicate that the interface layer height levels at 0.5 m and 1.0 m, respectively. Since the interface layer height is deduced through an algorithm using temperature data in thermocouple Tree 7, the algorithm used will result in erroneous predictions when a clear interface cannot be deduced from the temperature profile. Therefore, the measured and FDS prediction of interface height is erroneous. Video data indicates that the HGL reaches the floor at the fire at ~ 360 s. The HGL reaches the floor in most areas of the compartment before this time, leaving an area of air around the fire. The uncertainty in the CFAST prediction for the time the HGL reaches the floor at the fire is - 36 %.

Figure 5.2.4 shows the hot gas layer (HGL) temperature. The HGL temperature increases rapidly when the fire is increased and the heat lost to the boundaries is less rapid than the increase in the HRR of the fire. The measured HGL temperature transitions to a new rate of increase at ~ 180 s when the fire reaches a steady value of 1190 kW. The measured HGL increases until ~ 610 s when the fuel is shut off. CFAST and FDS predict the temperature to increase until ~ 600 s when the internal algorithms in the codes decrease the HRR. As mentioned above, the fuel was shut off at 630 s when the O2 concentration near the fire reached 14 % and the fire was observed to be nearly extinguished. Therefore, the internal algorithms in CFAST and FDS seem to perform reasonable well in simulating under-ventilated conditions and fire extinction for this test. CFAST and FDS over predict the peak HGL temperature by + 18 %, and + 4 %, respectively.

Figure 5.2.5 shows a comparison of the O_2 concentration predicted by CFAST and FDS with experimental measurement. Comparisons for FDS are shown for locations at O2-1 and O2-2 are shown. The trend predicted by CFAST and FDS are similar to measurements at O2-1. Measurements at O2-2 show oscillations in the concentration which is not predicted by FDS. These oscillations occur after the HGL has reached the floor and are possibly due to the lack of complete mixing of the hot gas which results in pockets of the gas containing higher levels of O_2. The uncertainties of the CFAST and FDS predictions are - 22 % for both codes.

Figure 5.2.6 compares the concentration of CO_2 predicted by CFAST and FDS in the HGL with experimental observation. CFAST and FDS predictions, and experimental observation show that the CO_2 from the combustion process builds up in the compartment since there are no vents releasing gases. The uncertainties in the predictions of CFAST and FDS are 0 % and - 8 %, respectively.

Figure 5.2.7 compares the concentration of CO predicted by CFAST and FDS in the HGL with experimental observation. Experimental observations indicate that CO production in the combustion process early in the transient is minimal. However, as the fire is under-ventilated toward the end of the transient, the CO production increases as is expected. The CFAST and FDS combustion models are simple and do not include the effect of O_2 concentrations on the CO production. The codes use a constant CO yield through the transient. Therefore, both codes show an increase in the CO level at the same rate through the transient.

Figure 5.2.8 compares the concentration of smoke predicted by CFAST and FDS in the HGL with experimental observation. Experimental observation indicates the smoke concentration increases to its peak value at ~465 s and decreases by about 30 % to the point when the fuel is shut off at ~ 630 s. This oscillatory behavior may result from first a weakening of the plume dynamics for the vitiated burning and then cooling of the gases when the flame is extinguished resulting in an increased smoke concentration. The simple combustion models in CFAST and FDS do not predict this oscillatory behavior. Table 5.3 lists the predicted and measured concentrations before the onset of the oscillatory behavior, and the uncertainties in the predictions. The uncertainties in the predictions of CFAST and FDS at the point noted above are + 52 % for both codes. However, it should be noted that this uncertainty does not represent the uncertainties expected for under-ventilated fires.

5.2.2 Local Gas Temperature

Figure 5.2.9 compares the gas temperatures in thermocouple Tree 2 predicted by FDS with measurement. The predicted and measured trends are similar. Experimental observation indicate a large increase and oscillations in gas temperature at Tree 2-7 at ~ 550 s (and some increase at Tree 2-5) possibly due to the lateral movement of the fire plume at the end of the transient, as observed in the fire video. This movement may cause the ceiling jet temperature to oscillate. The uncertainties of the predictions at 2-1, 2-5, and 2-7 are + 11 %, -6 %, and - 2 %.

Figure 5.2.10 compares the gas temperatures in thermocouple Tree 4 predicted by FDS with measurement. The predicted and measured trends are similar. Again measurement indicates an increase and oscillation in the gas temperature at Tree 4-8 at ~ 480 s. The uncertainty of the predictions at 4-8 is + 4 %.

Figure 5.2.11 compares the gas temperatures in thermocouple Tree 7 predicted by FDS with measurement. The predicted and measured trends are similar. The temperature profiles are similar to that of the average hot gas layer temperature discussed above. The uncertainties of the predictions at 7-1, 7-5, and 7-10 are 19 %, + 12 %, and - 2 %.

5.2.3 Heat Flux to Cable Targets

The following figures show comparisons of the incident radiative flux and the total heat flux predicted by CFAST and FDS with experiments. As indicated earlier, the total heat flux is measured by a gauge maintained at a constant temperature of ~ 75 C. The outputs from CFAST and FDS were modified to the extent possible to compare similar output quantities.

Figure 5.2.12 compares the radiative and total heat flux predicted by CFAST and FDS at Rad Gauge 1 and Total Gauge 2 with measurement. The trends of the predicted values are similar to experimental observation. The uncertainties in the predictions for CFAST at Rad Gauge 1 and Total Gauge 2 are + 161 % and + 35 %, respectively and; for FDS are + 44 % and - 15 %, respectively. Experimental observation indicates a larger convective heat flux (total heat flux - radiative heat flux) than predicted by both CFAST and FDS. The large discrepancy for CFAST prediction at Rad Gauge 1 is probably due to the use of the point source model in the code, and the height and orientation of the gauge.

Figure 5.2.13 compares the radiative and total heat flux predicted by CFAST and FDS at Rad Gauge 3 and Total Gauge 4 with measurement. A decrease in the measured radiative flux after ~ 400 s due to decrease in the intensity and size of the fire is noted. The CFAST and FDS do not model or predict these changes in the size of the fire. Otherwise, the trends of the predicted values are similar to experimental observation. The uncertainties in the predictions for CFAST at Rad Gauge 3 and Total Gauge 4 are + 67 % and + 8 %, respectively and; for FDS are + 7 % and - 22 %, respectively. Experimental observation indicates a larger convective heat flux (total heat flux - radiative heat flux) than predicted by both CFAST and FDS.

Figure 5.2.14 compares the radiative and total heat flux predicted by CFAST and FDS at Rad Gauge 5 and Total Gauge 6 with measurement. Again, a decrease in the measured radiative flux after ~ 400 s due to decrease in the intensity and size of the fire is noted. Generally, the trends of the predicted values are similar to experimental observation. The uncertainties in the predictions for CFAST at Rad Gauge 5 and Total Gauge 6 are - 17 % and - 32 %, respectively and; for FDS are - 25 % and - 40 %, respectively. Experimental observation indicates a larger convective heat flux (total heat flux - radiative heat flux) than predicted by both CFAST and FDS.

Figure 5.2.15 compares the radiative and total heat flux predicted by CFAST and FDS at Rad Gauge 10. Again, a decrease in the measured radiative flux after ~ 400 s due to decrease in the intensity and size of the fire is noted. The uncertainties in the predictions for CFAST and FDS at Rad Gauge 10 are - 14 % and - 41 %, respectively.

Interpretation of experimental results, and comparison of the predictions of heat flux with measurement is complicated by the various components of radiative heat flux from the fire, hot gas, and hot wall surfaces. Generally, experimental observations indicate higher convective heat fluxes than predicted by the codes.

5.2.4 Cable Temperature

Figure 5.2.16 shows a comparison of the control cable surface temperature at B-TS-14 predicted by CFAST and FDS with measurement. The uncertainties in the peak temperatures for CFAST and FDS are - 14 % and - 29 %, respectively. The figure shows that the heat up of the cables predicted by the models is slower than experimental observation. CFAST predicts a continued increase in target surface temperature even after the fire intensity is decreased by the code.

Figure 5.2.17 shows a comparison of the vertical cable surface temperature at TS-33 predicted by CFAST and FDS with measurement. The uncertainties in the peak temperatures for CFAST and FDS are + 30 % and - 9 %, respectively. The figure shows that the heat up of the cables predicted by CFAST is similar to experimental observation, whereas FDS predicts a smaller heat up. CFAST predicts a continued increase in target surface temperature even after the fire intensity is decreased by the code.

Figure 5.2.18 shows a comparison of the surface temperature of Slab E predicted by CFAST and FDS with measurement. There is a small change in the measured rate of temperature increase for Slab E possibly due to the softening of the PVC slab. The uncertainties in the peak temperatures for CFAST and FDS are - 22 % and - 36 %, respectively. CFAST predicts a continued increase in target surface temperature even after the fire intensity is decreased by the code.

Figure 5.2.19 shows a comparison of the control cable surface temperature at D-TS-12 predicted by CFAST and FDS with measurement. The uncertainties in the peak temperatures for CFAST and FDS are + 9 % and - 16 %, respectively. An increase and oscillation in the measured temperature is observed starting at ~ 580 s. This observation is similar to that noted for the gas temperatures, particularly at the higher elevations, and is possibly caused by the lateral movement of the fire plume about its vertical axis.

Figure 5.2.20 shows a comparison of the power cable surface temperature at F-TS-20 predicted by CFAST and FDS with measurement. The uncertainties in the peak temperatures for CFAST and FDS are - 7 % and - 25 %, respectively.

5.2.5 Heat Flux to Walls

Figure 5.2.21 shows a comparison of the net total heat flux to walls predicted by FDS with experimental observations. The uncertainties in the heat flux predicted by FDS for East U-4, West U-4, and Floor U-8 are - 27 %, - 27 %, and 0 %, respectively.

Figure 5.2.22 shows a comparison of the net heat flux to walls predicted by CFAST with experimental observations. The net heat fluxes to the east and west walls predicted by CFAST are identical and overlap. The trend of the predicted heat flux to the east and west walls, and the floor following the peak is the reverse of experimental observation. The uncertainties in the heat flux predicted by CFAST for East U-4, West U-4, and Floor U-8 are + 35 %,+ 35 %, and + 119 %, respectively.

5.2.6 Wall Temperature

Figure 5.2.23 shows a comparison of the wall temperatures predicted by FDS with experimental measurements. The trends predicted by FDS are similar to experimental observation. The uncertainties of the predictions by FDS for TC East U-4-2, TC West U-4-2, TC Ceiling C-5-2, and TC Floor U-8-2 are 29 %, + 38 %, - 14 % and + 63 %, respectively.

Figure 5.2.24 shows a comparison of the wall temperatures predicted by CFAST with experimental measurements. The predictions by CFAST are much higher than experimental observation and almost overlap. These predictions are probably due to errors in code implementation as opposed to weaknesses in the sub-models that predict these parameters. The uncertainties of the predictions by CFAST for TC East U-4-2, TC West U-4-2, TC Ceiling C-5-2, and TC Floor U-8-2 are + 50 %, + 60 %, - 45 % and + 158 %, respectively.

5.2.7 Conclusion

The simple extinction models in CFAST and FDS were accurate in predicting fire extinction for this scenario. CFAST and FDS predictions were similar to experimental observations for most parameters. Global parameters such as the HGL temperature, interface height, O2, and CO2 , were within 22 % of experimental values for CFAST and FDS. Larger deviations were observed for smoke and CO production which are dependent on the effects of ventilation on the fire. The effect of under ventilation on smoke and CO production in the combustion process is not modeled in CFAST or FDS. The codes use a constant yield for smoke and CO production. The prediction of compartment pressure was within 3 % for FDS. CFAST overestimated the pressure by 190 %. The local gas temperatures in the compartment predicted by FDS were within 19 % of experimental observations. Some local increases and oscillations in gas temperature, possibly due to the movement of the fire plume, were not predicted by FDS.

The heat flux to the cables predicted by CFAST and FDS deviated by as much as 161 % and 44 % from experimental observation, respectively and; the corresponding cable surface temperatures predicted by CFAST and FDS deviated by as much as 30 % and 36 % from experimental observation, respectively. The heat flux to the walls predicted by CFAST and FDS deviated by as much as 119 % and 27 % from experimental observation, respectively; and the corresponding wall surface temperatures predicted by CFAST and FDS deviated by as much as 158 % and 63 % from experimental observation, respectively.

The predictions for global parameters and local gas temperatures were generally more accurate than for heat fluxes and target response, except for the CFAST prediction of compartment over pressure. The extinction of the fire was fairly accurately predicted by the simple models in CFAST and FDS.

5.3 Test 3

Test 3 was designed as the base test for providing data to determine the predictively capability of models for scenarios with well ventilated conditions. The peak HRR was 1190 kW with a heptane fire located in the center of the compartment. The door was open during this test and the mechanical ventilation was turned off with the supply and exhaust vents sealed. XPE cable type was installed during this test.

The fire diameter for this test was about 1 m through observation of the fire pan after the test. The flame was observed to reach the ceiling of the compartment. The fire tilted toward the east wall away from the door due to the inflow of air. The oxygen near the fire (sensor O2-2) was maintained at ambient conditions through the transient by the air flow into the compartment through the open door, and the test was run to the planned completion time of 26 min. The smoke layer in the compartment was steady with slight oscillations of wave like motion in the layer. Observation of the steady state smoke layer during this test indicated the interface to be approximately 1.3 m above the compartment floor. There was no visible damage to the cables during this test, however, some discoloration (whitish) of the cables was observed.

5.3.1 Global Compartment Parameters

Figure 5.3.1 shows the HRR measured by the calorimeter and input to the CFAST and FDS codes. As in the experiment, the fire was increased linearly to 1190 kW in 3 minutes and then decreased linearly to zero after being maintained at the peak value for 20 minutes.

Figure 5.3.2 shows the predicted hot gas layer development predicted by CFAST and FDS, and measured in the experiment. CFAST, a two-zone model, calculates the interface height directly. However, the interface height is calculated from temperatures at a specific thermocouple tree for the experimental data and FDS calculation. The HGL interface height decreases rapidly initially until it reaches the top of the door after ~ 200 s at which point the hot gases flow out of door (see Figure 5.3.3). The measured interface height levels at 1.3 m, and CFAST and FDS predict the interface height to level at 1.1 m. The codes under predict the height at which the interface levels at by - 8 %.

Figure 5.3.3 shows the door flows. The steady state outflow predicted by CFAST is almost identical to the measured outflow of 1.9 kg/s from the door.

Figure 5.3.4 shows the hot gas layer (HGL) temperature. The HGL temperature increases rapidly when the fire is increased and the heat lost to the boundaries is less rapid than the increase in the HRR of the fire. The HGL temperature transitions to a new rate of increase in temperature at ~ 180 s when the fire reaches a steady value of 1190 kW. The HGL starts to decrease rapidly again once the ramp down of the fire is initiated. CFAST and FDS over predict the peak HGL temperature by + 28 % and + 10 %, respectively.

Figure 5.3.5 compares the concentration of CO_2 predicted by CFAST and FDS in the HGL with experimental observation. Both predictions and experimental observation shows that the CO_2 concentration reaches a steady state level at ~ 500 s after the flow of hot gas through the door reaches a steady level at ~ 240 s. The steady state concentration is determined by the flow of hot gas containing CO_2 through the door and the production of CO_2 in the combustion process. Table 5.3 lists the predicted and measured steady state concentrations, and the uncertainties in the predictions. The uncertainties in the predictions of CFAST and FDS are - 16 % and - 16 %, respectively.

Figure 5.3.6 compares the concentration of smoke predicted by CFAST and FDS in the HGL with experimental observation. Both predictions and experimental observation show that the smoke concentration reaches a steady state level at ~ 500 s after the flow of hot gas through the door reaches a steady level at ~ 240 s. The steady state concentration is determined by the flow of hot gas containing smoke through the door and the production of smoke in the combustion process. Table 5.3 lists the predicted and measured steady state concentrations, and the uncertainties in the predictions. The uncertainties in the predictions of CFAST and FDS are + 4 % and + 25 %, respectively.

Figure 5.3.7 compares the heat loss from the door predicted by FDS with experimental observation. The heat loss through the door increases with time through the transient due to the increase of the temperature of the hot gas. FDS over predicts the heat loss through the door by 29 %.

5.3.2 Local Gas Temperature

Figure 5.3.8 compares the gas temperatures in thermocouple Tree 7 predicted by FDS with measurement. The predicted and measured trends are similar. The temperature profiles are similar to that of the average hot gas layer temperature discussed above. The uncertainties of the predictions at 7-1, 7-4, and 7-10 are + 12 %, + 11 %, and + 5 %.

Figure 5.3.9 compares the gas temperatures in thermocouple Tree 2 predicted by FDS with measurement. The predicted and measured trends are similar. The uncertainties of the predictions at 2-1, 2-5, and 2-7 are + 14 %, + 4 %, and - 9 %.

5.3.3 Heat Flux to Cable Targets

The following figures show comparisons of the incident radiative flux and the total heat flux predicted by CFAST and FDS with experiments. As indicated earlier, the total heat flux is measured with a gauge maintained at a constant temperature of ~ 75 C. The outputs from CFAST and FDS were modified to the extent possible to compare similar output quantities.

Figure 5.3.10 compares the radiative and total heat flux predicted by CFAST and FDS at Rad Gauge 1 and Total Gauge 2 with measurement. The trends of the predicted values are similar to experimental observation. The uncertainties in the predictions for CFAST at Rad Gauge 1 and Total Gauge 2 are + 76 % and + 4 %, respectively; and for FDS + 17 % and - 27 %, respectively. Experimental observation indicates a larger convective heat flux (total heat flux - radiative heat flux) than predicted by CFAST.

Figure 5.3.11 compares the radiative and total heat flux predicted by CFAST and FDS at Rad Gauge 3 and Total Gauge 4 with measurement. The trends of the predicted values are similar to experimental observation. The uncertainties in the predictions for CFAST at Rad Gauge 3 and Total Gauge 4 are + 25 % and - 18 %, respectively; and for FDS are - 5 % and - 35 %, respectively. Experimental observation indicates a larger convective heat flux (total heat flux - radiative heat flux) than predicted by both CFAST and FDS.

Figure 5.3.12 compares the radiative and total heat flux predicted by CFAST and FDS at Rad Gauge 5 and Total Gauge 6 with measured values. The trends of the predicted values are similar to experimental observation. The uncertainties in the predictions for CFAST at Rad Gauge 5 and Total Gauge 6 are + 2 % and - 38 %, respectively and; for FDS are - 13 % and - 47 %, respectively. Experimental observation indicates a larger convective heat flux (total heat flux - radiative heat flux) than predicted by both CFAST and FDS.

Figure 5.3.13 compares the radiative and total heat flux predicted by CFAST and FDS at Rad Gauge 10 and Total Gauge 9 with measurement. The trends of the predicted values are similar to experimental observation. The uncertainties in the predictions for CFAST at Rad Gauge 10 and Total Gauge 9 are + 22 % and - 6 %, respectively and; for FDS are - 22 % and - 6 %, respectively. Experimental observation indicates a smaller convective heat flux (total heat flux - radiative heat flux).

Interpretation of experimental results, and comparison of predictions with measurement, of radiative and total heat flux is complicated by the various components of radiative heat flux from the fire, hot gas, and hot wall surfaces. Generally, experimental observations indicate higher convective heat fluxes than predicted by the codes.

5.3.4 Cable Temperature

Figure 3.1.14 shows a comparison of the control cable surface temperature at B-TS-14 predicted by CFAST and FDS with measurement. The uncertainties in the peak temperatures for CFAST and FDS are 0 % and - 24 %. The Figure shows that the heat up of the cables predicted by the models is slower than experimental observation. The measured peak cable surface temperature is within 15 C of the peak gas temperature (Tree 4-8) near it. The cable temperature is higher than the gas temperature due to radiative heating from the fire.

Figure 3.1.15 shows a comparison of the control cable surface temperature at C-TS-10 predicted by CFAST and FDS with measurement. Figure 3.1.15 also shows measurements indicating that the cable surface temperature at C-TS-10 (single cable) is ~ 60 C higher than the control cable surface temperature at D-TS-12 (cable in a bundle). Measurements indicate that the peak cable surface temperature is 20 C more than the peak gas temperature (Tree 3-9) near it. The Figure shows that the heat up of the cables predicted by the models is slower than experimental observation.

Figure 3.1.16 shows a comparison of the power cable surface temperature at F-TS-20 predicted by CFAST and FDS with measurement. The uncertainties in the peak temperatures for CFAST and FDS are - 18 % and - 40 %, respectively. Figure 3.1.16 also shows measurements indicating that the power cable surface temperature at F-TS-20 is ~ 15 C less than the control cable surface temperature at A-TS-18 near it. Measurements indicate that the peak control cable surface temperature (A-TS-18) is ~ 5 C more and the peak power cable surface temperature (F-TS-20) is ~ 11 C less than the peak gas temperature (Tree 3-9) near it. The Figure shows that the heat up of the cables predicted by the models is slower than experimental observation.

Figure 3.1.17 shows a comparison of the vertical cable surface temperature at TS-33 predicted by CFAST and FDS with measurement. The uncertainties in the peak temperatures for CFAST and FDS are + 32 % and - 27 %, respectively. Measurements indicate that the peak vertical cable surface temperature (TS-33) is ~ 22 C less than the peak gas temperature (Tree 2-5) near it. The Figure shows that the heat up of the cables predicted by CFAST is similar to experimental observation, whereas FDS predicts a smaller heat up.

5.3.5 Heat Flux to Walls

Figure 5.3.18 shows a comparison of the net total heat flux to walls predicted by FDS with experimental observations. The net heat flux to the ceiling peaks at ~ 180 s with the fire and then decreases sharply due to the heat up of the ceiling and radiative heat flux emitted from it. The trend of the heat flux to the ceiling predicted by FDS is similar to experimental observation. The heat flux to the floor increases sharply initially due to the ramp up of the fire and then increases with a smaller slope through the transient. The increase is due to the increase of temperature of the hot gas above it through the transient. This trend is also predicted by FDS. The measured net heat flux to the east and west walls remains constant after the initial ramp possible due to the balance between the increase in heat flux to the walls by the hot gas and the increase in radiative heat flux emitted from the walls through the transient. FDS predicts a small decrease in the heat flux to the walls after the initial ramp. The uncertainties in the heat flux predicted by FDS for East U-4, West U-4, Ceiling C-5, and Floor U-8 are - 38 %, - 32 %, + 45 %, and - 33 %, respectively.

Figure 5.3.19 shows a comparison of the net heat flux to walls predicted by CFAST with experimental observations. The net heat fluxes to the east and west walls predicted by CFAST are identical and overlap. Although the trend of the net heat flux to the ceiling is similar to experimental observation, the trend of the heat flux to the east and west walls, and the floor following the peak is the reverse of experimental observation. The uncertainties in the heat flux predicted by CFAST for East U-4, West U-4, Ceiling C-5, and Floor U-8 are + 33 %,+ 47 %, + 32 %, and + 47 %, respectively.

5.3.6 Wall Temperature

Figure 5.3.20 shows a comparison of the wall temperatures predicted by FDS with experimental measurements. The trends predicted by FDS are similar to experimental observation. The uncertainties of the predictions by FDS for TC East U-4-2, TC West U-4-2, TC Ceiling C-5-2, and TC Floor U-8-2 are + 20 %, + 21 %, - 14 % and + 39 %, respectively.

Figure 5.3.21 shows a comparison of the wall temperatures predicted by CFAST with experimental measurements. The trends predicted by CFAST are similar to experimental observation. The uncertainties of the predictions by CFAST for TC East U-4-2, TC West U-4-2, TC Ceiling C-5-2, and TC Floor U-8-2 are + 65 %, + 74 %, - 19 % and + 106 %, respectively.

Figure 5.3.22 and Figure 5.3.23 show pictures of the fire through the door and from the window on the south wall at steady state conditions. Figure 5.3.23 indicates that the flame is large reaching the ceiling of the compartment. Figure 5.3.24 shows an isosurface of the flame sheet (mixture fraction=0.062) at steady state conditions. FDS predicts the flame height to be about half of the compartment height. This accounts for the discrepancies of the FDS predictions for net heat flux to and temperature of the ceiling as shown in the Figures 5.3.18 and 5.3.20. The FDS prediction of the tilting of the fire plume due to flow into the compartment through the door is similar to experimental observation.

5.3.7 Conclusion

CFAST and FDS predictions were similar to experimental observations for most parameters. Global parameters such as the door heat flow, HGL temperature, interface height, CO2 and smoke concentration were within 28 % and 29 % of experimental values for CFAST and FDS, respectively. The local gas temperatures in the compartment predicted by FDS were within 14 % of experimental observations.

The heat flux to the cables predicted by CFAST and FDS deviated by as much as 76 % and 53 % from experimental observation, respectively and; the corresponding cable surface temperatures predicted by CFAST and FDS deviated by as much as 19 % and 43 % from experimental observation, respectively. The heat flux to the walls predicted by CFAST and FDS deviated by as much as 47 % and 45 % from experimental observation, respectively and; the corresponding wall surface temperatures predicted by CFAST and FDS deviated by as much as 106 % and 39 % from experimental observation, respectively.

The analysis indicates that the codes are more accurate in predicting global parameters and local gas temperatures than heat fluxes and target response for this scenario. The codes accurately predict the smoke concentration in this open door scenario.

5.4 Test 4

Test 4 was designed as a variation of Test 2 for providing data to determine the predictively capability of models for closed door scenarios with the mechanical ventilation system on. The peak HRR was 1200 kW with a heptane fire located in the center of the compartment. The door was closed during this test and the mechanical ventilation was turned on with the supply and exhaust vents open. XPE cable type was installed during this test.

The supply air from the mechanical ventilation system will generally come into the compartment in a horizontal direction. Due to the limitations in the design of the forced air system, optimal performance could not be achieved. This limitation resulted in the supply air entering the compartment in the upward direction at an angle of approximately 35 ° to the horizontal plane. The specified FDS calculation for this test was conducted with the supply air entering the compartment in a horizontal direction.

The fire diameter for this test was about 1 m through observation of the fire pan after the test. The flame was observed to reach the ceiling of the compartment. The oxygen near the fire (sensor O2-2) reached 14.8 % by volume at about 838 s when the test was terminated prior to the planned 26-minute transient, extending the duration of the run and fire by only 200 s as compared to Test 2. The fire was observed to become under ventilated through the transient becoming smaller and weaker toward the end of the transient. Further observations of the effects of oxygen depletion on the fire may be made from the videos in the accompanying DVDs. The average HGL temperature and cable temperature (B-TS-14) reached 219 C and 174 C, respectively during the peak of the transient. There was no visible damage to the cables during this test.

5.4.1 Global Compartment Parameters

Figure 5.4.1 shows the HRR input and calculated by the CFAST and FDS codes. The HRR input to the CFAST and FDS codes were set at the peak value of 1200 kW for 20 minutes after a 3-minute ramp up to the peak value. The internal algorithms in CFAST and FDS do not decrease the HRR in this simulation because the O2 levels remain higher than the LOL (see discussion below).

The remainder of the comparisons for this test is made at 800 s when the fuel was shutoff. These comparisons therefore do not account for the uncertainty in the model predictions due to the lack of ability to accurately predict fire extinction.

Figure 5.4.2 compares the compartment pressure predicted by CFAST and FDS with experimental observation. The CFAST and FDS calculations were conducted with the leakage for a closed compartment and does not account for the vents of the mechanical ventilation system. CFAST and FDS do not have the capability to model the details of a mechanical ventilation system and its feedback on compartment pressure during the build up of the fire. Therefore, the CFAST and FDS predictions of compartment pressure is much higher than observed in the experiment. This is discussed further later with vent flows. Experimental observation indicates a small pressure build up of ~ 59 Pa at the beginning of the transient (~ 70 s) and then a negative peak of ~ 76 Pa when the fuel is shut off.

Figure 5.4.3 shows the predicted hot gas layer development predicted by CFAST and FDS and measured in the experiment. CFAST, a two-zone model predicts the interface height to reach the floor at ~ 230 s. FDS and experimental observation both indicate that the interface layer height levels at ~ 1.0 m. The interface layer height is deduced through an algorithm using temperature data in thermocouple Tree 7. The algorithm used will result in erroneous predictions when a clear interface cannot be deduced from the temperature profile. Therefore, the measured and FDS prediction of interface height is probably erroneous. Video data indicates that the HGL reaches the floor at the fire at 420 s. The HGL reaches the floor in most areas of the compartment before this time leaving an area of air around the fire. The uncertainty for the CFAST prediction for the HGL to reach the floor at the fire is - 45 %.

Figure 5.4.4 shows a comparison of the vent flows predicted by CFAST and FDS with experimental observation. The supply and exhaust volumetric flowrates specified as input to CFAST and FDS was 1.1 m3/s which is the flowrate observed in the compartment without a fire. This translates to a mass flowrate of ~ 1.3 kg/s as shown in Figure 5.4.4. The supply mass flow predicted by CFAST and FDS remain constant as shown in the figure, however, the exhaust mass flow decreases with time due to the increase in the temperature of the hot gas. The exhaust flowrate calculated and used by CFAST and FDS decreases to ~ 0.7 kg/s. As shown in the figure, the supply flowrate quickly decreases from ~ 1.3 kg/s to 1 kg/s at the beginning of the transient due to the pressure build up in the compartment. On the other hand, the measured exhaust flowrate is seen to increase at the beginning of the transient due to the pressurization of the compartment from 1.3 kg/s to a peak of ~ 2 kg/s and then decreasing to a steady level of 1.4 kg/s. The above demonstrates the impact of the lack of the ability of the codes to include the coupling between the compartment and the mechanical ventilation system. It is difficult to realistically model the compartment fire scenario with mechanical ventilation without including a model of the coupling between the two.

Figure 5.4.5 shows the hot gas layer (HGL) temperature. The HGL temperature increases rapidly when the fire is increased and the heat lost to the boundaries is less rapid than the increase in the HRR of the fire. The measured HGL temperature transitions to a new rate of increase in temperature at ~ 180 s when the fire reaches a steady value of 1200 kW. The measured HGL increases until ~ 800 s when the fuel is shut off. As indicated earlier, CFAST and FDS codes do not decrease the HRR based on the LOLs used in the codes. At 800 s, CFAST and FDS over predict the peak HGL temperature by + 20 % and 14 %, respectively.

Figure 5.4.6 shows a comparison of the O2 concentration predicted by CFAST and FDS with experimental values. Comparisons for FDS are shown for locations at O2-1 and O2-2. The trend predicted by CFAST for the HGL and FDS at O2-2 are similar to measurements except a more rapid decrease in oxygen concentration is observed in the experiment than predicted for both codes. In fact, the FDS predicted concentration at O2-2 does not reach 15 %. This comparison indicates the importance of the prediction of local oxygen concentrations, and sensitivity to the LOL for predicting under-ventilated conditions and fire extinction. The uncertainties of the CFAST and FDS predictions at O2-1 are - 8 % and - 1 %, respectively. The uncertainty of the FDS prediction at O2-2 is - 7 %.

Figure 5.4.7 compares the concentration of CO2 predicted by CFAST and FDS in the HGL with experimental observation. CFAST and FDS predictions are similar to experimental observation showing that the CO_2 from the combustion process builds up in the compartment to an appreciable level even with the exhaust system functioning. Table 5.3 lists the predicted concentrations and the uncertainties in the predictions. The uncertainties in the predictions of CFAST and FDS are - 30 % and - 20%, respectively.

Figure 5.4.8 compares the concentration of CO predicted by CFAST and FDS in the HGL with experimental observation. The trends of the predictions are similar to experimental observation, except toward the end of the transient when the measured CO production starts to decrease possibly due to under ventilation and decrease in the HRR of the fire. The CFAST and FDS combustion models are simple and do not include the effect of O_2 concentrations on the CO production. A constant CO yield is used by the codes through the transient. Therefore, both codes show an increase in the CO level at the same rate through the transient.

Figure 5.4.9 compares the concentration of smoke predicted by CFAST and FDS in the HGL with experimental observation. Experimental observation indicates the smoke concentration increases to its peak value at ~480 s. This peak in smoke production early in the transient may result from the under ventilation and decrease in the HRR of the fire. The simple combustion models in CFAST and FDS do not predict this behavior.

Figure 5.4.10 shows a comparison of the heat loss from the vent predicted by FDS with experimental observation. A large discrepancy is seen due to the discrepancy in the exhaust mass flowrates discussed above.

5.4.2 Local Gas Temperature

Figure 5.4.11 compares the gas temperatures in thermocouple Tree 2 predicted by FDS with measurement. The predicted and measured trends are similar, except as noted earlier, the fire intensity is not reduced by FDS in this transient. Experimental observation indicate a large increase and oscillations in gas temperature at Tree 2-7 possibly due to the effect of the supply air coming into the compartment upward at an angle of approximately 35 ° to the horizontal plane. The uncertainties of the predictions at 2-1, 2-5, and 2-7 are - 7 %,+ 76 %, and - 2 %.

Figure 5.4.12 compares the gas temperatures in thermocouple Tree 4 predicted by FDS with measurement. The predicted and measured trends are similar, except at 4-8. This is due to the effect of the supply air coming into the compartment upward at an angle of approximately 35 ° to the horizontal plane and cooling the compartment around 4-8. Therefore, the uncertainty of the prediction at 4-8 is high at + 66 %.

Figure 5.4.13 compares the gas temperatures in thermocouple Tree 7 predicted by FDS with measurement. The predicted and measured trends are similar. The temperature profiles are similar to that of the average hot gas layer temperature discussed above. The uncertainties of the predictions at 7-1, 7-5, and 7-10 are + 4 %, + 20 %, and + 9 %.

5.4.3 Heat Flux to Cable Targets

The following figures show comparisons of the incident radiative flux and the total heat flux predicted by CFAST and FDS with experiments. As indicated earlier, the total heat flux is measured to a gauge maintained at a constant temperature of ~ 75 C. The outputs form CFAST and FDS were modified to the extent possible to compare similar output quantities.

Figure 5.4.14 compares the radiative and total heat flux predicted by CFAST and FDS at Rad Gauge 1 and Total Gauge 2 with measurement. The trends of the predicted values are similar to experimental observation. The uncertainties in the predictions at the peak of the measured fluxes for CFAST at Rad Gauge 1 and Total Gauge 2 are + 105 % and - 4 %, respectively; and for FDS are + 24 % and - 36 %, respectively. Experimental observation indicates a larger convective heat flux (total heat flux - radiative heat flux) than predicted by both CFAST and FDS. The large discrepancy for CFAST prediction at Rad gauge 1 is probably due to the use of the point source model in the code, and the height and orientation of the gauge.

Figure 5.4.15 compares the radiative and total heat flux predicted by CFAST and FDS at Rad Gauge 3 and Total Gauge 4 with measurement. A flattening and oscillation in the measured radiative flux after ~ 400 s is noted due to under ventilation and change in the combustion discussed earlier. The CFAST and FDS codes do not model or predict these changes in the size of the fire. Otherwise, the trends of the predicted values are similar to experimental observation. The uncertainties in the predictions for CFAST at Rad Gauge 3 and Total Gauge 4 are + 53 % and - 4 %, respectively and; for FDS are + 13 % and - 24 %, respectively. Experimental observation indicates a larger convective heat flux (total heat flux - radiative heat flux) than predicted by both CFAST and FDS.

Figure 5.4.16 compares the radiative and total heat flux predicted by CFAST and FDS at Rad Gauge 5 and Total Gauge 6 with measurement. Again, a decrease in the measured radiative flux after ~ 400 s is noted possibly due to the air entering the compartment and cooling the hot gas in the region around the flux gauge. Generally, the trends of the predicted values are similar to experimental observation. The uncertainties in the predictions for CFAST at Rad Gauge 5 and Total Gauge 6 are - 12 % and - 37 %, respectively; and for FDS are - 21 % and - 42 %, respectively. Experimental observation indicates a larger convective heat flux (total heat flux - radiative heat flux) than predicted by both CFAST and FDS.

Figure 5.4.17 compares the radiative and total heat flux predicted by CFAST and FDS at Rad Gauge 10 and Total Gauge 9. Again, a decrease in the measured radiative flux after ~ 400 s possible due to decrease in size of the fire is noted. The uncertainties in the predictions at Rad Gauge 10 and Total Gauge 9 are + 18 % and 0 %, respectively for CFAST; and - 6 % and - 18 %, respectively for FDS.

Interpretation of experimental results, and comparison of predictions with measurement, of radiative and total heat flux is complicated by the various components of radiative heat flux from the fire, hot gas, and hot wall surfaces. Generally, experimental observations indicate higher convective heat fluxes than predicted by the codes.

5.4.4 Cable Temperature

Figure 5.4.18 shows a comparison of the control cable surface temperature at B-TS-14 predicted by CFAST and FDS with measurement. The uncertainties in the temperatures, at the measured peak, for CFAST and FDS are + 14 % and - 8 %, respectively. The Figure shows that the heat up of the cables predicted by the models is slower than experimental observation.

Figure 5.4.19 shows a comparison of the vertical cable surface temperature at TS-33 predicted by CFAST and FDS with measurement. The uncertainties in the temperatures at the measured peak for CFAST and FDS are + 23 % and - 9 %, respectively.

Figure 5.4.20 shows a comparison of the control cable surface temperature at D-TS-12 predicted by CFAST and FDS with measurement. The uncertainties in the temperatures at the measured peak for CFAST and FDS are + 29 % and + 16 %.

Figure 5.4.21 shows a comparison of the power cable surface temperature at F-TS-20 predicted by CFAST and FDS with measurement. The uncertainties in the temperatures at the measured peak for CFAST and FDS are - 9 % and - 33 %.

5.4.5 Heat Flux to Walls

Figure 5.4.22 shows a comparison of the net total heat flux to walls predicted by FDS with experimental observations. The uncertainties in the heat flux predicted by FDS for East U-4, West U-4, Ceiling C-5, and Floor U-8 are - 36 %, - 36 %, 0 %, and - 7 %, respectively.

Figure 5.4.23 shows a comparison of the net heat flux to walls predicted by CFAST with experimental observations. The net heat fluxes to the east and west walls predicted by CFAST are identical and overlap. The trend of the heat flux to the east and west walls, and the floor following the peak is the reverse of experimental observation. The uncertainties in the peak heat flux predicted by CFAST for East U-4, West U-4, Ceiling C-5, and Floor U-8 are + 12 %,+ 12 %, + 4 %, and + 100 %, respectively.

5.4.6 Wall Temperature

Figure 5.4.24 shows a comparison of the wall temperatures predicted by FDS with experimental measurements. The uncertainties of the predictions by FDS for TC East U-4-2, TC West U-4-2, TC Ceiling C-5-2, and TC Floor U-8-2 are + 29 %, + 40 %, - 28 % and + 51 %, respectively.

Figure 5.4.25 shows a comparison of the wall temperatures predicted by CFAST with experimental measurements. The predictions by CFAST are much higher than experimental observation and almost overlap. These predictions are probably due to errors in code implementation as opposed to weaknesses in the sub-models that predict these parameters. The uncertainties of the predictions by CFAST for TC East U-4-2, TC West U-4-2, TC Ceiling C-5-2, and TC Floor U-8-2 are + 57 %, + 62 %, - 45 % and + 160 %, respectively.

5.4.7 Conclusion

CFAST and FDS predictions were similar to experimental observations for most parameters. Global parameters such as the HGL temperature, O2, and CO2 , were within 30 % and 20 % of experimental values for CFAST and FDS, respectively. Larger deviations were observed for CO and smoke which is dependent on the effects of ventilation on the fire which is not modeled in CFAST or FDS. The local gas temperatures in the compartment predicted by FDS were within 26 % of experimental observations, except for Tree 4-8 which is affected by the anomalous direction of the supply air.

The heat flux to the cables predicted by CFAST and FDS generally deviated by as much as 53 % and 42 % from experimental observation, respectively. A larger deviation for CFAST for Rad Gauge 1 was noted due to the assumption of the point source model in the code. The corresponding cable surface temperatures predicted by CFAST and FDS deviated by as much as 29 % and 33 % from experimental observation, respectively. The heat flux to the walls predicted by CFAST and FDS deviated by as much as 100 % and 36 % from experimental observation, respectively; and the corresponding predicted wall surface temperatures deviated by as much as 51 % and 160 % from experimental observation, respectively.

CFAST and FDS did not predict the extinction of the fire for this experiment. The use of an LOL in the codes did not result in an accurate prediction of fire development. The lack of ability to model the coupling of the compartment with the mechanical ventilation system results in errors in the predicted compartment pressure, ventilation flowrates, and O2 concentration.

5.5 Test 5

Test 5 was designed as a variation of Test 3 for providing data to determine the predictively capability of models for fires in well ventilated conditions with natural and mechanical ventilation. The peak HRR was 1190 kW with a heptane fire located in the center of the compartment. The door was open during this test and the mechanical ventilation was turned on with the supply and exhaust vents open. XPE cable type was installed during this test.

The fire diameter for this test was about 1 m through observation of the fire pan after the test. The fire tilted toward the east wall away from the door due to the inflow of air. The flame was observed to reach the ceiling of the compartment. The oxygen near the fire (sensor O2-2) was maintained at ambient conditions through the transient by the air flow into the compartment through the open door and by the mechanical ventilation system, and the test was run to the planned completion time of 26 min. The smoke layer in the compartment was steady with slight oscillations of wave like motion in the layer. The smoke layer development and height for this test were similar to that in Test 3. Further observations of the smoke layer development may be made from the videos in the accompanying DVDs. The average HGL temperature and cable temperature (B-TS-14) reached 200 C and 169 C, respectively during the peak of the transient. There was no visible damage to the cables during this test.

The compartment conditions resulting from this test are similar to those in Test 3 without mechanical ventilation. Therefore, an analysis of the global parameters and local gas temperatures are presented below to highlight the similar characteristics of this experiment and the ability of the codes to predict the compartment conditions even with mechanical ventilation. The uncertainties of the model predictions are similar to those for Test 3. Therefore, the uncertainties of the predictions are not discussed below or tabulated.

5.5.1 Global Compartment Parameters

Figure 5.5.1 shows the HRR input to the CFAST and FDS codes. The input to the CFAST and FDS codes were set at the nominal peak value of 1190 kW. As in the experiment, the fire was increased linearly to 1190 kW in 3 minutes and then ramped down linearly to zero after being maintained at the peak value for 20 minutes.

Figure 5.5.2 shows the pressure near the floor of the compartment predicted by the codes and measured as being identical in trend and magnitude. A small negative pressure develops resulting in the inflow of ambient air into the compartment.

Figure 5.5.3 shows the predicted hot gas layer development predicted by CFAST and FDS and measured in the experiment. The HGL interface height decreases rapidly initially until it reaches the top of the door after ~ 200 s at which point the hot gases flow out of door (see Figure 5.3.3). The measured and predicted interface heights are the same as in Test 3.

Figure 5.5.4 shows the door mass flows predicted by CFAST and measured. The figure shows that the CFAST prediction captures the trend and magnitude of the door mass flows.

Figure 5.5.5 shows a comparison of the vent flows predicted by CFAST and FDS with experimental observation. The supply and exhaust flowrate specified as input to CFAST and FDS was 1.1 m3/s according to the design specification of the experiment. This translates to a mass flowrate of ~ 1.3 kg/s as shown in Figure 5.5.4. The supply mass flow predicted by CFAST and FDS remain constant as shown in the figure, however, the exhaust mass flow decreases with time due to the increase in the temperature of the hot gas. The exhaust flowrate calculated and used by CFAST and FDS decreases to ~ 0.7 kg/s. As shown in the figure, the measured supply flowrate quickly decreases from ~ 1.2 kg/s to 1 kg/s at the beginning of the transient due to the pressure build up in the upper half of the compartment. On the other hand, the measured exhaust flowrate is seen to increase at the beginning of the transient due to the pressurization of the compartment to a peak of ~ 1.5 kg/s and then decreasing to a steady level that is about the same as the supply flowrate. The above demonstrates the impact of the lack of the ability of the codes to include the coupling between the compartment and the mechanical ventilation system. It is difficult to realistically model the a compartment fire scenario with mechanical ventilation without including a model of the coupling between the two.

Figure 5.5.6 shows the hot gas layer (HGL) temperature. The HGL temperature increases rapidly when the fire is ramped up and the heat lost to the boundaries is less rapid than the increase in the HRR of the fire. The HGL temperature transitions to a new rate of increase in temperature at ~ 180 s when the fire reaches a steady value of 1190 kW. The HGL starts to decrease rapidly again once the ramp down of the fire is initiated. CFAST and FDS predict the trend and magnitude of the hot gas temperature.

Figure 5.5.7 compares the concentration of CO2 predicted by CFAST and FDS in the HGL with experimental observation. Both predictions and experimental observation shows that the CO 2 concentration reaches a steady state level at ~ 500 s after the flow of hot gas through the door reaches a steady level at ~ 240 s. The steady state concentration is determined by the flow of hot gas containing CO2 through the door and the production of CO2 in the combustion process. CFAST and FDS predict the trend and magnitude of the hot gas temperature quite accurately.

Figure 5.5.8 compares the concentration of smoke predicted by CFAST and FDS in the HGL with experimental observation. Both predictions and experimental observation shows that the smoke concentration reaches a steady state level at ~ 500 s after the flow of hot gas through the door reaches a steady level at ~ 240 s. The steady state concentration is determined by the flow of hot gas containing smoke through the door and the production of smoke in the combustion process. CFAST and FDS predict the trend and magnitude of the smoke concentration in the compartment quite accurately, although a larger discrepancy for FDS is noted.

5.5.2 Local Gas Temperature

Figure 5.5.9 compares the gas temperatures in thermocouple Tree 2 predicted by FDS with measurement. The predicted and measured trends and magnitudes are similar. Oscillations in the temperature measured at Tree 2-7 are observed due to the direction of the flow into the compartment from the mechanical ventilation system, as discussed in Section 5.4 above.

Figure 5.5.10 compares the gas temperatures in thermocouple Tree 4 predicted by FDS with measurement. The predicted and measured trends and magnitudes are similar, except for the temperature at Tree 4-8. The measured temperature at Tree 4-8 is less than Tree 4-5 and Tree 4-2 because of the direction of the flow into the compartment from the mechanical ventilation system, as discussed in Section 5.4 above. This effect is not captured by FDS because of the different assumption of the direction of air flow into the compartment.

Figure 5.5.11 compares the gas temperatures in thermocouple Tree 7 predicted by FDS with measurement. Again, the predicted and measured trends and magnitudes are quite similar.

5.5.3 Conclusion

CFAST and FDS predictions were similar to experimental observations for most parameters. Global parameters such as the door mass flows, HGL temperature, interface height, CO_2 and smoke concentration were predicted quite accurately by CFAST and FDS. The local gas temperatures in the compartment predicted by FDS were also quite accurate. There was a discrepancy in predicting the effects of cooling by the mechanical ventilation system due to the different assumptions adopted for the FDS simulation. The lack of the ability of the codes to include the coupling between the compartment and the mechanical ventilation system is noted. It is difficult to realistically model a compartment fire scenario with mechanical ventilation without including a model of the coupling between the two.

The inclusion of mechanical ventilation in open door scenarios generally does not alter the predictive capabilities of the codes. The mechanical ventilation challenges the ability of the models to predict local cooling of targets that are in the flow path of the supply air.

5.6 Tests 7 to 10

Tests 7 to 10 were replicate tests of Tests 1, 2, 3, and 4. A discussion of the replicate tests including a comparison of the results with the base tests was presented in Section 5.4. The discussion in that section demonstrated the reproducibility of the tests, and thereby the confidence in the evaluation of the predictive capability of CFAST and FDS presented here.

5.7 Test 13

Test 13 was designed as a variation of Test 2 to provide data to determine the predictive capability of models for large fires in under ventilated conditions. The peak HRR was 2330 kW with a heptane fire located in the center of the compartment. The door was closed during this test and the mechanical ventilation was turned off with the supply and exhaust vents sealed. XPE cable type was installed during this test.

The fire diameter for this test was also about 1 m through observation of the fire pan after the test. The flame was observed to engulf the ceiling of the compartment over the fire. The oxygen near the fire (sensor O2-2) reached 13.8 % by volume at about 400 s. *The fire had extinguished itself at this time before the fuel was shut off.* The fire was observed to initially be large and engulfing and then becoming under ventilated through the transient becoming smaller and weaker toward the end of the transient. The visible color changed from yellow at the beginning of the transient to bluish-red toward the end possibly due to the under-ventilation of the fire and the flame temperature. Further observations of the effects of oxygen depletion on the fire may be made from the videos in the accompanying DVDs. The average HGL temperature and cable temperature (B-TS-14) reached 295 C and 218 C, respectively during the peak of the transient. There was no visible damage to the cables during this test.

5.7.1 Global Compartment Parameters

Figure 5.7.1 shows the HRR calculated by the CFAST and FDS codes. The HRR input to the CFAST and FDS codes were set at the peak value of 2330 kW for 20 minutes after a 3-minute ramp up to peak. FDS and CFAST start to decrease the HRR rapidly at ~ 340 s and ~ 300 s, respectively to account for under-ventilated conditions. The oscillation in the CFAST trend is due to limitations of the algorithm used to decrease the HRR.

Figure 5.7.2 compares the compartment pressure predicted by CFAST and FDS with experimental observation. The CFAST and FDS calculations were conducted with the leakage measured just before the test. CFAST and FDS predict pressure peaks at ~ 180 s when the HRR reaches its peak value. A negative peak is predicted by both codes and measured at the end of the transient when the fuel is shut off. The uncertainties in the CFAST and FDS predictions are 294 % and + 43 %, respectively.

Figure 5.7.3 shows the predicted hot gas layer development predicted by CFAST and FDS and measured in the experiment. CFAST, a two-zone model predicts the interface height to reach the floor at ~ 180 s. FDS and experimental observation indicate that the interface layer height levels at 0.5 m and 1.0 m, respectively. For FDS and experimental measurement, the interface layer height is deduced through an algorithm using temperature data in thermocouple Tree 7. The algorithm used will result in erroneous predictions when a clear interface cannot be deduced from the temperature profile. Therefore, the measured and FDS prediction of interface height is erroneous. Video data indicates the HGL reaches the floor at ~ 270 s. Based on this, the uncertainty of the CFAST prediction for the HGL to reach the floor is - 33 %.

Figure 5.7.4 shows the hot gas layer (HGL) temperature. The HGL temperature increases rapidly when the fire is increased and the heat lost to the boundaries is less rapid than the increase in the HRR of the fire. The measured HGL temperature transitions to a new rate of increase in temperature at ~ 180 s when the fire reaches a steady value of 2330 kW. The measured HGL increases until ~ 345 s when the fuel is shut off. CFAST and FDS predict the temperature to increase until the 300 s and 370 s, respectively when the internal algorithms in the codes decrease the HRR. As mentioned above, the fire extinguished itself in this test before the fuel was shut off. Therefore, the internal algorithm in CFAST with an LOL of 12 % performs well in simulating this under-ventilated fire and extinction. FDS also performs well in simulating under-ventilated conditions and fire extinction. CFAST and FDS over predict the peak HGL temperature by + 25 % and + 15 %.

Figure 5.7.5 shows a comparison of the O2 concentration predicted by CFAST and FDS with experimental measurement. Comparisons for FDS are shown for locations at O2-1 and O2-2. The trend predicted by CFAST and FDS are similar to measurements at O2-1. Measurements at O2-2 show oscillations in the concentration which are not predicted by FDS. These oscillations occur after the HGL has reached the floor and are possibly due to the lack of complete mixing of the hot gas resulting in pockets of the gas containing higher levels of O2. The uncertainties of the CFAST and FDS predictions at O2-1 are - 39 % and + 6 %, respectively.

Figure 5.7.6 compares the concentration of CO2 predicted by CFAST and FDS in the HGL with experimental observation. CFAST and FDS predictions, and experimental observation show that the CO2 from the combustion process builds up in the compartment since there are no vents releasing gases. The trends of the predictions and experimental observations are similar. Table 5.3 lists the predicted concentrations at the end of the transient, and the uncertainties in the predictions. The uncertainties in the predictions of CFAST and FDS are + 6 % and - 11 %, respectively.

Figure 5.7.7 compares the concentration of CO predicted by CFAST and FDS in the HGL with experimental observation. The trends of the predicted values are similar to experimental observation until ~ 236 s when measurement indicates a higher rate of increase in CO concentration. The CFAST and FDS combustion models are simple and do not include the effect of O2 concentrations on the CO production. The codes use a constant CO yield through the transient. Therefore, both codes show an increase in the CO level at the same rate through the transient. The uncertainties in the predictions of CFAST and FDS upto 230 s are + 5 % and - 8 %, respectively. However, it should be noted that this uncertainty does not represent the uncertainties expected for under-ventilated fires.

Figure 5.7.8 compares the concentration of smoke predicted by CFAST and FDS in the HGL with experimental observation. The trends of the predicted values and experimental observation are similar until 300 s when the measured value decreases. This is due to the under ventilation and extinction of the fire. The simple combustion models in CFAST and FDS do not predict this behavior. Table 5.3 lists the predicted and measured concentrations at 300 s before the decrease of the measured value, and the uncertainties in the predictions. The uncertainties in the predictions of CFAST and FDS are + 8 % and 17 %, respectively. However, it should be noted that this uncertainty does not represent the uncertainties expected for under-ventilated fires.

5.7.2 Local Gas Temperature

Figure 5.7.9 compares the gas temperatures in thermocouple Tree 2 predicted by FDS with measurement. The predicted and measured trends are similar. Experimental observation indicates a large increase and oscillations in gas temperature at Tree 2-7 at ~ 288 s (and some increase at Tree 2-5) possibly due to the lateral movement of the fire plume at the end of the transient, as observed in the fire video. This movement may cause the ceiling jet temperature to oscillate. The uncertainties of the predictions at 2-1, 2-5, and 2-7 at the time of the measured peak are + 16 %, + 6 %, and - 18 %.

Figure 5.7.10 compares the gas temperatures in thermocouple Tree 4 predicted by FDS with measurement. The predicted and measured trends are similar. The uncertainty of the prediction at 4-8 at the time of the measured peak is + 28 %.

Figure 5.7.11 compares the gas temperatures in thermocouple Tree 7 predicted by FDS with measurement. The predicted and measured trends are similar. The temperature profiles are similar to that of the average hot gas layer temperature discussed above. Experimental observation indicates an oscillation in the gas temperature at Tree 7-7 at ~ 288 s possibly due to the lateral movement of the fire plume at the end of the transient, as observed in the fire video. This movement may cause the ceiling jet temperature to oscillate. The uncertainties of the predictions at 7-1, 7-5, and 7-10 at the time of the measured peak are 23 %, + 21 %, and + 3 %.

5.7.3 Heat Flux to Cable Targets

The following figures show comparisons of the incident radiative flux and the total heat flux predicted by CFAST and FDS with experiments. As indicated earlier, the total heat flux is measured to a gauge maintained at a constant temperature of ~ 75 C. The outputs form CFAST and FDS were modified to the extent possible to compare similar output quantities.

Figure 5.7.12 compares the radiative and total heat flux predicted by CFAST and FDS at Rad Gauge 1 and Total Gauge 2 with measurement. The trends of the predicted values are similar to experimental observation. The uncertainties in the predictions for CFAST at Rad Gauge 1 and Total Gauge 2 at the peak of the measured flux are + 172 % and + 13 %, respectively; and for FDS are + 28 % and - 22 %, respectively. Experimental observation indicates a larger convective heat flux (total heat flux - radiative heat flux) than predicted by both CFAST and FDS. The large discrepancy for CFAST prediction at Rad Gauge 1 is probably due to the use of the point source model used in the code, and the height and orientation of the gauge.

Figure 5.7.13 compares the radiative and total heat flux predicted by CFAST and FDS at Rad Gauge 3 and Total Gauge 4 with measurement. The trends of the predicted values are similar to experimental observation. The uncertainties in the predictions for CFAST at Rad Gauge 3 and Total Gauge 4 at the measured peak of the flux are + 75 % and + 15 %, respectively; and for FDS are + 8 % and - 9 %, respectively. Experimental observation indicates a larger convective heat flux (total heat flux - radiative heat flux) than predicted by both CFAST and FDS.

Figure 5.7.14 compares the radiative and total heat flux predicted by CFAST and FDS at Rad Gauge 5 and Total Gauge 6 with measurement. The trends of the predicted values are similar to experimental observation, but peak at lower fluxes. The uncertainties in the predictions for CFAST at the time of the peaks of the measured fluxes at Rad Gauge 5 and Total Gauge 6 are - 18 % and - 34 %, respectively and; for FDS are - 13 % and - 34 %, respectively. Experimental observation indicates a larger convective heat flux (total heat flux - radiative heat flux) than predicted by both CFAST and FDS.

Figure 5.7.15 compares the radiative and total heat flux predicted by CFAST and FDS at Rad Gauge 10 and Total Gauge 9. The measured radiative flux decreases after ~ 200 s due to the descent of the HGL and its shielding of the radiative flux from the fire to the gauge. Both radiative and total measured fluxes show a sharp peak at ~ 350 s possibly due to the lateral movement of the fire plume at the end of the transient during under-ventilated conditions, as observed in the fire videos. The uncertainties in the predictions for CFAST and FDS at Rad Gauge 10 and Total Gauge 9 at the measured peak of the fluxes are - 12 % and - 8 %, respectively, and - 33 % and - 26 %, respectively.

Interpretation of experimental results, and comparison of predictions with measurement, of radiative and total heat flux is complicated by the various components of radiative heat flux from the fire, hot gas, and hot wall surfaces. Generally, experimental observations indicate higher convective heat fluxes than predicted by the codes.

5.7.4 Cable Temperature

Figure 5.7.16 shows a comparison of the control cable surface temperature at B-TS-14 predicted by CFAST and FDS with measurement. The uncertainties in the peak temperatures for CFAST and FDS at the measured peak temperature are - 9 % and - 43 %. CFAST predicts a continued increase in target surface temperature even after the fire intensity is decreased by the code.

Figure 5.7.17 shows a comparison of the power cable surface temperature at F-TS-20 predicted by CFAST and FDS with measurement. The uncertainties in the peak temperatures for CFAST and FDS are - 7 % and - 10 %.

Figure 5.7.18 shows a comparison of the vertical cable surface temperature at TS-33 predicted by CFAST and FDS with measurement. The uncertainties in the peak temperatures for CFAST and FDS are + 11 % and - 2 %. The Figure shows that the heat up of the cables predicted by CFAST is similar to experimental observation, whereas FDS predicts a slower heat up. CFAST predicts a continued increase in target surface temperature even after the fire intensity is decreased by the code.

Figure 5.7.19 shows a comparison of the control cable surface temperature at D-TS-12 predicted by CFAST and FDS with measurement. The uncertainties in the peak temperatures for CFAST and FDS are - 6 % and + 2 %. A small oscillation in the measured temperature is observed starting at ~ 270 s. This observation is similar to that noted for the gas temperatures, particularly at the higher elevations, and is possibly caused by the lateral movement of the fire about its vertical axis.

5.7.5 Heat Flux to Walls

Measurements of heat fluxes to the walls are not available for this test.

5.7.6 Wall Temperature

Figure 5.7.20 shows a comparison of the wall temperatures predicted by CFAST with experimental measurements. Except for the ceiling temperature, the predictions by CFAST are higher than experimental observation and almost overlap. These predictions are probably due to errors in code implementation as opposed to weaknesses in the sub-models that predict these parameters.

Figure 5.7.21 shows a comparison of the wall temperatures predicted by FDS with experimental measurements. The trends predicted by FDS are similar to experimental observation. The measured temperatures at TC East U-4-2 and TC West U-4-2 are not similar for this test, as expected. The uncertainties of the predictions by FDS for TC East U-4-2, TC West U-4-2, TC Ceiling C-5-2, and TC Floor U-8-2 are + 43 %, + 43 %, - 21 % and + 63 %, respectively.

5.7.7 Conclusion

CFAST and FDS predictions were similar to experimental observations for most parameters. Global parameters such as the HGL temperature, O_2, and CO_2 , were within 39 % and 17 % of experimental values for CFAST and FDS, respectively. Larger deviations were observed for smoke and CO production which are dependent on the effects of ventilation on the fire, but not modeled in CFAST and FDS. The pressurization of the compartment was overpredicted by CFAST. The local gas temperatures in the compartment predicted by FDS were within 28 % of experimental observations.

The heat flux to the cables predicted by CFAST and FDS deviated by as much as 141 % and 33 % from experimental observation, respectively and; the corresponding cable surface temperatures predicted by CFAST and FDS deviated by as much as 11 % and 43 % from experimental observation, respectively. The corresponding wall surface temperatures predicted by CFAST and FDS deviated by as much as - 118 % and - 63 % from experimental observation, respectively.

The simple extinction models in the codes and the LOL used fairly accurately predicted fire extinction.

5.8 Test 14

Test 14 was designed as a variation of Test 3 to provide data to determine the predictively capability of models for scenarios involving cable damage in an extreme thermal environment in well ventilated conditions that would sustain the fire through the transient. The test was also designed to investigate flame spread in vertical cable trays. The peak HRR was 1180 kW with a heptane fire located 1.8 m from the north wall on the east-west centerline near the vertical cable tray. The door was open during this test and the mechanical ventilation was turned off with the supply and exhaust vents sealed. XPE cable type was installed during this test.

The fire diameter for this test was about 1 m through observation of the fire pan after the test. The fire tilted toward the east wall away from the door due to the inflow of air. However, there was no visible tilt of the fire toward the north wall even though the fire was near the wall. The flame was observed to reach the ceiling of the compartment. Like Test 3, the oxygen near the fire (sensor O2-2) was maintained at ambient conditions through the transient by the air flow into the compartment through the open door, and the test was run to the planned completion time of 26 min. The smoke layer in the compartment was steady with slight oscillations of wave-like motion in the layer. Figures 5.11 and 5.12 in Section 3 show the hot gas smoke layer and the fire near the vertical cable tray. The average HGL temperature and cable temperature (TC-VS-32) reached 230 C and 378 C, respectively during the peak of the transient. There was extensive damage to the cables in the vertical cable tray (see Figure 5.13). The bottom of the cables in the tray reached higher temperatures than the top, as in Test 3. The damage appeared to be extensive around the center of the vertical run of the cables. Off-gases were observed to be emitted from the cables during the transient. The videos did not appear to indicate any presence of flame spread during the transient.

Since this test is a variation of Test 3, the analysis presented below is aimed at (1) confirming the predictive capabilities of the models when the fire is placed at a different location in the compartment; (2) determining the capability of the models to predict the spatial distribution and magnitude of heating of a vertical cable tray; and (3) examining the plume behavior of fires near a wall. Since a detailed discussion of the parameters and uncertainties of the predictions is presented in Section 5.3 for Test 3, the following discussion focuses on the above objectives for this analysis.

5.8.1 Global Parameters

Figures 5.8.1 to 5.8.7 present a comparison of the predicted trends with experimental measurement for the global parameters. Most predicted and measured trends are similar in this test as in Test 3, except as noted in the following. The discrepancy between the FDS prediction and measured heat loss through the door in Figure 5.8.4 is large as for Test 3 and Test 5. The measured heat loss is 300 kW in Test 14 and 335 kW in Test 3, while the FDS prediction is less for Test 3 . This may be due to a larger heat loss occurring through the north wall in the Test 14 due to the proximity of the fire to the wall than predicted by FDS. The measured peak CO 2 concentration in slightly higher in Test 14 (3.3 % vs 3.0 %) which may be due to the combustion of the XPE cables in the vertical cable tray which is not accounted for in the model predictions. The measured peak smoke concentrations in Test 3 at 115 mg/m3 and Test 14 at 89 mg/m3 are different, while the predicted peaks by the codes are the same. This may be due to the production of off-gases in Test 14 which may have caused measurement errors.

5.8.2 Local Gas Temperature

Figures 5.8.8 to 5.8.10 show a comparison of the predicted trends of hot gas temperature profiles in the compartment with experimental measurement. The comparison of FDS predictions and measurement are similar as for Test 3 except for Tree 2 shown in Figure 5.8.8. This discrepancy between prediction and measurement is due to the close proximity of Tree 2 to the fire in this experiment, and the resulting uncertainty of the thermocouple data.

5.8.3 Heat Flux to Cables

Figures 5.8.11 to 5.8.14 show a comparison of the predicted hear flux to cables with experimental data. The measured radiative flux in Figure 5.8.11 peaks at ~ 150 s at the time when the HGL descends below Rad Gauge 10 at 1.75 m and shields the radiative flux from the fire to the gauge. The HGL then reaches a steady level of 1.3 m. This trend is not predicted by CFAST or FDS. As in most of the other experiments, CFAST and FDS under predict the radiative and convective heat flux to the cable. Experimental observation indicates a larger convective heat flux (total heat flux - radiative heat flux) than predicted by both CFAST and FDS. Figures 5.8.12 and 5.8.13 show a comparison of predicted values with measurement for heat flux gauges 1 to 4 which point downward. Figure 5.8.14 shows the comparison for flux gauges 5 and 6 which point toward the north wall and the fire. It appears from these figures that the comparison of predicted and measured fluxes are better for FDS when the gauges are pointing downward. This is possibly due to the code under estimating the radiative heat flux from the fire and being more accurate when the radiative flux from the hot gas is prominent.

5.8.4 Cable Temperature

Figure 5.8.15 shows a comparison of predicted and measured temperature of the vertical cable (TS 33) and indicates that both CFAST and FDS under predict the cable temperature resulting from the under prediction of heat fluxes. Figures 5.8.16 and 5.8.17 show the measurements and predictions of the cable temperature in the vertical cable tray. Measurements indicate that the peak cable temperature is highest at TS 32 which is at 0.7 m from the floor under the HGL interface, whereas FDS predicts the peak cable temperature to increase with height in the cable tray. Again, this is possibly due to the under prediction of the radiative flux from the fire to the cables by FDS.

5.8.5 Conclusion

Changing the location of the fire to a different location in the compartment in this experiment did not change the predictively capability of the models for most global parameters and gas temperatures. FDS predicted that the plume behavior in this test did not vary from Test 3, as observed in the experiments.

Measurements indicate that the bottom of the vertical cable tray reaches higher temperatures than at the top. FDS predicted higher temperatures toward the top of the cable tray possibly due to the under prediction of the radiative flux from the fire to the cables by the code. This analysis demonstrates the complexity of predicting the spatial temperature distribution in vertical cable trays when fires sources are in its immediate vicinity.

5.9 Test 15

Test 15 was designed as a variation of Test 3 to provide data to determine the predictively capability of models for scenarios with well-ventilated conditions, with the fire directly under cable targets. Specifically, data on heat fluxes to cables in the fire plume, cable combustion, and flame spread was sought. The nominal peak HRR was 1180 kW with a heptane fire located 1.25 m from the south wall in the east-west centerline directly under cable B. The door was open during this test and the mechanical ventilation was turned off with the supply and exhaust vents sealed. PVC cable type was installed during this test.

The fire diameter for this test was about 1 m through observation of the fire pan after the test. The flame was observed to reach the ceiling of the compartment. The fire tilted toward the east wall away from the door due to the inflow of air. The fire also tilted toward the south wall, as discussed below. The oxygen concentration near the fire (sensor O2-2) was maintained at ambient conditions through the transient by the air flow into the compartment through the open door, and the test was run to the planned completion time of 26 min. The smoke layer in the compartment was steady with slight oscillations of wave like motion in the layer. Further observations of the smoke layer development and tilting of the fire may be made from the videos in the accompanying DVDs. The average HGL temperature reached 227 C during the peak of the transient. There was extensive damage to the cables, including combustion in localized areas (see Figures 5.15, 5.16, and 5.17). The videos did not appear to indicate any presence of flame spread during the transient.

The main objective of this test is to examine the nature of combustion of cables directly under a fire, and any subsequent flame spread. Other objectives of the test are to: (1) determine the predictive capabilities of the models when cable targets are in or near the fire plume; and (2) examine the plume behavior of fires near a wall. Since a detailed discussion of most of the parameters and uncertainties of the predictions are presented in Section 5.3 for Test 3, and in Section 5.8 for Test 14, the following discussion focuses on the above objectives for this analysis.

5.9.1 Global Parameters

The capabilities and uncertainties of the models for predicting global parameters in this experiment are the same as for Test 3 and Test 14. As for Test 14 and for the same reasons, a slightly larger discrepancy was noted for the door heat flow predicted by FDS.

5.9.2 Local Gas Temperature

Figures 5.9.1 to 5.9.4 show a comparison of the predicted trends of the hot gas temperature profiles in and near the fire plume with experimental measurement. Large discrepancies between FDS predictions and experimental measurements are noted in Figure 5.9.1. However, it should be noted there are large uncertainties associated with the temperatures measured by the thermocouples in the fire plume. Figure 5.9.2 shows a comparison of the predicted and measured temperatures at Tree 3-9 near Cable Targets C and D, and Tree 5-6 near Cable Targets A and F. The uncertainties of the predictions at these locations outside the fire plume are less than at Tree 4 in the fire plume. The uncertainty is larger for Tree 5-6 because it is possibly in the flaming region. The oscillations observed in the measured temperature at Tree 5-6 indicate the movement of the flame in and out of that region. The temperatures in Figures 5.9.3 and 5.9.4 indicate that the fire plume is tilted toward Tree 5 where the temperatures are higher and grouped together. Observation of the fire videos in the DVDs indicate the plume is tilted toward the east and south walls during the transient.

5.9.3 Heat Flux to Cables

Figures 5.9.5 to 5.9.8 show a comparison of the predicted heat fluxes to the cables with experimental measurement. The measured fluxes at Gauges 1 and 2 in Figure 5.9.5 show a small peak at ~ 200 s when the HGL descends to the level of the gauges. A small convective heat flux is noted at this location. Figure 5.9.6 shows that the measured fluxes at Gauges 3 and 4 in the fire plume is dominated by the radiative flux. The flux peaks at ~ 175 s when the HGL descends to the level of the gauges and shields the radiative flux from the fire to the gauges. Figure 5.9.7 shows a similar trend for measurements at Gauges 5 and 6, but the flux is dominated by the convective component due to the orientation of the gauges. CFAST uses a point source model and is not capable of predicting temperatures and fluxes within the fire plume. FDS predicts some of the trends discussed above to a much smaller degree. FDS under predicts the fluxes and temperatures in the plume region.

5.9.4 Cable Temperature

Cable temperatures were not available for this experiment. However, temperature data for thermocouples at cable locations is indicative of the cable temperatures in the experiment.

5.9.5 Conclusion

This test again confirmed that changing the location of the fire to a different location in the compartment does not change the predictively capability of the models for most global parameters and gas temperatures. The analysis for this experiment demonstrates the complexity of predicting heat fluxes and temperatures of cable targets in or near the fire plume. Fire plumes may tilt due to air flow into the compartment or due to entrainment patterns established for fires near a wall. The CFAST model is not capable of making such predictions. FDS under predicts the heat fluxes and temperatures in the fire plume.

5.10 Test 16

Test 16 was designed as a variation of Test 13 to provide data to determine the predictive capability of models for large fires in under ventilated conditions with the mechanical ventilation system on. The nominal peak HRR was 2330 kW with a heptane fire located in the center of the compartment. The door was closed during this test and the mechanical ventilation was turned on with the supply and exhaust vents open. PVC cable type was installed during this test

The fire diameter for this test was also about 1 m through observation of the fire pan after the test. The flame was observed to engulf the ceiling of the compartment over the fire. The oxygen near the fire (sensor O2-2) reached 14 % by volume at about 425 s when the test was terminated prior to the planned 26-minute transient, extending the test by only 25 s when compared to Test 13. The fire was observed to initially be large and engulfing at first and then becoming under ventilated through the transient, becoming smaller and weaker toward the end of the transient. The visible color changed from yellow at the beginning of the transient to bluish-red toward the end possibly due to the under-ventilation of the fire and the flame temperature. There was melting of the PVC cables during this test.

This test was not initially designed and included in the design specification of the test series. This test was planned during the test series in lieu of tests with toluene fuel which were not possible due to problems with the building smoke scrubbing system. Therefore, specified predictions for this experiment were not conducted and submitted to the impartial referee. For this reason, and because this test is very similar to Test 13 (the mechanical ventilation system only extended the test by 25 s), an analysis of this test is not presented here. The uncertainties of the code predictions are similar to those for Test 13.

5.11 Test 17

Test 17 was designed as a variation of Test 2 to provide data to determine the predictive capability of models for a different fuel, toluene, with under ventilated conditions. The peak HRR was 1160 kW with a toluene fire located in the center of the compartment. The door was closed during this test and the mechanical ventilation was turned off with the supply and exhaust vents sealed. PVC cable type was installed during this test.

The fire diameter for this test was about 1 m through observation of the fire pan after the test. The flame was observed to reach the ceiling of the compartment. The smoke development for this transient was much faster and dense when compared to Test 2. The fire was completely obstructed by the smoke and not visible at 273 s into the transient. At this point, the fuel was turned off for safety. Further observations of the dense smoke development from the fire may be made from the video in the accompanying DVDs.

Test 6 was designed before the test series was conducted as an open door test like Test 3, but with toluene fuel. Specified calculations were submitted for this test before the series was conducted. However, Test 6 was not conducted because of problems encountered with the building smoke scrubbing system. Test 17 was designed during the test series and conducted in lieu of Test 6. Therefore, specified calculations are not available for this test. An open calculation was conducted after the tests and is presented below.

5.11.1 Global Compartment Parameters

Figure 5.11.1 shows the HRR input to CFAST and FDS codes which was taken from experimental data, i.e. the fuel was shut off at 273 s. The HRR was not measured through calorimetry in this test because the compartment was sealed and had no openings.

Figure 5.11.2 shows the predicted hot gas layer development predicted by CFAST and FDS and measured in the experiment. CFAST, a two-zone model, calculates the interface height directly. However, the interface height is calculated from temperatures at a specific thermocouple tree in the experiment and FDS calculation. CFAST, a two-zone model predicts the interface height to reach the floor at ~ 260 s. FDS and experimental observation indicate that the interface layer height levels at ~ 0.5 m and ~ 1.0 m, respectively. The interface layer height is deduced through an algorithm using temperature data in thermocouple Tree 7. The algorithm used will result in erroneous predictions when a clear interface cannot be deduced from the temperature profile. Therefore, the measured and FDS prediction of interface height is erroneous. Video data indicates that the HGL reaches the floor at the fire at ~ 230 s. The HGL reaches the floor in most areas of the compartment before this time leaving a area of air around the fire. The uncertainty in the CFAST prediction for the time the HGL reaches the floor at the fire is + 12 %.

Figure 5.11.3 compares the compartment pressure predicted by CFAST and FDS with experimental observation. The CFAST and FDS calculations were conducted with the leakage measured just before the test. CFAST and FDS predict pressure peaks at ~ 180 s when the HRR reaches its peak value. A negative peak is predicted by both codes and measured at the end of the transient when the fuel is shut off. The uncertainties in the CFAST and FDS predictions are 47 % and - 25 %, respectively.

Figure 5.11.4 shows the hot gas layer (HGL) temperature. The HGL temperature increases rapidly when the fire is increased and the heat lost to the boundaries is less rapid than the increase in the HRR of the fire. The uncertainties of the CFAST and FDS predictions are + 30 % and + 25 %, respectively.

Figure 5.11.5 shows a comparison of the O2 concentration predicted by CFAST and FDS with experimental measurement. Comparisons for FDS are shown for locations at O2-1 and O2-2. The trend predicted by CFAST and FDS are similar to measurements at O2-1 and O2-2. The uncertainties of the CFAST and FDS predictions at O2-1 are - 37 % and + 19 %, respectively.

Figure 5.11.6 compares the concentration of CO2 predicted by CFAST and FDS in the HGL with experimental observation. CFAST and FDS predictions, and experimental observation show that the CO2 from the combustion process builds up in the compartment since there are no vents releasing gases. The uncertainties in the predictions of CFAST and FDS are - 14 % and - 23 %, respectively.

Figure 5.11.7 compares the concentration of smoke predicted by CFAST and FDS in the HGL with experimental observation. The measured smoke concentration increases upto 230 s when the fire was shut off. The measured smoke concentration for this test with toluene fuel is about 10 times larger (1000 mg/m3) than the concentrations (~ 100 mg/m3) in the other tests with heptane fuel. CFAST and FDS predict the smoke concentration for this test to be ~ 2000 mg/m3 at 230 s which is twice the measured value at the same point in time.

5.11.2 Local Gas Temperature

Figure 5.11.8 compares the gas temperatures in thermocouple Tree 2 predicted by FDS with measurement. The predicted and measured trends are similar. The uncertainties of the predictions at 2-1, 2-5, and 2-7 are + 20 %, + 17 %, and + 17 %.

Figure 5.11.9 compares the gas temperatures in thermocouple Tree 7 predicted by FDS with measurement. The predicted and measured trends are similar. The uncertainties of the predictions at 7-1, 7-5, and 7-10 are + 44 %, + 25 %, and - 8 %.

5.11.3 Heat Flux to Cable Targets

The following figures show comparisons of the incident radiative flux and the total heat flux predicted by CFAST and FDS with experiments. As indicated earlier, the total heat flux is measured by a gauge maintained at a constant temperature of ~ 75 C. The outputs form CFAST and FDS were modified to the extent possible to compare similar output quantities.

Figure 5.11.10 compares the radiative and total heat flux predicted by CFAST and FDS at Rad Gauge 1 and Total Gauge 2 with measurement. The trends of the predicted values are similar to experimental observation. The measured radiative flux increases rapidly upon ignition until ~ 100 s when the rate of increase becomes smaller possibly due to the descent of the HGL to the level of the gauges which shields the radiative heat flux from the fire to the gauge. This trend is predicted by FDS. The uncertainties in the predictions for CFAST at Rad Gauge 1 and Total Gauge 2 are + 178 % and + 68 %, respectively and; for FDS are + 56 % and + 16 %, respectively. Experimental observation indicates a larger convective heat flux (total heat flux - radiative heat flux) than predicted by both CFAST and FDS. The large discrepancy for CFAST prediction at Rad Gauge 1 is probably due to the use of the point source model and the height and orientation of the gauge (points to the floor).

Figure 5.11.11 compares the radiative and total heat flux predicted by CFAST and FDS at Rad Gauge 3 and Total Gauge 4 with measurement. The trends of the predicted values are similar to experimental observation. The measured radiative flux increases rapidly upon ignition until ~ 60 s when the rate of increase becomes smaller possibly due to the descent of the HGL to the gauges which shields the radiative heat flux from the fire to the gauge. This trend is predicted by FDS. The uncertainties in the predictions for CFAST at Rad Gauge 3 and Total Gauge 4 are + 108 % and + 38 %, respectively and; for FDS are + 38 % and + 4 %, respectively. Experimental observation indicates a larger convective heat flux (total heat flux - radiative heat flux) than predicted by both CFAST and FDS. The large discrepancy for CFAST prediction at Rad Gauge 3 is probably due to the use of the point source model, and the height and orientation (points to the floor) of the gauge.

Figure 5.11.12 compares the total heat flux predicted by CFAST and FDS at Total Gauge 6 with measurement. Generally, the trends of the predicted values are similar to experimental observation. The uncertainties in the predictions for CFAST and FDS for Total Gauge 6 are - 20 % and - 25 %, respectively.

Figure 5.11.13 compares the radiative and total heat flux predicted by CFAST and FDS at Rad Gauge 10 and Total Flux 9. The trends of the predicted values are similar to experimental observation. The measured radiative flux increases rapidly upon ignition until ~ 50 s when the rate of increase becomes smaller possibly due to the descent of the HGL to the gauges which shields the radiative heat flux from the fire to the gauge. This trend is predicted by FDS and CFAST. The uncertainties in the predictions for CFAST at Rad Gauge 10 and Total Gauge 9 are + 8 % and - 13 %, respectively and; for FDS are - 28 % and - 38 %, respectively.

Interpretation of experimental results, and comparison of predictions with measurement, of radiative and total heat flux is complicated by the various components of radiative heat flux from the fire, hot gas, and hot wall surfaces. Generally, experimental observations indicate higher convective heat fluxes than predicted by the codes.

5.11.4 Cable Temperature

Experimental measurements of cable temperatures were not available for this test.

5.11.5 Heat Flux to Walls

Experimental measurements of heat flux to walls were not available for this test.

5.11.6 Wall Temperature

Figure 5.11.14 shows a comparison of the wall temperatures predicted by CFAST with experimental measurements. Generally, the trends of the predicted values are similar to experimental observation. CFAST under estimates the ceiling temperature by a large amount because it uses a point source model for the fire. The uncertainties of the predictions by CFAST for TC East U-4-2, TC West U-4-2, TC Ceiling C-5-2, and TC Floor U-8-2 are 0 %, - 3 %, - 64 %, and + 155 %, respectively.

Figure 5.11.15 shows a comparison of the wall temperatures predicted by FDS with experimental measurements. The trends predicted by FDS are similar to experimental observation. The uncertainties of the predictions by FDS for TC East U-4-2, TC West U-4-2, TC Ceiling C-5-2, and TC Floor U-8-2 are + 25 %, + 4 %, - 6 % and + 45 %, respectively.

5.11.7 Conclusion

CFAST and FDS predictions were similar to experimental observations for most parameters. Global parameters such as the HGL temperature, interface height, O2, and CO2 , were within 37 % and 25 % of experimental values for CFAST and FDS, respectively. The local gas temperatures in the compartment predicted by FDS were within 44 % of experimental observations.

The heat flux to the cables predicted by CFAST and FDS deviated by as much as 178 % and 56 % from experimental observation, respectively. Experimental data for cable surface temperature and heat flux to the walls was not available for this test. The wall surface temperatures predicted by CFAST and FDS deviated by as much as 155 % and 45 % from experimental observation, respectively. The large discrepancy for the CFAST prediction of radiative heat flux is due to the use of the point source model in the code. The large discrepancy for the wall temperature is possibly due to an error in the code user interface.

5.12 Test 18

Test 18 was designed as a variation of Test 15 to provide data to determine the predictive capability of models for scenarios with well-ventilated conditions sustaining the fire, with the fire directly under cable targets. The peak HRR was 1180 kW with a heptane fire located 1.55 m from the south wall and 1.5 m east of the centerline directly under cable B. This test is similar to Test 15, except the fire was located east of the centerline compared to being located at the center between the east and west walls in Test 15. The door was open during this test and the mechanical ventilation was turned off with the supply and exhaust vents sealed. XPE cable type was installed during this test.

The fire diameter for this test was about 1 m through observation of the fire pan after the test. The flame was observed to reach the ceiling of the compartment. There was no visible tilt of the fire toward the wall even though the fire was near the south wall. The oxygen near the fire (sensor O2-2) was maintained at ambient conditions through the transient by the air flow into the compartment through the open door, and the test was run to the planned completion time of 26 min. The smoke layer in the compartment was steady with slight oscillations of wave-like motion in the layer. Further observations of the smoke layer development may be made from the videos in the accompanying DVDs. The average HGL temperature reached 227 C during the peak of the transient. There was extensive damage to the cables, including combustion in localized areas, with more damage to the control cables compared with the power cables (see Figures 5.18 and 5.19). The inside insulators of the power cables were intact at the end of the transient, whereas the copper wires were visible in the control cables. A thin whitish layer formed underneath the HGL possibly due to off-gases from combustion of the cables, and char from combusted cables was observed to fall to the floor during the transient. The smoke exhausting through the door also appeared to be whitish. The heating and combustion of the cables may be observed through the infrared camera recordings in the accompanying DVD. The videos did not appear to indicate any presence of flame spread during the transient.

As indicated, this test was designed to examine the nature of combustion of the cables directly under a fire, and any subsequent flame spread, as opposed to evaluating the predictive capabilities of the fire models. Therefore, an evaluation of the predictive capability of the models for this test is not presented here. The uncertainties in the code predictions of cable temperatures and fluxes during the transient will be the same as those for Test 15.

6 General Recommendations and Conclusions

The following provides conclusions and general recommendations as a result of this validation study.

6.1 Capabilities

Both CFAST and FDS demonstrated capabilities for modeling the phenomena in the transients investigated in this validation study. Generally, the prediction of open door tests is more simple and accurate. This is because the extinction models in CFAST and FDS employ simple algorithms for predicting fire extinction. However, even with these simple models, the codes provided fairly accurate predictions of fire extinction for closed door scenarios without mechanical ventilation. This is in part due to the accurate prediction of oxygen concentrations in most cases.

Generally, the predictions of global parameters such as HGL temperature, interface height, CO2, O2, CO, and smoke concentrations, and door heat and mass flows are more accurate than the prediction of heat fluxes and target responses. Tables 5.1 to 5.6 provide the errors in the predictions of each specific parameter for each test. The sub-models in both codes for predicting global parameters are generally robust.

6.2 Limitations

6.2.1 Extinction Models in CFAST and FDS

Both codes employ simple algorithms for fire behavior in under ventilated conditions. Although the predictions of fire extinction were reasonably good for some scenarios, the codes have difficulty predicting the mixing and local oxygen concentrations, especially for forced ventilation conditions. The lack of ability to model the coupling of the compartment with the mechanical ventilation system results in errors in the predicted compartment pressure, ventilation flowrates, and O2 concentration as discussed in Section 3.2.3.

For example, Figure 5.1.4 shows a comparison of the O2 concentration predicted by CFAST and FDS with experimental measurement for Test 1 without forced ventilation. The trends predicted by CFAST and FDS are similar but measurements show oscillations in the O2 concentration near the fire which is not predicted by CFAST or FDS. These oscillations are possibly due to the lack of complete mixing of the hot gas that results in pockets of the gas containing higher levels of O2. The uncertainties of the CFAST and FDS predictions are - 55 % and - 55 %, respectively which is quite high.

Again, Figure 5.2.5 and Figure 5.7.5 show comparisons of the O2 concentration predicted by CFAST and FDS with experimental the measurement for Test 2 and Test 13. Although the trends predicted by CFAST and FDS are similar to measurements, large oscillations in the oxygen concentration near the fire are not predicted by CFAST or FDS. These oscillations occur after the HGL has reached the floor.

Figure 5.4.6 shows a comparison of the O2 concentration predicted by CFAST and FDS with experimental values for Test 4 with forced ventilation. The trends predicted by CFAST for the HGL and FDS for the oxygen concentration near the fire are similar to measurements except a more rapid decrease in oxygen concentration is observed in the experiment than predicted by both codes. In fact, the FDS predicted concentration at O2-2 does not reach 15 %. Although the fire was terminated at 838 s due to under ventilation, the LOLs used in CFAST and FDS did not terminate the fire (see Figure 5.4.1) during the 26-minute transient. This comparison indicates the importance of the prediction of local oxygen concentrations, and sensitivity to the LOL for predicting under-ventilated conditions and fire extinction.

The codes have difficulty predicting the mixing and local oxygen concentrations, especially for forced ventilation conditions. Since both codes employ simple algorithms for fire behavior in under ventilated conditions, this leads to errors in the prediction of fire extinction.

6.2.2 Prediction of Combustion Products for Under Ventilated Fires by CFAST and FDS

The prediction of carbon monoxide and smoke, products of incomplete combustion, posed a challenge for the closed door experiments in which the fire became under ventilated. Both, CFAST and FDS do not account for the effects of under ventilation on carbon monoxide or smoke production. A constant yield for the quantities is used by the codes through the transient, whereas in reality the prediction of these species changes with the availability of oxygen during the combustion process. The smoke yield used in the calculations may also be dependent on the size of the fire.

Figure 5.7.7, 5.2.7, and 5.4.8 compare the concentration of CO predicted by CFAST and FDS in the HGL with experimental observation for Test 13, 2, and 4. In Figure 5.7.7 the trends of the predicted values are similar to experimental observation until ~ 236 s when measurement indicates a higher rate of increase in CO concentration. The CFAST and FDS combustion models are simple and do not include the effect of O2 concentrations on the CO production. The codes use a constant CO yield through the transient. Therefore, both codes show an increase in the CO level at the same rate through the transient. However, the fire becomes under ventilated at ~ 236 s at which point the yield of CO production increases as the measurement shows. The CFAST and FDS codes cannot predict the effects of under ventilation of a fire on the CO produced.

Figure 5.1.6, 5.2.8, 5.4.9, 5.7.8, and 5.11.7 compare the concentration of smoke predicted by CFAST and FDS in the HGL with experimental observation for Tests 1, 2, 4, 13, and 17. For example, in Figure 5.2.8 for Test 2 the experimental observation indicates the smoke concentration increases to its peak value at ~465 s and decreases by about 30 % to the point when the fuel is shut off at ~ 630 s. This peak and similar other peaks in smoke production in the figures for the other tests early in the transient is probably from the under ventilation and decrease in the HRR of the fire. The simple combustion models in CFAST and FDS do not predict this observed trend. Also a comparison of the figures shows that the smoke yield used is more accurate for the large fire in Test 13, as opposed to the smaller fires in Tests 1, 2, and 4.

CFAST and FDS do not account for the effects of under ventilation on carbon monoxide or smoke production. The constant yield for the quantities used by the codes through the transient leads to large inaccuracies in the prediction of these combustion products for under ventilated fires. Also, the amount of smoke produced as a function of the size of the fire is not modeled in the codes.

6.2.3 Modeling of Mechanical Ventilation Systems with CFAST and FDS

Figure 5.4.2 compares the compartment pressure predicted by CFAST and FDS with experimental observation for Test 4 with forced ventilation. The CFAST and FDS calculations were conducted with the leakage for a closed compartment and does not account for the vents of the mechanical ventilation system. CFAST and FDS do not have the capability to model the details of a mechanical ventilation system and its feedback on compartment pressure during the build up of the fire. Therefore, as shown in Figure 5.4.2, the CFAST and FDS predictions of compartment pressure is much higher than observed in the experiment.

Figure 5.4.4 shows a comparison of the vent flows predicted by CFAST and FDS with experimental observation for Test 4. The supply mass flow predicted by CFAST and FDS remain constant through the transient since the codes do not simulate the feedback from the ventilation system. The exhaust mass flow decreases with time only due to the increase in the temperature of the hot gas. However, as shown in the figure, the supply flowrate observed in the experiment quickly decreases at the beginning of the transient due to the pressure build up in the compartment. On the other hand, the measured exhaust flowrate is seen to increase at the beginning of the transient due to the pressurization of the compartment and then decreasing to a steady level. This figure illustrates the impact of the lack of the ability of the codes to include the coupling between the compartment and the mechanical ventilation system. Figure 5.5.5 for Test 5, an open door test, also shows similar trends and issues with the code predictions. It is difficult to realistically model the compartment fire scenario with mechanical ventilation without including a model of the coupling between the two. This limitation is also tied to the prediction of fire extinction, as discussed above.

6.2.4 Heat Flux Models in CFAST and FDS

Large inaccuracies were observed in the prediction of heat fluxes by CFAST and FDS. These inaccuracies are much larger than the uncertainties for the heat flux due measurement uncertainties. CFAST utilizes a point source model and predicts unrealistically high fluxes for gauge locations near and pointing toward the floor. The predictions of both components of heat flux, radiative and convective, have large errors depending on the location and orientation of the gauges, and the convective heat flux is under predicted in many of the transients. There are numerous plots presented in Chapter 5 that illustrate the above errors in the predictions. The following provides discussion of some of the plots, as examples.

Figures 5.1.11 and 5.2.12 compare the radiative and total heat flux predicted by CFAST and FDS. The error in the CFAST prediction of the radiative flux is ~ 150 % for both cases due to the use of the point source model in the code. Also noted in these two figures, a large convective flux (total - radiative) is measured but not predicted by the codes. This similar observation can be noted by examining similar plots for many other gauges and tests. Figures 5.3.10 to 5.3.13 show similar errors in the flux predictions for an open door test, and Figures 5.7.12 to 5.7.15 also show these errors for a large fire (2330 kW) in Test 13. The errors in the flux predictions for CFAST and FDS can be a high as 150 % and 47 %, respectively. Tables 5.1 to 5.6 provide the errors for the predictions for several gauges and tests. The errors in the FDS predictions are generally larger for gauges that point toward the fire, indicating larger errors in the predictions of radiative heat flux from the fire. The error in the prediction of the convective heat flux also seems to have a directional trend, a smaller error is noted for gauges pointing toward the floor in a horizontal direction. Figures 5.11.10 to 5.11.13 show similar trends in the errors for heat flux in Test 17 with toluene fuel.

Figures 5.8.16 and 5.8.17 show the measurements and predictions of the cable temperature in the vertical cable tray for Test 14 where the fire is near the tray. Measurements indicate that the peak cable temperature is highest at TS 32, which is at 0.7 m from the floor under the HGL interface, however, FDS predicts the peak cable temperature to increase with height in the cable tray. Again, this is due to the under prediction of the radiative flux from the fire to the cables by FDS. The prediction of the spatial flux and temperature distribution in vertical cable trays when fires sources are in its immediate vicinity is challenging and can be erroneous, even for FDS.

6.2.5 Target Models in CFAST and FDS

Large uncertainties are noted in the prediction of cable and walls temperatures by CFAST and FDS. A detailed heat transfer model for the cables and the trays used in the experiments will be fairly complex. The CFAST and FDS fire models are not capable of modeling complex multi-conductor cables, or cable tray configurations. The cable targets in these models are represented as rectangular slabs, the slabs were assumed to be of the same thickness as the cables. These limitations of CFAST and FDS for modeling cable targets were noted in ICFMP Benchmark Exercise # 1 [Dey, 2002].

Numerous plots are presented in Chapter 5 comparing the CFAST and FDS predictions of cable and wall temperatures with measurement. Although the temperature trends are predicted by both codes, there are considerable discrepancies in the peak values. Tables 5.1 to 5.6 tabulate the predictions and the uncertainties in the predictions. It should be noted that the thermal inertia of the cables reduce magnitude of the inaccuracies caused by the crude target models on the cable temperature predictions.

6.2.6 Prediction of Near Field Effects by FDS

Large uncertainties were observed in the prediction of gas temperatures and fluxes in the plume region by FDS. Certain increases and oscillations in the hot gas temperature or target temperature in localized areas were observed. Some of these oscillations are due to the movement of the fire plume, particularly if the fire is under ventilated. Oscillations in the local oxygen concentration due to the incomplete mixing of gases in closed compartment experiments were also observed. Prediction of these localized phenomena is difficult, even with a CFD code like FDS. The evaluation of target response in or near the fire can be challenging due to plume tilting and behavior.

Figures 5.9.1 and 5.9.2 show a comparison of the predicted trends of the hot gas temperature profiles in and near the fire plume with experimental measurement. Large discrepancies between FDS predictions and experimental measurements are noted in Figure 5.9.1. However, it should also be noted there are large uncertainties associated with the temperatures measured by the thermocouples in the fire plume. Figure 5.9.2 shows a comparison of the predicted and measured temperatures at Tree 3-9 near Cable Targets C and D, and Tree 5-6 near Cable Targets A and F. The uncertainties of the predictions at these locations outside the fire plume are less than at Tree 4 in the fire plume. The uncertainty is larger for Tree 5-6 because it is possibly in the flaming region. The oscillations observed in the measured temperature at Tree 5-6 indicate the movement of the flame in and out of that region. FDS is very limited in its ability to accurately predict gas temperatures in the plume and near-field region.

Figures 5.9.5 to 5.9.7 show a comparison of the predicted heat fluxes to the cables in the plume region with experimental measurement. Figure 5.9.6 shows that the measured fluxes at Gauges 3 and 4 in the fire plume is dominated by the radiative flux. The flux peaks at ~ 175 s when the HGL descends to the level of the gauges and shields the radiative flux from the fire to the gauges. Figure 5.9.7 shows a similar trend for measurements at Gauges 5 and 6, but the flux is dominated by the convective component due to the orientation of the gauges. CFAST uses a point source model and is not capable of predicting temperatures and fluxes within the fire plume. FDS predicts some of the trends discussed above to a much smaller degree, but grossly under predicts the radiative and convective fluxes in the plume region.

Figure 5.2.9 for Test 2 is an example of the movement of the fire plume which is not captured by FDS. The measured temperature at Tree 2-7 shows large oscillations due to the movement of the fire plume, particularly as it becomes under ventilated. These large oscillations are not observed in the FDS predictions. Similar oscillations at Tree 2-7 are noted for Test 4 in Figure 5.4.11, and for Test 13 in Figure 5.7.9.

Figures 5.1.4, 5.2.5, and 5.7.5 show comparisons of the O2 concentration predicted by CFAST and FDS with experimental measurement for Tests 1, 2, and 13. The figures show large oscillations in the oxygen concentration near the fire which are not predicted by FDS. These oscillations occur after the HGL has reached the floor and are possibly due to the lack of complete mixing of the hot gas which results in pockets of the gas containing higher levels of O2.

FDS is not capable of accurately predicting gas temperatures and fluxes in the plume region. Certain oscillations in the hot gas temperature or target temperature in localized areas were observed in the experiments, but not predicted by FDS. Some of these oscillations are due to the movement of the fire plume, particularly if the fire is under ventilated. Oscillations in the local oxygen concentration due to the incomplete mixing of gases in closed compartment experiments were also observed, but not predicted by FDS. Therefore, FDS cannot be used reliably to evaluate target response in or near the fire in the near-field region.

6.3 Benefits of Hand Calculations

In order to evaluate the benefits of hand calculations, specified calculations with FDTs [NRC, 2004] were conducted. A comparison of predicted results with measured values, and the uncertainties of the predicted values are tabulated in Table 6.1. The comparisons show that hand calculations could provide a method to quickly calculate global parameters (such as HGL temperature and interface height), as well as radiative fluxes to targets, using simple correlations. A large deviation is noted for the HGL temperature for Test 13 with a 2 MW fire, and for the radiative flux in Test 14 in which the fire was close to the flux gauge. Very large deviations for compartment pressure, and large deviations for smoke concentrations are noted. The correlation for compartment over pressure does not appear to predict realistic values. As discussed earlier, the prediction of smoke concentrations in closed compartment scenarios which become under ventilated is difficult, even for CFD codes. Therefore, the smoke concentrations predicted by FDTs which do not account for under ventilation are not realistic. Since the validity of the correlations in FDTs are narrow, the results are best suited for a screening calculation where a rough estimate is required, while acknowledging the answers may contain inaccuracies.

6.4 Need for Model Improvements

Although relatively good performance is noted above for most parameters, this validation study shows that the calculation of heat flux to targets and walls requires improvement for both CFAST and FDS. It should be noted that this validation test series was designed for and contains extensive data that can be used to improve the models for calculating heat fluxes in the codes.

The prediction of the effects of under ventilation on a fire is complex. Research is ongoing to improve the understanding of the basic combustion processes to be able to develop more robust combustion models. Although the performance of the simple combustion models in CFAST and FDS performed well in most of the scenarios examined here, further examination and development of combustion sub-models to cover a wide range of conditions is needed.

6.5 Need for Advanced Models

Simple hand calculations and zone models may be suitable for simple scenarios as in this validation study. CFD codes will be beneficial for calculating localized gas temperatures, e.g., near supply air from forced ventilation, to determine a more precise determination of target damage.

The computational requirements for CFD codes should be noted. The scenarios in this benchmark exercise required 68 hours - 189 hours to compute with FDS using different computers, whereas zone models can be executed in less than 10 s.

6.6 Need for Additional Test Programs

This test series provided a comprehensive data set for validating models for single compartment fire scenarios in nuclear power plants. As noted above, this test series was designed for and contains extensive data that can be used to improve the models for calculating heat fluxes. Therefore, other test programs for single compartment scenarios will be of limited benefit.

7 References

American Society of Testing and Materials, “Evaluating the Predictive Capability of Deterministic Fire Models,” ASTM E1355-05, West Conshohocken, PA (2005).

Dey, M., Ed., "International Collaborative Project to Evaluate Fire Models for Nuclear Power Plant Applications: International Panel Report on Benchmark Exercise # 1, Cable Tray Fires," U.S. Nuclear Regulatory Commission, NUREG-1758, June 2002, also National Institute of Standards and Technology, NISTIR-6872, June, 2002.

Hessling, W., "International Collaborative Project to Evaluate Fire Models for Nuclear Power Plant Applications: International Panel Report on Benchmark Exercise # 4, Large Fires in Compartments," to be published.

Institut de Radioprotection et de Sûreté Nucléaire (IRSN), France, “Probability Study Program on Fire Safety,” Laboratory on Research and Modeling of Fires, J. M. Such EF.30.15.R/96.442, 4/23/97.

Jones, W., Ed., “CFAST - Consolidated Model of Fire Growth and Smoke Transport (Version 5), National Institute of Standards and Technology, NIST Special Publication 1030, October 2004.

McGrattan, K., Ed., “Fire Dynamics Simulator (Version 4), Technical Reference Guide,” National Institute of Standards and Technology, NIST Special Publication 1018, September 2004.

Miles, S., "International Collaborative Project to Evaluate Fire Models for Nuclear Power Plant Applications: International Panel Report on Benchmark Exercise # 2, Pool Fires in Large Halls," Building Research Establishment Ltd., BRE Report Number 212214, May 2004.

Mitler, H. E., and Emmons, H. W., “Documentation for CFD V, the Fifth Harvard Computer Fire Code,” Harvard University, Division of Applied Sciences, Home Fire Project Technical Report No. 45, Cambridge, MA, Oct. 1981.

National Institute of Standards and Technology, “Report of Experimental Results for the International Fire Model Benchmarking and Validation Exercise # 3,” Hamins, A., et al, NIST Special Publication 1013, January 2005.

Riese, O., "International Collaborative Project to Evaluate Fire Models for Nuclear Power Plant Applications: International Panel Report on Benchmark Exercise # 5, Cable Tray Flame Spread," to be published.

U.S. Nuclear Regulatory Commission, “Investigation of Twenty-Foot Separation Distance as a Fire Protection Method as Specified in 10 CFR 50, Appendix R,” Douglas D. Cline, Walter A von Riesemann, James M. Chavez, NUREG/CR-3192, SAND83-0306, RP, October 1983.

U.S. Nuclear Regulatory Commission, “Enclosure Environment Characterization Testing for the Base Line Validation of Computer Fire Simulation Codes,” S. P. Nowlen, NUREG/CR 4681, SAND86-1296, RP, March 1987.

U.S. Nuclear Regulatory Commission, “An Experimental Investigation of Internally Ignited Fires in Nuclear Power Plant Control Cabinets,” J. M.Chavez, S. P. Nowlen, NUREG/CR-4527, SAND86-0336, Vol 2, November 1988.

U.S. Nuclear Regulatory Commission, "International Collaborative Project to Evaluate Fire Models for Nuclear Power Plant Applications: International Panel Report on Benchmark Exercise # 1, Cable Tray Fires," Dey, M., NUREG-1758, June, 2002.

U.S. Nuclear Regulatory Commission, " Fire Dynamics Tools (FDTs) Quantitative Fire Hazard Analysis Methods for the U.S. Nuclear Regulatory Commission Fire Protection Inspection Program," NUREG-1805, Washington DC, USA, November 2004.

U.S. Nuclear Regulatory Commission, "Validation of the CFAST and FDS Fire Models for Pool Fires in Multi-Level Turbine Halls in Nuclear Power Plants," Dey, M., NUREG-XXXX, April, 2005a, to be published.

U.S. Nuclear Regulatory Commission, "Validation of the CFAST and FDS Fire Models for Large Fires in Compartments," Dey, M, NUREG-XXXX, May, 2005b, to be published.

U.S. Nuclear Regulatory Commission, "Validation of the CFAST and FDS Fire Models for Cable Tray Flame Spread Experiments," Dey, M., NUREG-XXXX, May, 2005c, to be published.

Table 5.1 Summary of Predictions for Test 1
Specified Predictions

Parameter	Sensor	Model prediction at peak CFAST	Model prediction at peak FDS	Measured value at peak	Initial measured value	Uncertainty CFAST	Uncertainty FDS
Global Parameters							
HGL Temp. (avg.)-C	Tree 7	173.0	152.0	139.0	27.0	30%	12%
HGL Interface Ht - time to floor (s)	Fire videos	500.0	NA	510.0	NA	- 2 %	NA
Smoke Conc. - mg/m3 - NA	Smoke Obs./Conc.	NA					
O2 Conc. - Vol %	O2-1	12.2	12.8	15.2	20.7	-55%	-55%
CO2 Conc. - Vol %	CO2	4.8	4.6	3.9	0.0	23%	18%
CO Conc. - ppm	CO	NA					
Pressure - Pa	Comp P	113.0	42.0	59.0	0.0	92%	-29%
Flame Height - m	From fire videos	NA					
Local Gas Temperature							
Hot Gas Temp. (point values) - C	Tree 4.8		154.0	132.0	27.0		21%
	Tree 2-1		117.0	90.0	27.0		43%
	Tree 2-5		142.0	123.0	27.0		20%
	Tree 2-7		154.0	137.0	27.0		15%
	Tree 3-9		162.0	147.0	27.0		13%

	Tree 5-6		144.0	134.0	27.0		9%
	Tree 7-1		122.0	88.0	27.0		56%
	Tree 7-5		146.0	120.0	27.0		28%
Plume Temp.- C	NA						
Ceiling Jet Temp.-C	Tree 7-10		174.0	173.0	27.0		1%
Heat Flux to Cables							
Radiative Heat Flux to Cables - kW/m2	Cable Rad Flux Gauge 1	2.1	1.1	0.9	0.0	133%	22%
	Cable Rad Flux Gauge 3	2.2	1.4	1.1	0.0	100%	27%
	Cable Rad Flux Gauge 5	2.3	1.7	2.2	0.0	5%	-23%
	Cable Rad Flux Gauge 10	2.3	1.4	1.5	0.0	53%	-7%
Total Heat Flux to Cables - kW/m2	Cable Total Flux Gauge 2	2.4	1.5	1.6	0.0	50%	-6%
	Cable Total Flux Gauge 4	2.4	1.7	1.8	0.0	33%	-6%
	Cable Total Flux Gauge 6	2.4	1.9	2.8	0.0	-14%	-32%
	Cable Total Flux Gauge 9 - NA						
Cable Temperature							

Cable Surface Temp. - C	B-TS-14 (control cable)	141.0	104.0	130.0	27.0	11%	-25%
	TS-33 (vertical cable)	132.0	88.0	88.0	27.0	72%	0%
	E-TS-16 (slab)	141.0	104.0	137.0	27.0	4%	-30%
	D-TS-12 (cable in bundle/tray) -	NA					
	F-TS-20 (power cable)	115.0	87.0	106.0	27.0	11%	-24%
Heat Flux to Walls							
Total Heat Flux to Walls - kW/m2	East U-4	1.5	0.7	0.9	0.0	67%	-22%
	West U-4	1.5	0.7	0.9	0.0	67%	-22%
	Ceiling C-5	1.5	1.1	1.0	0.0	50%	10%
	Floor U-8	1.6	0.6	0.6	0.0	167%	0%
Wall Temperature							
Wall Surface Temp. - C	TC East U-4-2	144.0	111.0	84.0	27.0	105%	47%
	TC West U-4-2	144.0	111.0	81.0	27.0	117%	56%
	TC Ceiling C-5-2	144.0	156.0	187.0	27.0	-27%	-19%
	TC Floor U-8-2	144.0	89.0	57.0	27.0	290%	107%

Notes: NA - Not available or applicable. See main text for formula used to calculate uncertainty.

Table 5.2 Summary of Predictions for Test 2
Specified Predictions

Parameter	Sensor	Model prediction at peak		Measured value at peak	Initial measured value	Uncertainty	
		CFAST	FDS			CFAST	FDS
Global Parameters							
HGL Temp. (avg.)-C	Tree 7	273.0	244.0	235.0	27.0	18%	4%
HGL Interface Ht - time to floor (s)	Fire videos	230.0	NA	360.0	NA	- 36 % %	NA
Smoke Conc. - mg/m3	Smoke Obs./Conc.	185.0	185.0	122.0	0.0	52%	52%
O2 Conc. - Vol %	O2-1	10.1	11.4	12.0	20.7	-22%	-22%
CO2 Conc. - Vol %	CO2	6.0	5.5	6.0	0.0	0%	-8%
CO Conc. - ppm	CO	NA					
Pressure - Pa	Comp P	835.0	298.0	288.0	0.0	190%	3%
Flame Height - m	From fire videos	NA					
Local Gas Temperature							
Hot Gas Temp. (point values) - C	Tree 4.8		249.0	241.0	27.0		4%
	Tree 2-1		180.0	165.0	27.0		11%
	Tree 2-5		221.0	233.0	27.0		-6%
	Tree 2-7		257.0	262.0	27.0		-2%
	Tree 3-9		263.0	244.0	27.0		9%

	Tree 5-6		221.0	212.0	27.0		5%
	Tree 7-1		188.0	162.0	27.0		19%
	Tree 7-5		231.0	209.0	27.0		12%
Plume Temp.- C	NA						
Ceiling Jet Temp.-C	Tree 7-10		286.0	291.0	27.0		-2%
Heat Flux to Cables							
Radiative Heat Flux to Cables - kW/m2	Cable Rad Flux Gauge 1	4.7	2.6	1.8	0.0	161%	44%
	Cable Rad Flux Gauge 3	5.0	3.2	3.0	0.0	67%	7%
	Cable Rad Flux Gauge 5	5.0	4.5	6.0	0.0	-17%	-25%
	Cable Rad Flux Gauge 10	5.1	3.5	5.9	0.0	-14%	-41%
Total Heat Flux to Cables - kW/m2	Cable Total Flux Gauge 2	5.4	3.4	4.0	0.0	35%	-15%
	Cable Total Flux Gauge 4	5.4	3.9	5.0	0.0	8%	-22%
	Cable Total Flux Gauge 6	5.4	4.8	8.0	0.0	-32%	-40%
	Cable Total Flux Gauge 9 - NA						
Cable Temperature							

Cable Surface Temp. - C	B-TS-14 (control cable)	177.0	151.0	202.0	27.0	-14%	-29%
	TS-33 (vertical cable)	165.0	123.0	133.0	27.0	30%	-9%
	E-TS-16 (slab)	176.0	149.0	219.0	27.0	-22%	-36%
	D-TS-12 (cable in bundle/tray) -	166.0	134.0	154.0	27.0	9%	-16%
	F-TS-20 (power cable)	145.0	122.0	154.0	27.0	-7%	-25%
Heat Flux to Walls							
Total Heat Flux to Walls - kW/m2	East U-4	3.5	1.9	2.6	0	35%	-27%
	West U-4	3.5	1.9	2.6	0	35%	-27%
	Ceiling C-5						
	Floor U-8	3.5	1.6	1.6	0	119%	0%
Wall Temperature							
Wall Surface Temp. - C	TC East U-4-2	195.0	172.0	139.0	27.0	50%	29%
	TC West U-4-2	195.0	172.0	132.0	27.0	60%	38%
	TC Ceiling C-5-2	195.0	291.0	334.0	27.0	-45%	-14%
	TC Floor U-8-2	195.0	133.0	92.0	27.0	158%	63%

Notes: NA - Not available or applicable. See main text for formula used to calculate uncertainty.

Table 5.3 Summary of Predictions for Test 3
Specified Predictions

Parameter	Sensor	Model prediction at peak CFAST	Model prediction at peak FDS	Measured value at peak	Initial measured value	Uncertainty CFAST	Uncertainty FDS
Global Parameters							
HGL Temp. (avg.)-C	Tree 7	283.0	247.0	227.0	27.0	28%	10%
HGL Interface Ht -	Fire videos	1.1	1.0	1.3	3.8	- 8 %	- 12 %
Smoke Conc. - mg/m3 - NA	Smoke Obs./Conc.	120.0	144.0	115.0	0.0	4%	25%
O2 Conc. - Vol %	O2-1	NA					
CO2 Conc. - Vol %	CO2	2.6	2.6	3.1	0.0	-16%	-16%
CO Conc. - ppm	CO	NA					
Pressure - Pa	Comp P	-2.0	NA	-1.9	0.0	5%	NA
Flame Height - m	From fire videos	NA					
Local Gas Temperature							
Hot Gas Temp. (point values) - C	Tree 4.8		241.0	245.0	27.0		-2%
	Tree 2-1		91.0	83.0	27.0		14%
	Tree 2-5		227.0	220.0	27.0		4%
	Tree 2-7		246.0	268.0	27.0		-9%
	Tree 3-9		263.0	284.0	27.0		-8%
	Tree 5-6		229.0	236.0	27.0		-3%

	Tree 7-1		114.0	105.0	27.0		12%
	Tree 7-5		231.0	210.0	27.0		11%
Plume Temp.- C	NA						
Ceiling Jet Temp.-C	Tree 7-10		281.0	269.0	27.0		5%
Heat Flux to Cables							
Radiative Heat Flux to Cables - kW/m2	Cable Rad Flux Gauge 1	5.1	3.4	2.9	0.0	76%	17%
	Cable Rad Flux Gauge 3	5.5	4.2	4.4	0.0	25%	-5%
	Cable Rad Flux Gauge 5	5.6	4.8	5.5	0.0	2%	-13%
	Cable Rad Flux Gauge 10	6.0	3.8	4.9	0.0	22%	-22%
Total Heat Flux to Cables - kW/m2	Cable Total Flux Gauge 2	5.4	3.8	5.2	0.0	4%	-27%
	Cable Total Flux Gauge 4	5.6	4.4	6.8	0.0	-18%	-35%
	Cable Total Flux Gauge 6	5.6	4.8	9.0	0.0	-38%	-47%
	Cable Total Flux Gauge 9	6.0	3.7	6.4	0.0	-6%	-42%
Cable Temperature							
Cable Surface Temp. - C	B-TS-14 (control cable)	257.0	201.0	256.0	27.0	0%	-24%

	TS-33 (vertical cable)	254.0	153.0	199.0	27.0	32%	-27%
	E-TS-16 (slab)	NA					
	D-TS-12 (cable in bundle/tray) -	230.0	188.0	240.0	27.0	-5%	-24%
	F-TS-20 (power cable)	215.0	164.0	255.0	27.0	-18%	-40%
Heat Flux to Walls							
Total Heat Flux to Walls - kW/m2	East U-4	2.8	1.3	2.1	0.0	33%	-38%
	West U-4	2.8	1.3	1.9	0.0	47%	-32%
	Ceiling C-5	2.9	3.2	2.2	0.0	32%	45%
	Floor U-8	2.2	1	1.5	0.0	47%	-33%
Wall Temperature							
Wall Surface Temp. - C	TC East U-4-2	255.0	193.0	165.0	27.0	65%	20%
	TC West U-4-2	255.0	186.0	158.0	27.0	74%	21%
	TC Ceiling C-5-2	255.0	270.0	310.0	27.0	-19%	-14%
	TC Floor U-8-2	206.0	148.0	114.0	27.0	106%	39%

Notes: NA - Not available or applicable. See main text for formula used to calculate uncertainty.

Table 5.4 Summary of Predictions for Test 4
Specified Predictions

Parameter	Sensor	Model prediction at peak CFAST	Model prediction at peak FDS	Measured value at peak	Initial measured value	Uncertainty CFAST	Uncertainty FDS
Global Parameters							
HGL Temp. (avg.)-C	Tree 7	259.0	247.0	220.0	27.0	20%	14%
HGL Interface Ht - time to floor (s)	Fire videos	500.0	NA	510.0	0.0	- 2 %	NA
Smoke Conc. - mg/m3 - NA	Smoke Obs./Conc.	NA					
O2 Conc. - Vol %	O2-1	14.2	13.7	13.6	20.7	-8%	-1%
CO2 Conc. - Vol %	CO2	3.5	4.0	5.0	0.0	-30%	-20%
CO Conc. - ppm	CO	NA					
Pressure - Pa	Comp P	959.0	490.0	59.0	0.0	1525%	731%
Flame Height - m	From fire videos	NA					
Local Gas Temperature							
Hot Gas Temp. (point values) - C	Tree 4.8		246.0	159.0	27.0		66%
	Tree 2-1		166.0	177.0	27.0		-7%
	Tree 2-5		226.0	213.0	27.0		7%
	Tree 2-7		252.0	257.0	27.0		-2%
	Tree 3-9		267.0	218.0	27.0		26%

	Tree 5-6		208.0	210.0	27.0		-1%
	Tree 7-1		163.0	158.0	27.0		4%
	Tree 7-5		233.0	198.0	27.0		20%
Plume Temp.- C	NA						
Ceiling Jet Temp.-C	Tree 7-10		274.0	253.0	27.0		9%
Heat Flux to Cables							
Radiative Heat Flux to Cables - kW/m2	Cable Rad Flux Gauge 1	4.3	2.6	2.1	0.0	105%	24%
	Cable Rad Flux Gauge 3	4.6	3.4	3.0	0.0	53%	13%
	Cable Rad Flux Gauge 5	4.6	4.1	5.2	0.0	-12%	-21%
	Cable Rad Flux Gauge 10	5.9	4.7	5.0	0.0	18%	-6%
Total Heat Flux to Cables - kW/m2	Cable Total Flux Gauge 2	4.8	3.2	5.0	0.0	-4%	-36%
	Cable Total Flux Gauge 4	4.9	3.9	5.1	0.0	-4%	-24%
	Cable Total Flux Gauge 6	4.8	4.4	7.6	0.0	-37%	-42%
	Cable Total Flux Gauge 9	6.0	4.9	6.0	0.0	0%	-18%
Cable Temperature							

Cable Surface Temp. - C	B-TS-14 (control cable)	195.0	162.0	174.0	27.0	14%	-8%
	TS-33 (vertical cable)	180.0	140.0	151.0	27.0	23%	-9%
	E-TS-16 (slab)				27.0	0%	0%
	D-TS-12 (cable in bundle/tray) -	171.0	157.0	139.0	27.0	29%	16%
	F-TS-20 (power cable)	160.0	125.0	173.0	27.0	-9%	-33%
Heat Flux to Walls							
Total Heat Flux to Walls - kW/m2	East U-4	2.8	1.6	2.5	0.0	12%	-36%
	West U-4	2.8	1.6	2.5	0.0	12%	-36%
	Ceiling C-5	2.8	2.7	2.7	0.0	4%	0%
	Floor U-8	2.8	1.3	1.4	0.0	100%	-7%
Wall Temperature							
Wall Surface Temp. - C	TC East U-4-2	204.0	173.0	140.0	27.0	57%	29%
	TC West U-4-2	204.0	180.0	136.0	27.0	62%	40%
	TC Ceiling C-5-2	204.0	260.0	349.0	27.0	-45%	-28%
	TC Floor U-8-2	204.0	130.0	95.0	27.0	160%	51%

Notes: NA - Not available or applicable. See main text for formula used to calculate uncertainty.

Table 5.5 Summary of Predictions for Test 13
Specified Predictions

Parameter	Sensor	Model prediction at peak CFAST	Model prediction at peak FDS	Measured value at peak	Initial measured value	Uncertainty CFAST	Uncertainty FDS
Global Parameters							
HGL Temp. (avg.)-C	Tree 7	352.0	328.0	288.0	27.0	25%	15%
HGL Interface Ht	Fire videos - time to floor (s)	180.0	NA	270.0	0.0	33%	NA
Smoke Conc. - mg/m3	Smoke Obs./Conc. (Upto 300 s)	245.0	265.0	226.0	0.0	8%	17%
O2 Conc. - Vol %	O2-1	9.6	10.5	12.7	20.7	-39%	6%
CO2 Conc. - Vol %	CO2	5.6	4.7	5.3	0.0	6%	-11%
CO Conc. - ppm	CO (upto 230 s)	114.0	100.0	109.0	0.0	5%	-8%
Pressure - Pa	Comp P	945.0	343.0	240.0	0.0	294%	43%
Flame Height - m	From fire videos	NA					
Local Gas Temperature							
Hot Gas Temp. (point values) - C	Tree 4.8		342.0	274.0	27.0		28%
	Tree 2-1		249.0	218.0	27.0		16%
	Tree 2-5		293.0	278.0	27.0		6%
	Tree 2-7		331.0	399.0	27.0		-18%

	Tree 3-9		360.0	357.0	27.0		1%
	Tree 5-6		305.0	270.0	27.0		14%
	Tree 7-1		254.0	211.0	27.0		23%
	Tree 7-5		310.0	261.0	27.0		21%
Plume Temp.- C	NA						
Ceiling Jet Temp.-C	Tree 7-10		387.0	377.0	27.0		3%
Heat Flux to Cables							
Radiative Heat Flux to Cables - kW/m2	Cable Rad Flux Gauge 1	7.9	3.7	2.9	0.0	172%	28%
	Cable Rad Flux Gauge 3	8.4	5.2	4.8	0.0	75%	8%
	Cable Rad Flux Gauge 5	8.5	9.0	10.4	0.0	-18%	-13%
	Cable Rad Flux Gauge 10	8.8	6.7	10.0	0.0	-12%	-33%
Total Heat Flux to Cables - kW/m2	Cable Total Flux Gauge 2	8.9	6.2	7.9	0.0	13%	-22%
	Cable Total Flux Gauge 4	9.2	7.3	8.0	0.0	15%	-9%
	Cable Total Flux Gauge 6	9.2	9.3	14.0	0.0	-34%	-34%
	Cable Total Flux Gauge 9	9.5	7.6	10.3	0.0	-8%	-26%
Cable Temperature							

Cable Surface Temp. - C	B-TS-14 (control cable)	201.0	204.0	219.0	27.0	-9%	-43%
	TS-33 (vertical cable)	183.0	164.0	167.0	27.0	11%	-2%
	E-TS-16 (slab)	NA					
	D-TS-12 (cable in bundle/tray)	197.0	210.0	207.0	27.0	-6%	2%
	F-TS-20 (power cable)	167.0	163.0	178.0	27.0	-7%	-10%
Heat Flux to Walls							
Total Heat Flux to Walls - kW/m2	East U-4 - NA	NA					
	West U-4 - NA	NA					
	Ceiling C-5 - NA	NA					
	Floor U-8 - NA	NA					
Wall Temperature							
Wall Surface Temp. - C	TC East U-4-2	230.0	237.0	174.0	27.0	38%	43%
	TC West U-4-2	230.0	237.0	174.0	27.0	38%	43%
	TC Ceiling C-5-2	230.0	430.0	535.0	27.0	-60%	-21%
	TC Floor U-8-2	230.0	179.0	120.0	27.0	118%	63%

Notes: NA - Not available or applicable. See main text for formula used to calculate uncertainty.

Table 5.6 Summary of Predictions for Test 17

Parameter	Sensor	Model prediction at peak CFAST	Model prediction at peak FDS	Measured value at peak	Initial measured value	Uncertainty CFAST	Uncertainty FDS
Global Parameters							
HGL Temp. (avg.)-C	Tree 7 - NA	187.0	181.0	150.0	27.0	30%	25%
HGL Interface Ht	Fire videos time to floor - s	260.0	NA	230.0	0.0	16%	NA
Smoke Conc. - mg/m3	Smoke Obs./Conc.	NA					
O2 Conc. - Vol %	O2-1	17.0	17.7	18.0	20.7	-37%	19%
CO2 Conc. - Vol %	CO2	1.9	1.7	2.2	0.0	-14%	-23%
CO Conc. - ppm	CO	NA					
Pressure - Pa	Comp P	294.0	151.0	200.0	0.0	47%	-25%
Flame Height - m	From fire videos						
Local Gas Temperatures							
Hot Gas Temp. (point values) - C	Tree 4.8	NA					
	Tree 2-1		122.0	106.0	27.0		20%
	Tree 2-5		163.0	143.0	27.0		17%
	Tree 2-7		203.0	177.0	27.0		17%
	Tree 3-9		192.0	180.0	27.0		8%
	Tree 5-6		162.0	145.0	27.0		14%

	Tree 7-1		119.0	91.0	27.0		44%
	Tree 7-5		167.0	139.0	27.0		25%
Plume Temp.- C	NA						
Ceiling Jet Temp.-C	Tree 7-10		168.0	180.0	27.0		-8%
Heat Flux to Cables							
Radiative Heat Flux to Cables - kW/m2	Cable Rad Flux Gauge 1	2.5	1.4	0.9	0.0	178%	56%
	Cable Rad Flux Gauge 3	2.7	1.8	1.3	0.0	108%	38%
	Cable Rad Flux Gauge 5	NA					
	Cable Rad Flux Gauge 10	2.7	1.8	2.5	0.0	8%	-28%
Total Heat Flux to Cables - kW/m2	Cable Total Flux Gauge 2	3.2	2.2	1.9	0.0	68%	16%
	Cable Total Flux Gauge 4	3.3	2.5	2.4	0.0	38%	4%
	Cable Total Flux Gauge 6	3.2	3.0	4.0	0.0	-20%	-25%
	Cable Total Flux Gauge 9	3.2	2.3	3.2	0.0	-13%	-38%
Cable Temperature							
Cable Surface Temp. - C	B-TS-14 (control cable)	NA					

	TS-33 (vertical cable)	NA					
	E-TS-16 (slab)	NA					
	D-TS-12 (cable in bundle/tray)	NA					
	F-TS-20 (power cable)				27.0	0%	0%
Heat Flux to Walls							
Total Heat Flux to Walls - kW/m2 - NA	East U-4						
	West U-4			NA			
	Ceiling C-5						
	Floor U-8						
Wall Temperature							
Wall Surface Temp. - C	TC East U-4-2	84.0	98.0	84.0	27.0	0%	25%
	TC West U-4-2	93.0	98.0	95.0	27.0	-3%	4%
	TC Ceiling C-5-2	99.0	214.0	226.0	27.0	-64%	-6%
	TC Floor U-8-2	83.0	59.0	49.0	27.0	155%	45%

Notes: NA - Not available or applicable. See main text for formula used to calculate uncertainty.

Table 6.1 Summary of Predictions with FDTs

Parameter	Sensor	Model Prediction	Measured Value at Peak	Initial Measured Value	Uncertainty %
Test 1					
HGL Temp. - C @ 1200 s	Tree 7	133.00	139.00	27.00	44%
Interface Ht - m	Tree 7	NA			
Smoke Conc. - mg/m3 @ 1200 s	Smoke Obs./Conc.	277.00	38.00	0.00	??
Pressure - Pa	Comp P	43450.00	58.00	0.00	500%
Heat Flux to Targets - kW/m2	Rad Gauge 5	1.20	3.80	0.00	50%
	Rad Gauge 10	1.90	1.50	0.00	??
Test 2					
HGL Temp. - C	Tree 7	333.00	235.00	27.00	??
Interface Ht - m	Tree 7	NA			
Smoke Conc. - mg/m3 @ 625 s	Smoke Obs./Conc.	414.00	122.00	0.00	-283%
Pressure - Pa	Comp P	124150.00	288.00	0.00	1509%
Heat Flux to Targets - kW/m2	Rad Gauge 5	7.10	6.00	0.00	-1738%
	Rad Gauge 10	5.60	5.90	0.00	5040%

Test 3					
HGL Temp. - C @ 1200 s	Tree 7	288.00	227.00	27.00	-3260%
Interface Ht - m @ 60 s	Tree 7	1.77	1.31	3.82	-666%
Smoke Conc. - mg/m3	Smoke Obs./Conc.	NA			
Pressure - Pa	Comp P	NA			
Heat Flux to Targets - kW/m2	Rad Gauge 5	7.10	5.50	0.00	??
	Rad Gauge 10	5.60	4.90	0.00	340%
Test 4					
HGL Temp. - C	Tree 7	327.00	220.00	27.00	-45%
Interface Ht - m	Tree 7	NA			
Smoke Conc. - mg/m3	Smoke Obs./Conc.	NA			
Pressure - Pa	Comp P	NA			
Heat Flux to Targets - kW/m2	Rad Gauge 5	7.10	5.20	0.00	-12%
	Rad Gauge 10	5.60	5.00	0.00	-100%
Test 13					
HGL Temp. - C	Tree 7	626.00	288.00	27.00	-275%
Interface Ht - m	Tree 7	NA			

Smoke Conc. - mg/m3 @ 365 s	Smoke Obs./Conc.	1058.00	266.00	0.00	??
Pressure - Pa	Comp P	248300.00	221.00	0.00	78%
Heat Flux to Targets - kW/m2	Rad Gauge 5	13.90	10.40	0.00	-73%
	Rad Gauge 10	8.00	10.00	0.00	??
Test 14					
HGL Temp. - C	Tree 7	Same as Test 3			
Interface Ht - m	Tree 7	Same as Test 3			
Smoke Conc. - mg/m3	Smoke Obs./Conc.	NA			
Pressure - Pa	Comp P	NA			
Heat Flux to Targets - kW/m2	Rad Gauge 5	3.40	4.00	0.00	94%
	Rad Gauge 10	18.10	7.00	0.00	55%
Test 15					
HGL Temp. - C	Tree 7	Same as Test 3			
Interface Ht - m	Tree 7	Same as Test 3			
Smoke Conc. - mg/m3	Smoke Obs./Conc.	NA			
Pressure - Pa	Comp P	NA			
Heat Flux to Targets	Rad Gauge 5	NA			
	Rad Gauge 10	2.10	3.60	0.00	??

Figures for Test 1

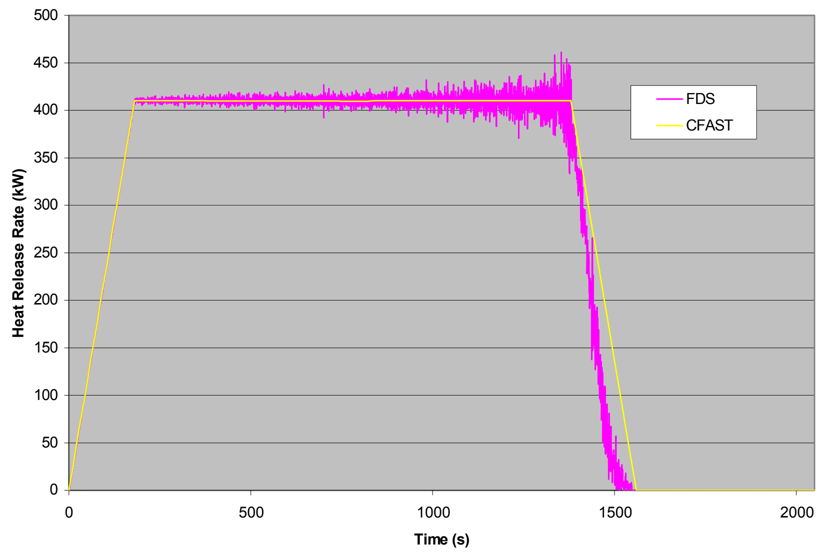

Figure 3.1.1 Heat Release Rate - Test 1

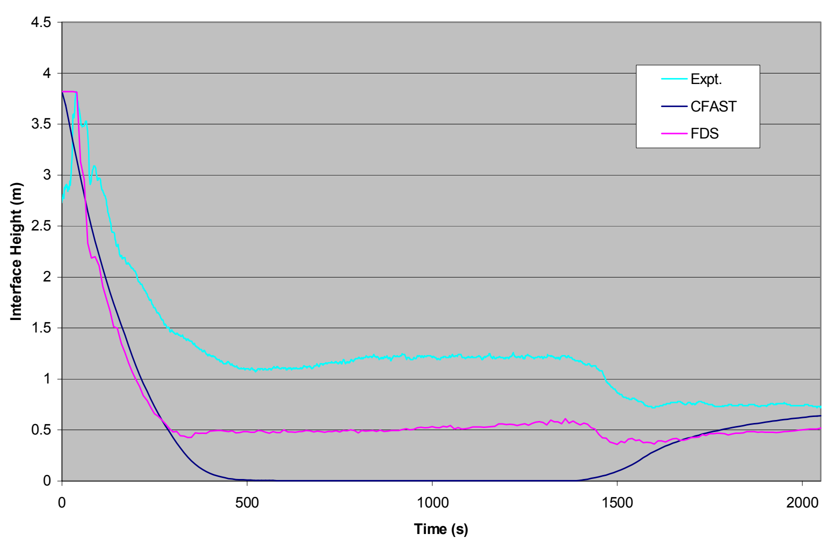

Figure 5.1.2 Hot Gas Layer Development - Test 1

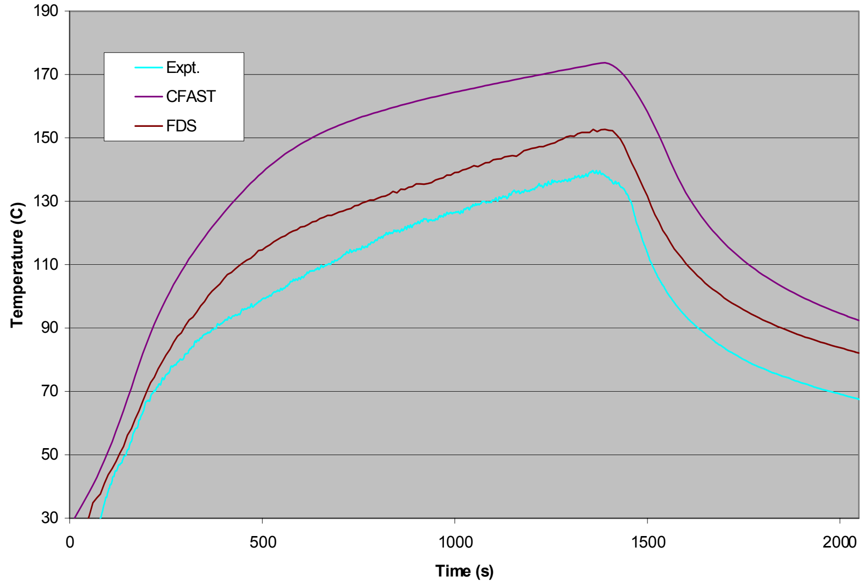

Figure 5.1.3 Hot Gas Layer Temperature - Test 1

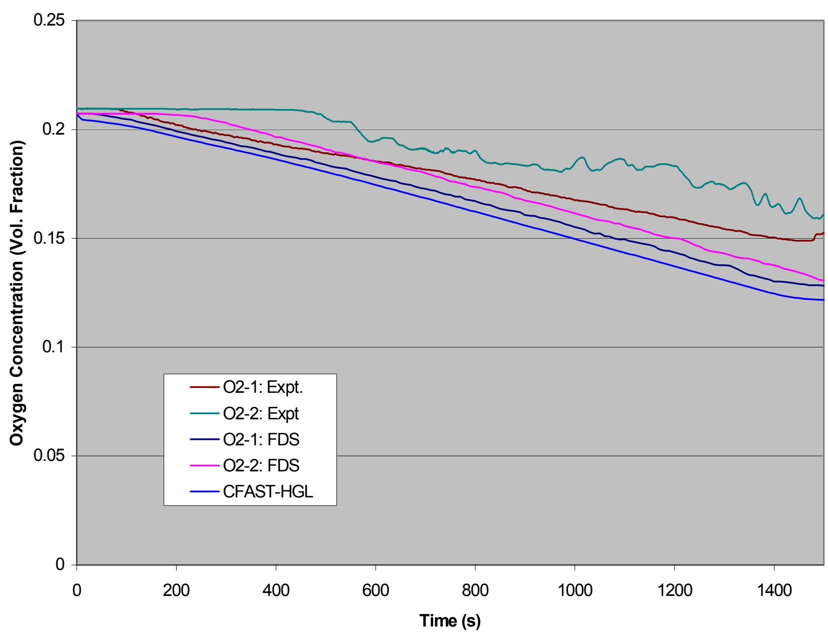

Figure 5.1.4 Oxygen Depletion - Test 1

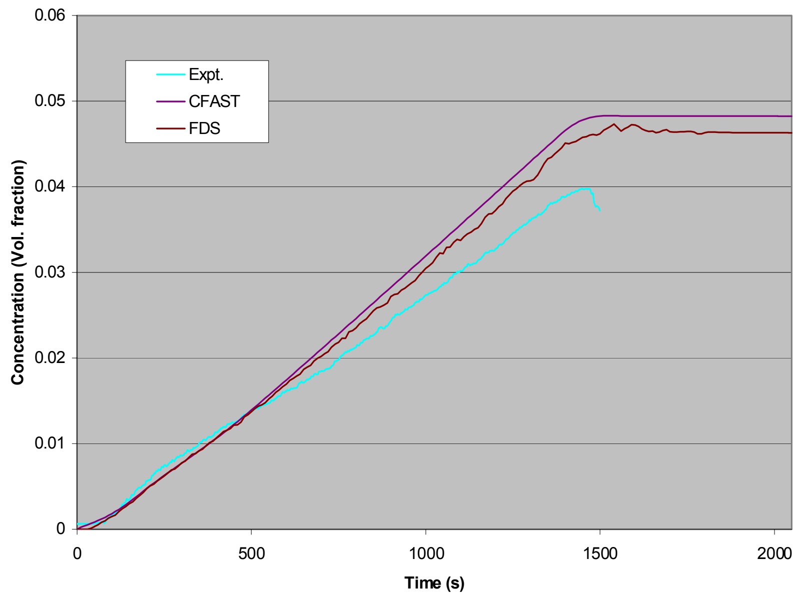

Figure 5.1.5 CO2 Concentration - Test 1

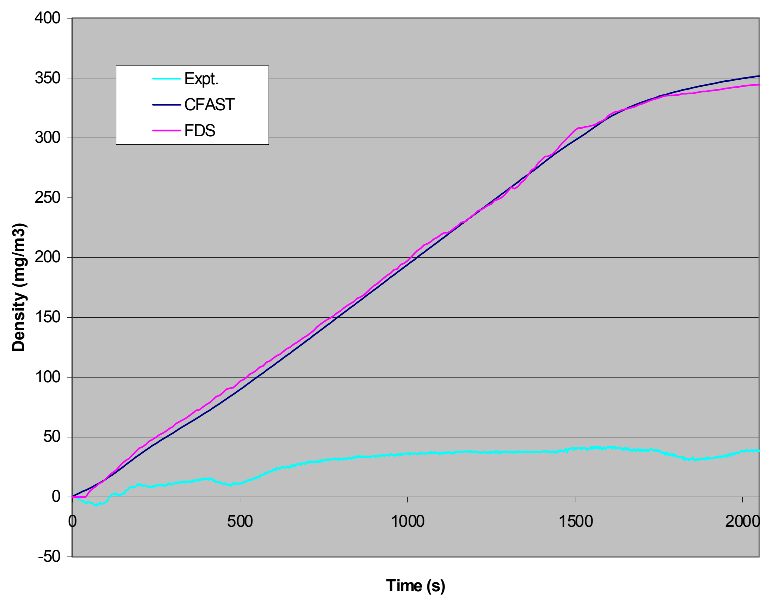

Figure 5.1.6 Smoke Concentration - Test 1

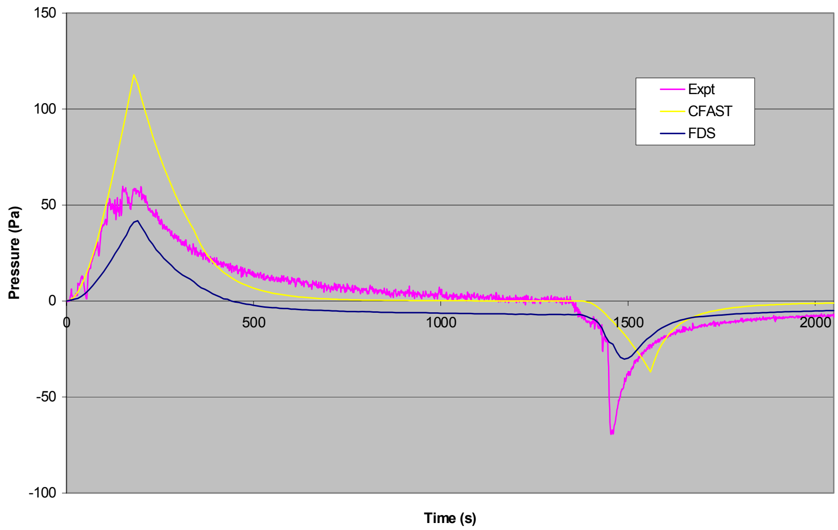

Figure 5.1.7 Compartment Pressure - Test 1

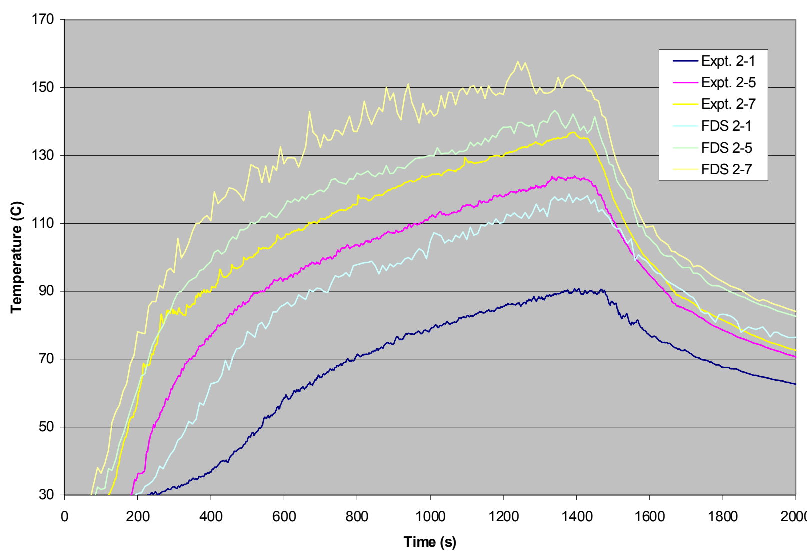

Figure 5.1.8 TC Tree 2 - Test 1

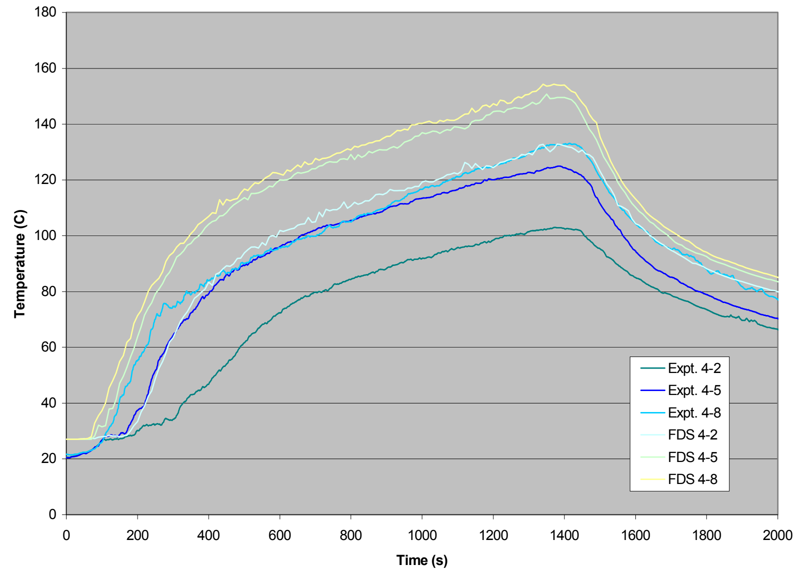

Figure 5.1.9 TC Tree 4 - Test 1

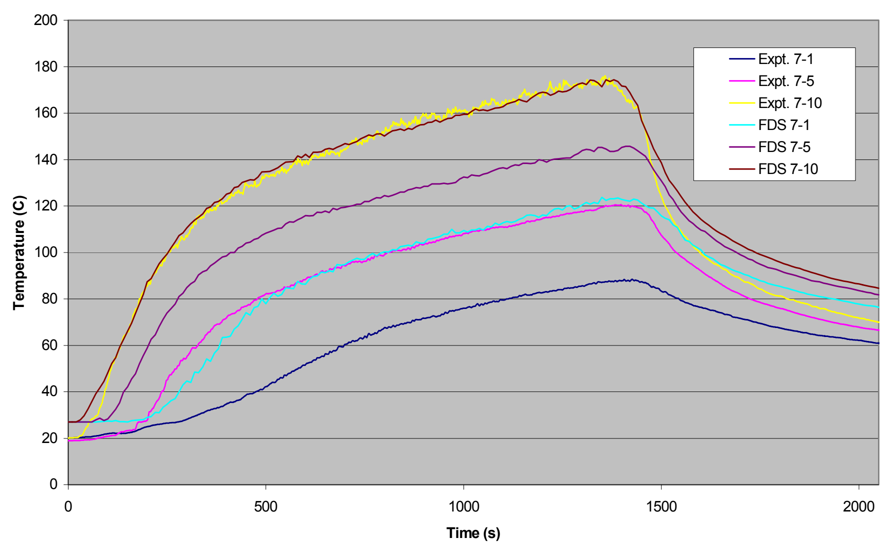

Figure 5.1.10 TC Tree 7 - Test 1

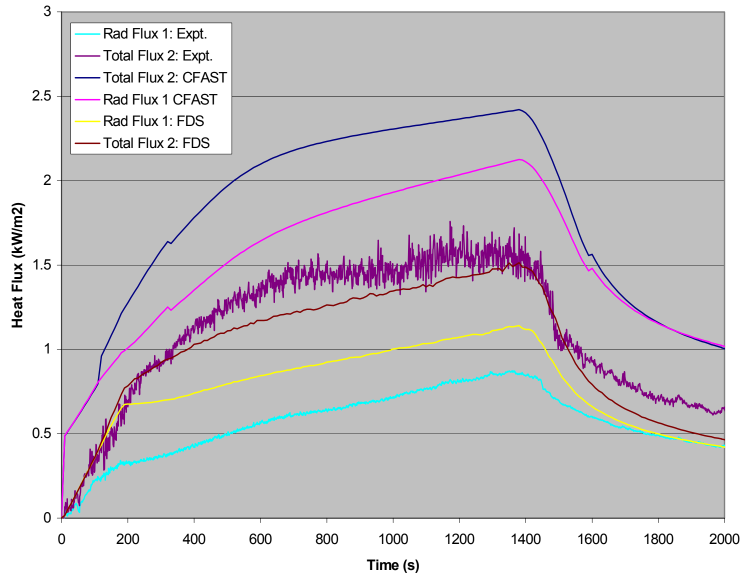

Figure 5.1.11 Heat Flux to Cables (1& 2) - Test 1

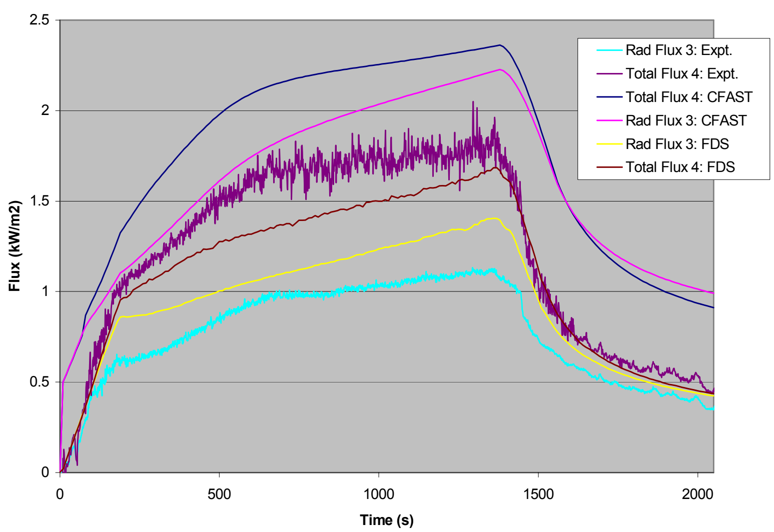

Figure 5.1.12 Heat Flux to Cables (3 & 4) - Test 1

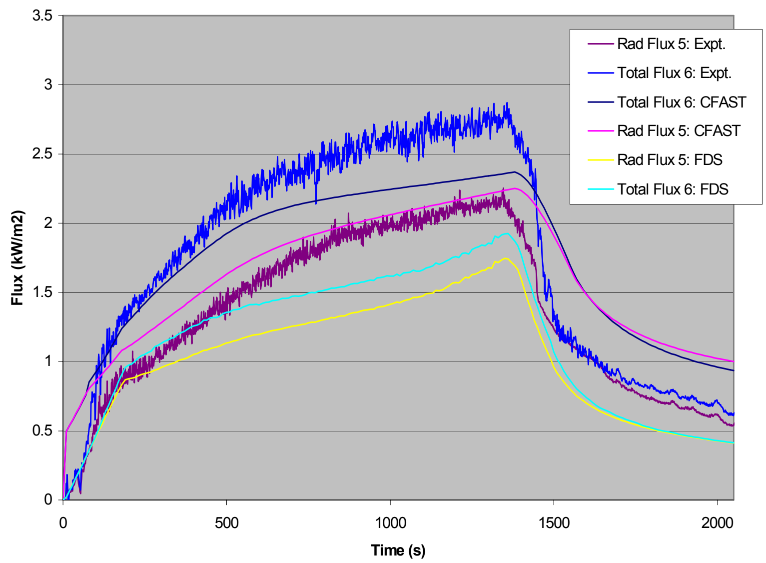

Figure 5.1.13 Heat Flux to Cables (3 & 4) - Test 1

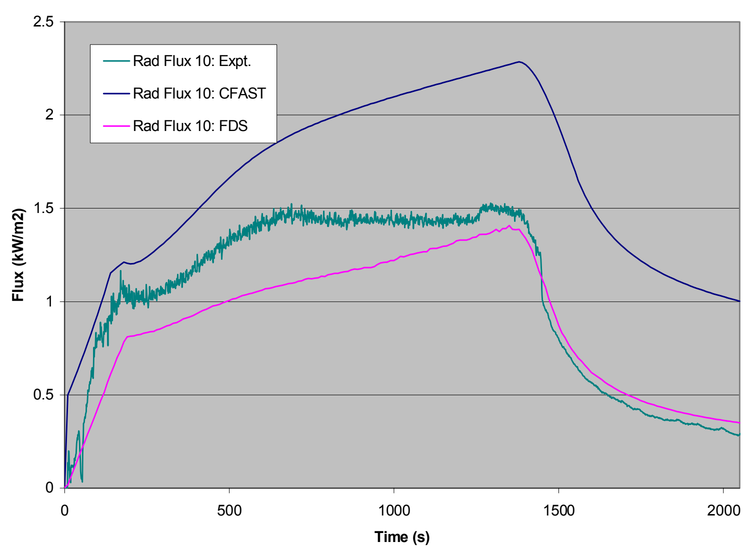

Figure 5.1.14 Heat Flux to Cables (9) - Test 1

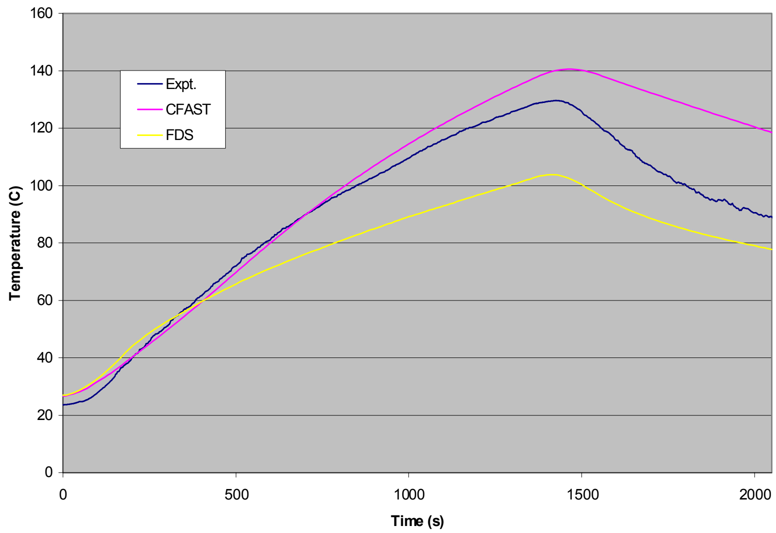

Figure 5.1.15 Control Cable Temperature (B-TS-14) - Test 1

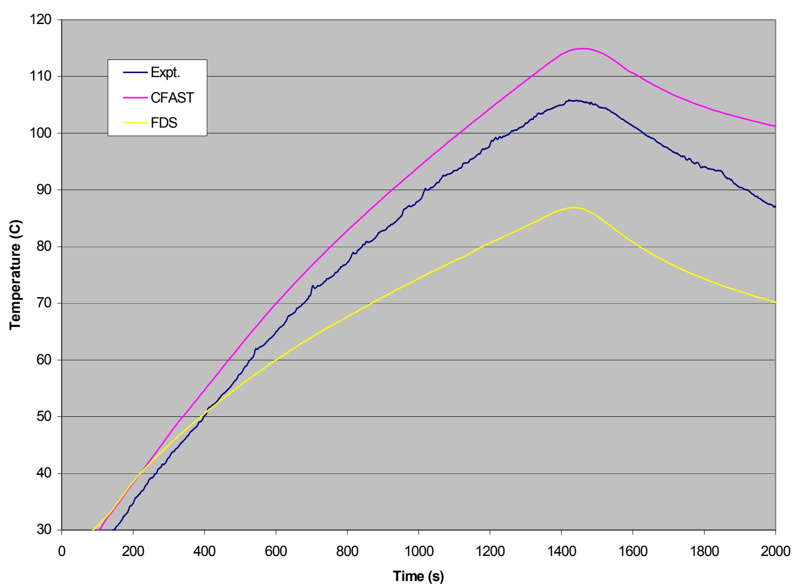

Figure 5.1.16 Power Cable Temperature (F-TS-20) - Test 1

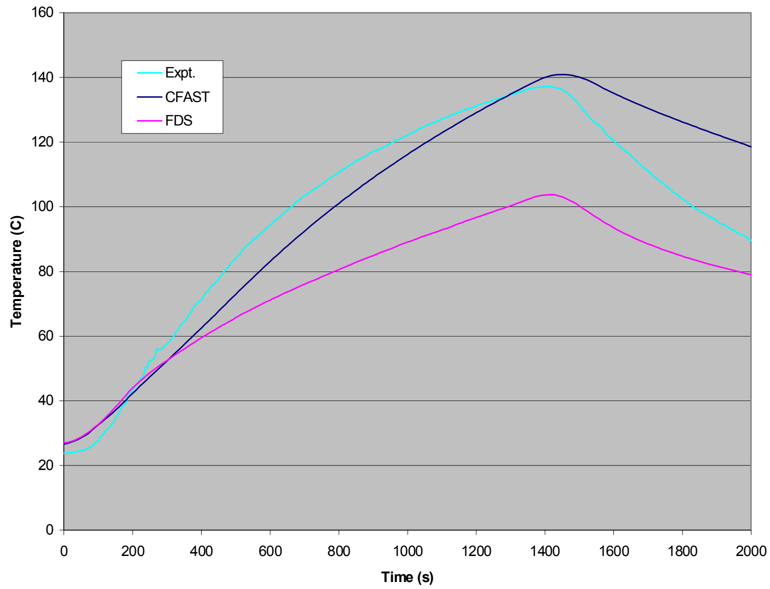

Figure 5.1.17 Slab E Temperature (E-TS-16 bottom) - Test 1

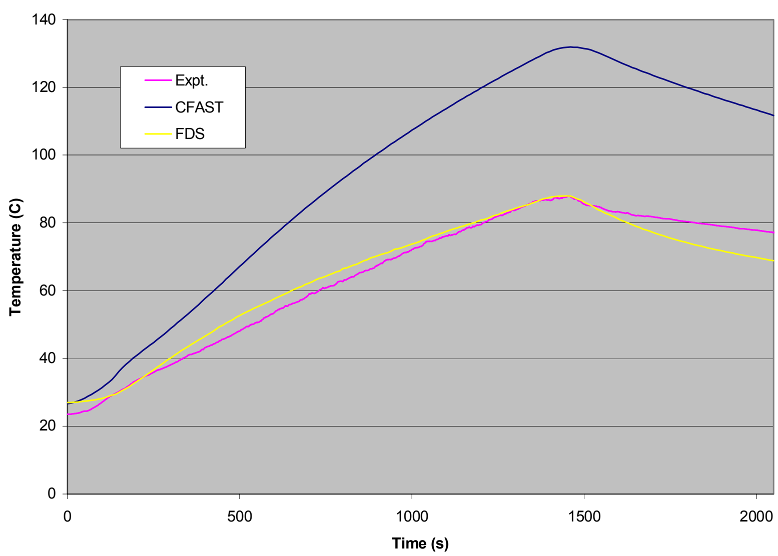

Figure 5.1.18 Vertical Cable Temperature (TS-33) - Test 1

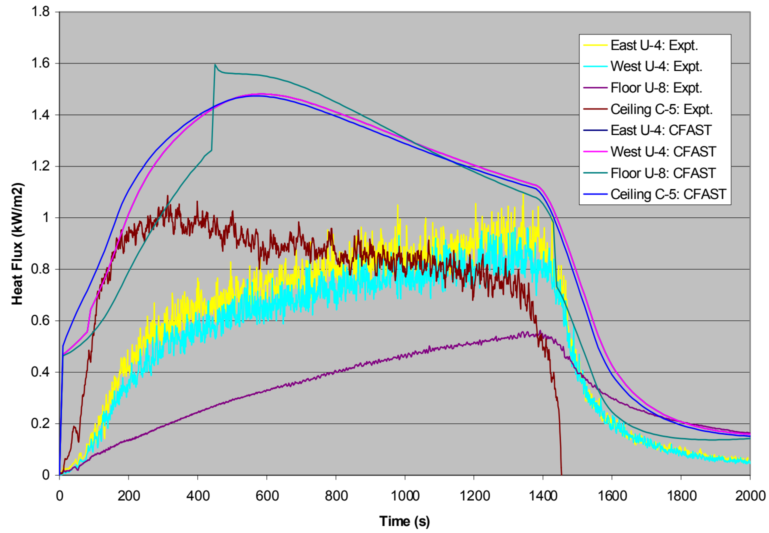

Figure 5.1.19 Heat Flux to Walls (CFAST) - Test 1

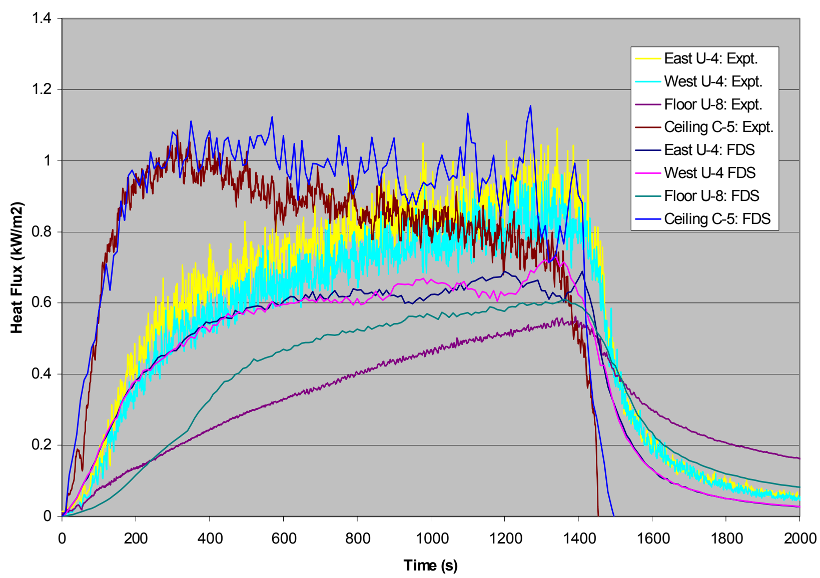

Figure 5.1.20 Heat Flux to Walls (FDS) - Test 1

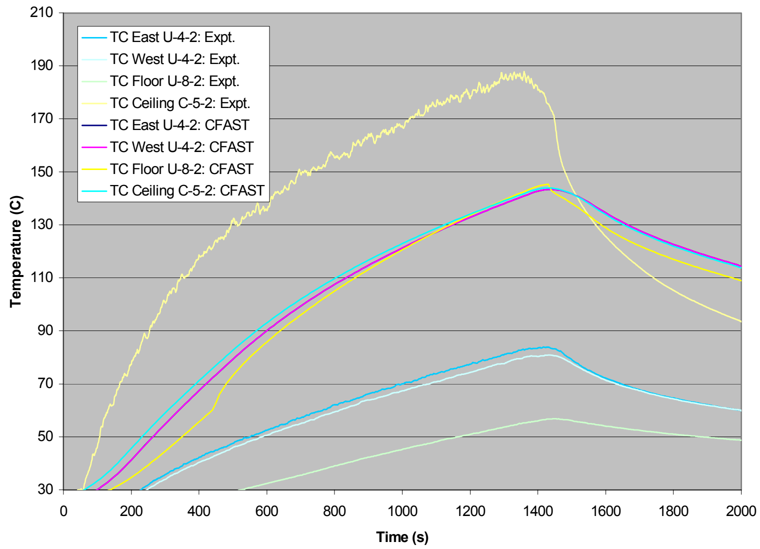

Figure 5.1.21 Wall Temperature (CFAST) - Test 1

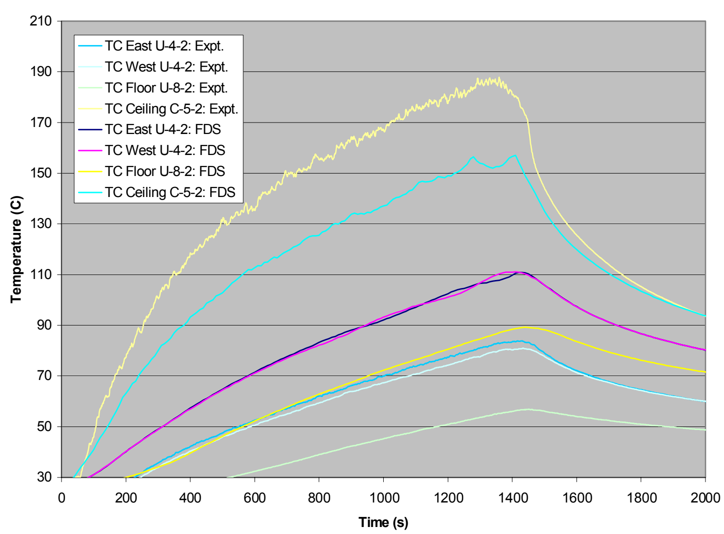

Figure 5.1.22 Wall Temperature (FDS) - Test 1

Figures for Test 2

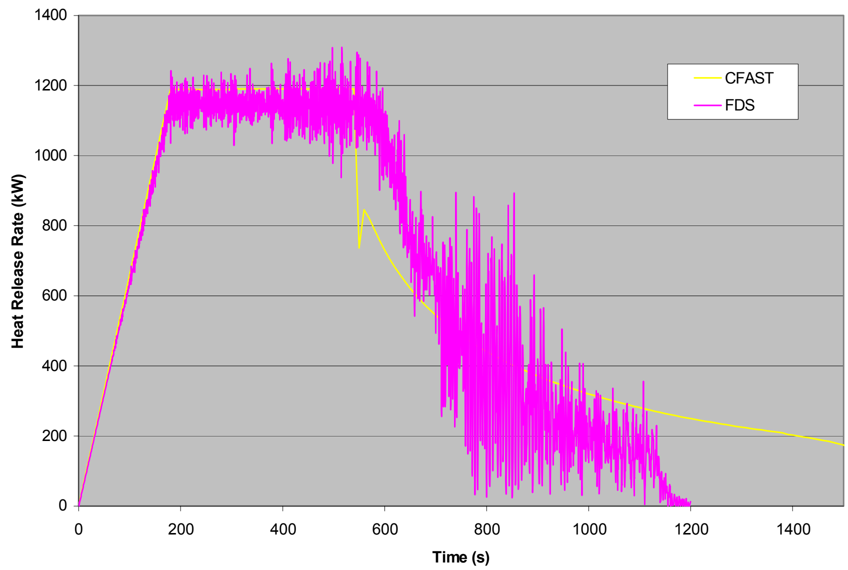

Figure 5.2.1 Heat Release Rate - Test 2

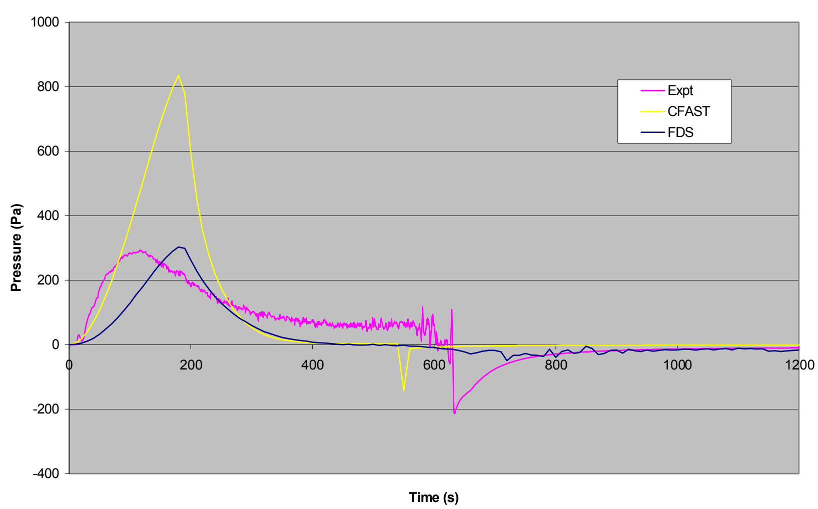

Figure 5.2.2 Compartment Pressure - Test 2

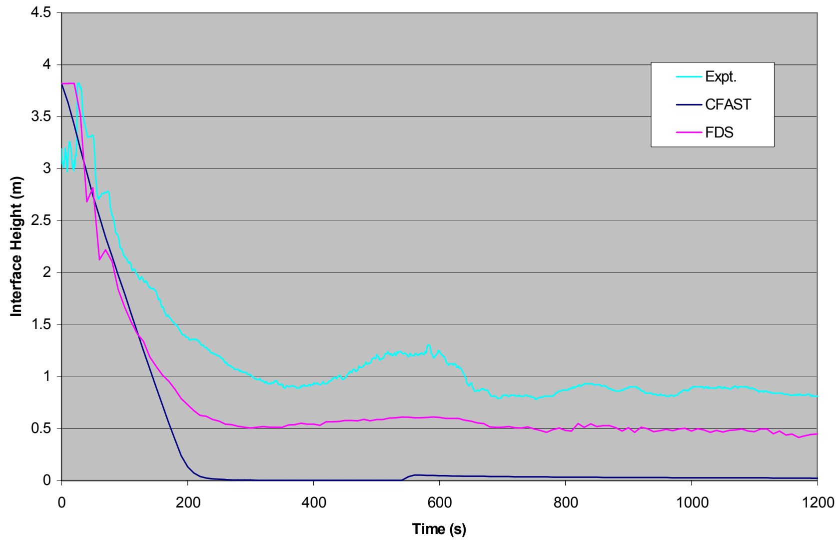

Figure 5.2.3 Hot Gas Layer Development - Test 2

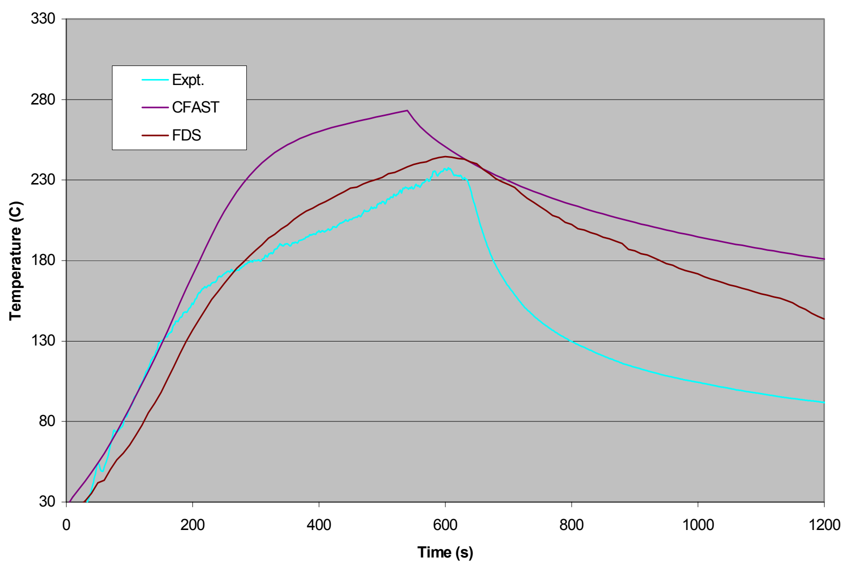

Figure 5.2.4 Hot Gas Layer Temperature - Test 2

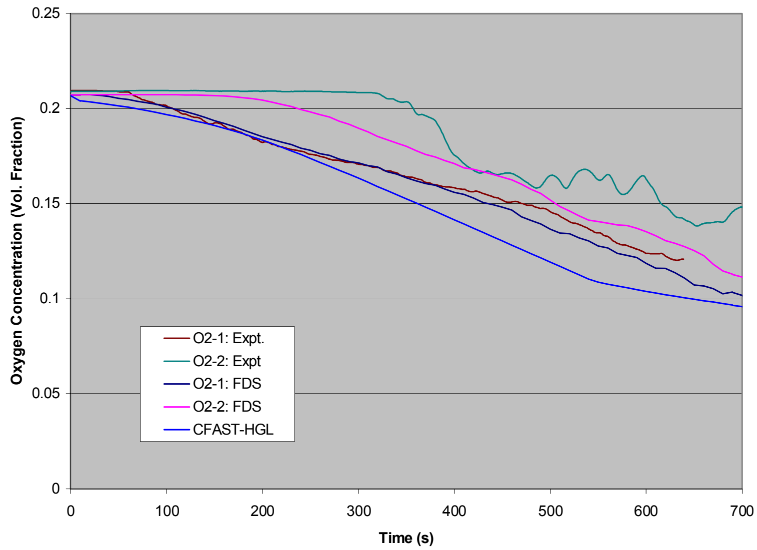

Figure 5.2.5 Oxygen Concentration - Test 2

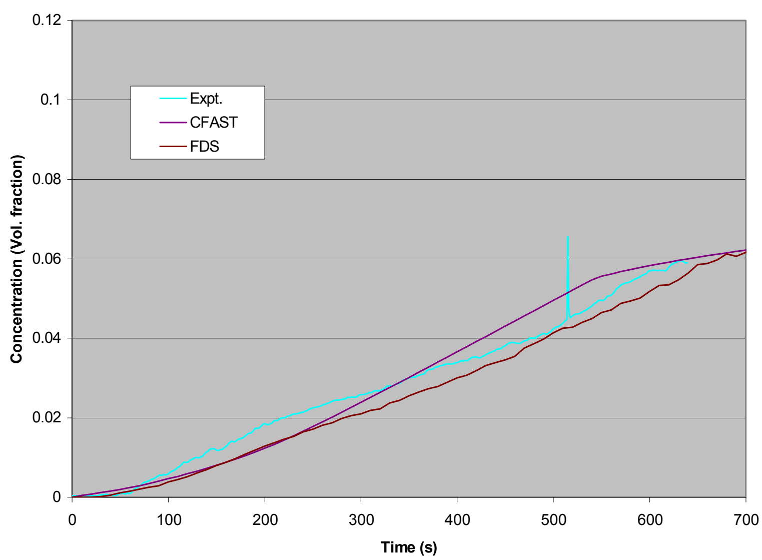

Figure 5.2.6 CO2 Concentration - Test 2

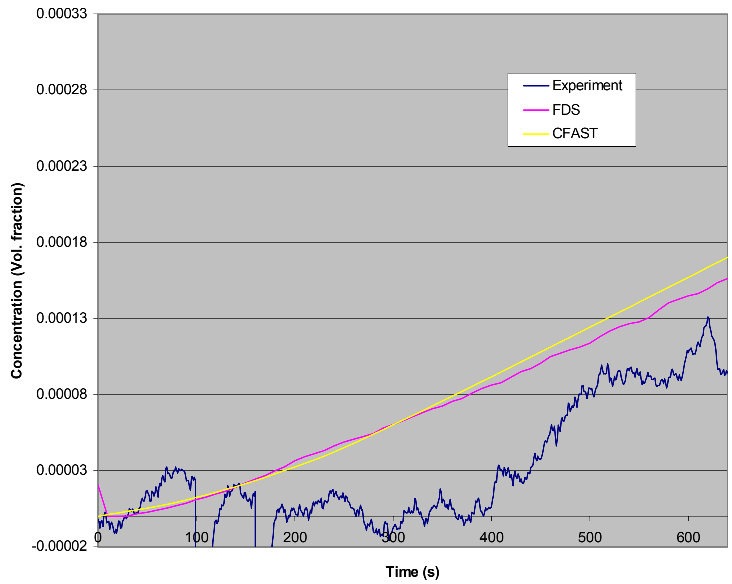

Figure 5.2.7 CO Concentration - Test 2

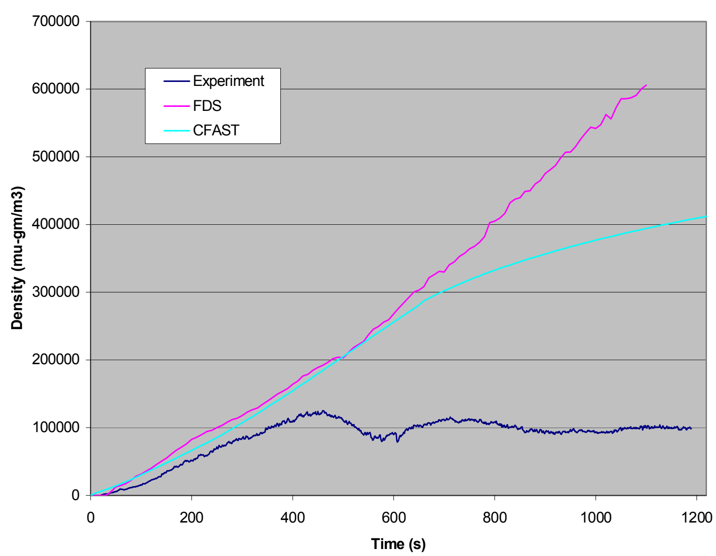

Figure 5.2.8 Smoke Concentration - Test 2

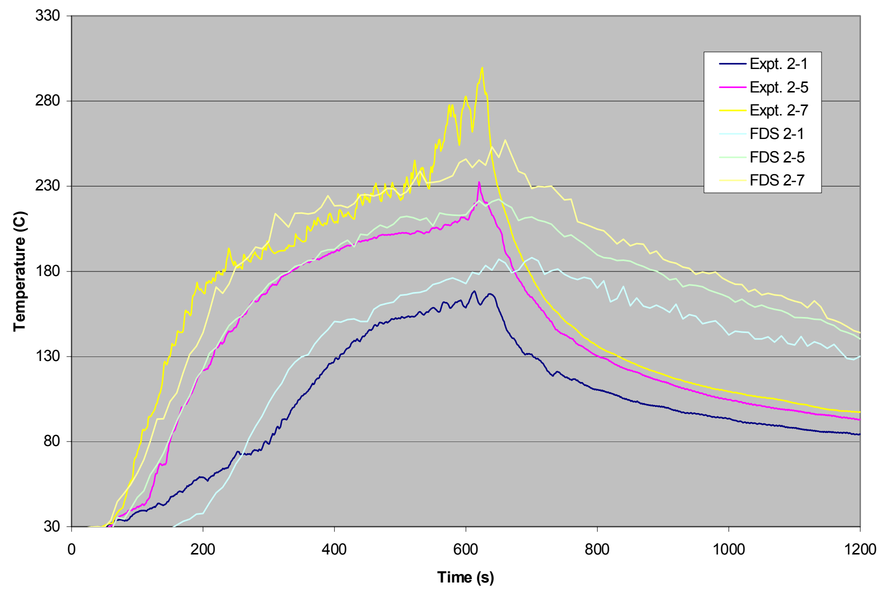

Figure 5.2.9 Compartment Temperature (Tree 2) - Test 2

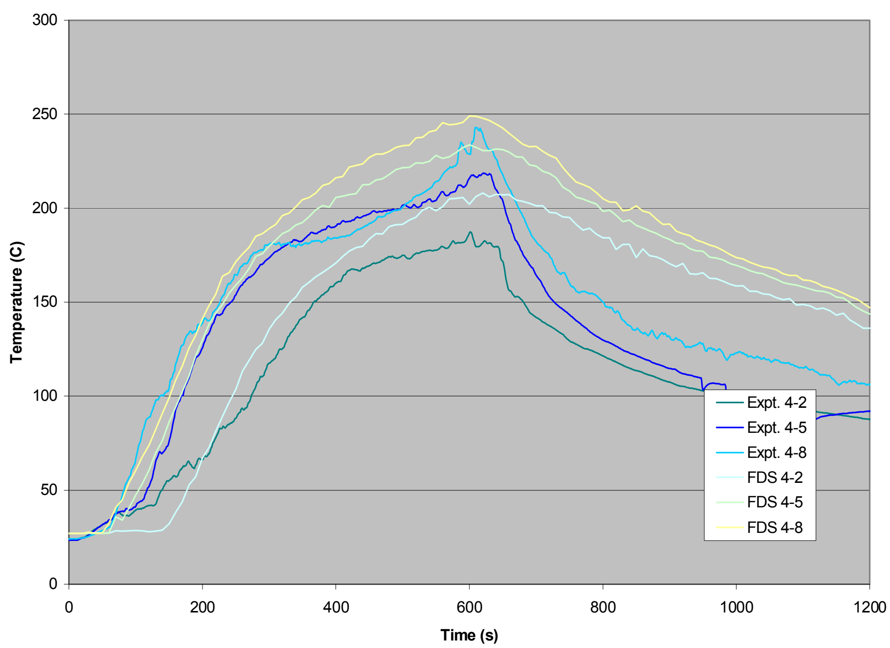

Figure 5.2.10 Compartment Temperature (Tree 4) - Test 2

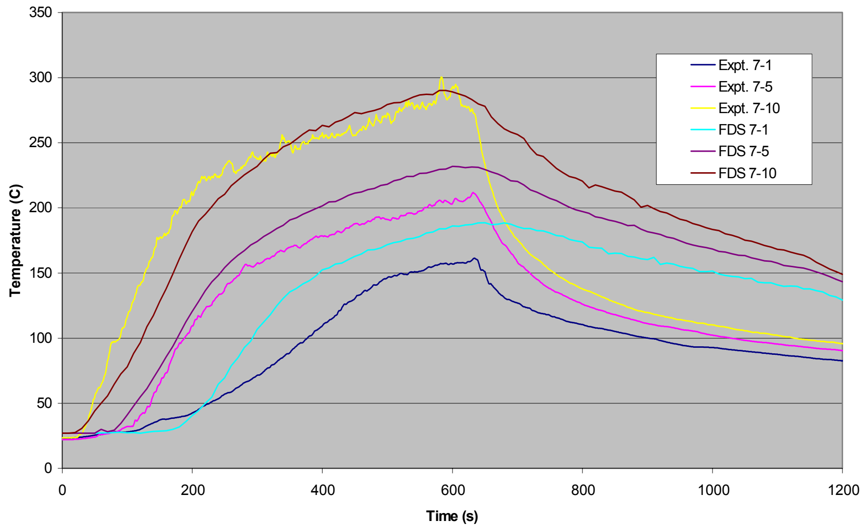

Figure 5.2.11 Compartment Temperature (Tree 7) - Test 2

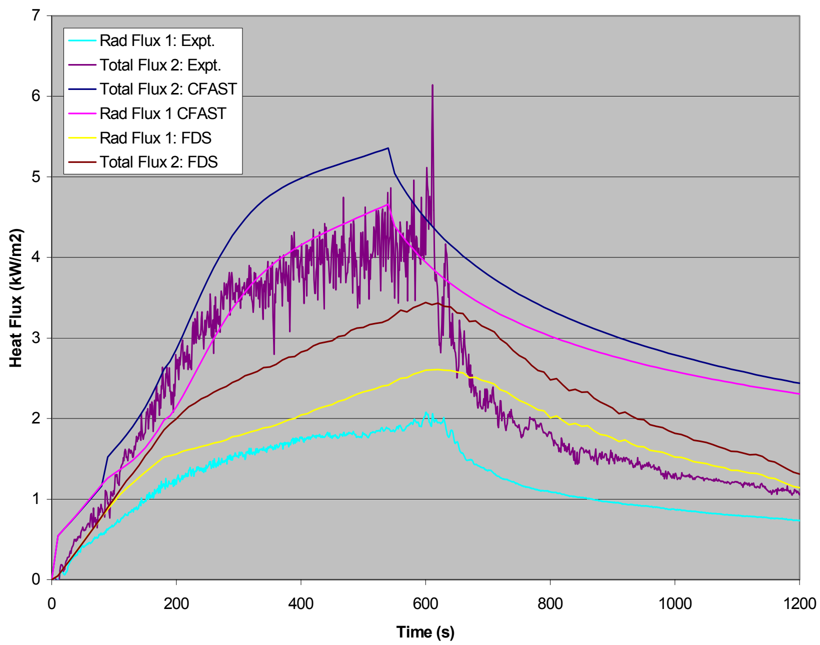

Figure 5.2.12 Heat Flux to Cables(Gauges 1 & 2) - Test 2

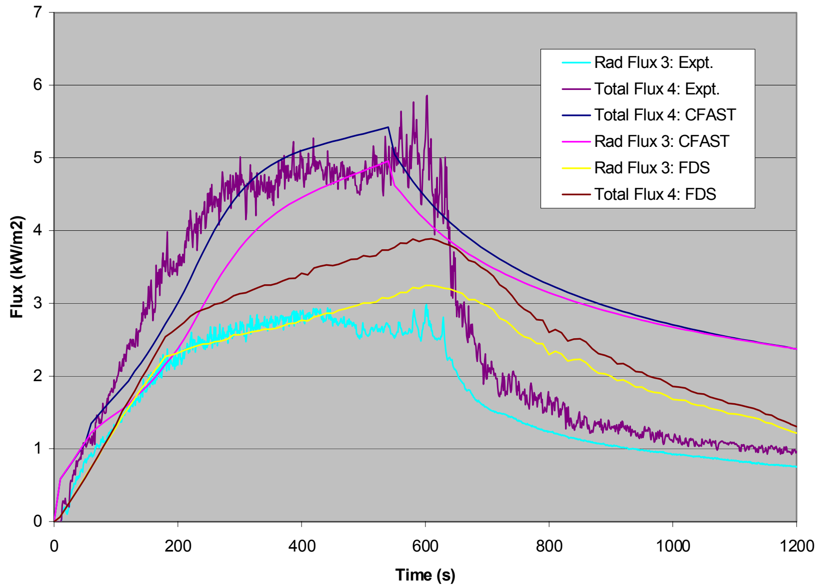

Figure 5.2.13 Heat Flux to Cables (Gauges 3 &4) - Test 2

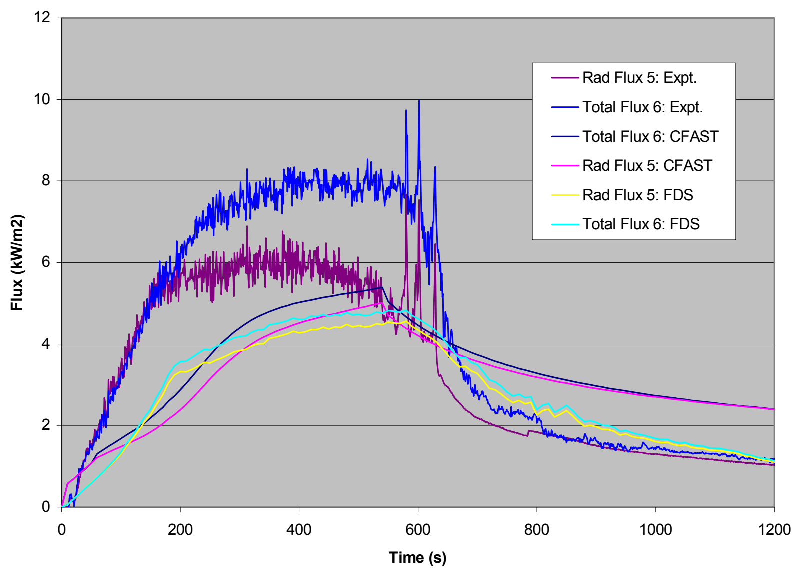

Figure 5.2.14 Heat Flux to Cables (Gauges 5 & 6) - Test 2

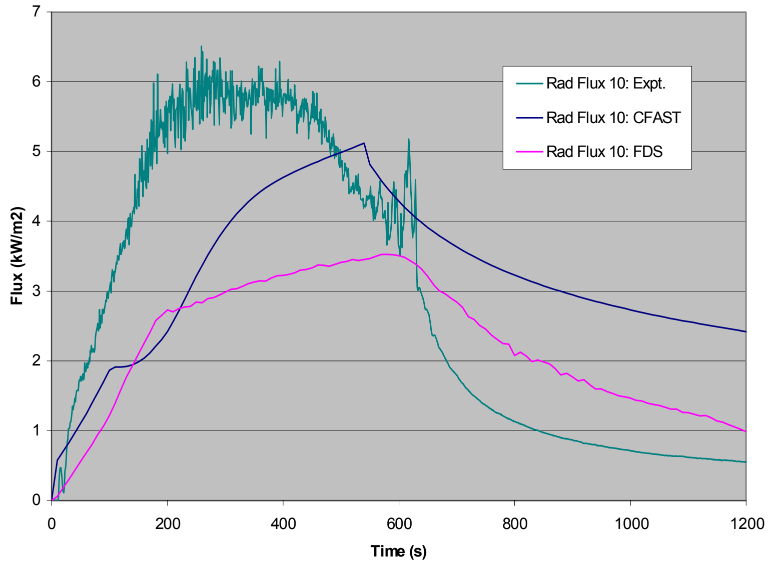

Figure 5.2.15 Heat Flux to Cables (Gauge 10) - Test 2

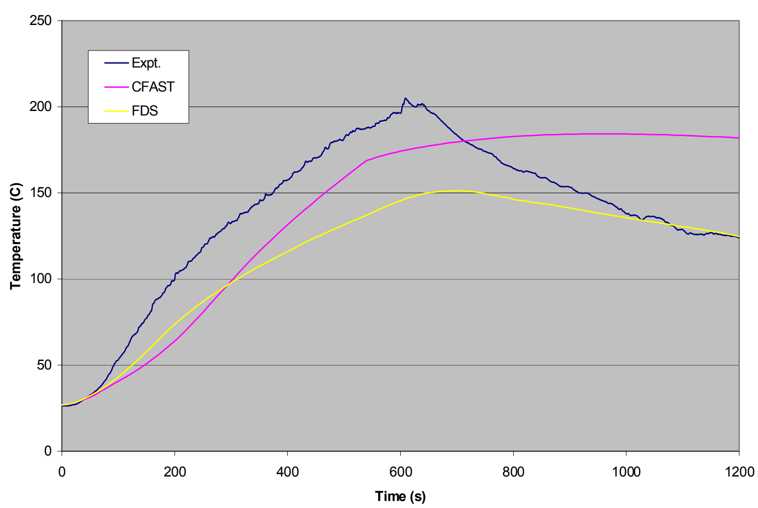

Figure 5.2.16 Control Cable Temperature (B-TS-14) - Test 2

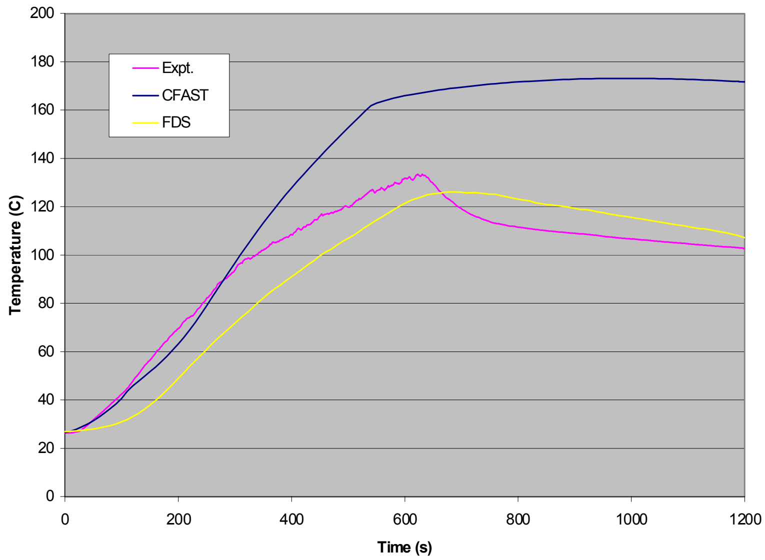

Figure 5.2.17 Vertical Cable Temperature (TS-33) - Test 2

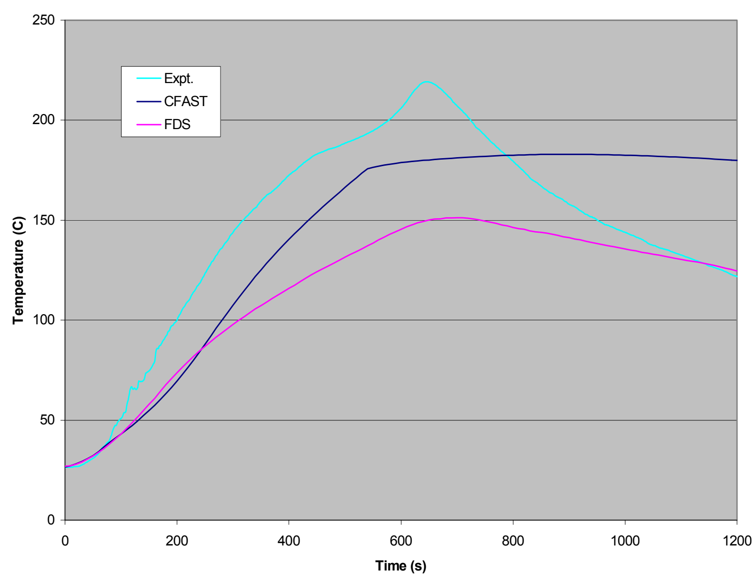

Figure 5.2.18 Slab E Temperature (E-TS-16 Bottom) - Test 2

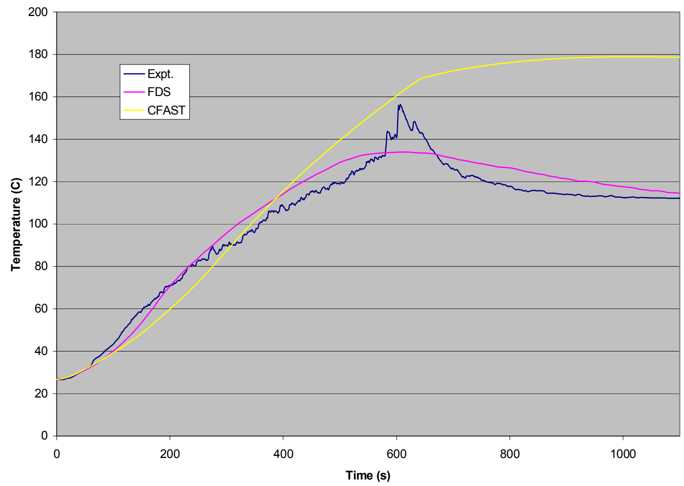

Figure 5.2.19 Control Cable Temperature (D-TS-12) - Test 2

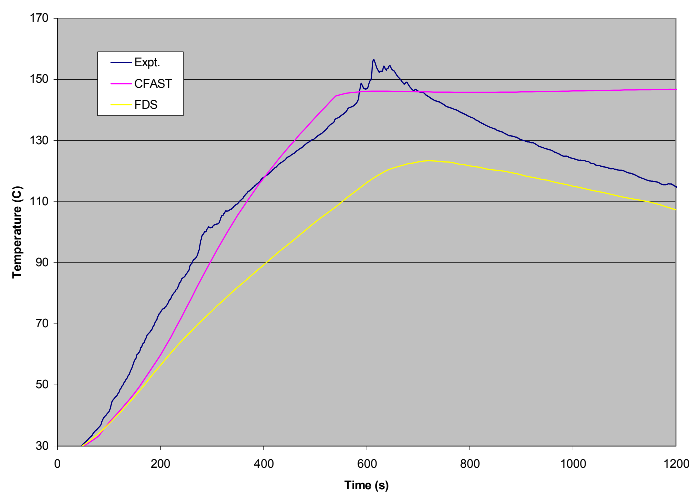

Figure 5.2.20 Power Cable Temperature (F-TS-20) - Test 2

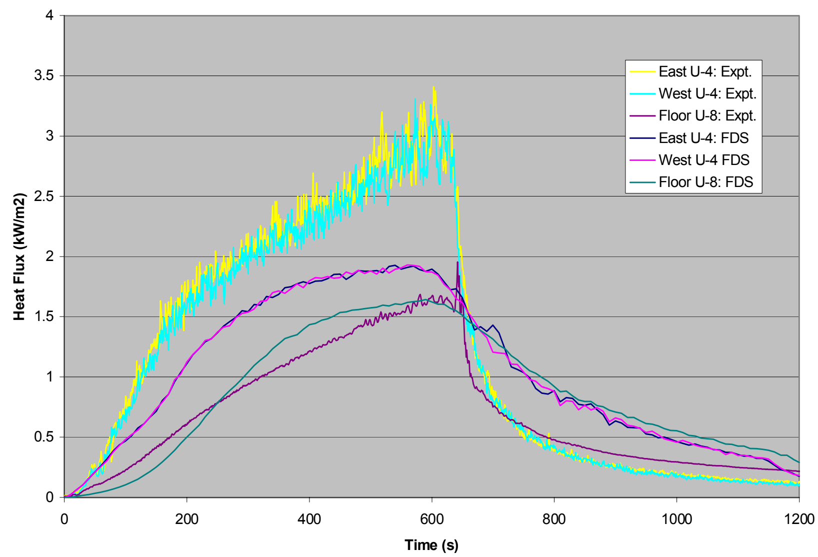

Figure 5.2.21 Heat Flux to Walls (FDS) - Test 2

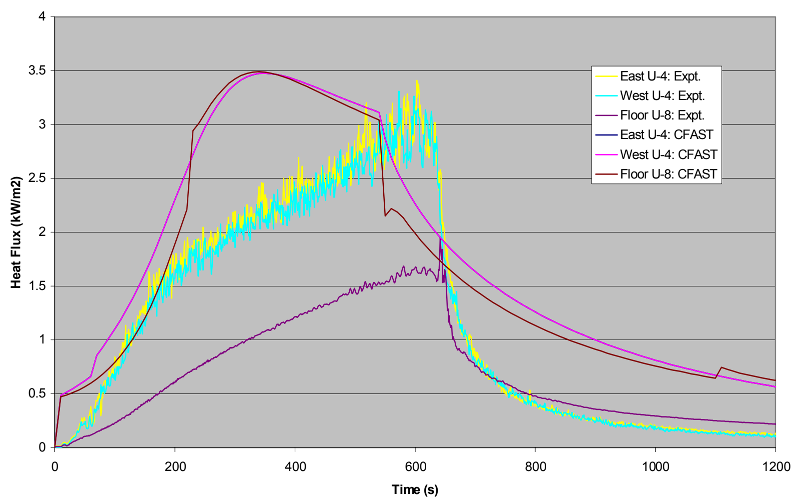

Figure 5.2.22 Heat Flux to Walls (CFAST) - Test 2

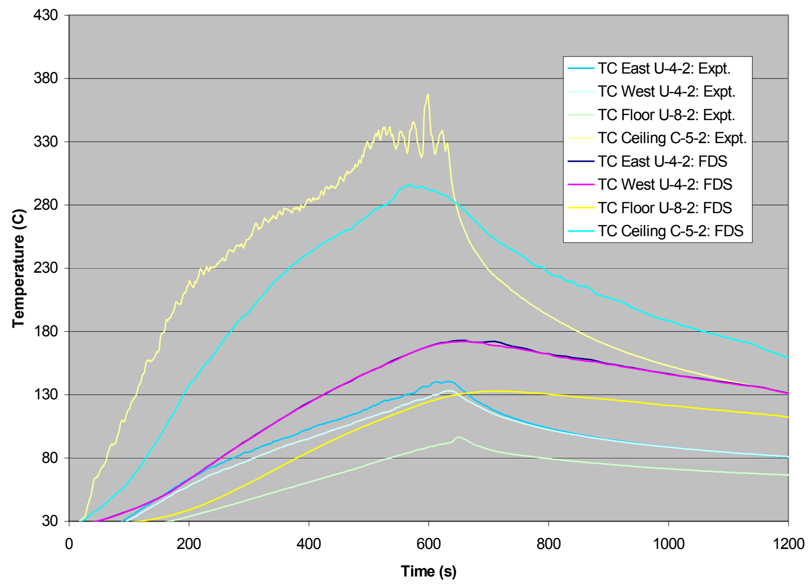

Figure 5.2.23 Wall Temperature (FDS) - Test 2

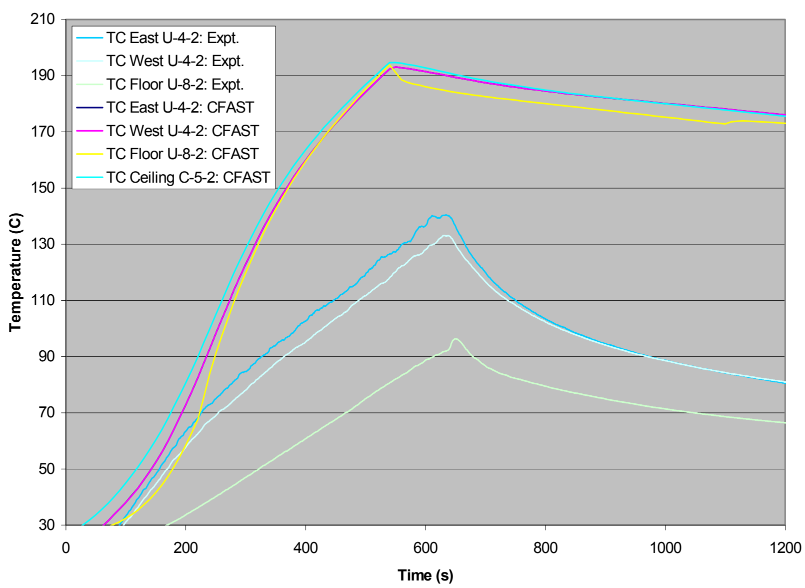

Figure 5.2.24 Wall Temperature (CFAST) - Test 2

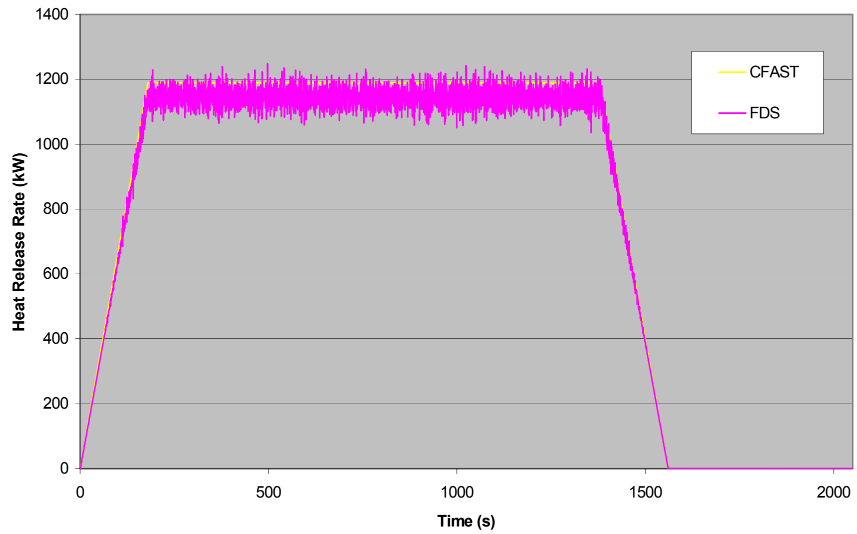

Figure 5.3.1 Heat Release Rate - Test 3

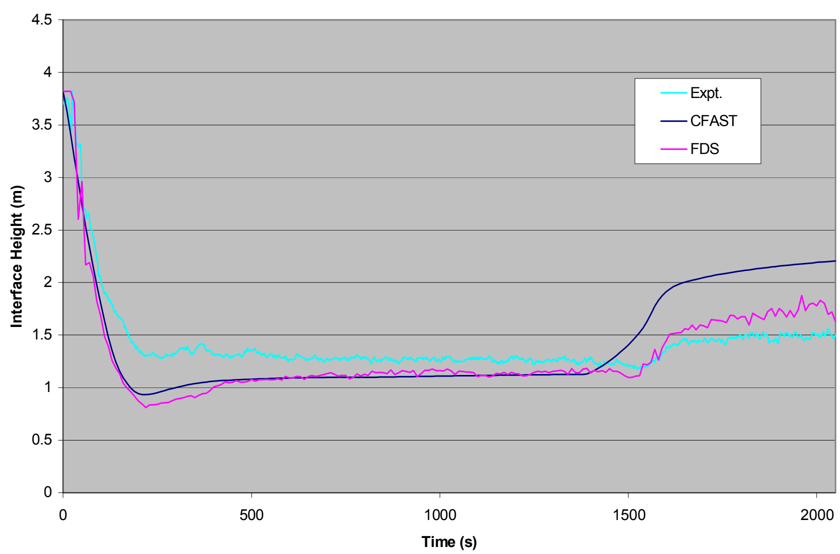

Figure 5.3.2 Hot Gas Layer Development - Test 3

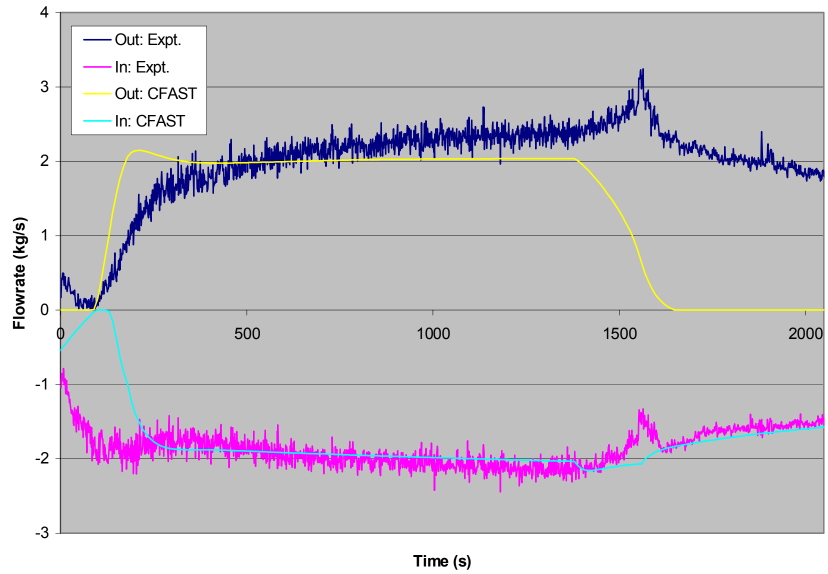

Figure 5.3.3 Door Flows - Test 3

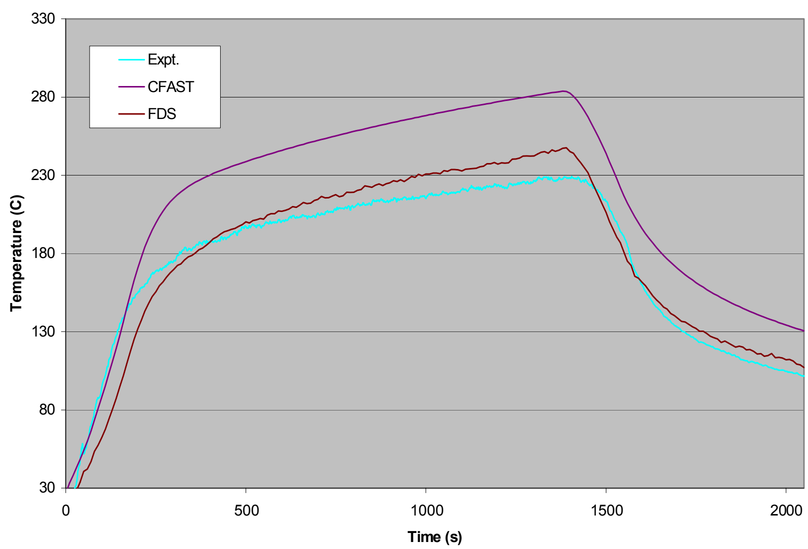

Figure 5.3.4 Hot Gas Layer Temperature - Test 3

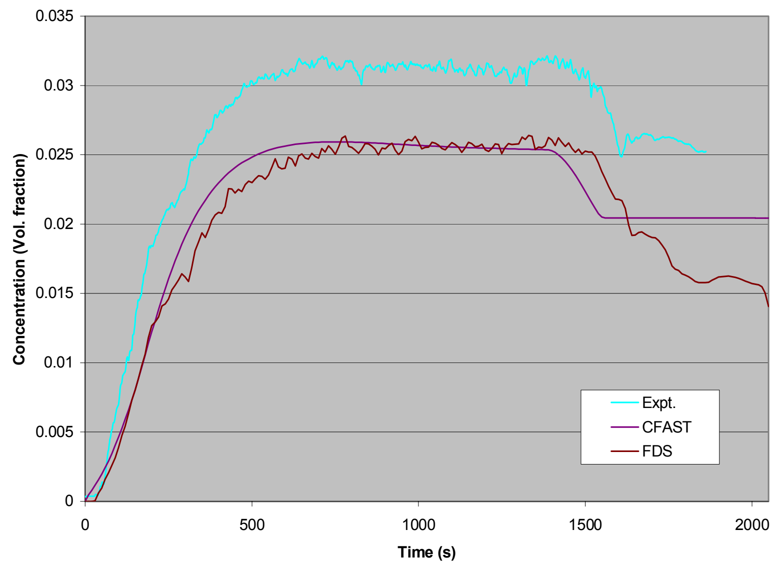

Figure 5.3.5 CO2 Concentration - Test 3

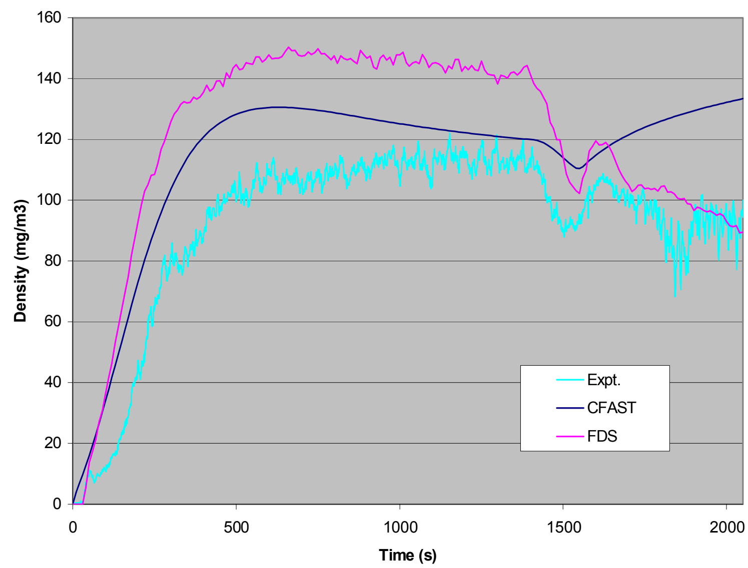

Figure 5.3.6 Smoke Concentration - Test 3

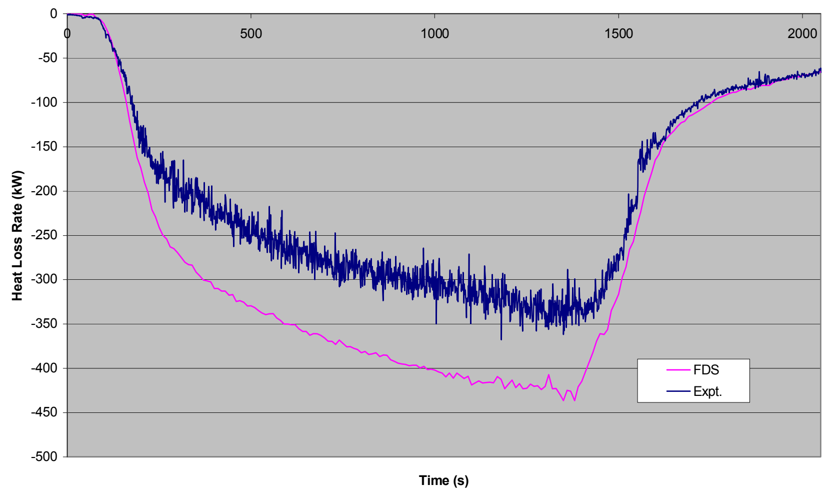

Figure 5.3.7 Heat Loss from Door - Test 3

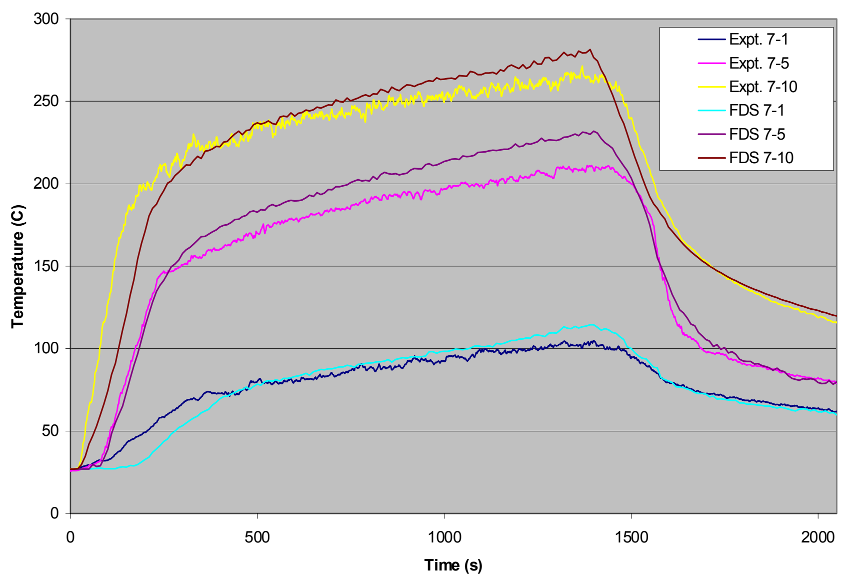

Figure 5.3.8 Compartment Temperature (Tree 7) - Test 3

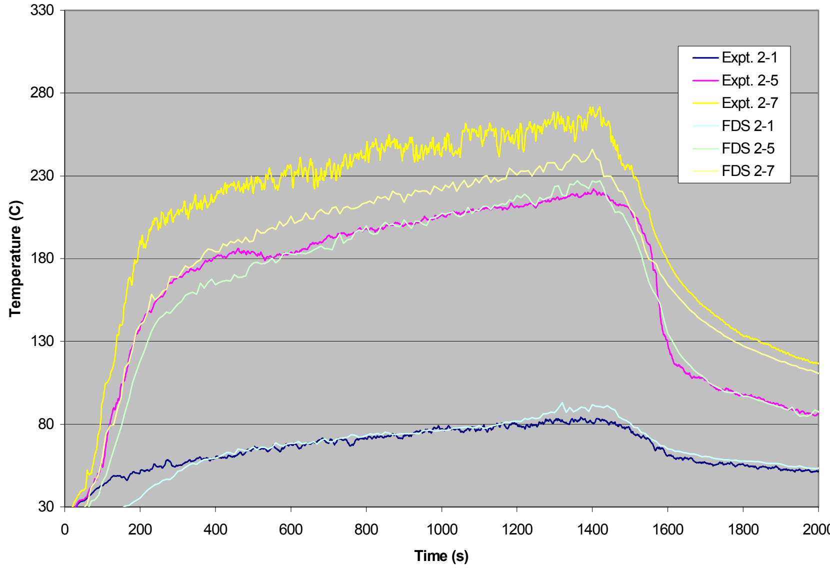

Figure 5.3.9 Compartment Temperature (Tree 2) - Test 3

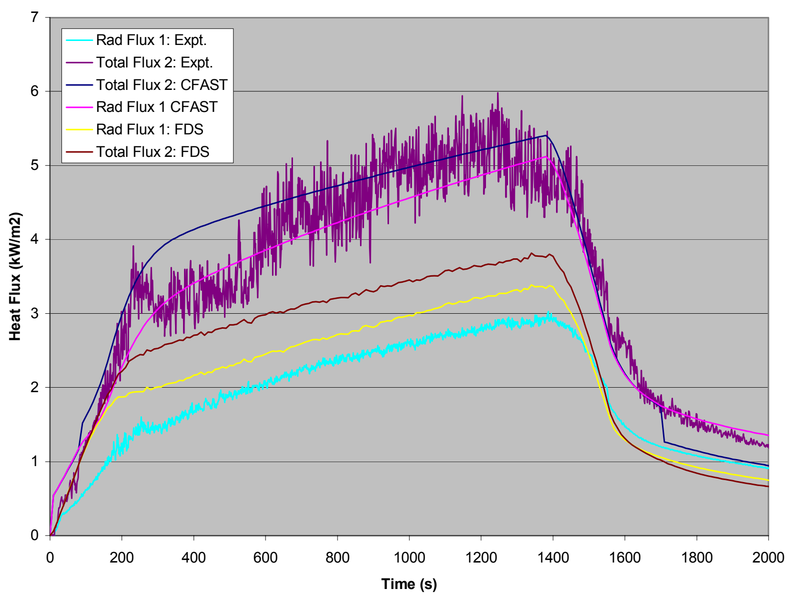

Figure 5.3.10 Heat Flux to Cables (1 & 2) - Test 3

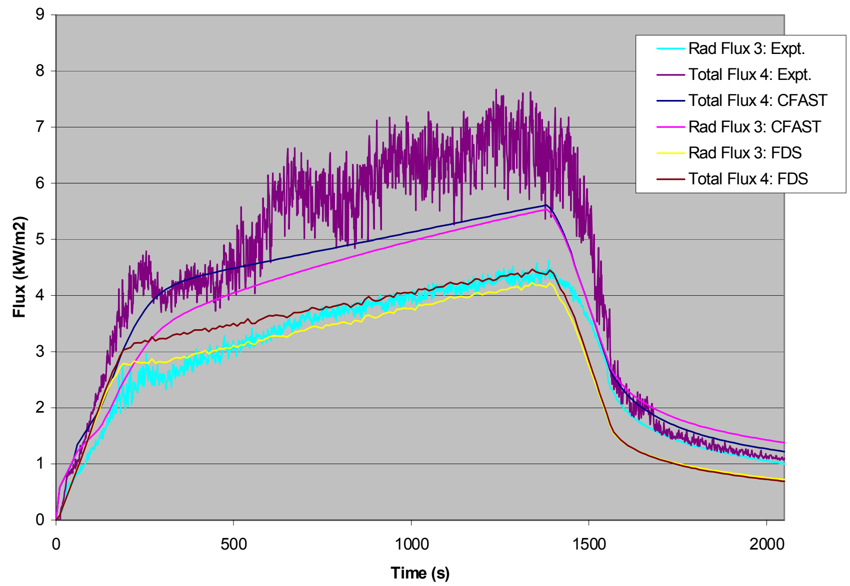

Figure 5.3.11 Heat Flux to Cables (3 &4) - Test 3

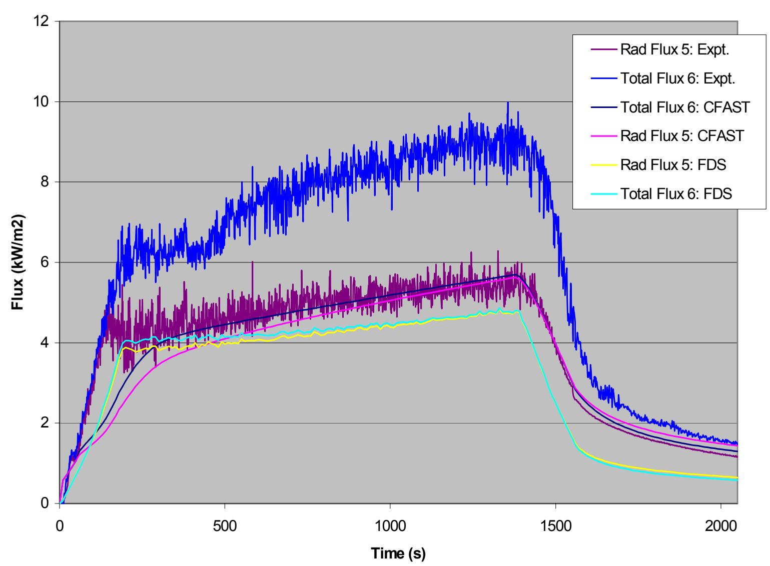

Figure 5.3.12 Heat Flux to cables (5&6) - Test 3

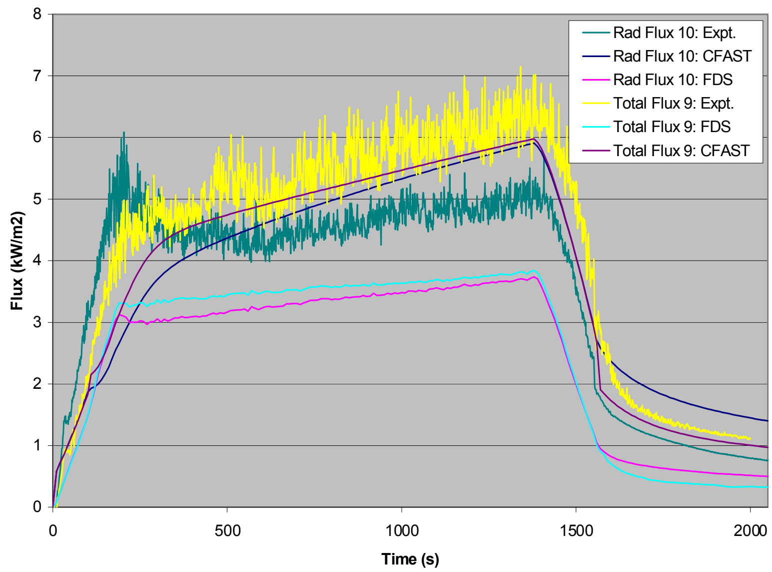

Figure 5.3.13 Heat Flux to Cables (9 & 10) - Test 3

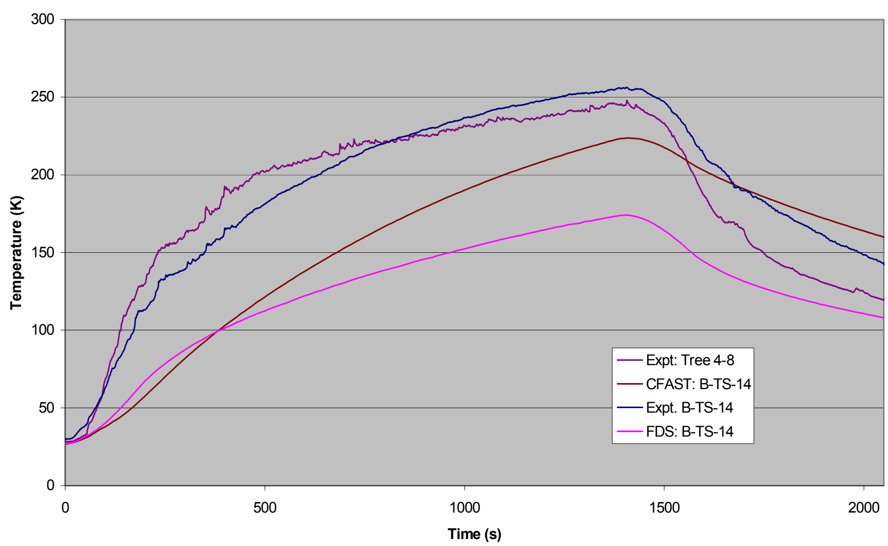

Figure 5.3.14 Control Cable Temperature (B-TS-14) - Test 3

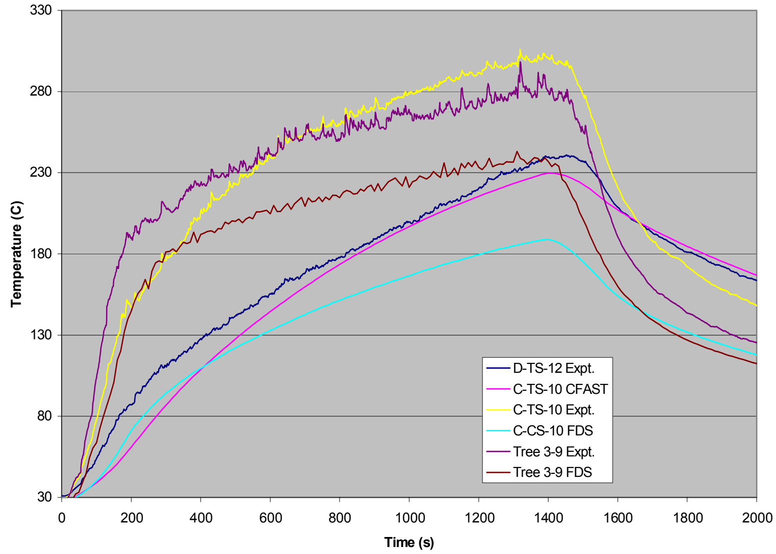

Figure 5.3.15 Control Cable Temperature (C-TS-10) - Test 3

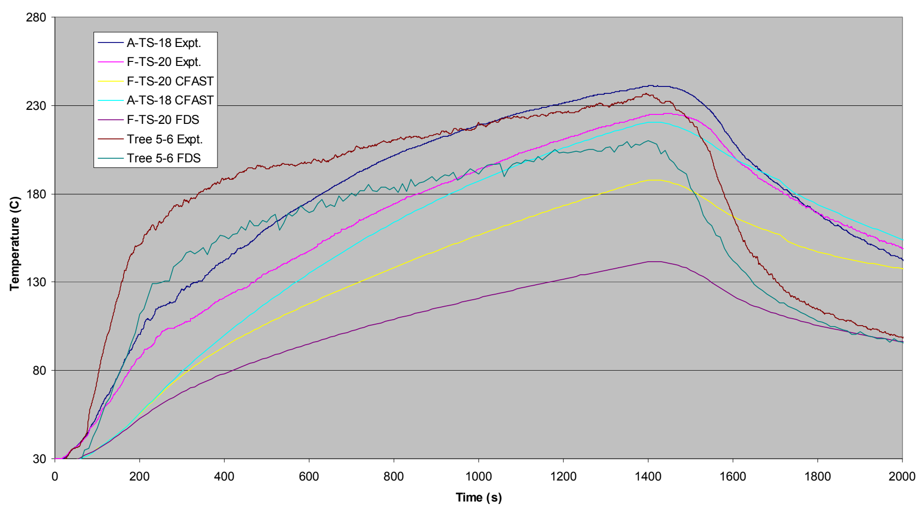

Figure 5.3.16 Power Cable Temperature (F-TS-20)

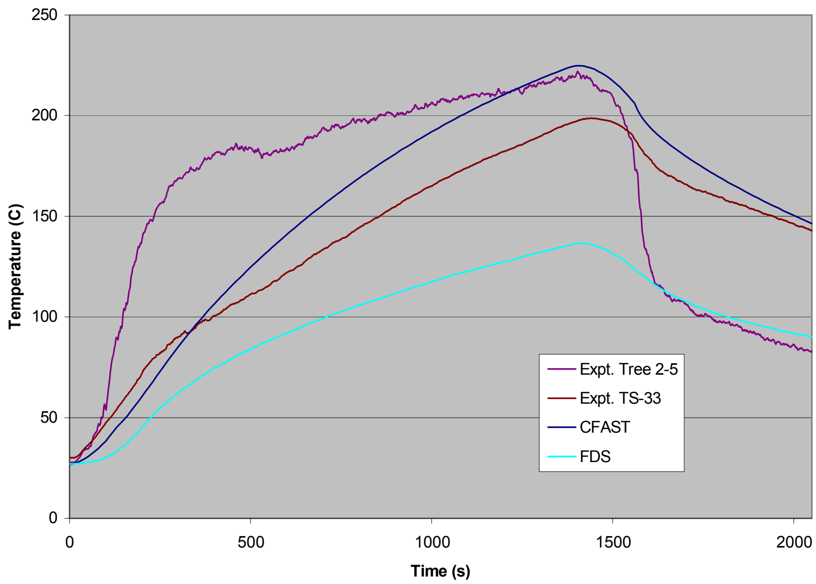

Figure 5.3.17 Vertical Cable Temperature (TS-33) - Test 3

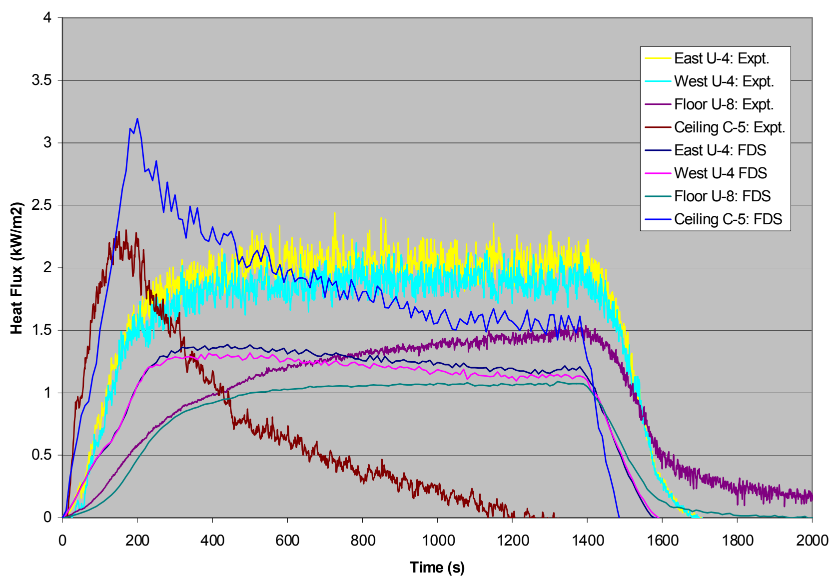

Figure 5.3.18 Heat flux to Walls (FDS) - Test 3

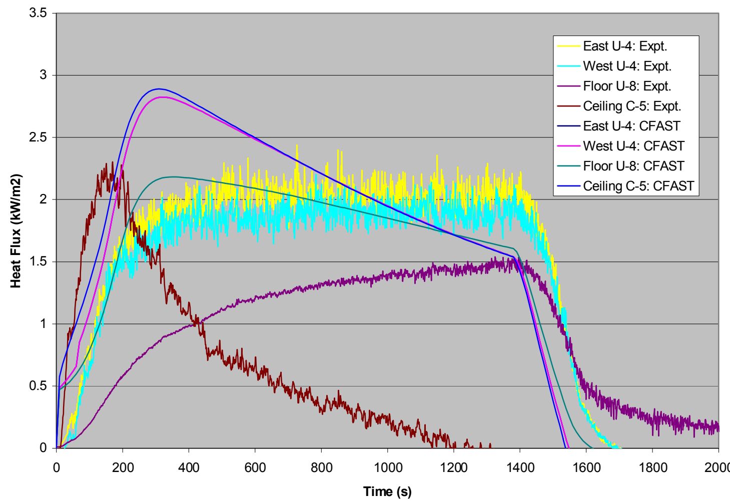

Figure 5.3.19 Heat Flux to Walls (CFAST) - Test 3

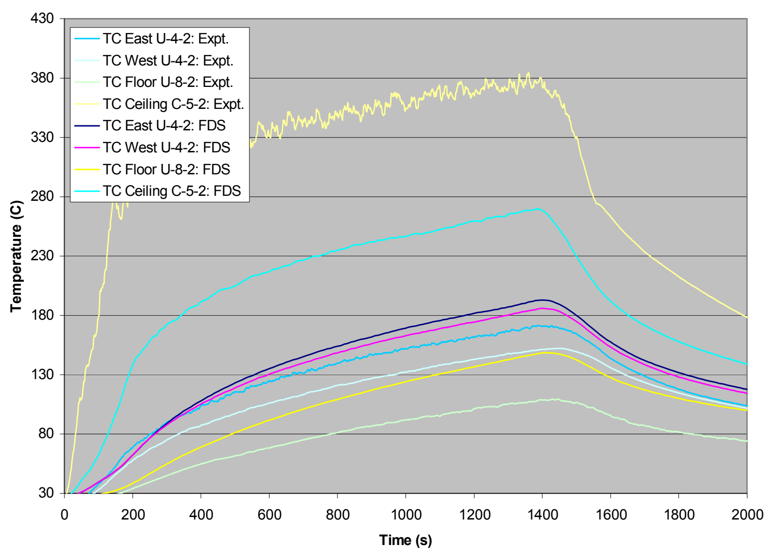

Figure 5.3.20 Wall Temperature (FDS) - Test 3

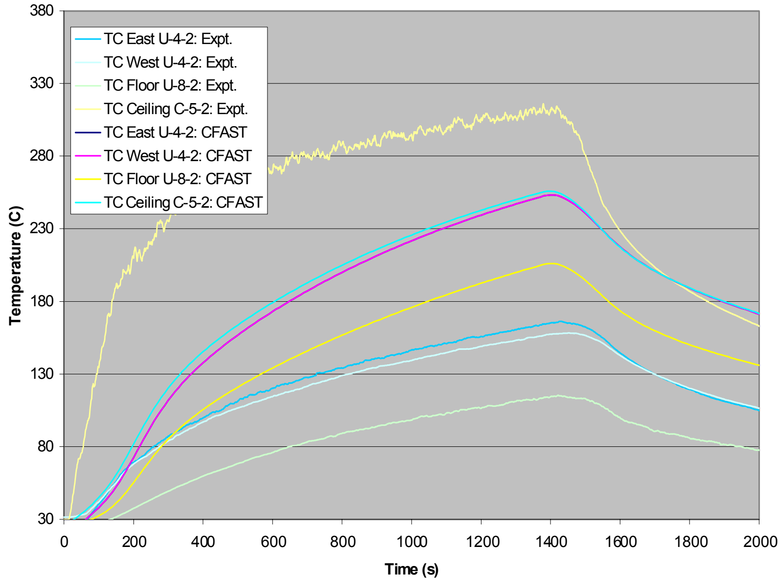

Figure 5.3.21 Wall Temperature (CFAST) - Test 3

Figure 5.3.22 Hot Gas Layer (steady state) - Test 3

Figure 5.3.23 Fire Plume Tilt - Test 3

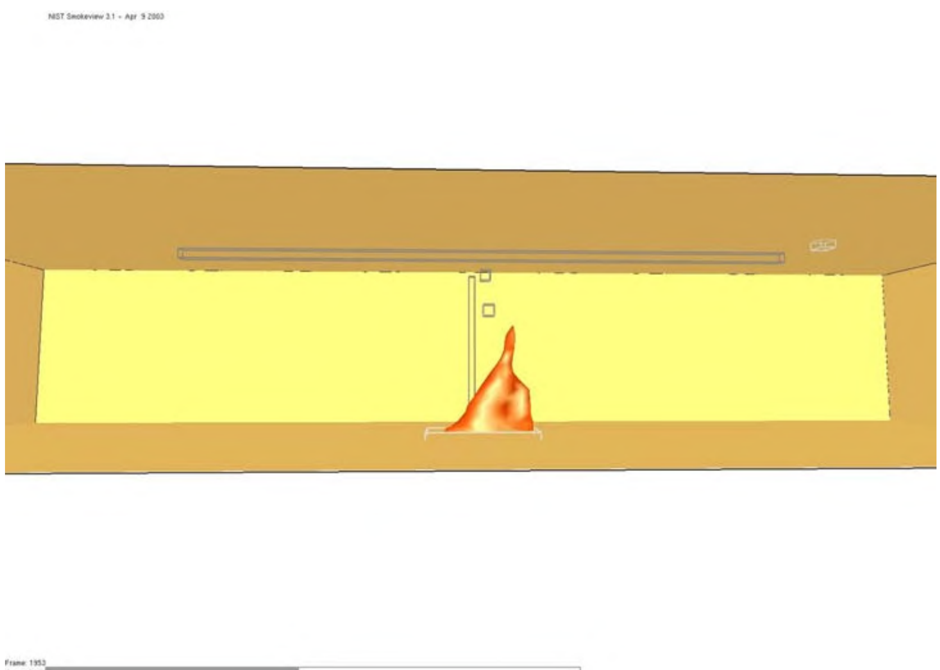

Figure 5.3.24 Isosurface of Flame sheet (FDS) - Test 3

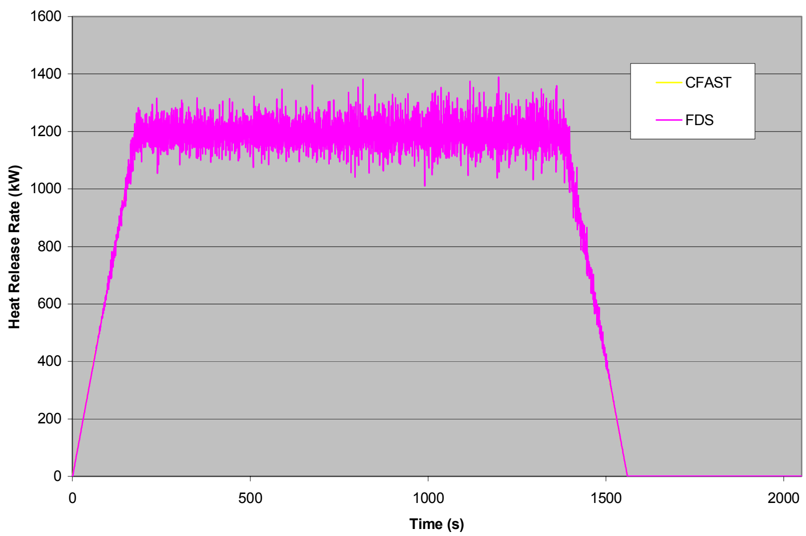

Figure 5.4.1 Heat Release Rate - Test 4

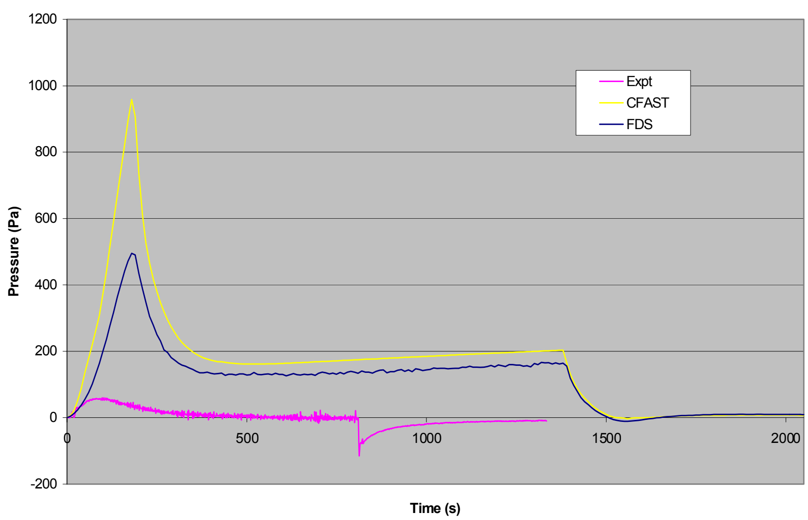

Figure 5.4.2 Compartment Pressure - Test 4

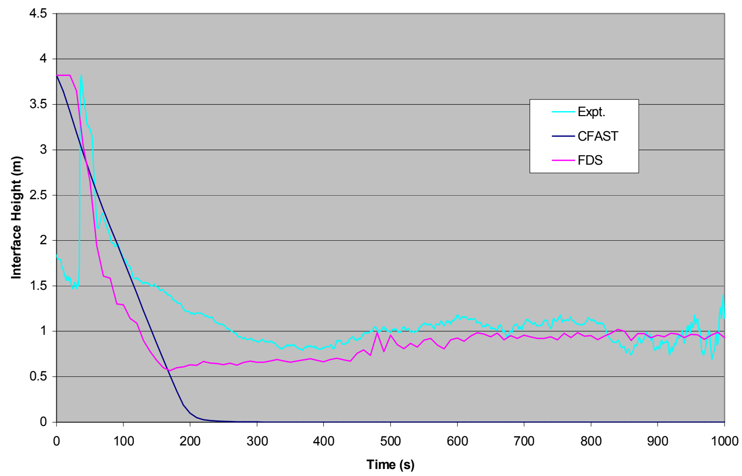

Figure 5.4.3 Hot Gas Layer Development - Test 4

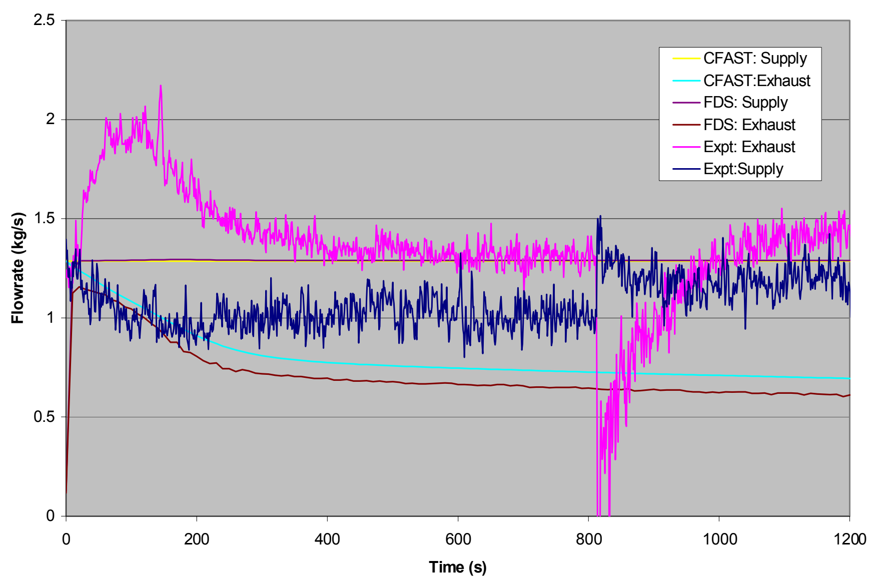

Figure 5.4.4 Vent Flows - Test 4

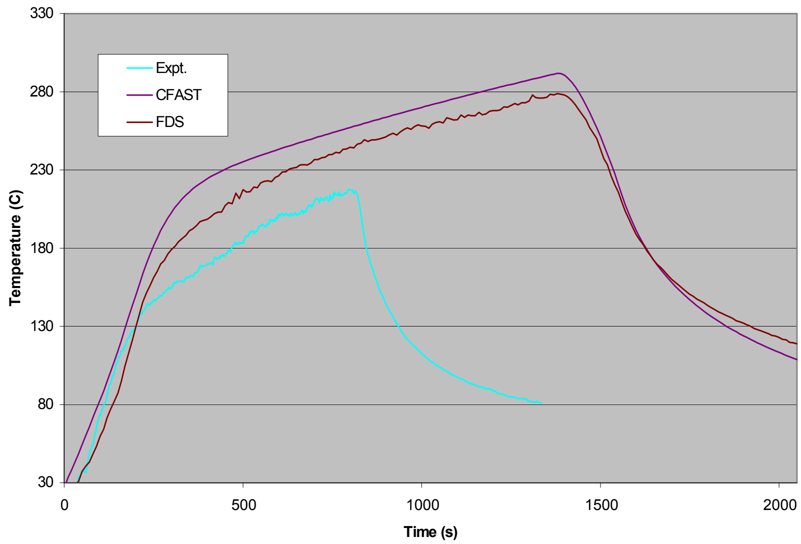

Figure 5.4.5 Hot Gas Layer Temperature - Test 4

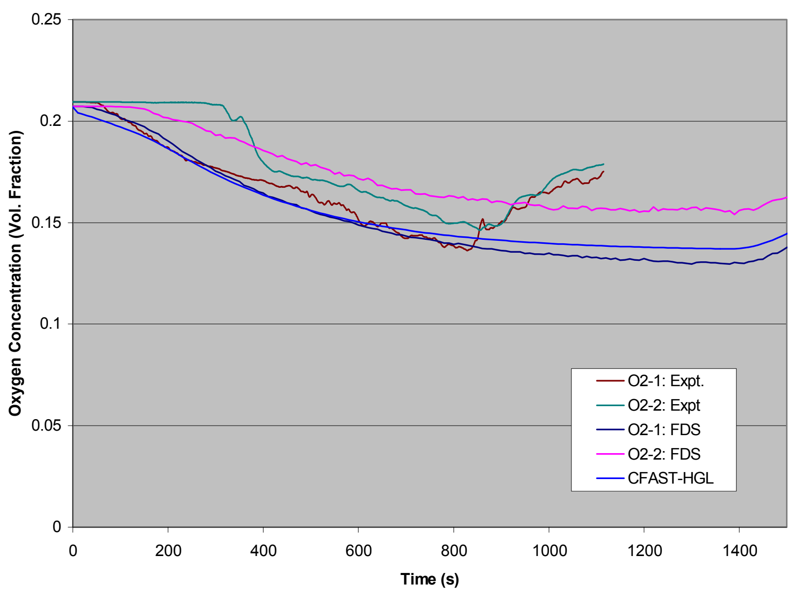

Figure 5.4.6 Oxygen Concentration - Test 4

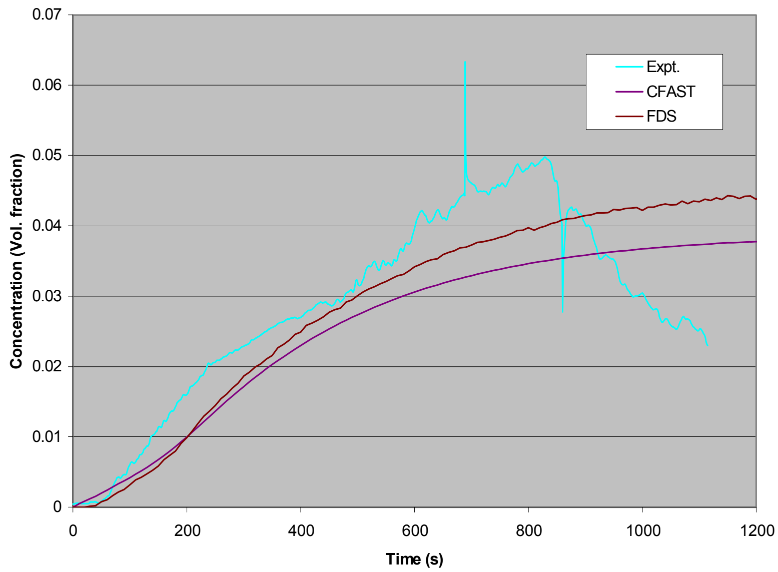

Figure 5.4.7 CO2 Concentration - Test 4

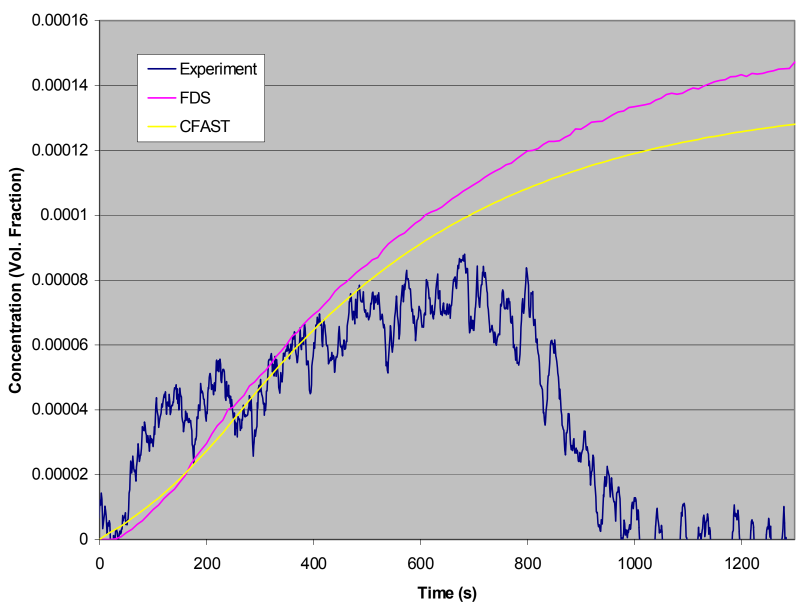

Figure 5.4.8 CO Concentration - Test 4

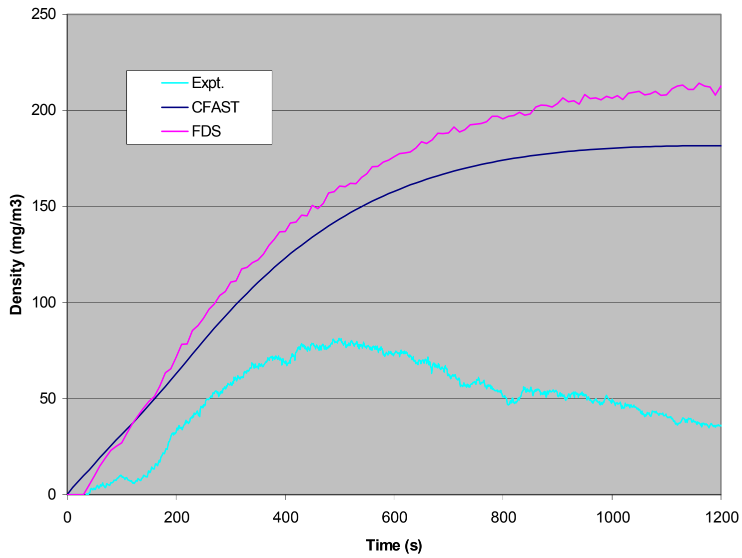

Figure 5.4.9 Smoke Concentration - Test 4

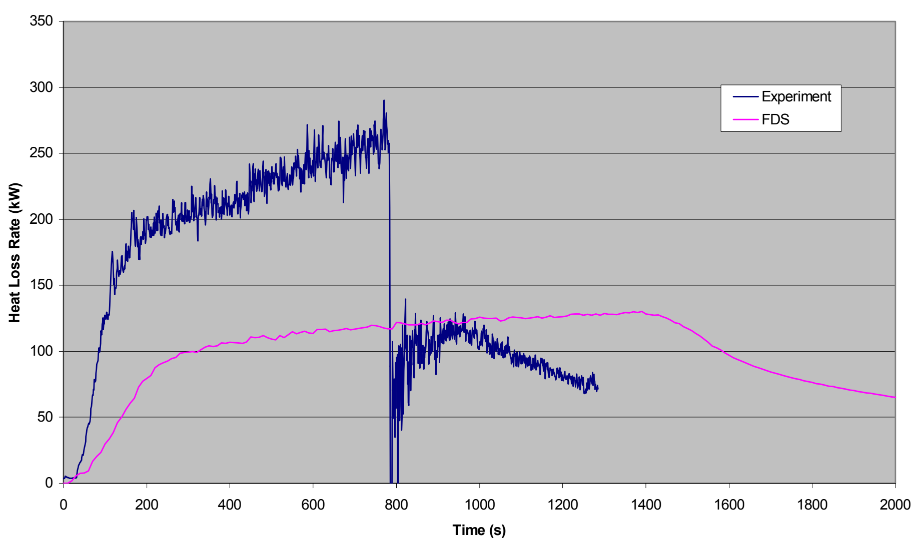

Figure 5.4.10 Heat Loss from Vents - Test 4

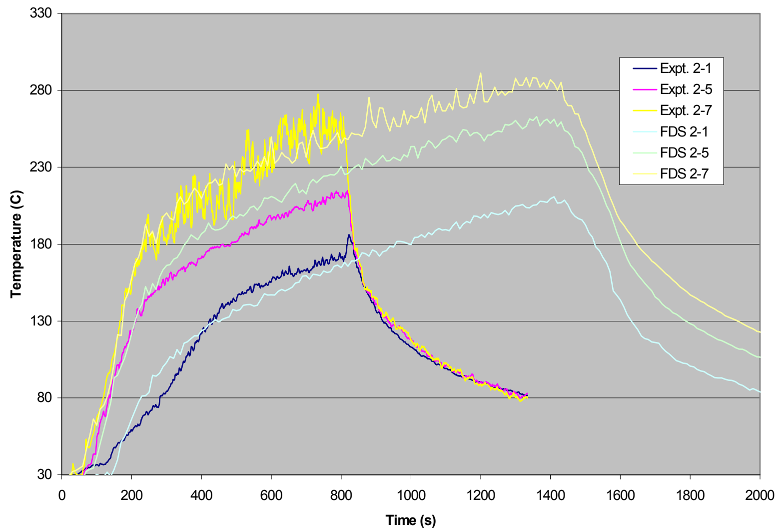

Figure 5.4.11 Compartment Temperature (Tree 2) - Test 4

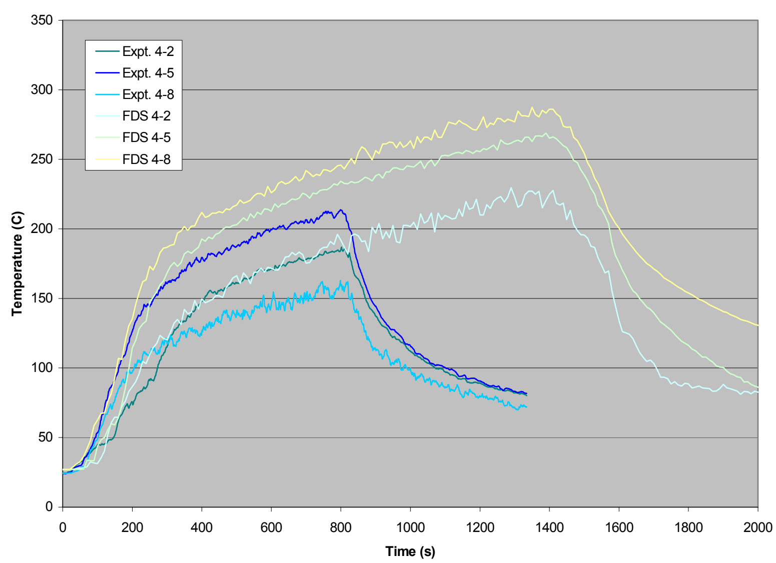

Figure 5.4.12 Compartment Temperature (Tree 4) - Test 4

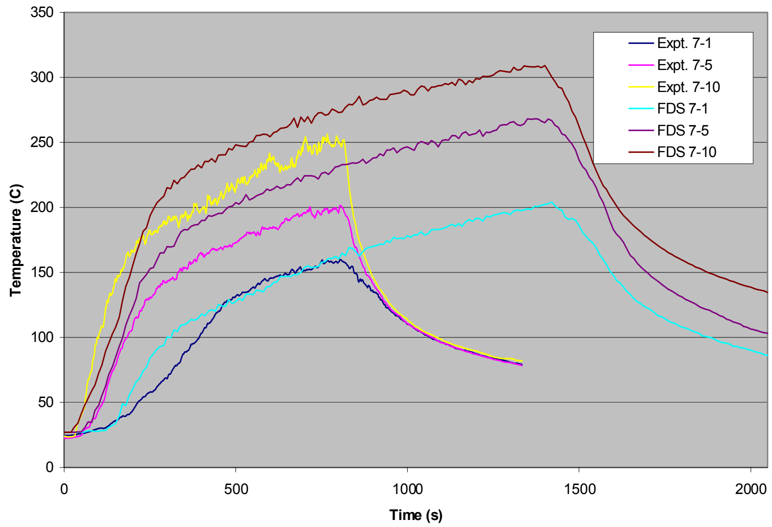

Figure 5.4.13 Compartment Temperature (Tree 7) - Test 4

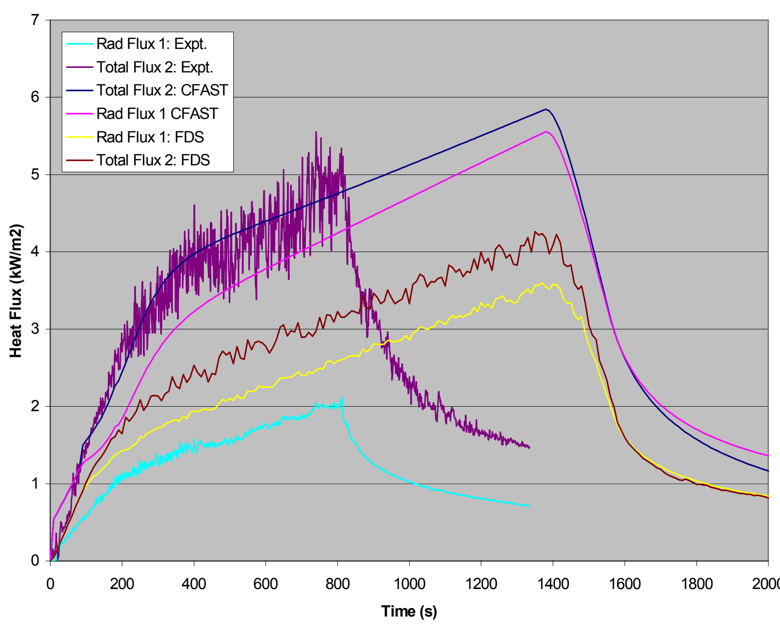

Figure 5.4.14 Heat Flux to Cables (Gauges 1 & 2) - Test 4

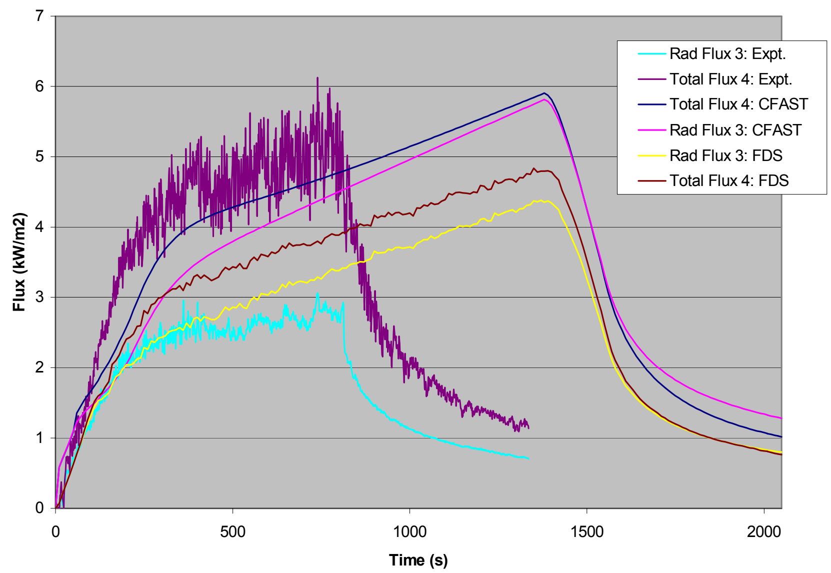

Figure 5.4.15 Heat Flux to Cables (Gauges 3 & 4) - Test 4

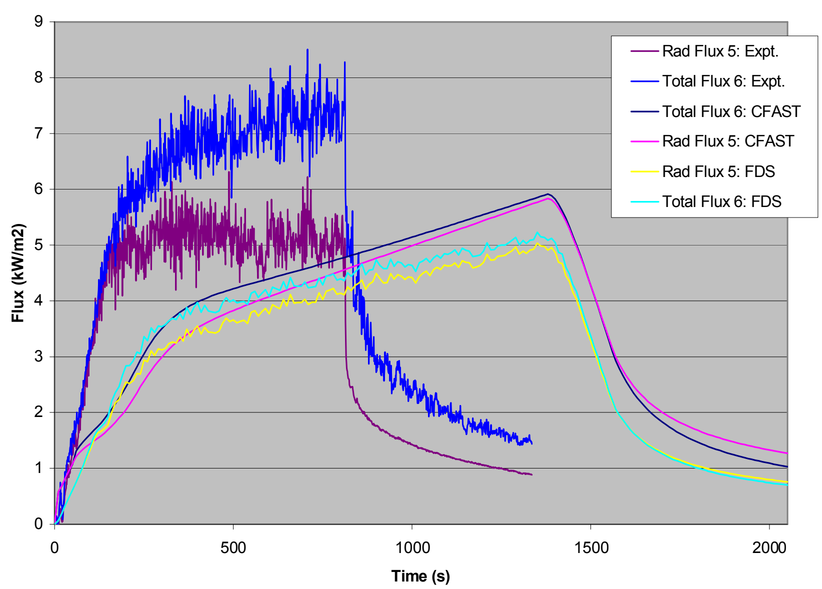

Figure 5.4.16 Heat Flux to Cables (Gauges 5 & 6) - Test 4

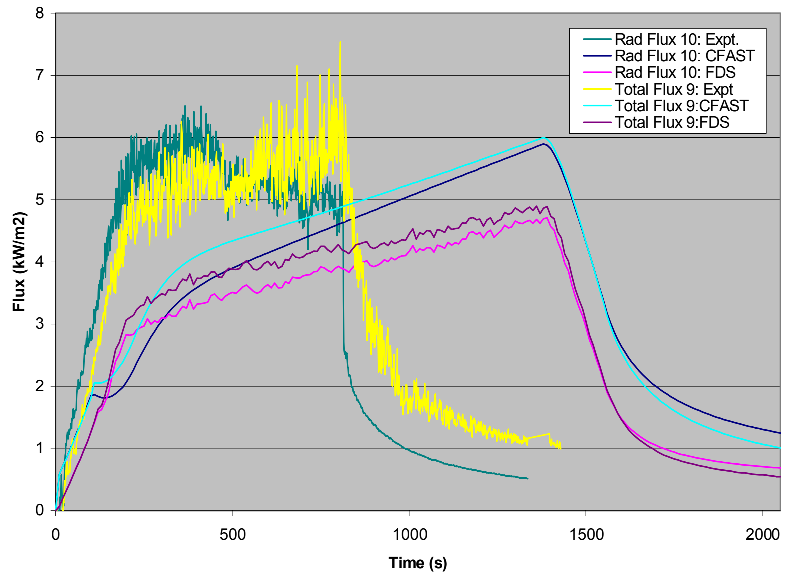

Figure 5.4.17 Heat Flux to Cables (Gauges 9 & 10) - Test 4

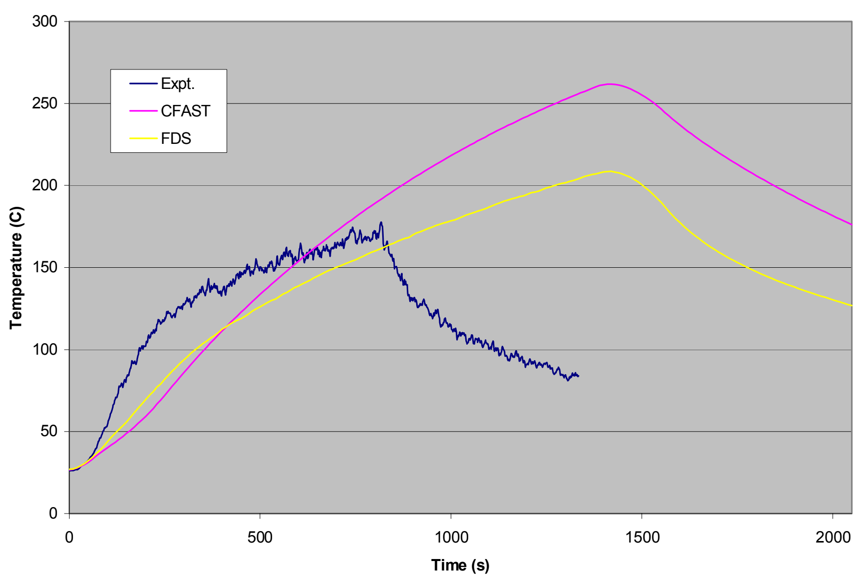

Figure 5.4.18 Control Cable Temperature (B-TS-14) - Test 4

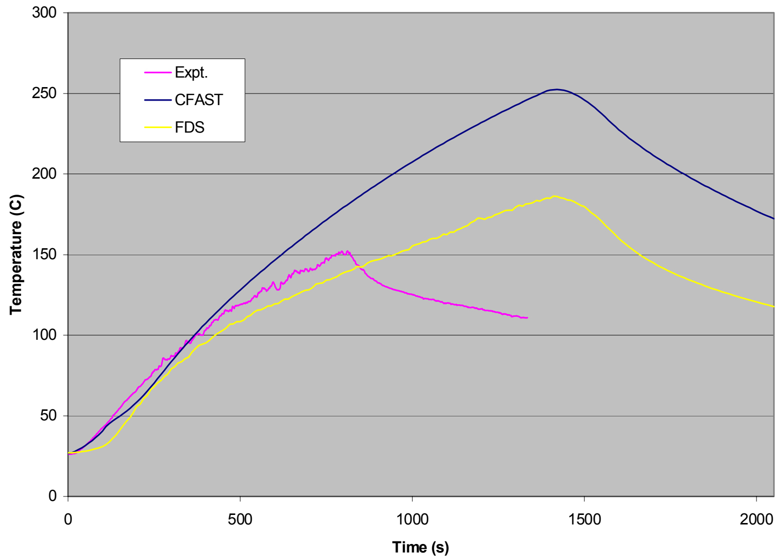

Figure 5.4.19 Vertical Cable Temperature (TS-33) - Test 4

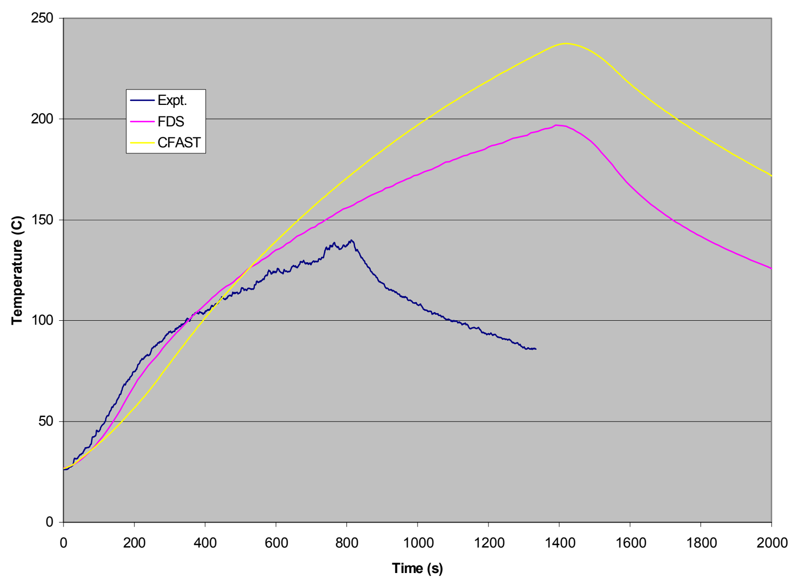

Figure 5.4.20 Control Cable Temperature (D-TS-12) - Test 4

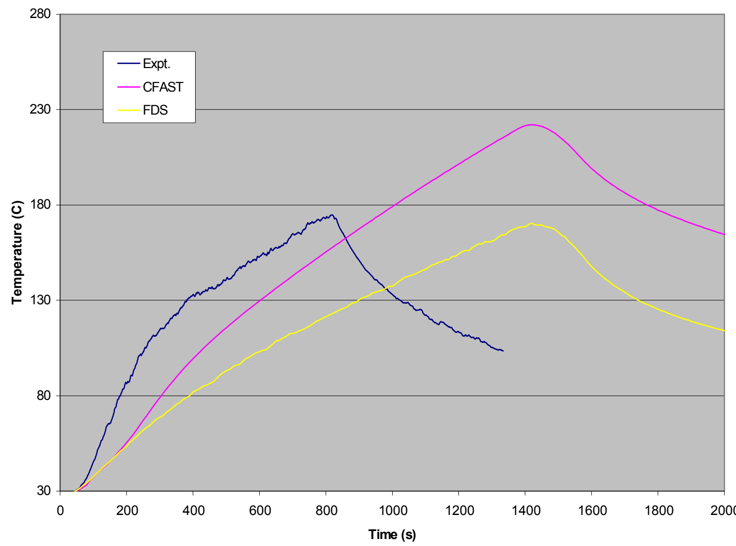

Figure 5.4.21 Power Cable Temperature (F-TS-20) - Test 4

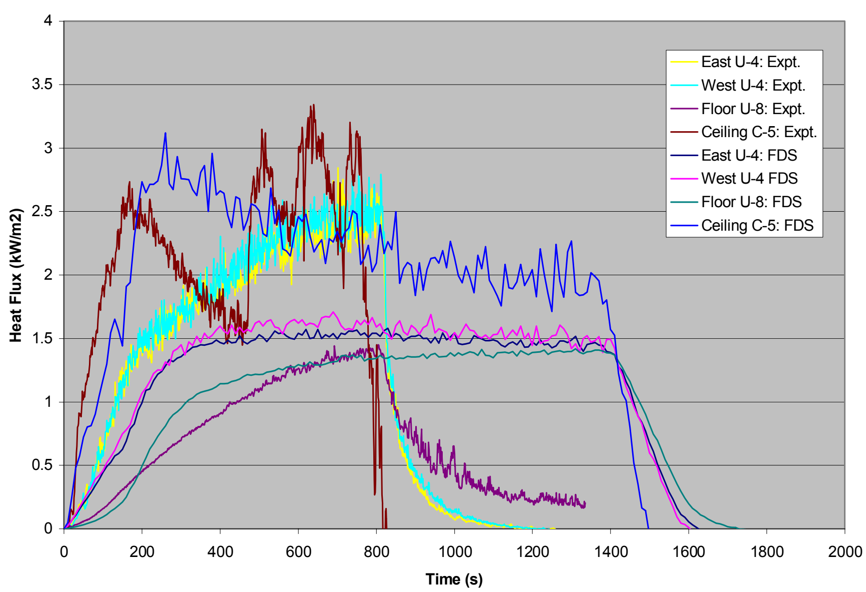

Figure 5.4.22 Heat Flux on Walls (FDS) - Test 4

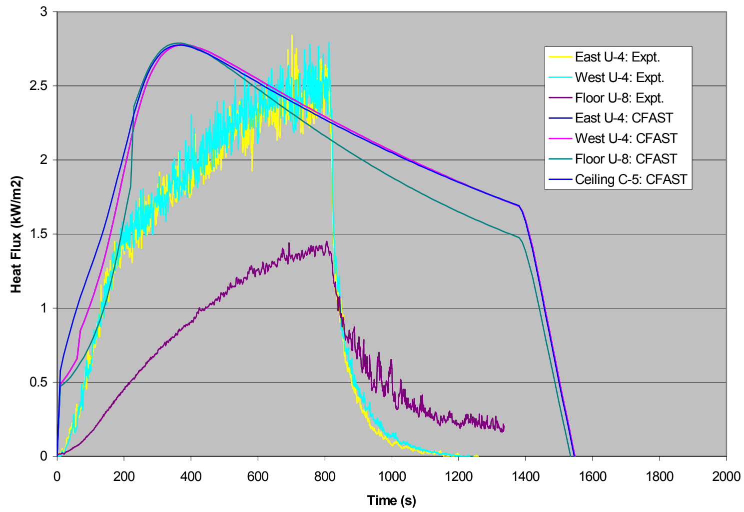

Figure 5.4.23 Heat Flux to Walls (CFAST) - Test 4

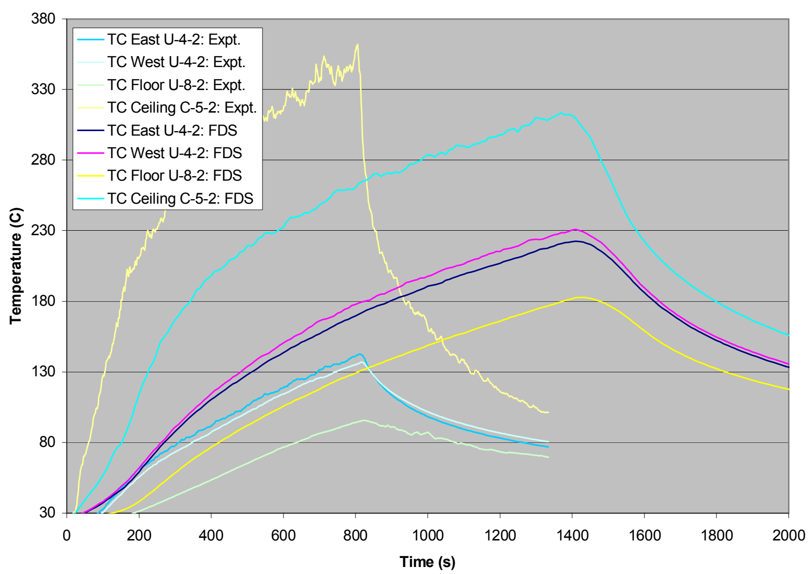

Figure 5.4.24 Wall Temperature (FDS) - Test 4

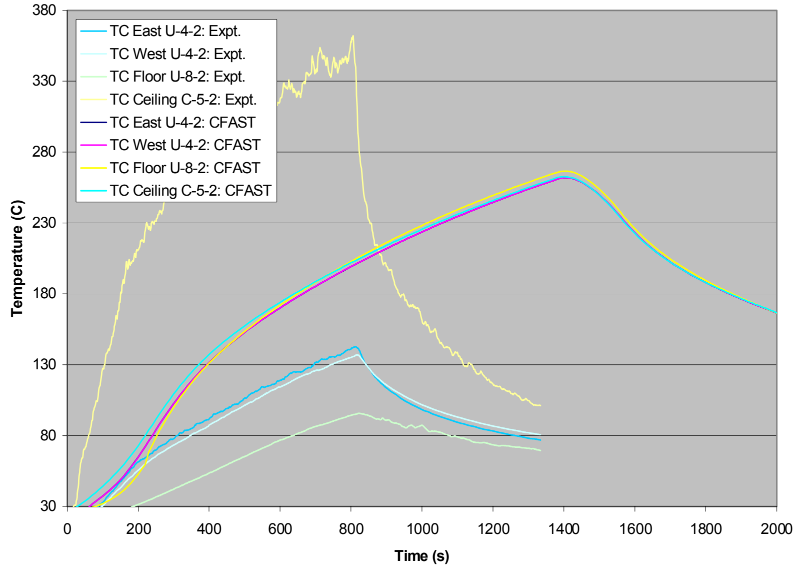

Figure 5.4.25 Wall Temperature (CFAST) - Test 4

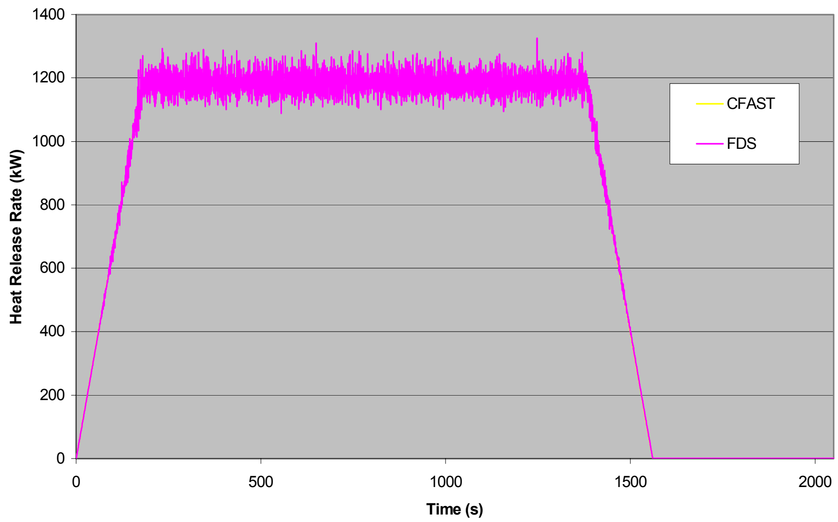

Figure 5.5.1 Heat Release Rate - Test 5

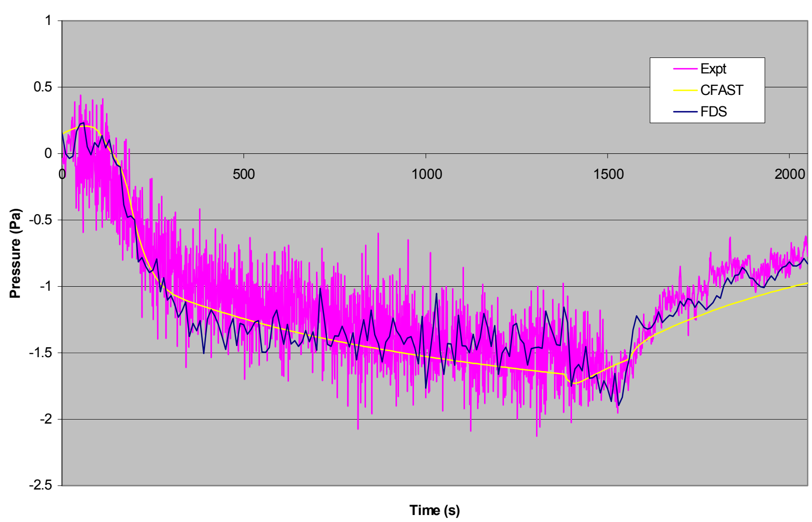

Figure 5.5.2 Compartment Pressure - Test 5

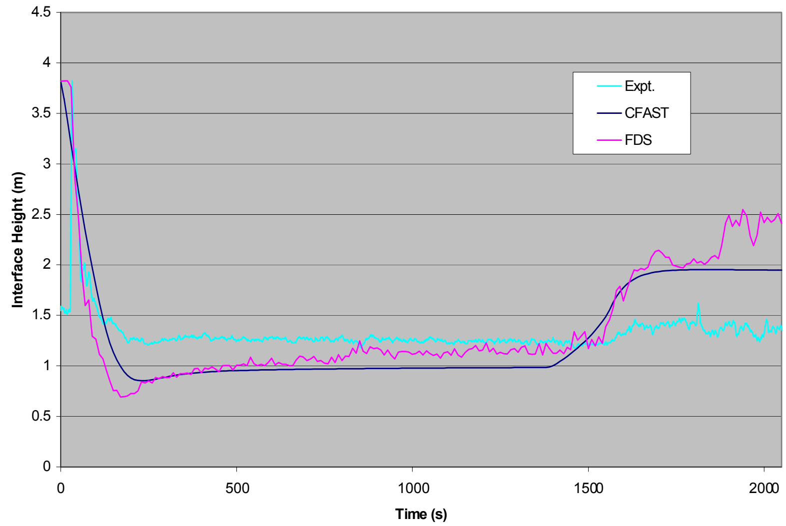

Figure 5.5.3 Hot Gas Layer Development - Test 4

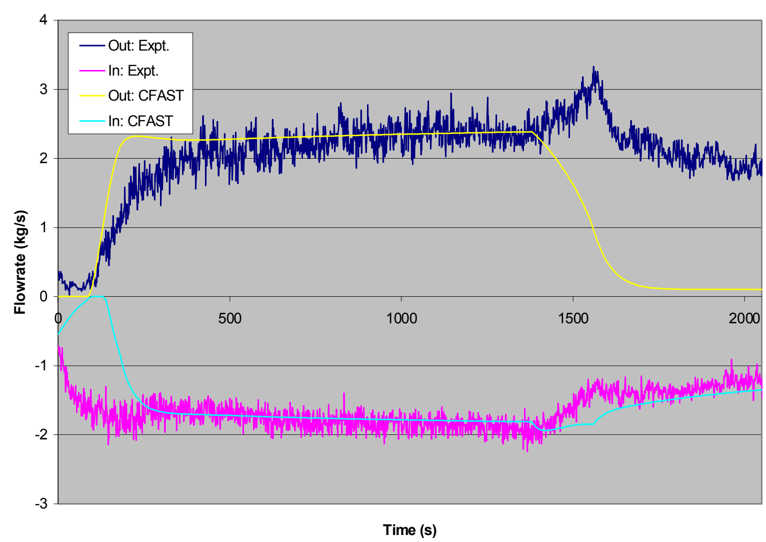

Figure 5.5.4 Door Mass Flow - Test 5

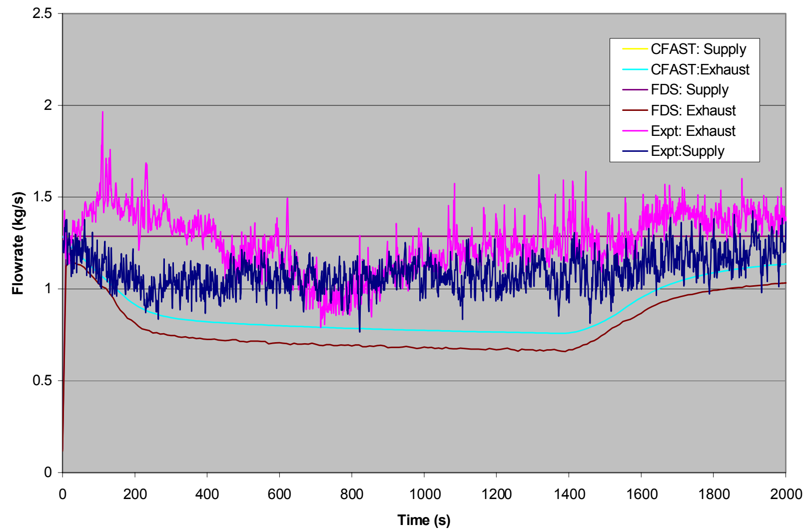

Figure 5.5.5 Vent Mass Flow - Test 5

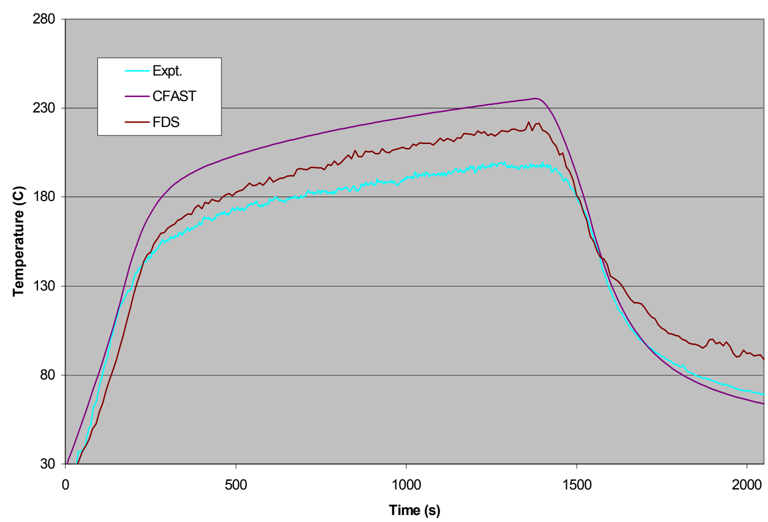

Figure 5.5.6 Hot Gas Layer Temperature - Test 5

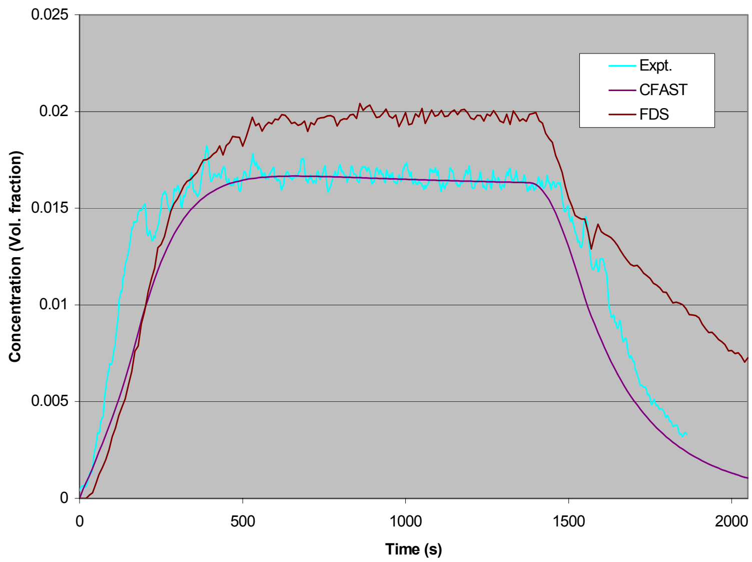

Figure 5.5.7 CO2 Concentration - Test 5

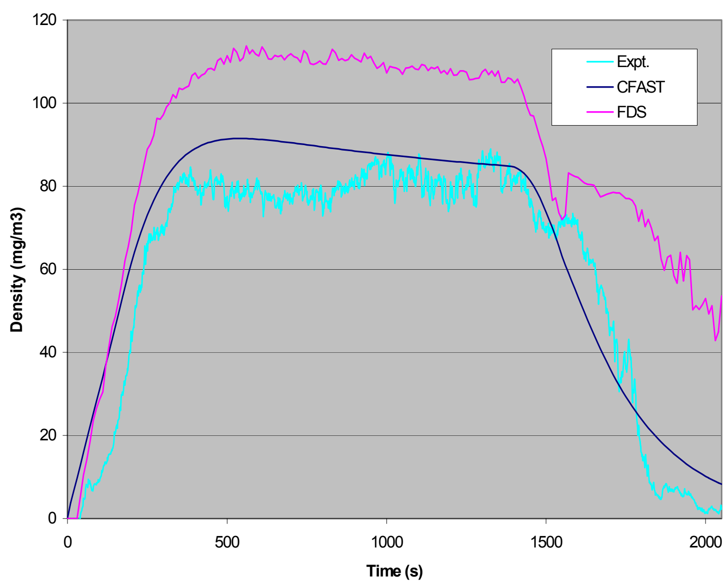

Figure 5.5.8 Smoke Concentration - Test 5

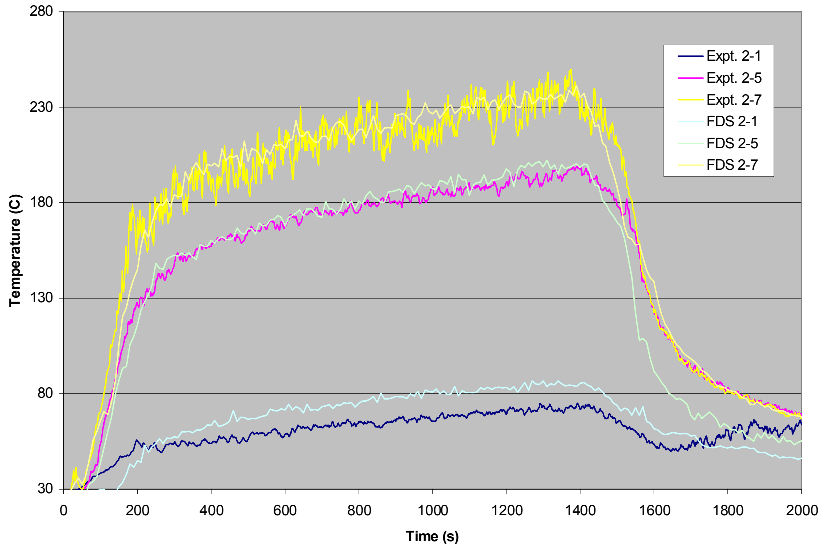

Figure 5.5.9 Hot Gas Temperature (Tree 2) - Test 5

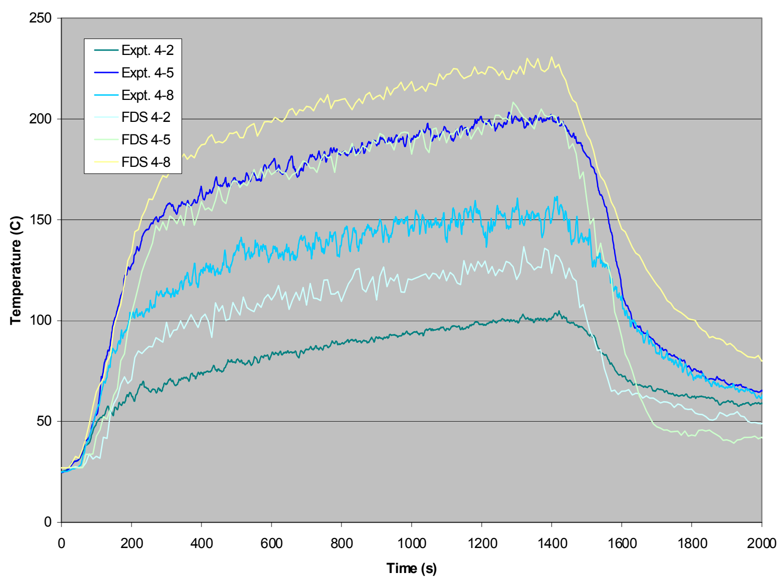

Figure 5.5.10 Hot Gas Temperature (Tree 4) - Test 5

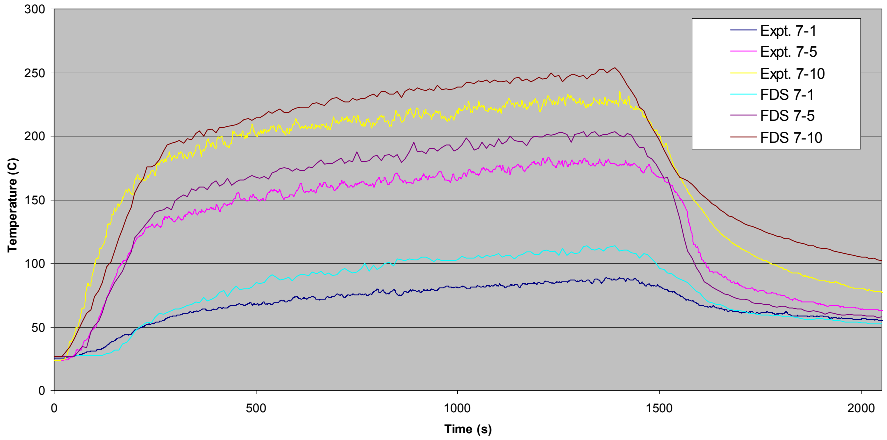

Figure 5.5.11 Hot Gas Temperature (Tree 7) - Test 5

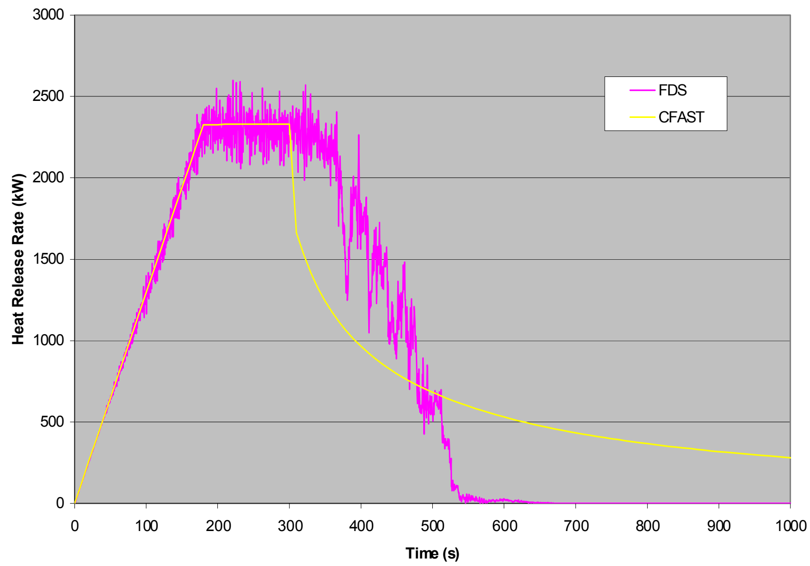

Figure 5.7.1 Heat Release Rate - Test 13

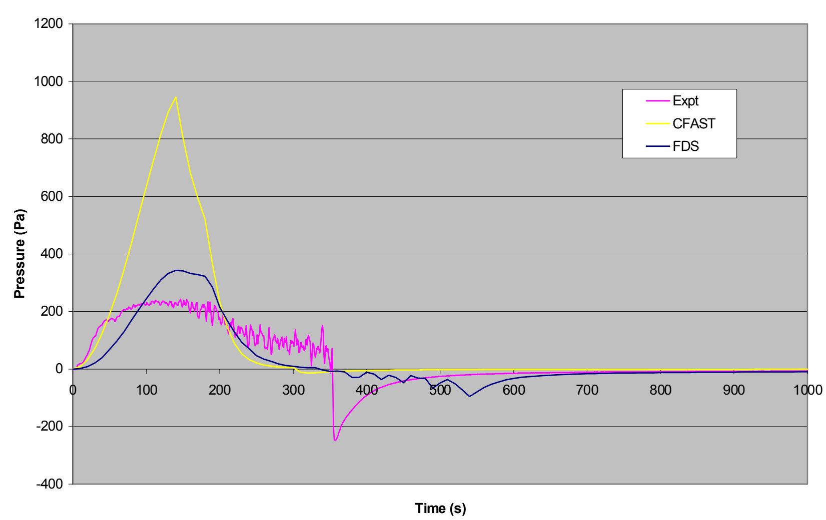

Figure 5.7.2 Compartment Pressure - Test 13

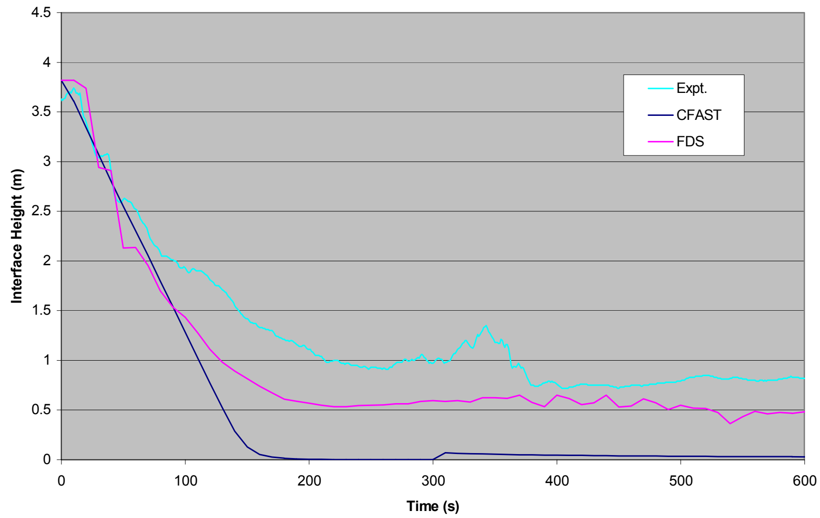

Figure 5.7.3 Hot Gas Layer Development - Test 13

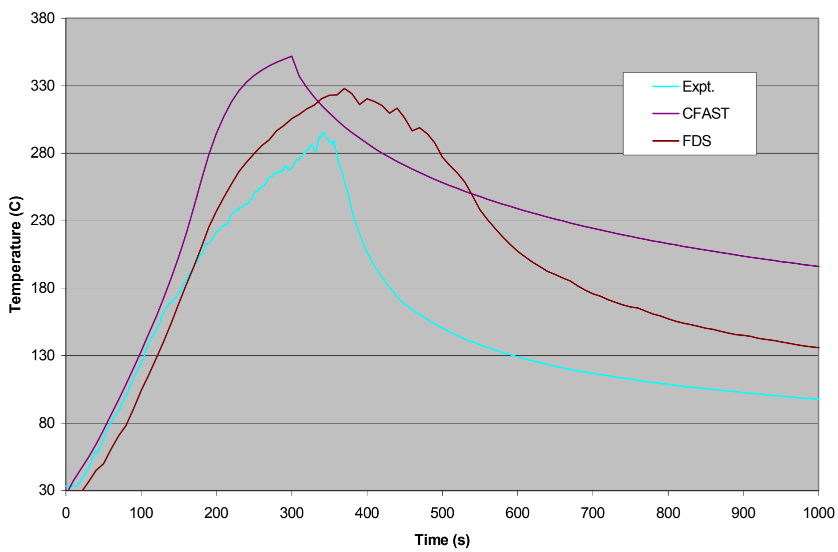

Figure 5.7.4 Hot Gas Layer Temperature - Test 13

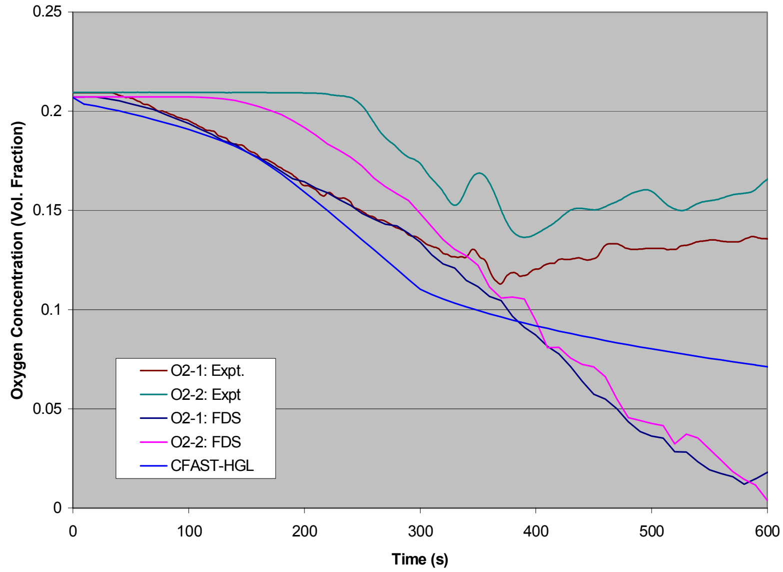

Figure 5.7.5 Oxygen Depletion - Test 13

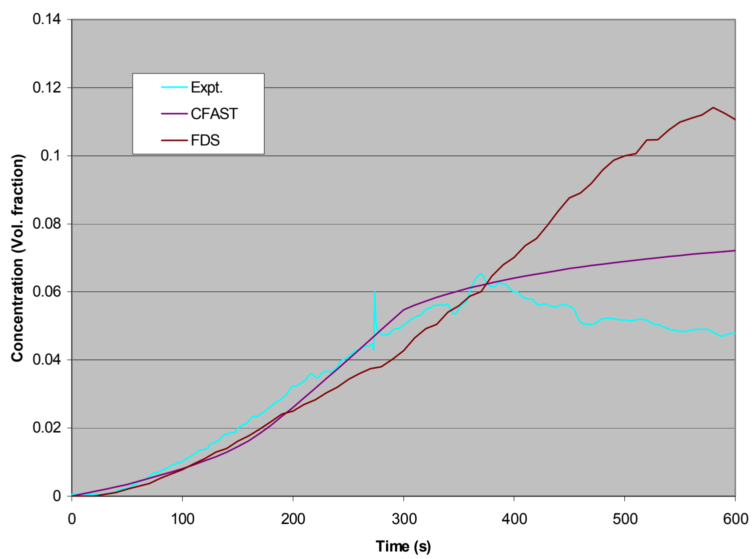

Figure 5.7.6 CO 2 Concentration - Test 13

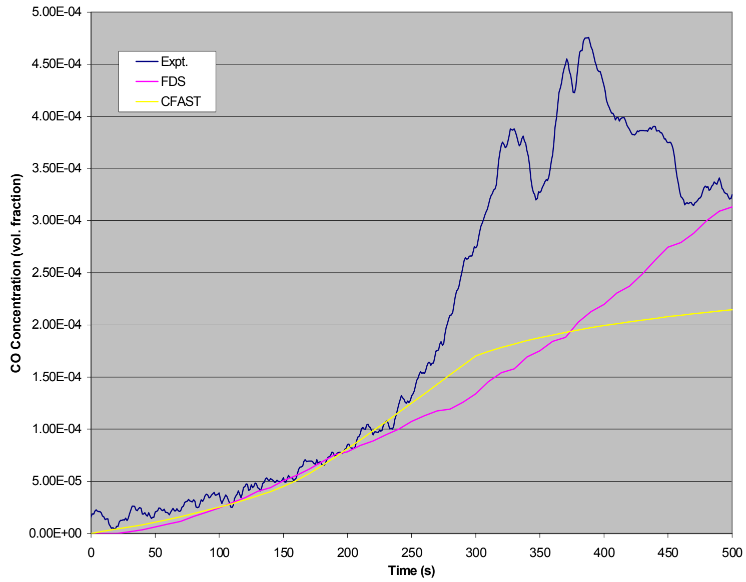

Figure 5.7.7 CO Concentration - Test 13

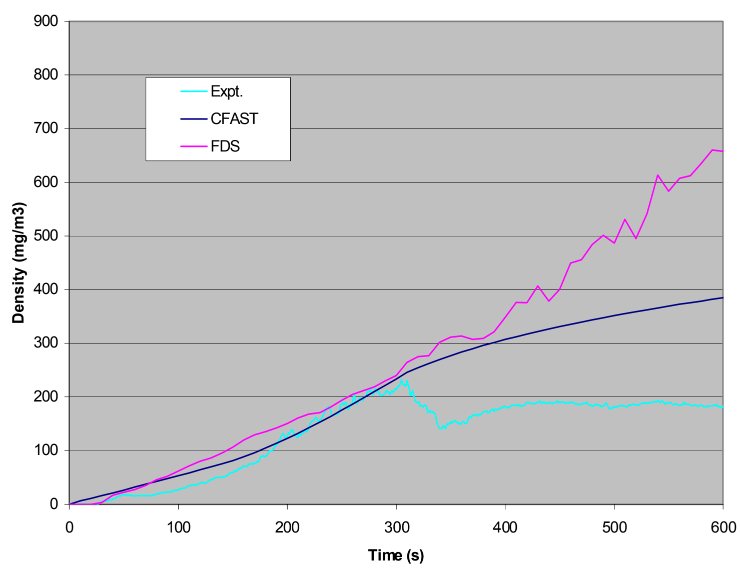

Figure 5.7.8 Smoke Density - Test 13

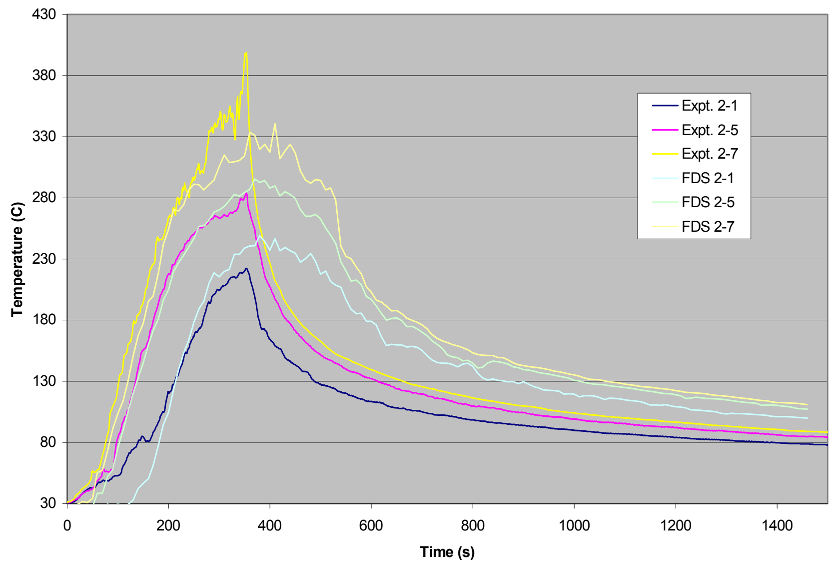

Figure 5.7.9 TC Tree 2 - Test 13

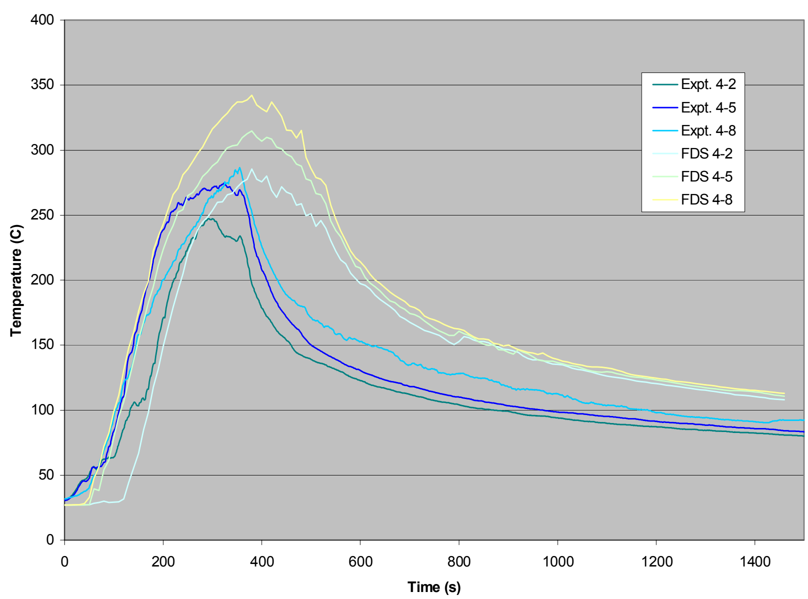

Figure 5.7.10 TC Tree 4 -Test 13

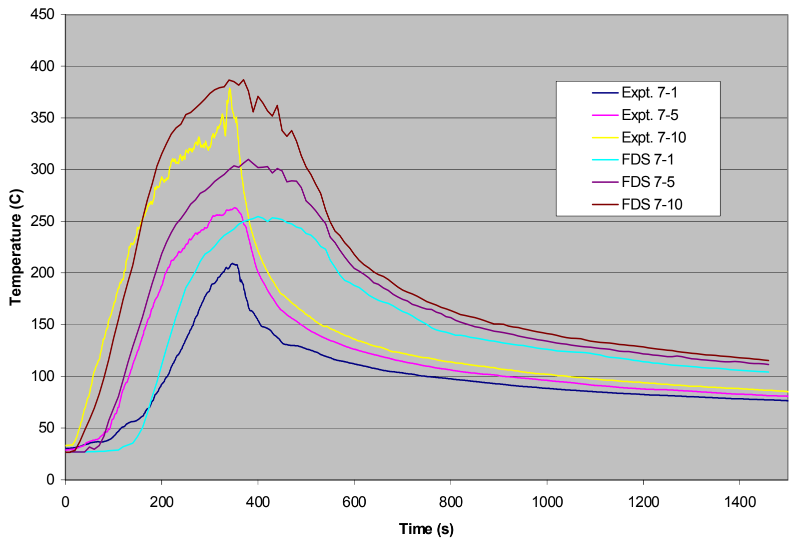

Figure 5.7.11 TC Tree 7 - Test 13

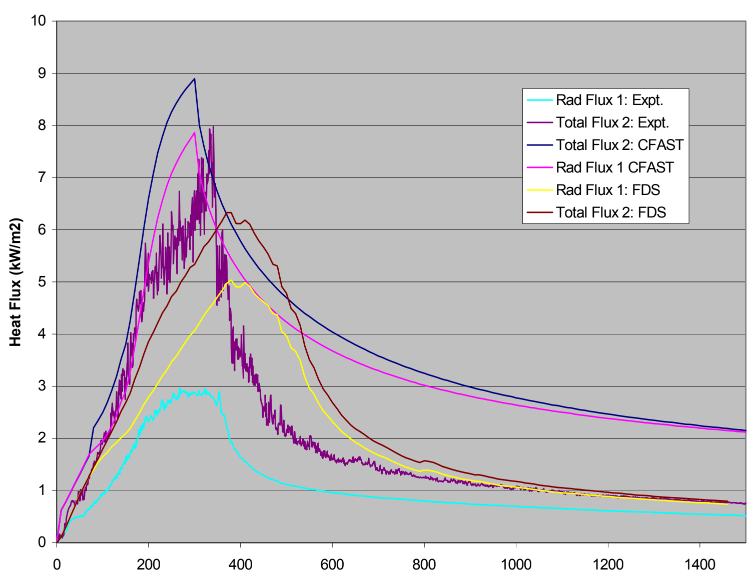

Figure 5.7.12 Heat Flux to Cables (1 & 2) - Test 13

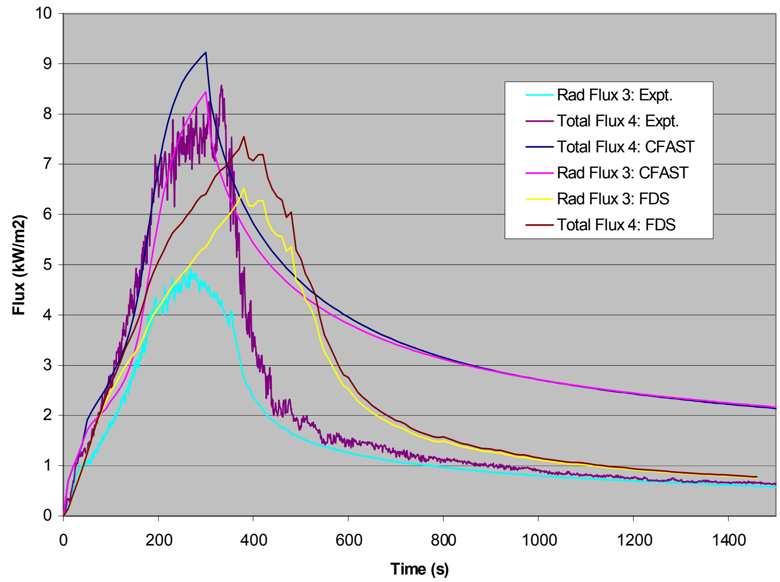

Figure 5.7.13 Heat Flux to Cables (3 & 4) - Test 13

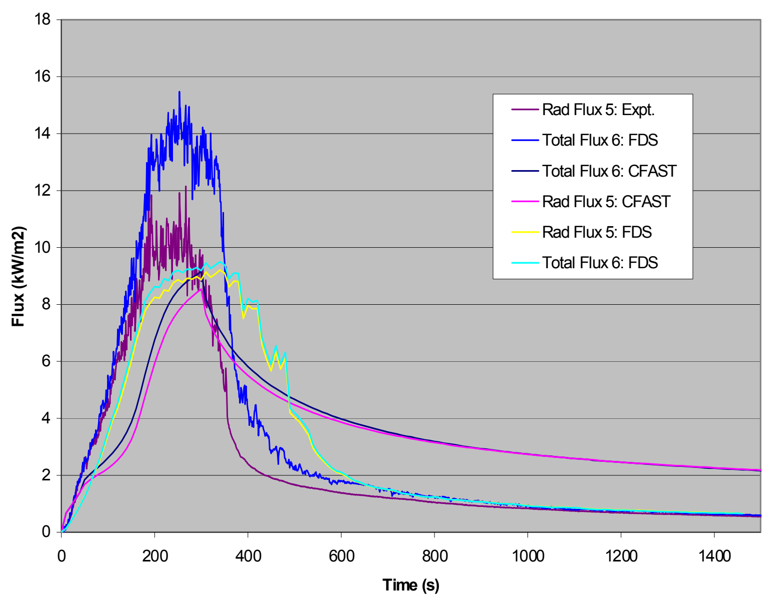

Figure 5.7.14 Heat Flux to Cables (5 & 6) - Test 13

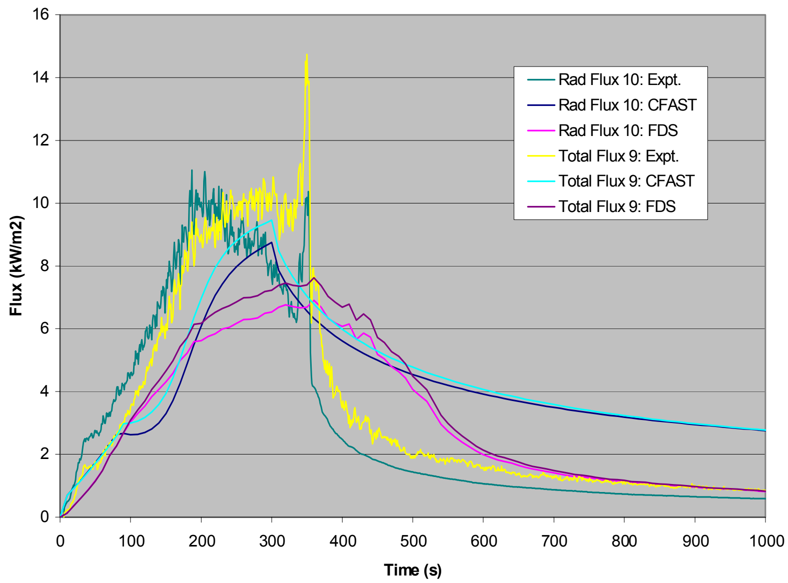

Figure 5.7.15 Heat Flux to Cables (9 & 10) - Test 13

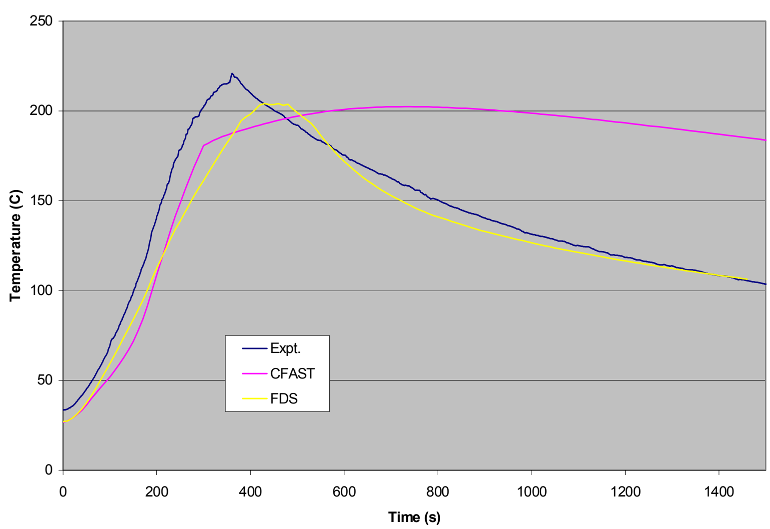

Figure 5.7.16 Control Cable Temperature (B-TS-14) - Test 13

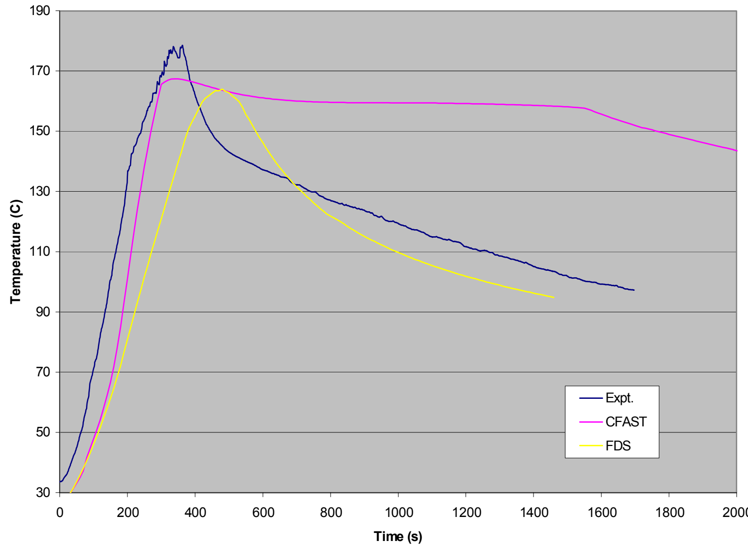

Figure 5.7.17 Power Cable Temperature (F-TS-20) - Test 13

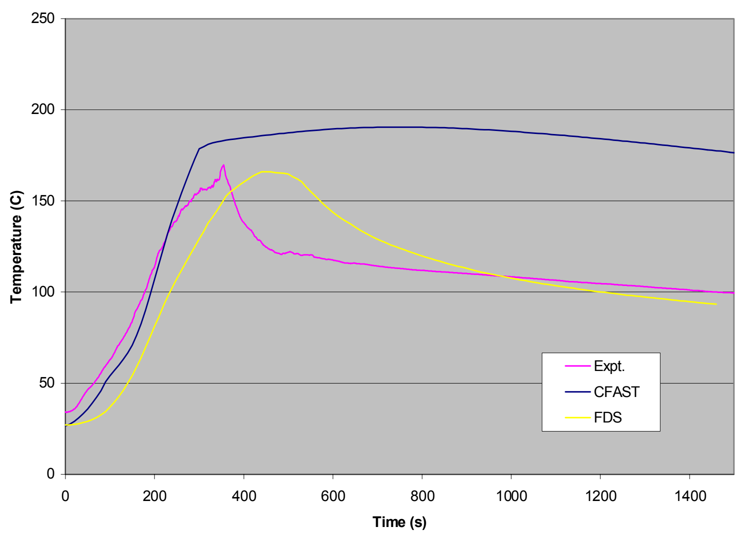

Figure 5.7.18 Vertical Cable Temperature (TS-33) - Test 13

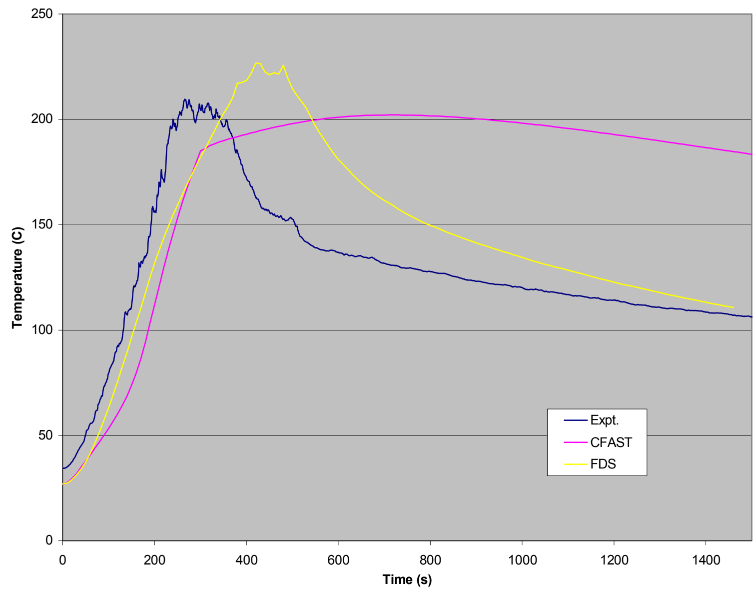

Figure 5.7.19 Control Cable Temperature (D-TS-12) - Test 13

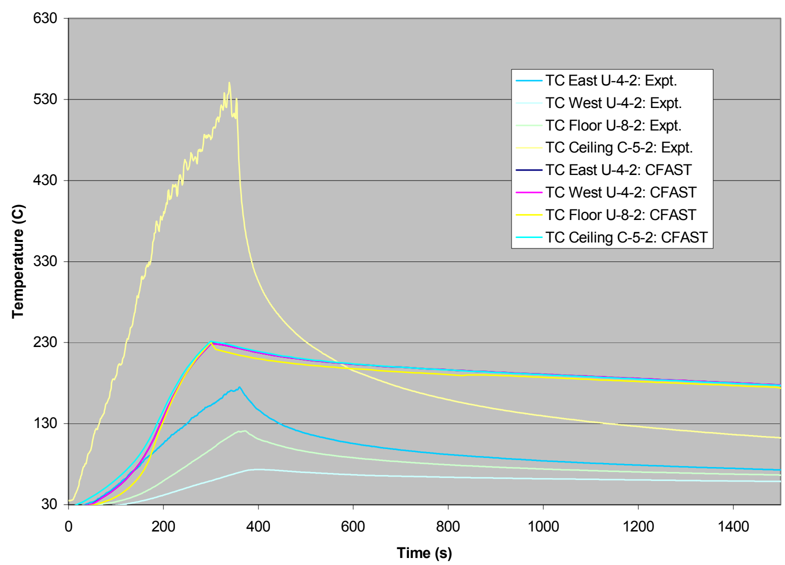

Figure 5.7.20 Wall Temperature (CFAST) - Test 13

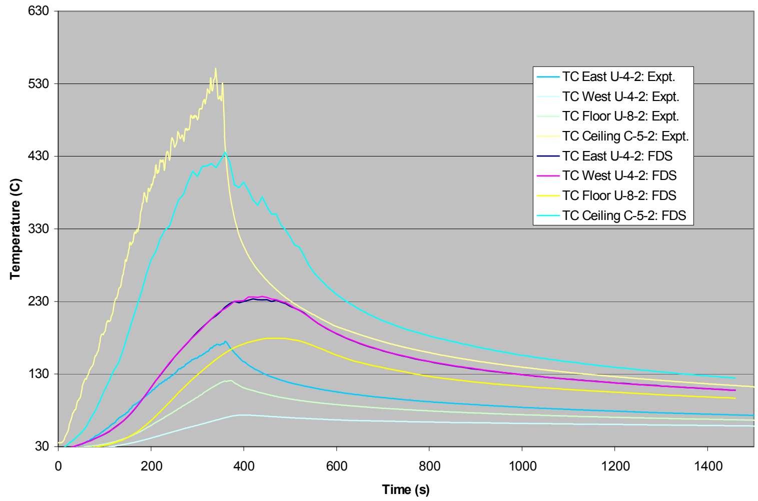

Figure 5.7.21 Wall Temperature (FDS) - Test 13

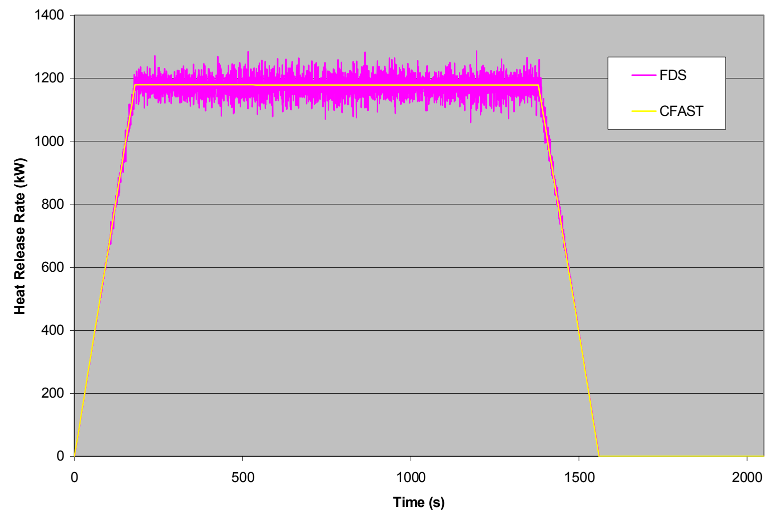

Figure 5.8.1 Heat Release Rate - Test 14

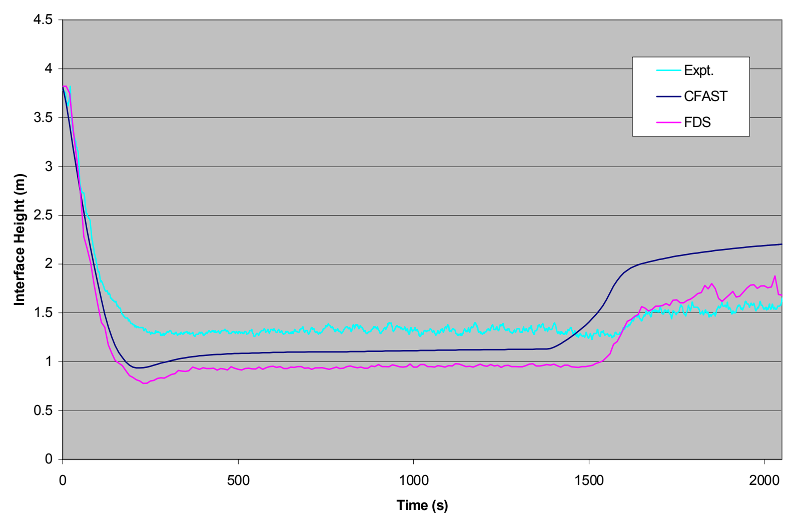

Figure 5.8.2 Hot Gas Layer Development - Test 14

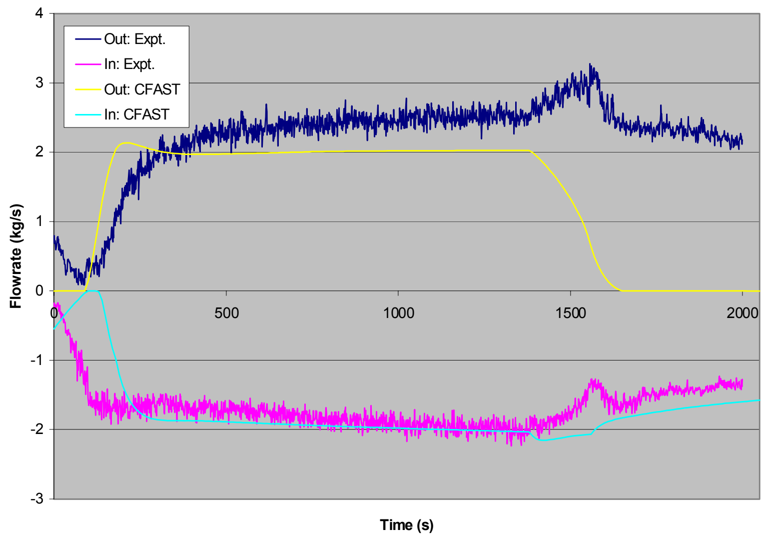

Figure 5.8.3 Door Mass Flows - Test 14

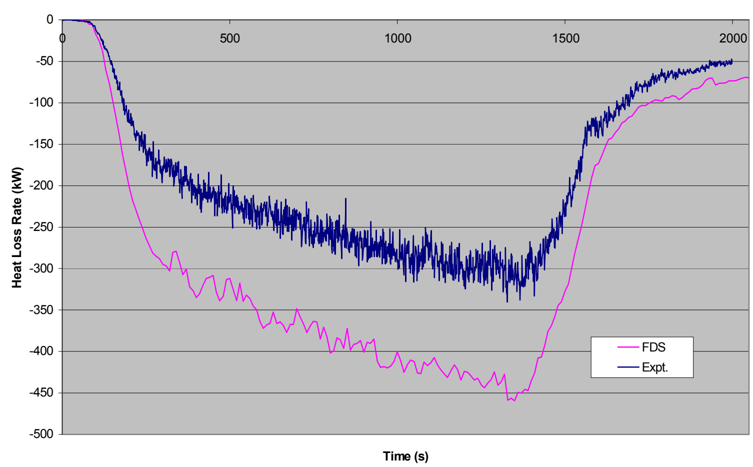

Figure 5.8.4 Door Heat Flow - Test 14

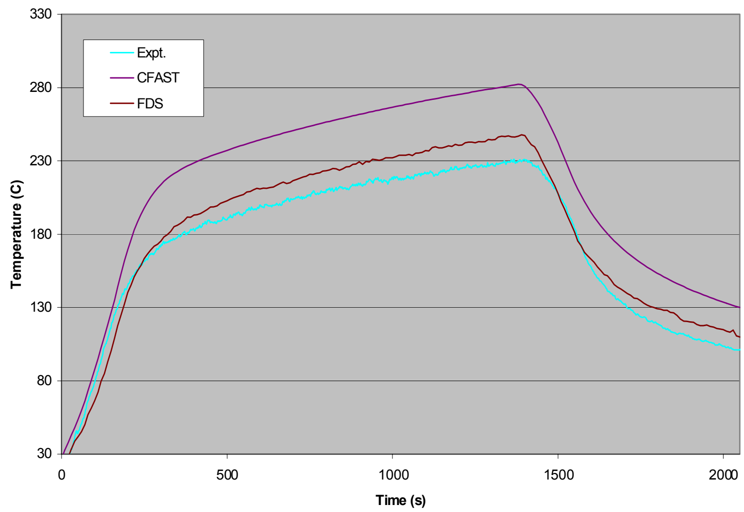

Figure 5.8.5 Hot Gas Temperature - Test 14

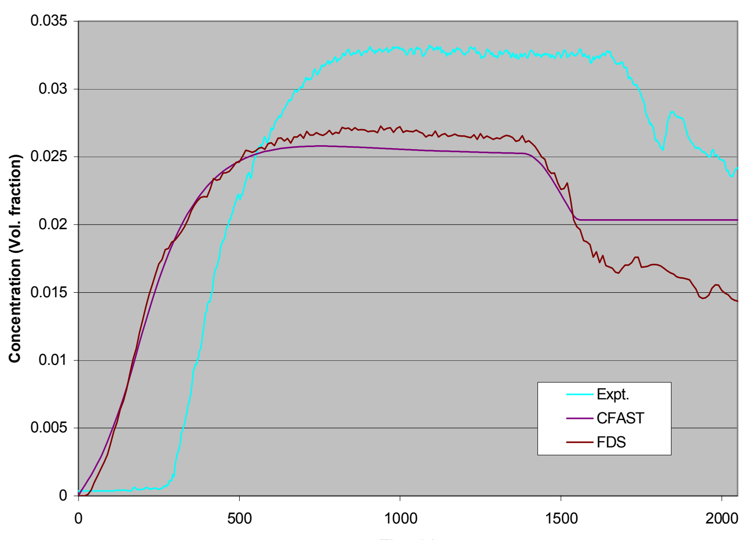

Figure 5.8.6 CO2 Concentration - Test 14

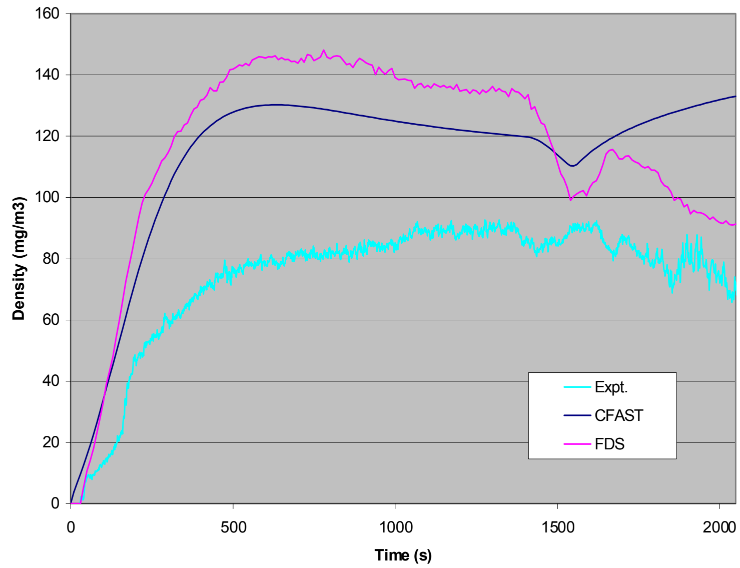

Figure 5.8.7 Smoke Concentration - Test 14

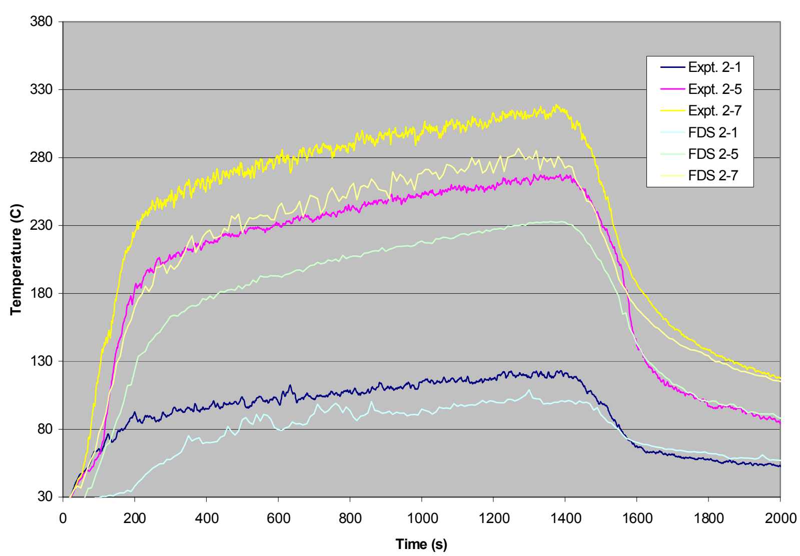

Figure 5.8.8 Hot Gas Temperature (Tree 2) - Test 14

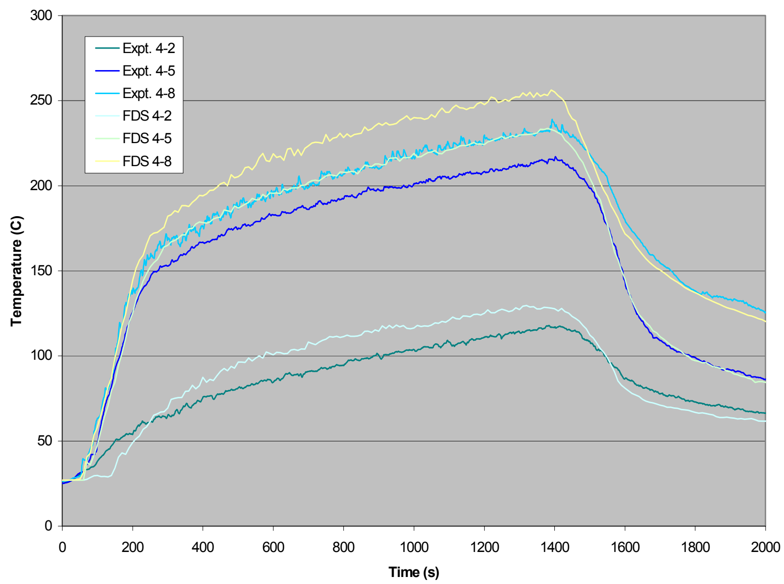

Figure 5.8.9 Hot Gas Temperature (Tree 4) - Test 14

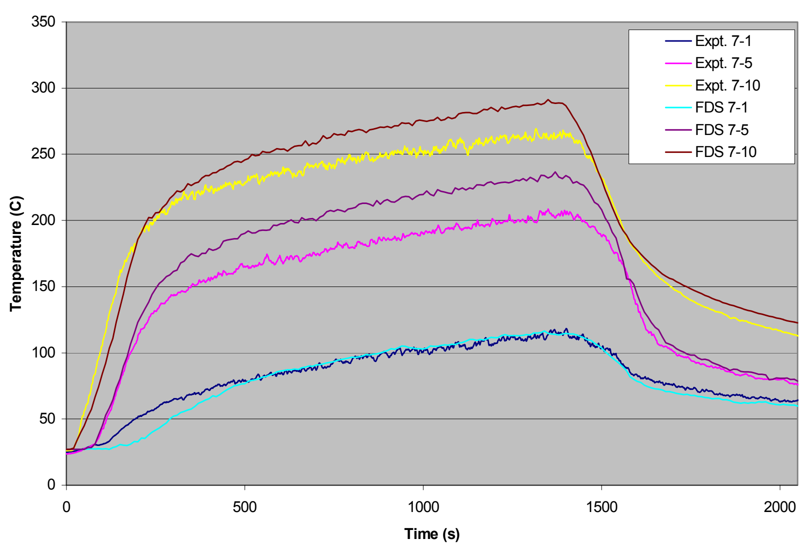

Figure 5.8.10 Hot Gas Temperature (Tree 7) - Test 14

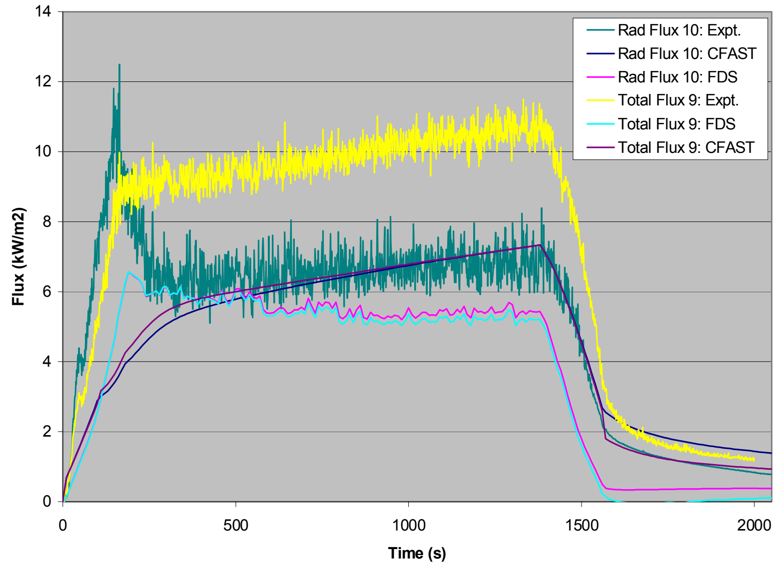

Figure 5.8.11 Heat Flux to Vertical Cables (Gauges 9 & 10) - Test 14

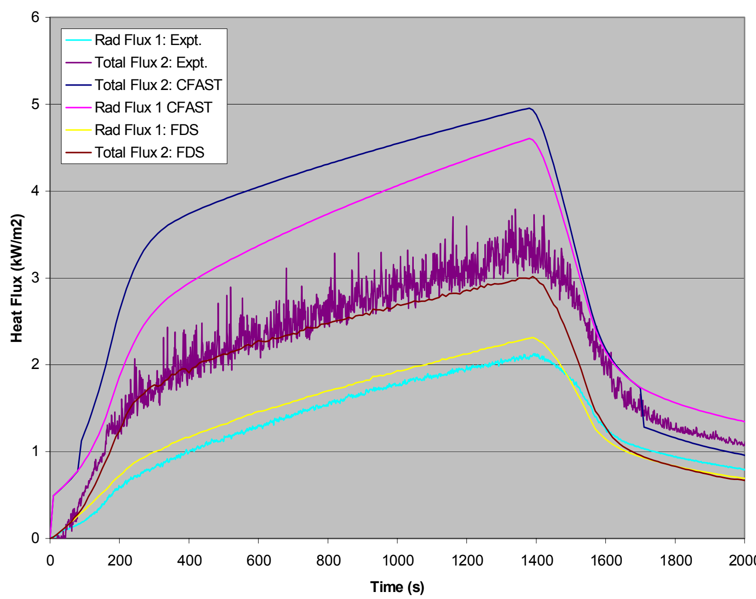

Figure 5.8.12 - Heat Flux to Cables (Gauges 1 & 2) - Test 14

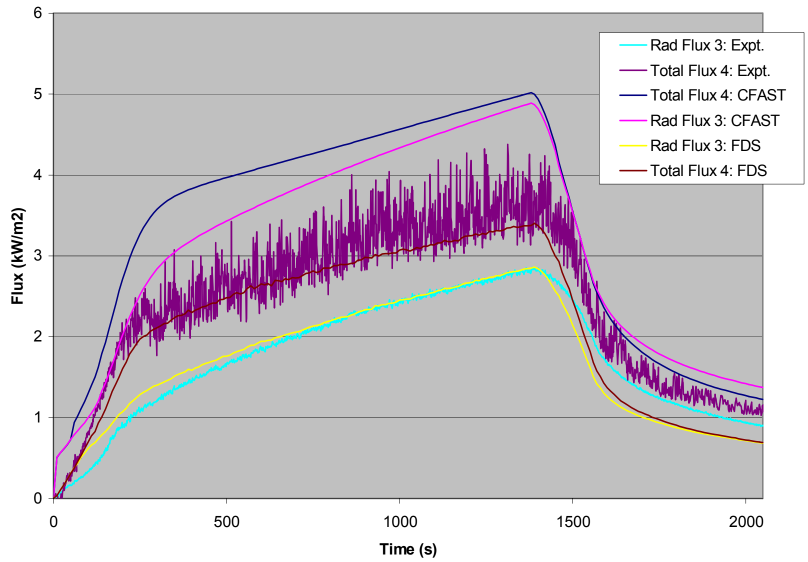

Figure 5.8.13 Heat Flux to Cables (Gauges 3 & 4) - Test 14

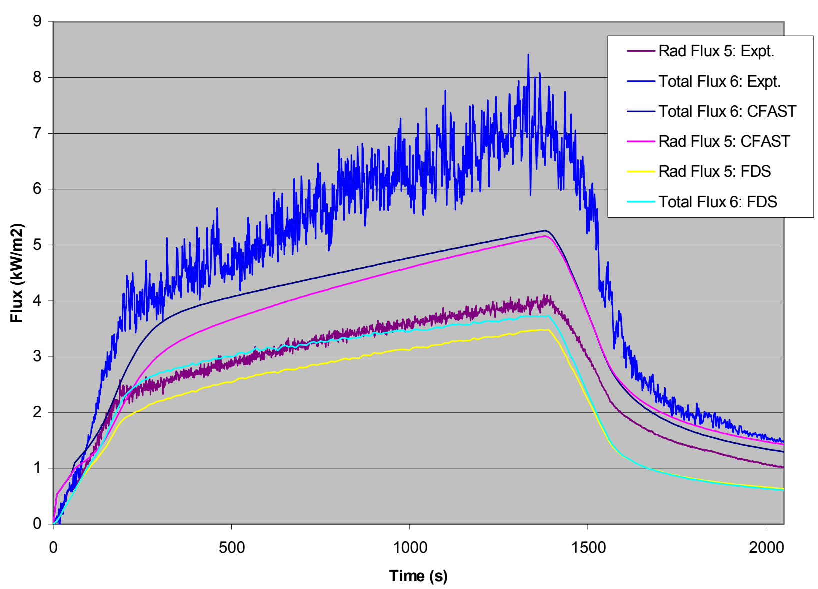

Figure 5.8.14 Heat Flux to Cables (Gauges 5 & 6) - Test 14

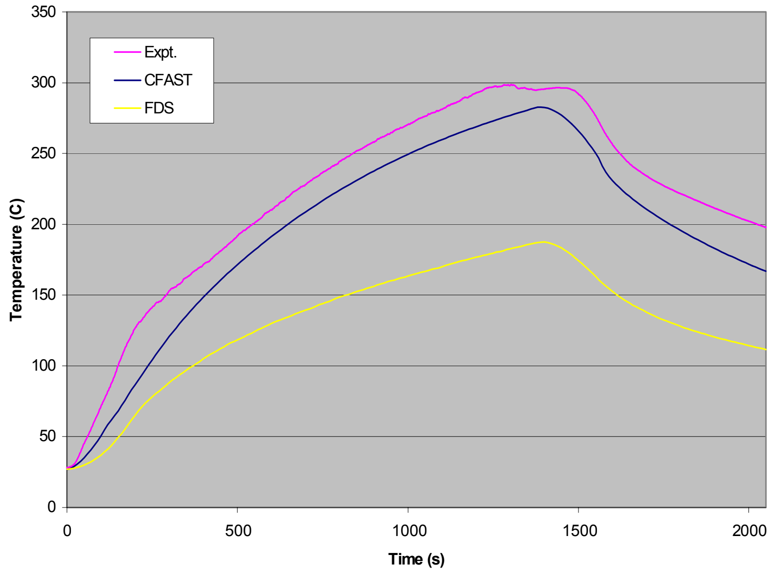

Figure 5.8.15 Vertical Cable Temperature (TS 33) - Test 14

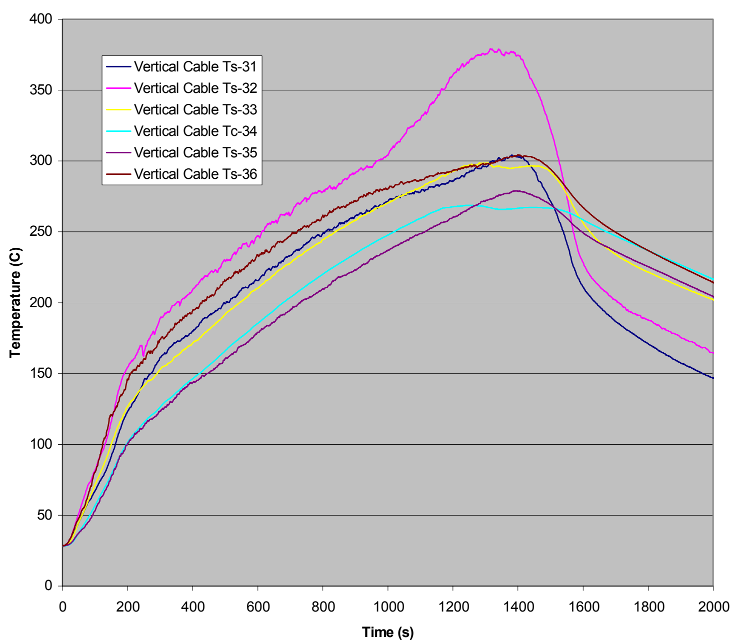

Figure 5.8.16 Vertical Cable Temperatures (Expt.) - Test 14

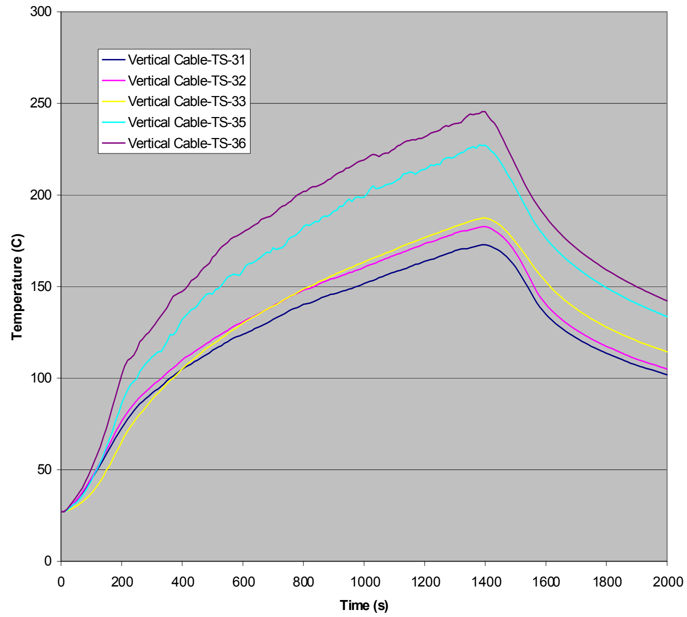

Figure 5.8.17 Vertical Cable Temperatures (FDS) - Test 14

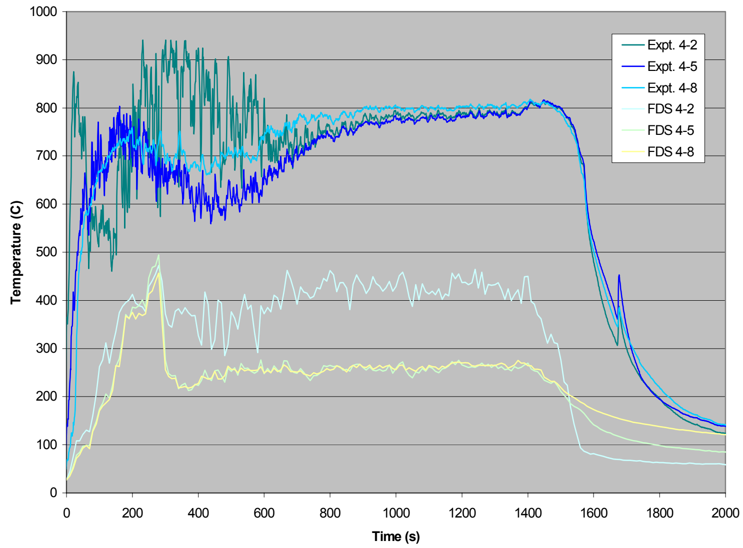

Figure 5.9.1 Plume Temperature (Tree 4) - Test 15

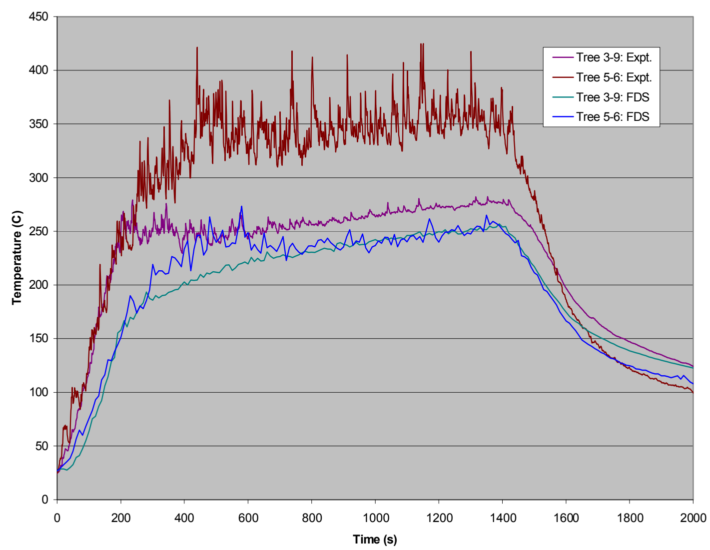

Figure 5.9.2 Hot Gas Temperature (3-9 & 5-6) - Test 15

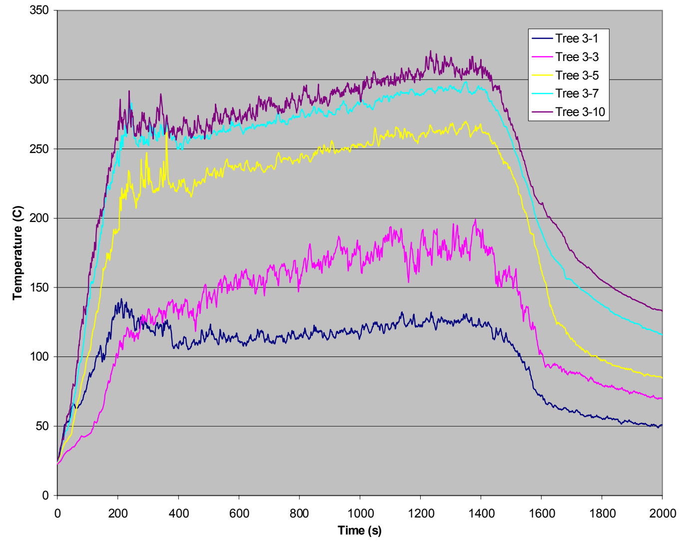

Figure 5.9.3 Hot Gas Temperature (Tree 3, Expt.) - Test 15

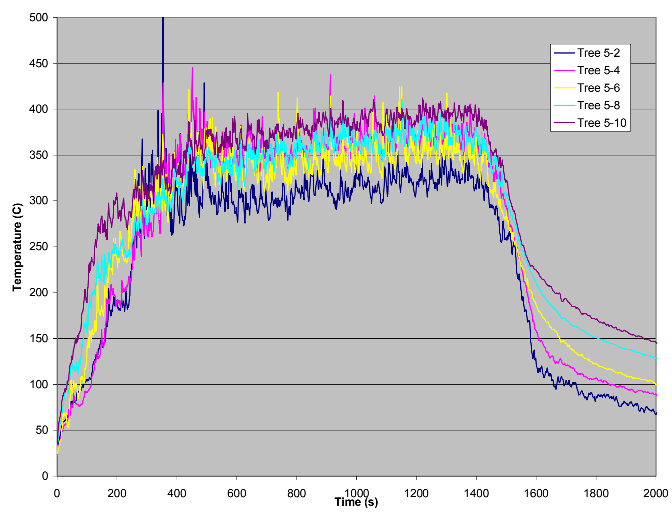

Figure 5.9.4 Hot Gas Temperature (Tree 5-Expt.) - Test 15

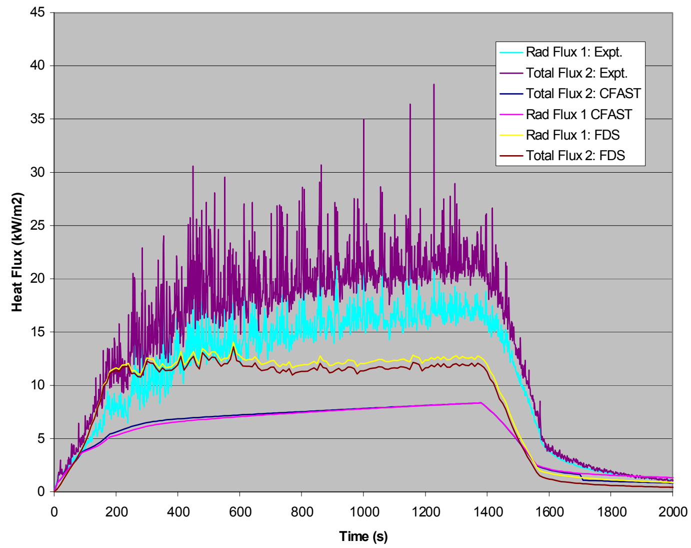

Figure 5.9.5 Heat Flux to Cables (Gauges 1 & 2) - Test 15

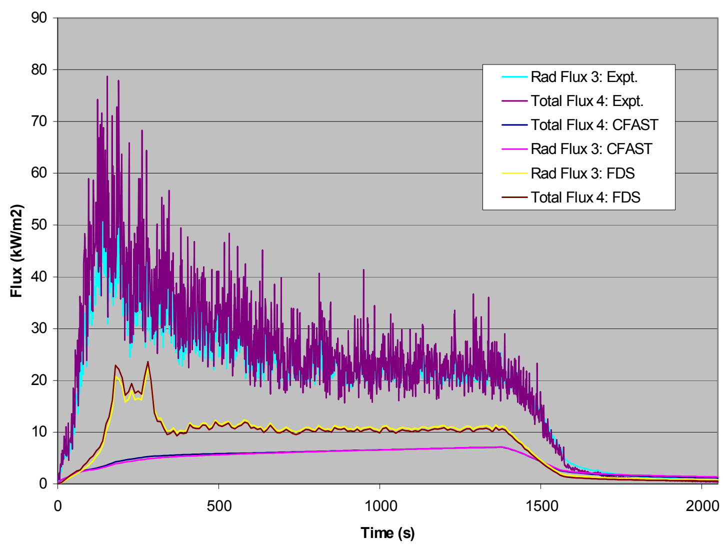

Figure 5.9.6 Heat Flux to Cables (Gauges 3 & 4) - Test 15

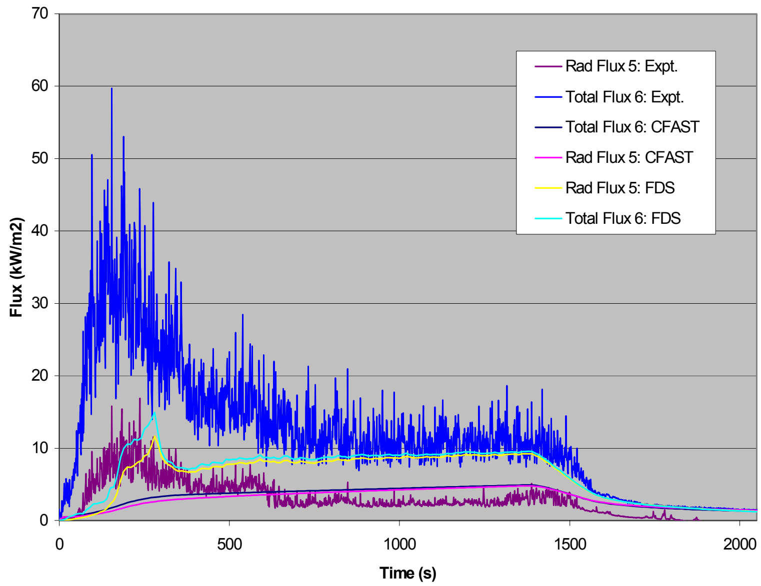

Figure 5.9.7 Heat Flux to Cables (Gauges 5 & 6) - Test 15

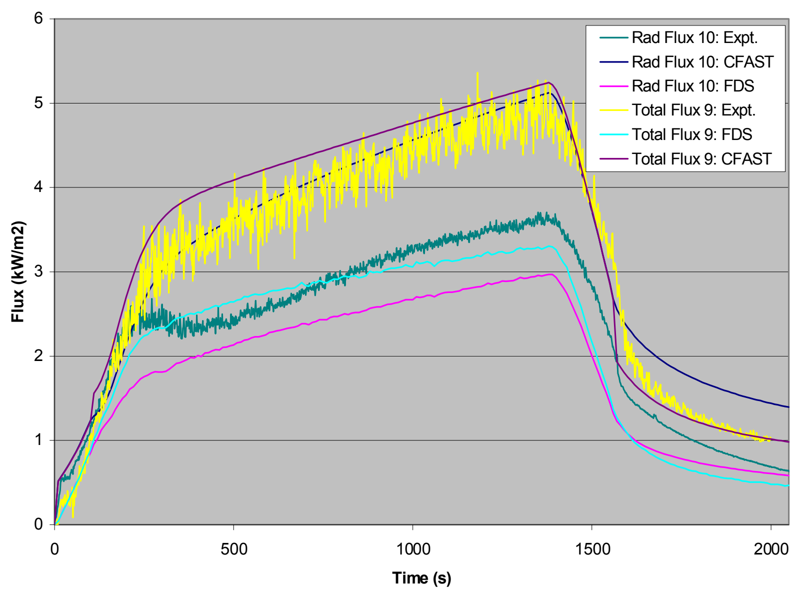

Figure 5.9.8 Heat Flux to Cables (Gauges 9 & 10) - Test 15

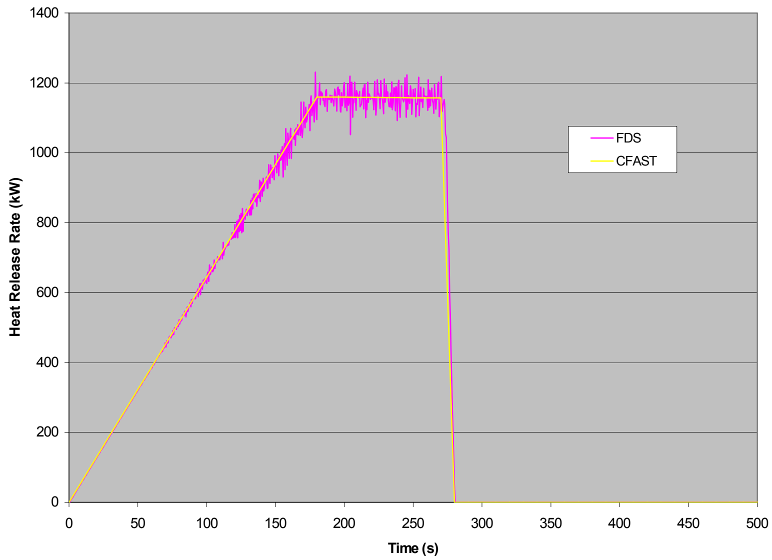

Figure 5.11.1 Heat Release Rate - Test 17

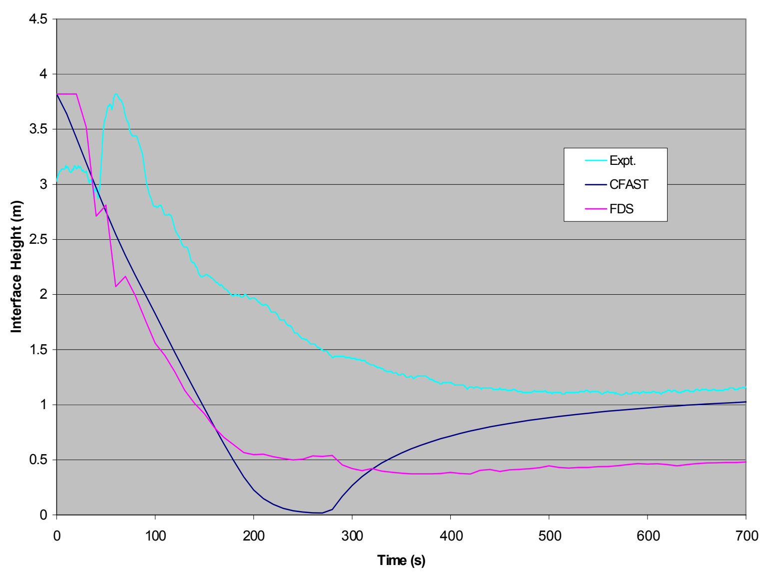

Figure 5.11.2 Hot Gas Layer Development - Test 17

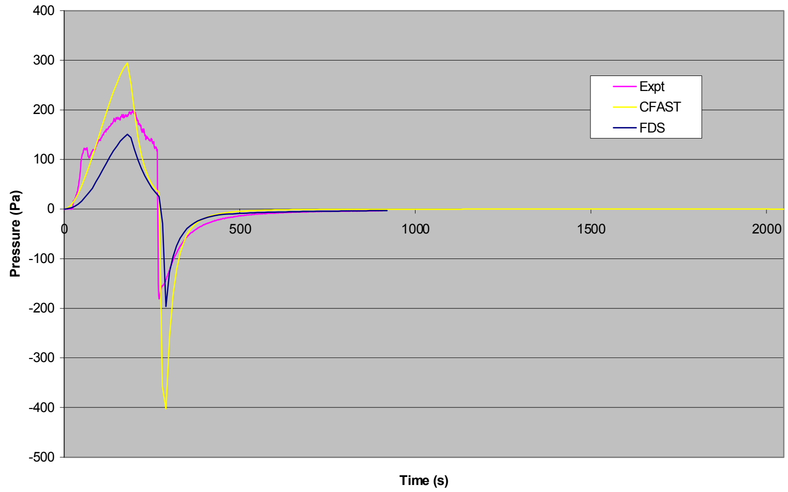

Figure 5.11.3 Compartment Pressure - Test 17

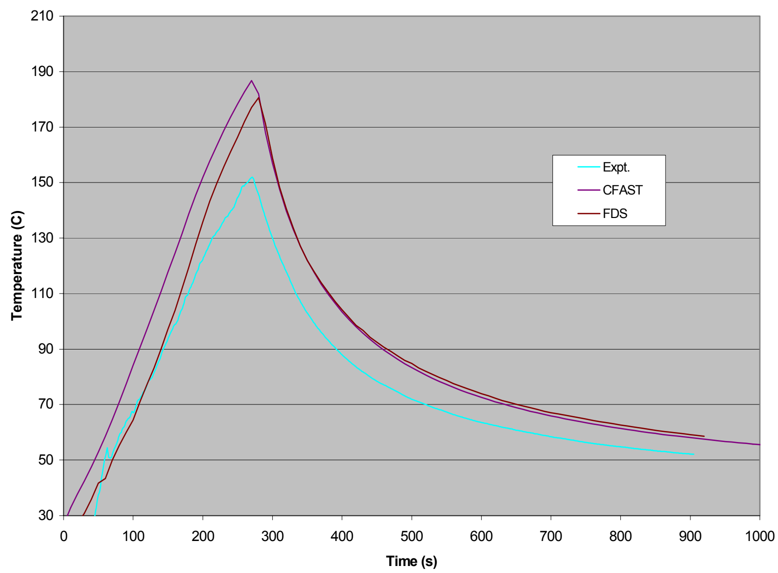

Figure 5.11.4 HGL Temperature - Test 17

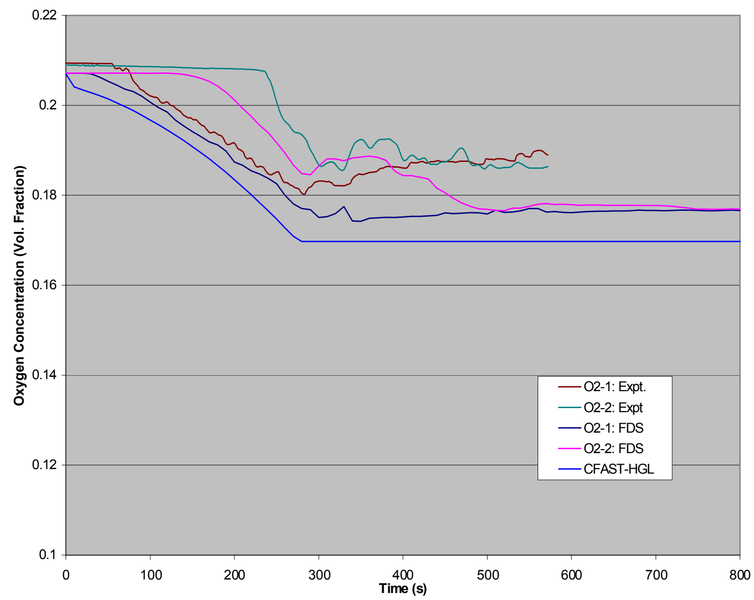

Figure 5.11.5 Oxygen Concentration - Test 17

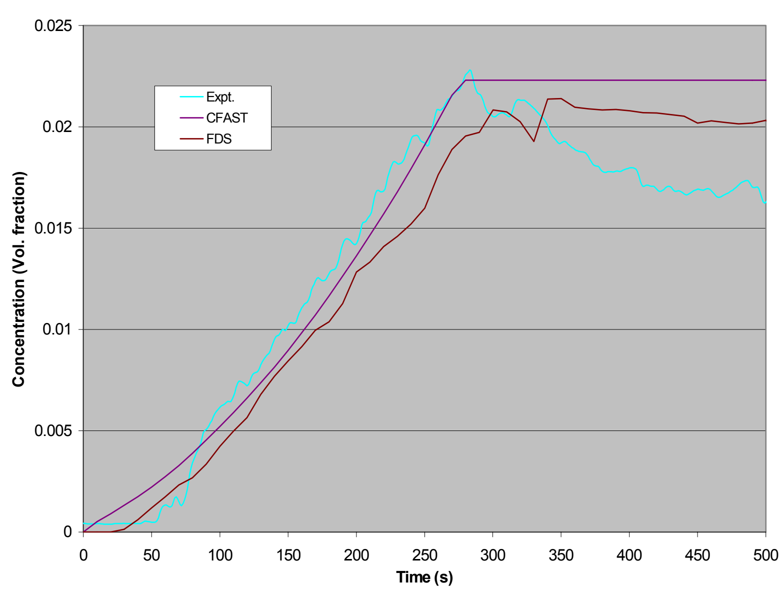

Figure 5.11.6 CO2 Concentration - Test 17

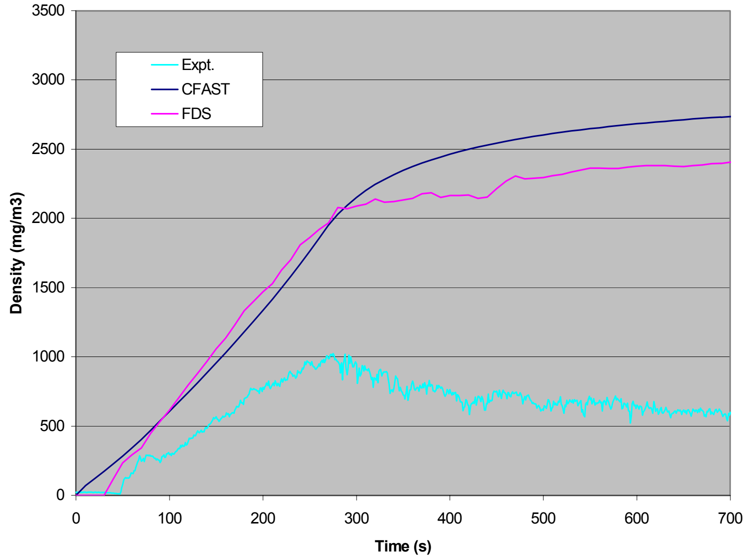

Figure 5.11.7 Smoke Development - Test 17

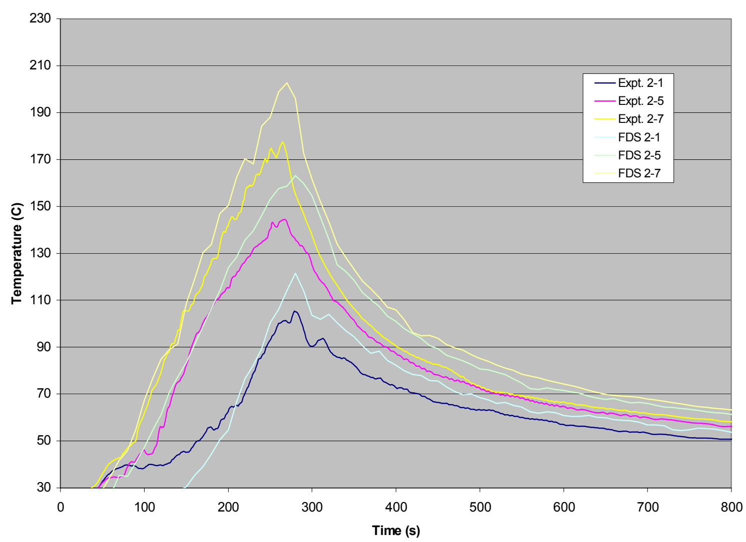

Figure 5.11.8 TC Tree 2 - Test 17

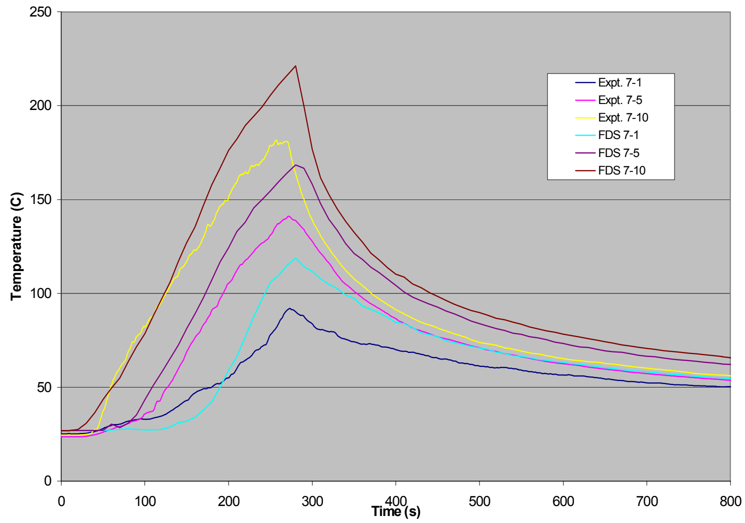

Figure 5.11.9 TC Tree 7 - Test 17

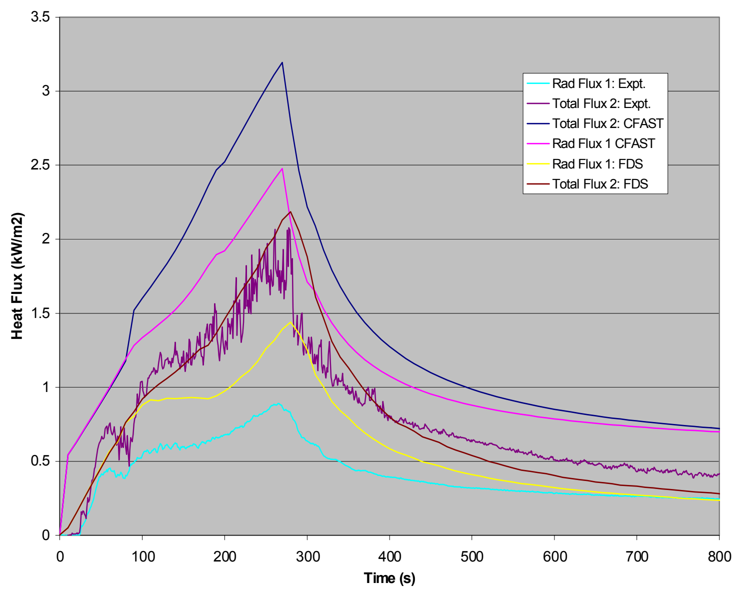

Figure 5.11.10 Heat Flux to Cables (1 & 2) - Test 17

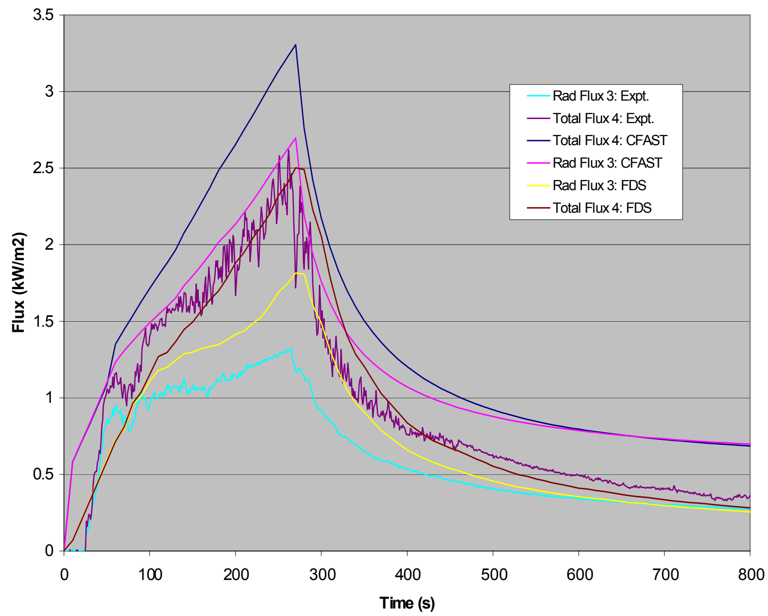

Figure 5.11.11 Heat Flux to Cables (3 & 4) - Test 17

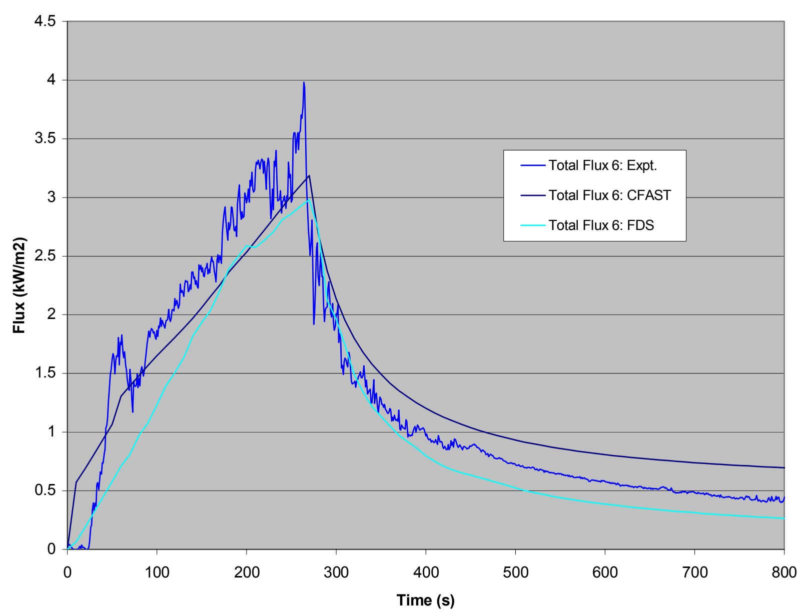

Figure 5.11.12 Heat Flux to Cables (6) - Test 17

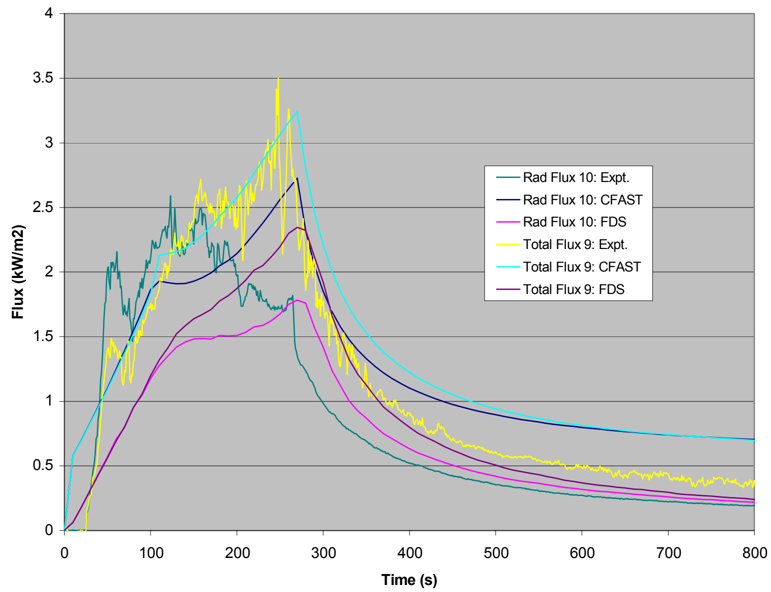

Figure 5.11.13 Heat Flux to Cables (9 & 10) - Test 17

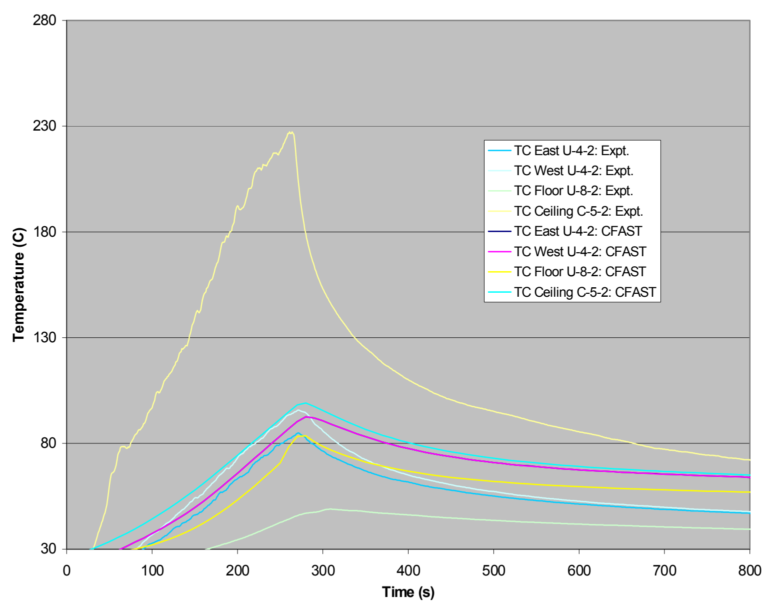

Figure 5.11.14 Wall Temperature (CFAST) - Test 17

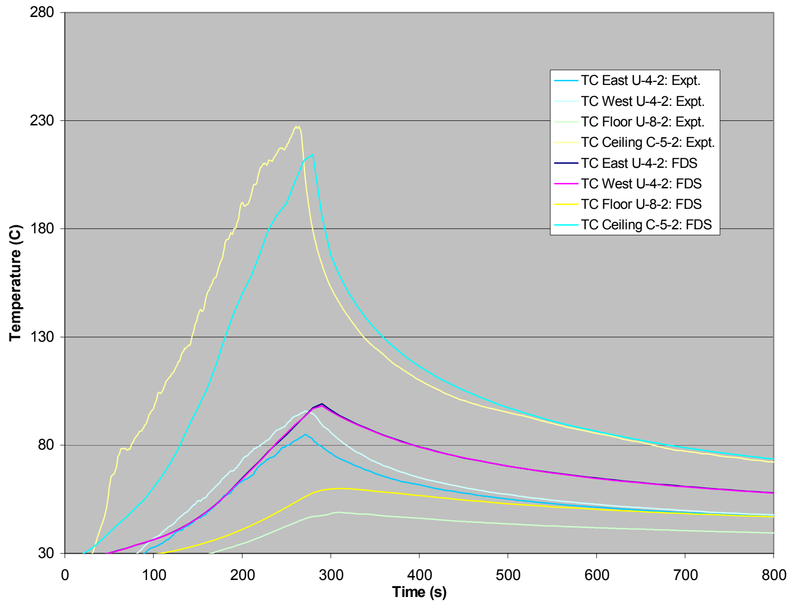

Figure 5.11.15 Wall Temperature (FDS) - Test 17

Appendix A: Comments on Design of Experiments

A.1 Introduction

A draft specification of ICFMP Benchmark Exercise # 3 was issued to participants in the International Collaborative Fire Model Project (ICFMP) on September 6, 2002. Written comments on the draft specification were received from participants. The draft test specification was also presented at the 6th ICFMP meeting at British Research Establishment (BRE), UK on October 10-11, 2002 when verbal comments from participants in the meeting were received and documented. This Appendix documents the written and verbal comments received on the draft specification of the ICFMP Benchmark Exercise # 3, including the resolution and disposition of the comments. The final specification used for ICFMP Benchmark Exercise # 3 and presented in the main report includes the modifications resulting from the comments received and presented here.

A.2 Comments at 6th ICFMP Meeting

The following presents the disposition of comments received on the draft specification at the 6th ICFMP Meeting.

1. Comment: Contact resistance between marinite slabs will be challenging to calculate -

Disposition: The contact resistance between the marinite slabs will be measured.

2. Comment: Include a target geometry that can be directly modeled by most fire models, i.e. a slab geometry with the same thermal inertia and surface area as a cable

Disposition: Revise geometry of PVC target to a rectangular slab 25 mm thick by 100 mm wide

3. Comment: IRSN has collected data on leak tightness of compartments in NPPs which can be provided for the benchmark exercise

Disposition: IRSN has provided NRC with proprietary data on the leak tightness of compartments in French NPPs which will be reviewed for use in the benchmark exercise.

4. Comment: The specific dimensions of the cables should be provided. AWG should be defined or some other international standard should be used in the test plan

Disposition: The specific dimensions of cables defined per the American Wire Gauge standard has been included in the test specification.

5. Comments: The effect of various parameters that may affect the symmetry of the fire should be examined, e.g. pressure variations

Disposition: The targets have been relocated so that they do not rely on the symmetry of the fire.

6. The effect of pressure variations on the fuel spray flow should be assessed

NIST Disposition: The fuel delivery system incorporates a positive displacement fuel delivery pump. Once the flow rate has been selected, the system operates at a uniform pressure.

7. Comment: The use of a symmetrical fire source should be a goal in the test series

Disposition: The targets have been relocated so that they do not rely on the symmetry of the fire. Therefore, achieving a symmetrical fire source is no longer a key issue for the test series.

8. Comment: A flame stabilizer should be used to achieve symmetry of the fire

Disposition: The targets have been relocated so that they do not rely on the symmetry of the fire, so a flame stabilizer is no longer necessary.

9. Comment: The fire source should be simple (can be modeled easily) and accurate for the benchmark exercise.

Disposition: A spray burner will be utilized with toluene and heptane fuels. The fuels will be characterized for soot yield and fraction of heat released as radiation.

10. Comment: Since the test series involve full-scale experiments, the focus of the benchmark exercise should be on parameters/data that can only be obtained through full-scale tests.

Disposition: Several measurements shall be made to focus on parameters/data that can only be obtained through full-scale tests.

11. Comment: Natural gas has a low soot concentration and therefore will not be an effective fuel for examining the effect of soot on the fire environment.

Disposition: Heptane and toluene have been chosen to allow examination of soot concentration on fire effects.

12. Comment: The use of methanol (clean fuel) and heptane (high soot yield) could provide a diverse set of fuel sources.

Disposition: Heptane and toluene have been chosen to allow examination of the soot concentration on fire effects. Toluene has a high soot yield similar to PVC and lube oil.

13. Comment: The cable targets should be located so that they are exposed to the hot gas layer (HGL).

Disposition: The cable targets have been repositioned to locations above the top of the door so that they will be exposed to the HGL when the door is open.

14. Comment: Consider the option of maintaining symmetry in the y-direction (as opposed to the x-direction as proposed). The targets can then be varied along the y-direction.

Disposition: In order to maintain a simple target configuration, and not rely on the symmetry of the fire, targets have been located in the same vicinity of the fire compartment to allow comparisons of target heating.

15. Comment: The flow velocity of the mechanical ventilation system in the test series should be similar to that in real NPP configurations

Disposition: The velocity for a mechanical ventilation rate of 5 volume changes per hour is 1.6 m/s for a the specified vent area of 0.5 m2. This velocity is similar to that in real NPP configurations.

16. Comment: One flow rate (as opposed to the two proposed) for the mechanical ventilation system should be sufficient for the test series.

Disposition: Only one flow rate of 5 volume changes per hour will be used for the test series.

17. The flow characteristics of the test mechanical ventilation system should be measured, i.e. the flow versus pressure curves. The pressures at the entrance and exit of the mechanical ventilation systems should be measured

NIST Disposition: The supply and exhaust vents will be equipped with bidiectional probes. These measurements together with temperature measurements will be used to determine flow rates trough the systems during testing.

18. Comment: Gas burner fires can be controlled the most, but care and attention is needed to ensure safety.

Disposition: Spray burners with heptane and toluene fuels will be used. These fuel sources should be safer to use than gas burners.

19. Comment: The effect of combustion efficiency in determining the heat release rate profile should be assessed for determining an appropriate fuel source

Disposition: As indicated above, spray burners with heptane and toluene fuels will be used in the test series. The combustion efficiency of the fuels under various ventilation conditions will be measured and provided to participants in the benchmark exercise.

20. Comment: A scenario with an elevated fire source should be considered

Disposition: The inclusion of an elevated fire source will add complexity and cost to the 1st test series which will challenge the current schedule and allotted budget. Therefore, an elevated fire will be considered for the 2nd test series.

21. Comment: The pressure should be measured at a high and low point in the compartment

NIST Disposition: The uncertainty in the pressure measurement would be significantly larger than the measured pressure difference. Such a measurement would be of little utility.

22. Comment: The visibility should be directly measured.

Disposition: The visibility will be directly measured, as suggested.

23. Comment: Consideration should be given to measuring plume temperatures.

Disposition: Plume temperatures will be measured, as suggested.

24. A 1 mm and 200 micron thermocouple should be placed at the same location to estimate the uncertainties in measuring convective and radiative heat flux

NIST Disposition: The measurement technique that utilizes different size thermocouples to estimate uncertainties in convective and radiative fluxes is not appropriate in a soot-filled environment where the effective size of a thermocouple changes as soot deposits occur. Instead, heat flux measurements will be undertaken using a number of Schmidt-Bolter total heat flux gauges and ellipsoidal radiometers. The Schmidt Bolter gauges will be cooled by an elevated temperature water flow to avoid condensation on the sensing element of the gauge. The radiometers are wide-angle, N_2 purged devices. A comparison of the fluxes between the ellipsoidal and Schmidt-Bolter measurements will allow differentiation of radiative and convective heat flux. Convective heat flux is expected to be small compared to the radiative heat flux. Additional instrumentation will be used to measure heat losses to the walls and ceiling.

25. Comment: The total and radiative heat flux should be measured.

Disposition: The total and radiative heat flux will be measured, as suggested.

26. Comment: CO, CO_2, and O_2 should be measured.

Disposition: CO, CO_2, O_2 will be measured, as suggested.

27. Grab samples should be used in making the measurements suggested above (ref: MRL, SNL?)

NIST Disposition: A continuous sampling loop will be used to measure O_2, CO and CO_2 in the hot layer. Additionally O_2 will also be measured in the lower layer.

28. Comment: A video recording should be made of the fire scenarios in the test series.

Disposition: A video recording will be made of the fire scenarios in the test series, as suggested.

29. Comment: SI units should be consistently used in the test plan.

Disposition: SI units will be used for all documents related to the test series, including the specification of the scenarios and the test plan.

30. Comment: The cables should be located such that they are thermally stressed, but do not ignite.

Disposition: The cables will be located such that they are thermally stressed, but do not ignite.

A.3 Written Comments

The following presents the disposition of written comments received on the draft specification.

R. Bertrand (IRSN)

1) Comment: The insulation of control cables are in XPE and the insulation of all the power cables is in PVC. Could you indicate the reason of this choice? It would be interesting to carry

out some tests with power cables having a thermoset insulation in order to appreciate the influence of the insulation material.
Disposition: The test series will include both power and control cables with XPE and PVC insulation to examine the effect of the insulation material and size of the cables.

2) Comment: The tray D contains 9 cables on 2 rows (the first row with 6 cables, the second with 3 cables). In NPPs, the number of rows and cables can be higher. So, it would be interesting in one test or two tests to see if the number of rows has an influence on the cable temperature evolution.
Disposition: The test series will include cable trays loaded with 2 and 3 rows of cables to examine the influence of loading on cable temperature evolution.

3) Comment: The tray is located in the lower part of the compartment. To have a higher increasing of the cable temperature, it would be better to put it in the hot zone. More over, it would be interesting to carry out some tests with the tray inside the plume, in order to appreciate the influence of the cable location.
Disposition: All targets have been repositioned so that they are in the upper compartment and in the HGL for scenarios in which the door is open. One scenario has been included to evaluate the heating of a target in the fire plume region.

4) Comment: In order to make easier the comparison of the cable temperature evolution, it would be better to install the alone cable near the tray. Disposition: The single control cables have been moved to near the cable tray, rectangular insulation slab target, and power cable to make the comparison of the temperature evolution more accurate.

5) Comment: Is it foreseen to reach the damage temperature of the cable?
Disposition: The duration of the tests will be established so the target approaches the damage temperature.

6) Comment: It is not foreseen to install instrument cables. It would be interesting to test this kind of cable that have lower thermal inertia.
Disposition: In order to maintain a limit on the scope of the 1st test series, instrument cables will be examined later in the program.

7) Comment: The PVC cylinder has a diameter of 50 mm. How was chosen this diameter? Moreover, it would be interesting to see if a rectangular slab can be used for a cable model.
Disposition: The 50 mm diameter was chosen as equivalent to the diameter of typical power cables. The geometry of the PVC target will be revised to be a rectangular slab.

C. Casselman (IRSN)

Generalities
The general objective of the tests is to obtain data for testing models for target temperature elevation which are used in fire codes.
Different targets are submitted to different thermal conditions ; parameters are :
Elevation of targets
Fire HRR
Fraction of produced soot (emissivity of gases)
Position of the fire in the room
Ventilation of the room : closed room, natural or mechanical ventilation

Fire scenarios

Comments and questions

Closed room scenarios : Take care of the overpressure as the fire will be ignited and also of the under-pressure at the extinction ; is the test room designed to withstand these stresses?

Comment: Do you plan to determine the leakage of the room itself in function of the pressure to get input data for codes?
Disposition: The leakage of the room as a function of pressure will be established to be similar to that in NPP compartments and measured before the test series.

Comment - Also for tests with mechanical ventilation, you could have peaks of over pressure and under pressure which depend of the ventilation network aeraulic characteristics.
Disposition: This phenomenon will be noted in the design of the instrumentation for the ventilation system.

Comment: Cables in the plume (test 16) : one or several cables could ignite and burn ; is it of interest for this study? In this case, will the cable fire HRR be correctly estimated in the test?

Disposition: Since cable heating in the plume region is of interest in fire risk studies, this case is included in the test series. The duration of the tests will be established so that the cables approach damage temperature, but do not ignite.

Suggestions

Comment: why not one or two scenarios with both mechanical and natural ventilation?
Disposition: One scenario with both mechanical and natural ventilation (door open) will be included in the test series.

Comments: Are electric measurements planed for the cables to know the instant of no-functioning? If not, what is the precise objective related to the cables? Only temperature elevation?
Disposition: Measurements of the cable circuitry are not planned for this test program. The objective of this set of test series is to evaluate and validate the ability of current fire models to predict cable temperature evolution in NPP compartment fires.

Fire position in the room
Comments and questions

Fire in a corner or near the walls : the particular objective is to have another temperature distribution in the room? a different air entrainment flow rate (a different evolution of the interface height)?

Suggestions

Comment: Why the burner are not exactly against the walls (in contact with the walls)? If there is a distance between the wall and the edge of the fire, the effect of the fire will be weak.
Comment: For fire of low HRR (<550 kW), in our tests, we observe no effect of the position of the fire (near a wall in comparison with the centre of the room); above 550 kW, the

effect appears essentially for the plume and the flame structure (flow velocity and temperature) ; but the global thermal behaviour is not notably different for a fire near the wall in comparison with the fire in the centre of the room.
Disposition: Based on the above suggestion indicating that the global thermal behavior is not notably different for a fire near the wall or corner in comparison with a fire in the center of the room, the tests with the fire in the corner and near the wall will be deleted from the test series.

Some lessons learned from previous study

Comment: Measurements of room leakages are of great importance for the scenarios without ventilation ; without the good knowledge of the leakage versus temperature and pressure, it is not possible to calculate correctly the pressure in the room
Disposition: The leakage of the room as a function of pressure will be established to be similar to that in NPP compartments and measured before the test series.

Comment: Scenarios in natural ventilation can be compared with test LIC 2.12 (800 kW) in which we observed a ghosting flame. But the opening in these test is larger ; so the probability for the ghosting flame is low.

Disposition: A video recording of the ghosting flame will made if it is observed during the test.

Radiometers for radiative fluxes : radiative MEDTHERM ellipsoidal type or with a saphir window? The first is better because soot deposit affects the measurement for the second. -

NIST Disposition: MEDTHERM radiometers will be used.

Material for the walls
Comment: What is "marinite"? insulating material?
Disposition: Marinite is a material used for walls, like gypsum board.

Comment: Before the test, will this material be characterized accurately (thermal capacity, thermal conductivity, density, emissivity)?

Disposition: Yes, this material and the cables will be characterized (specific heat, thermal conductivity, density, emissivity) accurately for the benchmark exercise.

Measurements
Questions

Comment: Measurement of HRR from oxygen concentration in the case of open doors : is there a delay in the case of a long volume like the test room?

NIST Disposition: There will be a long delay.

Comment: What is the exact location of the thermocouples and radiometers on the targets?
Disposition: The exact locations of the thermocouples and radiometers are shown in the Figures in this Report.

Comment: Is the number of thermocouples for targets sufficient?
Disposition: The number of thermocouples for the targets have been increased.

Suggestions

Comment: Some video recordings could be of help to visualize the flame extinction and the interface (soot zone) evolution, also outside of the room at the door to observe the interface height.
Disposition: Video recordings of the tests will be made, as suggested.

Comment: Some measurements on a tree for extinction coefficient measurements to follow the interface height from the optical characteristic of the gas at several elevations.
Disposition: Extinction coefficient measurements will be made, as suggested.

Comments: Several thermocouples on a vertical axe above the burner to get information for plume and also for extinction.
Disposition: Plume temperatures will be recorded, as suggested.

S. Miles (BRE)

1) Comment: The process of securing the fuel if the oxygen concentration falls below 15% is a bit unclear, in particular in respect to how to incorporate this into the modeling.

NIST Disposition: The fuel will be remotely secured once the lower compartment oxygen concentration reaches 15.0%. At that point the fire will be extinguished. During modeling this can be simulated by removing the heating source.
2) Comment: I assume the individual thermocouple tree readings will be documented in the data spreadsheet, allowing detailed comparison with CFD and lumped parameter model predictions.

Disposition: Thermocouple tree readings will be documented in the data spreadsheet to allow detailed comparison with CFD and lumped parameter model predictions.
3) Comment: Have we possibly made the blind simulation period too short (recalling that Christmas will occupy some of the period)? This applies in particular to CFD models, which take time to run. Obviously, the experimental data will be very useful for open simulations for many years ahead, but the opportunity for blind predictions is one off, and maybe we will not get the maximum benefit if the number of predictions is curtailed due to the time available.

Disposition: The schedule has been revised to incorporate the comment.

A.4 NRC and NIST Comments

<u>E. Connell, M Salley and N Iqbal (USNRC)</u>

1. Comment: Why are power cables being selected for testing? Power cables are the least susceptible to fire induced failure. These cables are generally the cables of least concern with respect to fire damage and fire safe shutdown (FSSD) analysis. These cables generally have the largest physical mass (based on their requirement to safety carry higher current) which allows the cables to act as a larger heat sink for a given thermal insult from a fire. These cables typically

constitute the largest sizes of conductors used in nuclear power plant (NPP) (#14 AWG up through 750 MCM).

Instrument and control cables are more susceptible to fire induced failures than power cables. This can be attributed to their size and sensitivity.

It is suggested that the testing be performed using control and instrumentation cables rather than power cables with a representative mixture of thermoset and thermoplastic cable construction.

Disposition: Power cables are included since they can be important for certain fire scenarios that are important in risk assessments. Both power (3 conductors, #6 AWG) and control cables (7conductors, # 14 AWG) in both thermoset (XPE) and thermoplastic (PVC) construction will be used in the test series.

2. Comment: The test plan needs a better description of cable construction (Section 4.2.2). What type of cable jacketing materials has been selected to carry out the testing? Again it is suggested that the testing be performed using mixed thermoset and thermoplastic cable jacketing materials that is commonly encountered in the U.S. commercial NPPs.

Disposition: The cable jacketing material will be PVC for cables with PVC insulation, and Hypalon for cables with XPE insulation.

3. Comment: Section 4.2.2, Figure 1, shows the compartment content layout for full-scale experiments. This setup shows only one cable tray and several individual cable targets. The contents of the compartment are limited for the size of the experiment and this type of configuration is not representative of a NPP compartment. This is not an economic use of the fire test. It is recommended that the experimental setup be revised. Instead of several individual cable targets, add an array of cables trays in middle as well as along the walls of the test compartment. Steel and aluminum conduits should also be added.

Disposition: The objective of the 1st test series is to use a test configuration so that the predictive capabilities of fire models may be evaluated. A complex compartment configuration was not chosen for the 1st test series so the evaluation would not be complicated by several compounding factors. The objective is to conduct the set of test series in a progressive manner from the simple to more complex geometries.

4. Comment: What is a solid PVC cylinder target representing in this testing? It is not a representative target found in a NPP compartment. It is suggested to add better representative targets (as found in NPP) such as metal junction boxes (mounted on wall/ceiling), floor mounted motor control center (MCC) etc. A small section of structural steel (I-beam) would also provide a good target in compartment overhead.

Disposition: A PVC slab is included as a target in the test series to allow the evaluation of the predictive capability of fire models that model a target in a slab geometry. This will allow a focused and accurate evaluation of the target submodel. A metal junction box will be included as a target, as suggested.

5. Comment: Section 4.3 discussed test configuration and fire scenario. The maximum fire durations have been selected for five, and ten minutes for various fire sizes. Why such a short

fire duration been selected? The fire duration should be one hour or until failure to get the complete results.

Disposition: The durations of the fire scenarios will be revised and established so that the targets approach damage temperatures.

6. Comment: Section 4.4, discussed the thermocouples (TCs) tree setup in experiments. 10 TCs are presently placed along the 3.72/m level. It is recommended that for greater accuracy place 1 TC every foot.

TCs on cables will be used to measure surface and core cable temperatures. 16 TCs on cable are also too few to measure the surface temperature. It is recommended that a minimum of 1 TC per meter to should be placed to measure cable surface temperature. How will the TCs be attached and orientated on the cables? This could be critical to the measurements.

Disposition: The spacing of the thermocouples in the draft test plan is about 1 TC per meter. The TCs will be attached and oriented to result in meaningful results.

7. Comment: Section 1.2 discussed a review of previous work done in cable testing. This review does not address an important Thermo-Lag testing study sponsored by the U.S. Nuclear Regulatory Commission, Office of Nuclear Reactor Regulation, and performed by the Sandia National Laboratories (SNL) title, "An Evaluation of the Fire Barrier System Thermo-Lag 330-1," SANDIA 94-0146, Sandia National Laboratories, Albuquerque, New Mexico, September, 1994. - NRC

Disposition: A reference will be added, as suggested.

8. Comment: Section 3.0 discussed the testing program to simulate an unobstructed compartment. In a NPP almost every compartment is filled with overhead obstructions, there are no unobstructed compartments. Therefore, it is suggested to add more targets such as cables trays, ducts, pipes etc.

Disposition: See response to Comment # 3.

9. Comment: Section 4.2.1 discussed the compartment wall, ceiling, and floor materials. Why is the floor covered with 25 mm gypsum? and walls and ceilings are covered with 25 mm marinite?. In a NPP compartments enclosing surfaces construct with thick concrete. Could the testing with marinite and gypsum be more representative? (e.g., heat conduction and other thermal properties of concrete vs. marinite and gypsum are very different).

Disposition: The materials for and thickness of the walls and floors were chosen to be representative of concrete walls in NPPs.

10. Is there mechanical ventilation installed in the test compartment? Figure 1 does not show a mechanical ventilation installed in the test compartment.

Disposition: Figure 1 will be modified to clearly show the mechanical ventilation system.

11. Comment: Section 4.2, discussed the compartment size and construction (Figure 2). What is this compartment configuration attempting to represent in a NPP?

Disposition: The compartment dimensions are similar to the compartment analyzed in Benchmark Exercise # 1 which represented a typical switchgear room.

12. Comment: Section 4.3 discussed test configuration and fire scenarios to examine certain effects. The following effects are not included in the list:

Fire source located in center of the compartment
Compartment door closed
Mechanical ventilation on, door open
Mechanical ventilation on, door closed
Mechanical ventilation off, door open
Mechanical ventilation off, door closed
Compartment flashover

Disposition: Most of the above affects were included in the specification. A scenario with mechanical and natural ventilation (door open) has been added. Compartment flashover may be investigated later in the test program.

13. Comment: Section 4.3 also discusses the fire sizes and burn duration. Why was the fire heat release rates (HRRs) of 350 kW, 1.0 MW, and 2.0 MW selected for testing? What is the growth rate of these fires?

It is recommended that fire sizes of 500 kW, 800 kW, 1200 kW, 1500 kW, 1800 kW be included to examine effects. How will HRR be measured and controlled during testing?

Disposition: 350 kW, 1.0 MW, and 2 MW were selected to cover a range of fire intensities of interest in fire risk analysis. The measurement of HRR will be discussed in the test plan. Although it would be interesting to obtain information on the effects of other fire sizes, additional scenarios have not been included due to the costs of adding tests and the need to investigate other important effects.

14. Comment: Section 4.4 provides a list of parameters plan to measure during testing. The following parameters are not included in the list:

Flame height
Ignition temperature
Flame spread rate on cables
Visibility
Species concentration (e.g., Soot, CO, CO2 unburnt hydrocarbons, etc.).

Disposition: Information regarding flame height will be obtained through video recordings. Measurements of ignition temperature and flame spread rate on cables are planned for later test in the program. Visibility and species concentrations (soot, CO, CO2) will be measured.

15. Comment: Section 4.5 discussed test matrix to performed eighteen tests. In Table 2, Test 9 through Test 13 are listed as replicate tests. Provide test number for these replicate in the test matrix.

Disposition: The test matrix has been revised and will be numbered appropriately.

Kevin McGrattan (NIST)

1. Comment: Metric units should be used throughout. English units OK if in ( ). Pressure in Pa, not torr.

SI units will be used in all documents related to the test program.

2. Comment: Data Analysis looks sketchy. The way I read it, someone is just going to hand you a data file full of numbers. I think they ought to talk about how they are going to reduce the data and ensure that the measurements are consistent in terms of the overall energy balance.

Disposition: Measurements of heat loss to the boundaries will be made so that one can evaluate the performance of the fire models for predicting overall energy balances.

3. Comment: Define AWG for cables.

Disposition: The specific dimensions of cables defined per the American Wire Gauge standard has been included in the test specification.

4. Comment: Figure 2 is not clear.

Disposition: Figure 2 has been revised and clarified.

5. Comment: I realize that these experiments are to be close to Benchmark 1. I recommend some bigger fires if the compartment proves to be strong enough to take it.

Disposition: Due to considerations of safety, it has been decided that the fire size will be limited to 2 MW for this test series.

Appendix B Input Data Files for CFAST and FDS

Deytec, Inc.

Nuclear Engineering Services